THE BEHAVIOUR OF CONCRETE AND REINFORCED CONCRETE UNDER SHORT TERM STEADY STATE TEMPERATURES

by

AZIZ FARUQUE SARKAR

A thesis submitted to the School of Graduate Studies, University of Ottawa, in partial fulfilment of the requirement for the degree of Master of Applied Science in Civil Engineering.

OTTAWA, ONTARIO

CANADA

March, 1972

TABLE OF CONTENTS

SYNOPSIS

Experimental and analytical investigations of the thermal coefficient of expansion and the modulus of elasticity of plain and reinforced concrete under short-term steady state temperatures (-100^0F to $+150^0$F) were carried out. Tests were conducted on one hundred and twenty-five 12 in. x 4 in. x 3 in. slab*specimens and thirty-six 12 in. x 3 in. x 3 in. prism specimens.

The slab specimens were used to determine the thermal coefficient of expansion. The one hundred and twenty-five specimens consisted of seventeen series of seven specimens each and one series of six specimens. In each series the reinforcements in the slabs varied from 0% to 5%. Nine of these series were symmetrically reinforced and the other nine were unsymmetrically reinforced. Among these nine series of each reinforcement type, five series were dry-cured; they were kept in water (68^0F to 70^0F) for seven days, after which they were taken out and stored in the laboratory (68^0F to 72^0F temperature and 65% to 75% RH) until tested. The remaining four series were wet-cured; they were kept in water (68^0F to 72^0F) until tested. The last dry-cured series in both the symmetrical and unsymmetrical reinforced types were tested at the age of one year. The other series were tested at three different ages, viz. 7, 28 and 84 days.

The prism specimens were used to determine the dynamic modulus of elasticity of concrete by the resonant frequency method. Two prism specimens were cast with each series of slab specimens. They were cured

---

* A segment of the reinforced concrete slab of a steel-concrete composite section.

and treated in the same way as the slab specimens. The prism specimens were tested simultaneously with the slab specimens at each test age. Along with the slab and prism specimens five 6 in. x 12 in. control cylinders were cast for each series. They were used to determine concrete strengths and the initial tangent modulus of elasticity at the various test ages.

At each steady state temperature the fundamental relations of equilibrium of forces and moments and the compatibility of linear deformations were considered for the slab specimens. From these conditions analytical expressions were derived for the strains and the coefficient of thermal expansion of reinforced concrete. A computer programme was used to calculate the coefficient of expansion and the force developed in concrete at each test temperature. These results are presented in graphical and tabular form.

From the experimental work measured deformations of slab specimens were curve fitted by the least square method. The fitted curves and the actual deformations were plotted using a special plotter programme. The coefficient of correlation and the estimate of error for the curve fit were computed. Experimental and analytical values were compared and the correlation was found good.

The variations of the coefficients of expansion of plain and reinforced concrete with the different variables, viz. water-cement ratio, method of curing, arrangement and amount of longitudinal steel and age, were investigated. Definite patterns of relations between the different variables were found and are reported in the form of figures and tables.

The dynamic modulus of elasticity values were calculated and curve fitted using a separate computer programme. The rate of variation of the dynamic modulus of elasticity with age, water-cement ratio and type of curing was reported. The results, presented in the form of graphs and tables, show that a definite pattern of relations exists between these variables.

The coefficient of expansion values decreased with an increase in the water-cement ratio and increased over the age. For plain concrete the coefficient of expansion varied from 4.60×10^{-6} in./in./°F (w/c 0.445 - 7 days wet-cured) to 3.34×10^{-6} in./in./°F (w/c 0.672 - 84 days wet-cured). For the reinforced section the values varied from 5.74×10^{-6} in./in./°F (w/c 0.445 - 84 days dry-cured; 5% steel; unsymmetric face 1*) to 2.80×10^{-6} in./in./°F (w/c 0.672 - 7 days wet-cured; 5% steel; unsymmetric face 2**). The coefficient of expansion of symmetrically reinforced concrete increased with an increase in the percentage of steel reinforcement (3.64×10^{-6} in./in./°F for 0% to 4.32×10^{-6} in./in./°F for 5% - ASD 0.577; 7 day old). For unsymmetrically reinforced concrete the coefficient of expansion for the concrete face near the reinforcement increased significantly with an increase in the percentage of steel (3.64×10^{-6} in/in./°F for 0% to 5.11×10^{-6} in./in./°F for 5% - Series AUD 0.577; 7 days old), while that for the concrete face away from the reinforcement decreased slightly (3.64×10^{-6} in./in./°F for 0% to 3.42×10^{-6} in./in./°F for 5% - Series AUD 0.577; 7 days old). The wet-cured speciments had lower coefficients of expansion than those for the dry-cured specimens.

---

* Face 1 - near the steel reinforcement
** Face 2 - away from the steel reinforcement

The dynamic modulus of elasticity of wet-cured concrete increased with age (5079 KSI at 7 days to 5503 KSI at 84 days - Series ASW 0.487), while that for the dry-cured concrete decreased with age (5209 KSI at 7 days to 4635 KSI at 84 days - Series ASD 0.487). The modulus of elasticity increased with a decrease in temperature (4729 KSI at 153.6°F to 5796 KSI at -100.2°F - Series ASD 0.487; 28 days old), having different rates of change in slopes for below (-11.15 KSI/°F; ASD 0.487; 28 days old) and above (-1.28 KSI/°F; ASD 0.487; 28 days old) the freezing point. The rates of change in the slopes of the modulus of elasticity were greater with a higher water-cement ratio. With the exception of the above freezing changes in the slopes of the dynamic-E of the wet-cured concrete, the rates of change generally decreased with age (-10.03 KSI/°F at 7 days to -2.50 KSI/°F at 84 days - Series ASD 0.445; below freezing slopes).

LIST OF FIGURES

LIST OF TABLES

LIST OF PHOTOGRAPHIC PLATES

LIST OF FLOW CHARTS AND SUBROUTINES

CHAPTER 1

INTRODUCTION

1.1 GENERAL

Concrete is invariably used in conjunction with steel. Reinforced and prestressed concrete and composite structures contain varied percentages of steel. These two materials - steel and concrete - have different thermal and physical properties.

The thermal coefficient of expansion of steel ($\alpha_s = 6.5 \times 10^{-6}$ in./in./^{0}F; A.I.S.C. manual 1966) is normally greater than that of concrete ($\alpha_c = 3.56 \times 10^{-6}$ in./in./^{0}F for water-cement ratio = 0.672, age = 7 days and temperature 32^0F - 150^0F). In a structural member, the section of which is composed of steel and concrete, the deformation of steel would be greater than that of concrete if these materials were considered separate and underwent a change in temperature. The two components of the structural member are attached firmly to each other by means of bond, shear connectors, etc. Therefore, the steel and concrete must deform together to produce compatible linear deformations across the section. This will give rise to internal stress in both steel and concrete, the magnitude of which will depend on the amount of steel used in conjunction with the concrete. Composite structures, because of a high percentage of steel, are most seriously affected in case of a temperature change.

In a simple span composite bridge of reinforced concrete slab and steel beam a negative flexural effect will be produced across the bridge with a decrease in temperature. This is opposite to the normal loading effect. With an increase in temperature the effect will be similar to the normal loading effect, i.e. a positive curvature across the bridge. These effects, which are due to changes in temperature, might be more significant when accompanied by a difference in temperature between the slab and the beam. Such a difference may occur due to a warming of the slab by the sun while the girder is shaded, freezing rain or snow suddenly cooling the slab, or a rapid increase or decrease in air temperature, which is quickly reached in the steel beam. For unidirectionally extended structures, such as multistoried buildings, tall towers or continuous composite bridges, the above effects will be particularly severe.

The different components of concrete are cement, aggregate and water. The characteristics and amount of these components affect the characteristics and physical properties of the resulting concrete. In the analysis of deformation and stress of concrete structures undergoing temperature change, it is necessary to know the extent of variation of the properties (modulus of elasticity and coefficient of thermal expansion) of the concrete with temperature.

1.2 OBJECT

Deformation characteristics of reinforced concrete slab sections under steady state temperature conditions (-100^0F to $+150^0$F) were the principal objects of this investigation. Both the experimental investigation and the analytical study were undertaken. Specific properties investigated were the coefficient of expansion of concrete and reinforced concrete and dynamic modulus of elasticity of concrete under temperature change. The effects of arrangement and amount of reinforcement, the water-cement ratio of concrete, age and method of curing on coefficient values and their interactions were investigated. Also observed were the variations of modulus of elasticity with the water-cement ratio of concrete, age and method of curing. Short-term steady state conditions of temperature were applied with changes affected by low temperature gradients.

One hundred and twenty-five slab specimens of 12 in. x 4 in. x 3 in. dimensions and thirty-six prism specimens of 12 in. x 3 in. x 3 in. dimensions were tested under temperatures between -100^0F (-73.5^0C) and $+150^0$F ($+65.5^0$C). The variables were method of curing (dry and wet), amount (0% to 5%) and position (symmetrical and unsymmetrical) of the longitudinal steel and the age of the specimens. The dry-cured specimens - slabs, cylinders and prisms - were kept in water (at 68^0F to 70^0F) for 7 days. Then they were taken out and stored in the laboratory (temperature 68^0F to 70^0F; 65% to 75% RH) until tested. The wet-cured specimens were kept in water (68 to 70^0F) until tested.

The one hundred and twenty-five slab specimens and thirty-six prism specimens were divided into eighteen series - nine (five dry-cured and four wet-cured) series were symmetrically reinforced and nine unsymmetrically reinforced. Except the fifth dry series (which was one year old) of both types of reinforcement, the dry and wet series were each tested at three different ages - 7, 28 and 84 days. Each series, irrespective of age, was tested over the full range of test temperatures. At each temperature increment thermal deformations and the dynamic modulus of elasticity of concrete were computed.

From the equilibrium of forces, moments and compatibility of strains, analytical expressions were developed for strains and thermal coefficients of linear expansion. Analytical and experimental results were compared. Curve-fitting and correlation programmes were used to analyze the experimental data.

1.3 EARLIER INVESTIGATIONS:

The information on the thermal properties of concrete and its aggregates is limited.

An early investigation of the thermal expansion of aggregates over the temperature range 35^0F to 135^0F was carried out by Callan (ref. 1). The coefficients of expansion of coarse aggregates varied from 1.9×10^{-6} in./in./^{0}F (for limestone) to 5.4×10^{-6} in./in./^{0}F (for quartzite). The fine aggregate mortars showed generally high values with 4.4×10^{-6} in./in./^{0}F for limestone (min.) and 7.0×10^{-6} in./in./^{0}F for siliceas (max.). The concrete combinations were tested for durability. No attempt was made to find the coefficients of expansion of the concrete combinations. The water-cement ratios of mortar and concrete specimens were kept constant at 0.49 and 0.51 respectively. They were cured for 7 days at 70^0F and 100% R.H.

Mitchell (ref. 2) reported tests on aggregates, neat cements and concretes at temperatures ranging from 10^0F to 70^0F. The aggregates were found to have varying coefficients of thermal expansion ranging from 1.1×10^{-6} in./in./^{0}F to 9.5×10^{-6} in./in./^{0}F. The thermal expansions of limestone, sandstone and many other rocks were significantly different for similar rocks from different sources. The coefficients for limestone aggregates ranged from 1.2 to 6.5×10^{-6} in./in./^{0}F. The thermal coefficients of expansion of neat cement were approximately the same for oven-dried ($\alpha = 6.4 \times 10^{-6}$ in./in./^{0}F for sample No. A59) and vacuum-saturated ($\alpha = 7 \times 10^{-6}$ in./in./^{0}F for A59) specimens but were considerably higher at intermediate moisture contents ($\alpha = 11.6 \times 10^{-6}$ in./in./^{0}F for A59). In the range of 80 to 90% saturation the coefficient increased as much as 100%. There was much less variation in concrete. The coefficient of expansion varied from 2.4 to 5.8×10^{-6} in./in./^{0}F for concrete with controlled aggregate minerals. The water-cement ratios varied between 0.21 to 0.35 for neat cement and were constant at 0.45 and 0.51 for mortar and concrete specimens respectively.

Saemann and Washa (ref. 3) conducted tests on the variations with temperature (-70^{0}F to 450^{0}F) of mortar and concrete properties (moisture content, compressive strength, tensile strength, transverse strength, stiffness, toughness and coefficient of thermal expansion). Two mortars and three concretes (w/c 0.48, 0.81 and 0.84) were used in the investigation. The mortar and concrete specimens were moist-cured at normal room temperature for 14 days, stored in air at 70^{0}F and 50% RH for 13 days and then held at test temperature for 24 hours before test. The thermal coefficients of expansion for mortars varied from 5.3×10^{-6} in./in./^{0}F (w/c 0.84) to 5.8×10^{-6} in./in./^{0}F (w/c 0.48) and those of concrete varied between 3.9×10^{-6} in./in./^{0}F and 4.4×10^{-6} in./in./^{0}F (w/c 0.48). The other properties generally increased with the decrease of temperature.

Tokuda and Ito (ref. 4) published results of experimental work on thermal diffusivity, conductivity and coefficients of expansion of concretes. The effects of mix-quantity of aggregates on the properties were the object of the investigation. The coefficients of expansion of concretes (w/c 0.42 constant; age 28 days) varied from 8.5×10^{-6} cm./cm./^{0}C (4.45×10^{-6} in./in./^{0}F) for an aggregate content* of 0.8 to 12×10^{-6} cm./cm./^{0}C (6.66×10^{-6} in./in./^{0}F) for an aggregate content of 0.4. Graywacke rock type aggregates were used.

Dettling (ref. 5) in 1964 published a compilation of the contents of various investigations on coefficients of expansion of concretes and aggregates. He also conducted tests on the variations of the coefficients of expansion due to the different chemical composition of cements and aggregates. The thermal coefficients of the aggregates varied widely. The coefficients of expansion of limestone and quartz aggregates were 5×10^{-6} cm./cm./^{0}C and 12×10^{-6} cm./cm./^{0}C respectively. The tests were limited to plain concrete and aggregates.

Monfore and Lentz (ref. 6) reported an investigation of compressive strengths, splitting strengths, modulus of elasticity and thermal contractions of three sand and gravel concretes (cement content 574 lbs./yd.^{3}) at various temperatures from 75^{0}F to -250^{0}F. They noted that the moisture present in the concrete influenced the above properties. The modulus of elasticity of moist concrete (cement content 517 lbs./yd.^{3};

---

* by Absolute Volume (m^3)

curing: 28 days in fog + 63 days sealed) increased from 5.5×10^6 psi. at 75^0F to 8.5×10^6 psi. at -250^0F. The air-cured concrete (cement content 517 lbs./yd.^{3}; curing: 28 days in fog + 40 days sealed + 80 days at 50% RH) increased from 5.0×10^6 psi. at 75^0F to 5.4×10^6 psi. at -250^0F. But the dry concrete (cement content 517 lbs/yd.^{3}; curing: 28 days in fog + 94 days sealed + 35 days at 50% RH + 10 days at 105^0C) did not show any change ($E = 4.3 \times 10^6$ psi.) over the temperature range. Similarly, the measured thermal contractions over the temperature range were $1,420 \times 10^{-6}$ in./in. ($\alpha = 4.4 \times 10^{-6}$ in./in./^{0}F), $1,280 \times 10^{-6}$ in./in. ($\alpha = 3.94 \times 10^{-6}$ in./in./^{0}F) and $1,240 \times 10^{-6}$ in./in. ($\alpha = 3.80 \times 10^{-6}$ in./in./^{0}F) for the moist, air-cured and dry concrete respectively.

Cran (ref. 7) was the first investigator who attempted to find experimentally the effects of reinforcement on bridge deck slabs under temperature change. Plain and reinforced concrete slabs were subjected to temperatures varying from -30^0F to 75^0F. He found that, while the compressive strength of concrete (2,400 psi. to 4,800 psi.) and percentage of steel reinforcement (0% to 5%) increased significantly, the coefficient of expansion of the reinforced concrete increased only modestly (6% to 9%). The modulus of elasticity increased by 2% (2 year old) to 17% (14 days air-cured).

Berwanger (ref. 8) presented theoretical expressions for strain and deformation of reinforced concrete slabs. His experimental investigation was based on Cran's (ref. 7) test data. He reported that the modulus of elasticity of concrete increased sharply below freezing temperatures. The rates of change in the modulus of elasticity of concrete (w/c 0.57; age 55 days) at above and below freezing points were 0.00016×10^6 and 0.00739×10^6 psi./^{0}F respectively. The rate of change below the freezing point decreased with age (0.0161×10^6 psi./^{0}F at 42 days; 0.0012×10^6 psi./^{0}F at 761 days). The coefficient of expansion of the concrete was greater for a smaller water-cement ratio ($\alpha_c = 5.49 \times 10^{-6}$ in./in./^{0}F for w/c 0.57; $\alpha_c = 4.94 \times 10^{-6}$ in./in./^{0}F for w/c 0.75). He concluded that, due to random variations in the test results, further testing would be required to establish the relationship more fully.

Cruz (ref. 9) subjected concrete made with 4 types of aggregates to elevated temperatures in order to determine the moduli of elasticity and shear. All tests were carried out at the age of 28 days and two ranges (4,000-4,500 psi. and 6,000-6,500 psi.) of design compressive strengths were considered. The test temperatures were 75^{0}F, 300^{0}F, 600^{0}F, 900^{0}F and 1,200^{0}F respectively. The moduli of elasticity of concrete decreased with the increase in temperature. The modulus of the concrete (4,000-4,500 psi.) made from Elgin sand and crushed limestone decreased from 5.35×10^{-6} in./in./^{0}F at 75^{0}F to 2.07×10^{-6} in./in./^{0}F at 1,200^{0}F.

Berdichevskii and Svirdov (ref. 10) reported tests on reinforced concrete members at low temperatures (20^{0}C to-50^{0}C; 68^{0}F to -58^{0}F). Properties investigated consisted of cube strength, bending strength, bond failure and static modulus of elasticity. The modulus of elasticity of the concrete (w/c 0.40 constant) increased from

404×10^3 kg./cm.^{2} (5.74×10^6 psi.) at 20°C (68°F) to 474×10^3 kg./cm.^{2} (6.73×10^6 psi.) at -50°C (-58°F).

Moskvin, Kapkin and Anatov (ref. 11) reported tests on concrete (w/c 0.43 constant) between temperatures of -10°C (14°F) and -60°C (-76°F). He investigated concrete strength and the modulus of elasticity of concrete. He reported the influence of the saturation* of water in the character changes of the specimens. The saturation of water depended upon the degree of temperature. The modulus of elasticity decreased with temperature in general. Samples with 6.5% to 8% water increased by 33% at -30°C (-22°F) and 41% at -50°C (-58°F).

Hansen and Erickson (ref. 12) presented results of an experimental investigation of the heating effects on the deflection of neat cement and mortar beams under load between 20°C (68°F) and 70°C (158°F). The modulus of elasticity decreased from 3.37×10^5 kg./cm.^{2} (4.8×10^6 psi.) at 20°C (68°F) to 2.81×10^5 kg./cm.^{2} (4.0×10^6 psi.) at 70°C (158°F). They concluded that a rapid increase in temperature permanently reduced the modulus of elasticity of cement mortar, indicating an internal deterioration of the material structure.

Berwanger (ref. 13) reported an analysis of the strains measured during the lowering of the bridge superstructure. A parallel shift in the strains occurred due to the thermal strains produced by temperature changes. The coefficient of expansion of concrete was assumed to be 4.9×10^{-6} in./in./°F.

Samelson and Tor (ref. 14) reported an investigation of underground reinforced concrete cylindrical tanks containing liquids, the

---

* water content in % by weight

temperatures of which varied from 50^0F to 500^0F as a function of time. Their effort was concentrated on stress under both straight line and transient temperature gradients. They assumed values of E_c (3×10^{-6} psi.) and α_c (5.5×10^{-6} in./in./^{0}F).

Fintel and Khan (ref. 15) recommended a design temperature for exposed concrete members. A graphical method was presented for a rapid and accurate determination of isotherms, gradients and average temperatures. The effects of bowing and length changes of partially exposed columns were discussed. The design values of coefficients of linear expansion, thermal conductivity and heat capacity of concrete were assumed.

Sadana and Verma (ref. 16) presented a method of analysis of reinforced concrete frames, taking into consideration the uniform temperature changes in the beams comprising a frame. Deformation properties of concrete were assumed ($\alpha_c = 6.5 \times 10^{-6}$ in./in./^{0}F) and emphasis was given on the stress analysis.

The early investigations (ref. 1, 2, 3) generally dealt with the coefficient of expansion of aggregates. The normal assumption made was that the concrete resulting would have the same coefficient of expansion as its aggregate. Mitchell (ref. 2) showed that this assumption was in error. Further efforts (ref. 4, 5) were made to determine the influence of the amount and composition of aggregates on the coefficient of expansion of concrete.

Monfore and Lentz (ref. 6) reported the effect of moisture on both the coefficient of expansion and the modulus of elasticity of concrete. Their findings were similar to those of Mitchell (ref. 2).

Later investigators (ref. 7, 8) extended the investigation to include the effect of the reinforcing steel on the coefficient of expansion of concrete at low temperatures. Due to random variations in test results Berwanger (ref. 8) suggested further testing.

Various investigations were reported on the variations of the modulus of elasticity of concrete (ref. 6-11) and cement mortar (ref. 12) with temperature. Most investigators (ref. 6, 7, 9-11) considered variation of the modulus of elasticity with the strength of the concrete. Berwanger (ref. 8) reported the effect of the water-cement ratio on the modulus of elasticity of concrete.

In the theoretical investigations (ref. 14-16) of thermal deformation and stress analysis, values of the coefficient of expansion and modulus of elasticity of concrete were often assumed.

In the test series reported here investigations of the coefficient of thermal expansion of plain and reinforced concrete and the modulus of elasticity of plain concrete were undertaken. The test temperatures varied from -100^0F to $+150^0$F. Other variables were the water-cement ratio (0.434 to 0.708), age (7, 28 and 84 days), method of curing (water and air-cured), amount (0% to 5%) of longitudinal steel and arrangement (symmetrical and unsymmetrical) of the reinforcing bars.

1.4 IMPORTANCE OF STUDY:

The stabilization of the concrete structure both thermally and volumetrically is of prime importance. The extensive use of concrete in various structures under temperature extremes especially warrants a knowledge of the temperature effects on the concretes used in conjunction with steel. For the purpose of design, analysis and prediction of behaviour of all structures from the building of lightweight concrete in which insulation is a major factor to large massive structures in which artificial temperature control is employed, the true thermal deformation of the reinforced concrete should be known. Many multistoried buildings have exposed columns subjected to seasonal temperature variation. The exposed exterior columns change in length relative to the interior columns, which remain unchanged in a controlled environment. Similar consideration must be given in accurately analyzing for temperature effects other exposed structures, such as continuous composite steel-concrete bridges.

While a few attempts have been made to find the general effects of temperature change on the physical and deformation properties of concrete, very little information is available as to the effects of the different variables (water-cement ratio, age, curing process and steel reinforcement) on such properties. An undertaking of a well-planned and detailed study to establish the trends of change of these properties in a more predictable form is sorely needed. This would facilitate the obtaining of significantly precise values of the properties for the purpose of design and analysis of structures under temperature change.

In most investigations of thermal stress problems assumed values of the coefficient of expansion and the modulus of elasticity of concrete were used. Therefore, they lack true deformation and consequently true stress consideration.

An attempt was made in this thesis to derive analytical expressions for strains and coefficients of expansion of reinforced concrete under temperature change. Experimental investigations of the coefficient of expansion and the modulus of elasticity were made. A number of factors may influence these properties - the temperature range, water-cement ratio, age, type of aggregate and the method of curing. Additional factors which may effect the coefficient of expansion of reinforced concrete slabs are the amount and position of the reinforcing steel. The influence of all of these variables, except type of aggregate, were studied in this investigation.

1.5 ACKNOWLEDGEMENTS:

The tests were performed in the Structures and Materials Behaviour Testing Laboratories of the Civil Engineering Department at the University of Ottawa. The writer expresses his sincere gratitude and appreciation to his supervisor, Professor Carl Berwanger, for suggesting the problem and for his guidance throughout the project. The research was funded through grants held by Professor Berwanger from the National Research Council of Canada. Funds were used to obtain equipment and materials and employ summer help.

Messrs. Dennis MacKinnon and Pierre Marion assisted with the experimental work and their help is sincerely acknowledged. Mention must also be made of the generous use allowed of the facilities of the Computing Centre at the University of Ottawa.

Finally, the writer wishes to thank his wife, Suzanne, who painstakingly typed the thesis and encouraged him throughout the entire project.

1.6 NOTATION:

Symbols are defined where they first appear in the thesis. In this section the symbols are arranged for convenient reference.

A_c = area of concrete section

A_s = area of steel reinforcement

b = width of specimen

c, c_1, c_2 = distances from the centroid of the section

d = distance of steel centroid from opposite face of section

D = 0.1035 L/bt for prism (dynamic-E)

e = eccentricity

E = Young's modulus of elasticity

E_c = Young's modulus of elasticity of concrete

E_{cd}, E_{cs} = dynamic and static modulus of elasticity of concrete respectively

E_R = longitudinal resonance modulus of elasticity

E_s = Young's modulus of elasticity of steel

f'_c = compressive strength of concrete for 6 in. x 12 in. cylinders

F, F_c, F_s = forces developed

I_c = moment of inertia of the concrete section of the slabs

L_i, L = length of specimen

n' = fundamental longitudinal frequency

t = depth of specimens

T, T_i, T_f = temperatures in ^0F

W = weight of prism specimen

w/c = water-cement ratio of concrete

$\bar{y}$ = location of the centroid of the concrete section referenced to the gross slab centroid

α = thermal coefficient of expansion

α_c = coefficient of expansion of concrete

$\alpha^s_{RC}, \alpha^u_{RC}$ = coefficients of expansion of symmetrically and unsymmetrically reinforced concrete

α_s = coefficient of expansion of steel

Δ = change of,

$\varepsilon_c, \varepsilon^u_{c_1}, \varepsilon^u_{c_2}$ = strains in concrete

$\varepsilon_s, \varepsilon^u_s$ = strains in steel

NOTE: sub '1' = Face 1
sub '2' = Face 2

In the case of unsymmetrically reinforced slabs, steel reinforcements are placed nearer Face 1.

CHAPTER 2

THEORY

2.1 TEMPERATURE-MODULUS OF ELASTICITY RELATIONSHIP:

Berwanger (ref. 8) pointed out that, as the temperature of a solid decreases, the material shrinks and the particles are subjected to stronger cohesive forces. A given external load causes a smaller strain at low than at high temperatures; that is, the material has a higher modulus at the low temperatures. This is illustrated in the variations of Young's modulus of elasticity with temperature (fig. 4.33) for steel (ref. 32). The slope is 0.00316×10^6 psi/^{0}F. Therefore it is expected that concrete undergoing temperature changes will show similar effects. The modulus of elasticity of concrete will increase with decreasing temperature. Other investigators (ref. 7, 9, 10, 11) reported similar behaviour.

There are further complications in the case of concrete due to free and absorbed moisture present. From their experiments with concretes of various moisture contents, Monfore and Lentz (ref. 6) found that, while all moist concrete increased somewhat in elastic modulus, concrete that had been oven-dried and sealed against moisture absorption during testing showed a constant concrete modulus over a wide range of temperatures (75^0F to -250^0F or 23^0C to -157^0C). The increase in the concrete modulus is directly related to the moisture present in the concrete, with the saturated concrete having the largest increase (50%).

The amount of moisture available depends upon the water-cement ratio of the concrete, age and curing. With a lower water-cement ratio, increasing age and dry curing, the available moisture content will decrease. Thus it is expected that concrete with a high water-cement ratio will have a greater change in modulus of elasticity. Similarly, concrete of the same water-cement ratio at a greater age will have a smaller rate of change in modulus of elasticity.

2.2 TEMPERATURE-COEFFICIENT OF EXPANSION RELATIONSHIP:

Mitchell (ref. 2) found that there were significantly higher coefficients of expansion for the concrete (min. 3.2×10^{-6} in./in./^{0}F for limestone) as compared to the aggregates (min. 2.0×10^{-6} in./in./^{0}F for limestone) used in the concrete. The difference appeared to be directly related to the moisture content of the specimens.

Verbeck and Kleiger (ref. 17) and Berwanger (ref. 8) reported that a linear relationship existed between temperature and concrete strains down to the freezing point of water. Below this freezing point the strains were found to be smaller.

As the temperature of concrete is decreased below 32^0F, the amount of water which is frozen progressively increases. There are two opposing effects at these temperatures; ice that has been formed contracts with further cooling but the additional ice formed during this further cooling causes further expansion.

1. Effect of Water Content:

The amount of water freezing at a particular instant depends upon the total amount of moisture available. This again is dependent on any one or all of the following criteria:

(a) Water-Cement Ratio:

Verbeck and Kleiger (ref. 17) reported an increase in the water frozen with an increase in the water-cement ratio. The concrete with a higher water-cement ratio will have more water available to be frozen at any time than a concrete with a lower water-cement ratio when both the concretes have been cast at the same time and have undergone similar curing processes.

(b) Age:

As the hydration process continues, more and more water is used up in the chemical reaction. Therefore, the amount of available water which may freeze at sub-freezing temperatures decreases with time, with the curing process remaining unaltered.

(c) Type of Curing:

The amount of moisture present in the concrete will depend on the curing conditions. Specimens of the same concrete cured in dry air and in water will have different amounts of available moisture. Since the coefficients of expansion of concrete vary with moisture content (ref. 2), the curing process will have a definite influence on the coefficient of expansion of the concrete.

2. Effect of Reinforcement:

The coefficient of expansion of reinforcing steel ($\alpha_s = 6.5 \times 10^{-6}$ in./in./^{0}F between 45^{0}F and 200^{0}F; ref. 18) is greater than that of concrete ($\alpha_c = 4.25 \times 10^{-6}$ in./in./^{0}F for water-cement ratio = 0.41 and age = 200 days; ref. 8). For a reinforced concrete slab undergoing temperature change, the unrestrained strain and deformation produced in steel will be considerably greater than those of concrete. These deformations become altered satisfying the compatibility condition of linear deformations. Consequently, the strain and coefficient of expansion of concrete will be affected. The extent of this effect will depend upon the arrangement and amount of reinforcement (equations 11, 12, 21, 23 and 24).

2.3 BASIC ASSUMPTIONS:

The following are the basic assumptions used by the author to develop the analytical expressions for coefficients of expansion, strains and deformations in reinforced concrete sections subjected to thermal ambient change.

(a) Concrete Strain Distribution: The Bernoulli-Navier hypothesis of plane section remaining plane after bending has been extended to the sections under thermal ambient change.

(b) Stress-Strain Relationship of Concrete: Since the effect of temperature change over the range produces small deformations, a linear stress-strain relationship of concrete is assumed.

(c) Bond between Concrete and Reinforcing Steel: It is assumed that there was no slip between concrete and reinforcing steel as the stresses and strains are low (ref. 27).

(d) The coefficient of expansion of steel is taken normally to be higher than that of plain concrete. This is in fair agreement with the findings of previous investigations (ref. 8).

(e) It is assumed that concrete behaves as a homogeneous mass under low stress.

(f) The curvature produced under temperature changes in sections with unsymmetrical reinforcing steel is neglected as small, considering the small gauge length.

(g) Short-term steady state conditions of temperatures have been considered.

2.4 DEVELOPMENT OF ANALYTICAL EXPRESSIONS FOR LINEAR EXPANSION OF REINFORCED CONCRETE:

(a) Symmetrically Reinforced:

The slab in fig. 2.1 is subjected to a temperature increase. If the concrete and the steel were both allowed to expand independently of each other, the temperature change would produce a change in length in the concrete:

$$\Delta L_c = \alpha_c \cdot (T_f - T_i) \cdot L_i = \alpha_c \cdot \Delta T \cdot L_i \qquad \text{......(1)}$$

and in steel:

$$\Delta L_s = \alpha_s \cdot (T_f - T_i) \cdot L_i = \alpha_s \cdot \Delta T \cdot L_i \qquad \text{......(2)}$$

Where T_i, T_f = inital and final temperature in ^{0}F

L_i = initial length of slab in inches

α_c, α_s = coefficient of expansion of concrete and steel in in./in./^{0}F

$\alpha_s > \alpha_c$ therefore, $\Delta L_s > \Delta L_c$

For compatibility of linear deformations of the slab, equal and opposite forces F_c (in concrete) and F_s (in steel) will be produced.

The deformations produced are:

in concrete:

$$L_i \cdot \varepsilon_c = \Delta L_{RC} - \Delta L_c \qquad \ldots\ldots(3)$$

and in steel:

$$L_i \cdot \varepsilon_s = \Delta L_s - \Delta L_{RC} \qquad \ldots\ldots(4)$$

Where ε_c, ε_s = unit strains in concrete and steel respectively

and ΔL_{RC}, the deformation of reinforced slab

is given by:

$$\Delta L_{RC} = \alpha^s_{RC} \cdot \Delta T \cdot L_i \qquad \ldots\ldots(5)$$

Where α^s_{RC} = coefficient of expansion of symmetrically reinforced concrete in in./in./^{0}F

Therefore from equations (3) and (4):

$$\Delta L_{RC} = L_i \cdot \varepsilon_c + \Delta L_c = \Delta L_s - L_i \cdot \varepsilon_s \qquad \ldots\ldots(6)$$

Considering small deformations

in concrete:

$$L_i \cdot \varepsilon_c = \frac{F \cdot L_i}{A_c \cdot E_c} \qquad \ldots\ldots(7)$$

in steel:

$$L_i \cdot \varepsilon_s = \frac{F \cdot L_i}{A_s \cdot E_s} \qquad \text{......(8)}$$

Where $\quad F_c = F_s = F$ for equilibrium

A_c, A_s = net area of concrete and steel respectively in in.^{2}

E_c, E_s = modulus of elasticity of concrete and steel respectively in psi.

Substituting in equation (6):

$$\Delta L_{RC} = \alpha_c \cdot \Delta T \cdot L_i + \frac{F \cdot L_i}{A_c \cdot E_c} = \alpha_s \cdot \Delta T \cdot L_i - \frac{F \cdot L_i}{A_s \cdot E_s} \quad \text{..(9)}$$

and rearranging:

$$(\alpha_s - \alpha_c) \cdot L_i \cdot \Delta T = F \cdot L_i \left[\frac{1}{A_s \cdot E_s} + \frac{1}{A_c \cdot E_c}\right]$$

$$\text{or} \quad F = \frac{\Delta T \cdot (\alpha_s - \alpha_c)}{\left[\frac{1}{A_s \cdot E_s} + \frac{1}{A_c \cdot E_c}\right]} \qquad \text{.....(10)}$$

From equations (5) and (9) substituting values of F and dividing by $\Delta T \cdot L_i$:

$$\alpha^S_{RC} = \alpha_c + \frac{(\alpha_s - \alpha_c)}{\left[\frac{A_c \cdot E_c}{A_s \cdot E_s} + 1\right]} = \alpha_s - \frac{(\alpha_s - \alpha_c)}{\left[1 + \frac{A_s \cdot E_s}{A_c \cdot E_c}\right]} \qquad \text{.....(11)}$$

and the unit deformation of the slab is:

$$\varepsilon_{RC} = \Delta T \cdot \left[\alpha_c + \frac{(\alpha_s - \alpha_c)}{\left[\frac{A_c \cdot E_c}{A_s \cdot E_s} + 1\right]}\right] = \Delta T \cdot \left[\alpha_s - \frac{(\alpha_s - \alpha_c)}{\left[1 + \frac{A_s \cdot E_s}{A_c \cdot E_c}\right]}\right] \quad \ldots(12)$$

E_c, E_s, α_c and α_s are temperature dependent.

(b) Unsymmetrically Reinforced:

The analysis of deformation behaviour and the derivation of analytical expressions of unsymmetrically reinforced slabs follow procedures similar to those of the symmetrically reinforced slabs. Slabs with reinforcement in a single layer are considered (fig. 2.2).

The unrestrained temperature deformation of the concrete is:

$$\Delta L_c = \alpha_c \cdot \Delta T \cdot L_i$$

and of steel:

$$\Delta L_s = \alpha_s \cdot \Delta T \cdot L_i$$

$$\Delta L_s > \Delta L_c \qquad \text{since} \qquad \alpha_s > \alpha_c$$

For compatibility of deformation, interaction of the two slab materials will produce slab deformation in the steel:

$$\Delta L^u_{RC} = \Delta L_s - L_i \cdot \varepsilon_s = \alpha_s \cdot \Delta T \cdot L_i - \frac{F \cdot L_i}{A_s \cdot E_s} \quad \ldots\ldots(13)$$

Where F is the force developed in steel. This force will transfer an equal but opposite force in concrete which is eccentric to the centroid of the concrete section.

The location of the centroid of the concrete section can be determined. Taking moment about the gross slab centroid (fig. 2.2):

$$(b.t - A_s) \;.\; \bar{y} = A_s \;.\; (d - \frac{t}{2})$$

Therefore:

$$\bar{y} = A_s . \frac{(d - \frac{t}{2})}{(b.t - A_s)} \qquad ......(14)$$

Where A_s = area of reinforcing steel in tension in in.^{2}

b = width of section in in.

t = total depth of slab in in.

d = effective depth of reinforced concrete slab in in.

$\bar{y}$ = location of the centroid of the concrete section referenced to the gross slab centroid.

Therefore, the eccentricity of the force acting on concrete section is:

$$e = (d - \frac{t}{2} + \bar{y}) \qquad ......(15)$$

The concrete section properties are:

Area: $A_c = (b.t - A_s)$

and moment of inertia:

$$I_c = (\frac{b.t^3}{12} + b.t \;.\; \bar{y}^2 - A_s \;.\; e^2) \qquad ......(16)$$

Therefore the slab deformation at steel centroid is:

$$\Delta L^u{}_{RC} = \Delta L_c + \varepsilon_c \cdot L_i = \alpha_c \cdot L_i \cdot \Delta T + \frac{F \cdot L_i}{A_c \cdot E_c} + \frac{F \cdot L_i \cdot e^2}{E_c \cdot I_c}$$

$$= \alpha_c \cdot L_i \cdot \Delta T + F \cdot L_i \left[\frac{1}{A_c \cdot E_c} + \frac{e^2}{E_c \cdot E_c}\right] \quad \ldots\ldots(17)$$

From equations (13) and (17):

$$\Delta L^u{}_{RC} = \alpha_s \cdot \Delta T \cdot L_i - \frac{F \cdot L_i}{A_s \cdot E_s}$$

$$= \alpha_c \cdot L_i \cdot \Delta T + F \cdot L_i \left[\frac{1}{A_c \cdot E_c} + \frac{e^2}{E_c \cdot E_c}\right] \quad \ldots\ldots(18)$$

Dividing by L_i and rearranging:

$$F \left[\frac{1}{A_c \cdot E_c} + \frac{e^2}{E_c \cdot I_c} + \frac{1}{A_s \cdot E_s}\right] = (\alpha_s - \alpha_c) \cdot \Delta T$$

or

$$F = \frac{(\alpha_s - \alpha_c) \cdot \Delta T}{\left[\frac{1}{A_c \cdot E_c} + \frac{e^2}{E_c \cdot I_c} + \frac{1}{A_s \cdot E_s}\right]} \quad \ldots\ldots(19)$$

This value of F can be substituted back into equation (18).

The generalized expression for deformation of the unsymmetrically reinforced concrete slab can be shown to be:

$$\Delta L^u{}_{RC} = \alpha_c \cdot L_i \cdot \Delta T + F \cdot L_i \left[\frac{1}{A_c \cdot E_c} + \frac{e \cdot c}{E_c \cdot I_c}\right]$$

$$= \alpha_c \cdot L_i \cdot \Delta T + \frac{(\alpha_s - \alpha_c) \cdot \Delta T \cdot L_i}{\left[\frac{1}{A_c \cdot E_c} + \frac{e^2}{E_c \cdot I_c} + \frac{1}{A_s \cdot E_s}\right]} \cdot \left[\frac{1}{A_c \cdot E_c} + \frac{e \cdot c}{E_c \cdot I_c}\right]$$

$$= L_i \cdot \Delta T \quad \alpha_c + \frac{(\alpha_s - \alpha_c) \cdot \left[\frac{1}{A_c \cdot E_c} + \frac{e \cdot c}{E_c \cdot I_c}\right]}{\left[\frac{1}{A_c \cdot E_c} + \frac{e^2}{E_c \cdot I_c} + \frac{1}{A_s \cdot E_s}\right]} \quad \ldots\ldots(20)$$

Where c = distance from the neutral axis.

Since:

$$\alpha^u_{RC} = \frac{\Delta L^u_{RC}}{\Delta T \cdot L_i}$$

Therefore:

$$\alpha^u_{RC} = \alpha_c + \frac{(\alpha_s - \alpha_c) \cdot \left[\frac{1}{A_c \cdot E_c} + \frac{e \cdot c}{E_c \cdot I_c}\right]}{\left[\frac{1}{A_c \cdot E_c} + \frac{e^2}{E_c \cdot I_c} + \frac{1}{A_s \cdot E_s}\right]} \quad \ldots\ldots(21)$$

Where α^u_{RC} = coefficient of expansion of unsymmetrically reinforced concrete slab;

and the strain expressions become:

for steel:

$$\varepsilon^u_s = \alpha_s \cdot \Delta T - \frac{F}{A_s \cdot E_s}$$

$$= \alpha_s \cdot \Delta T - \frac{(\alpha_s - \alpha_c) \cdot \Delta T}{A_s \cdot E_s \left[\frac{1}{A_c \cdot E_c} + \frac{e^2}{E_c \cdot I_c} + \frac{1}{A_s \cdot E_s}\right]} \quad \ldots\ldots(22)$$

and for the concrete slab:

at face 1 (near the steel reinforcement):

$$\varepsilon^u_{c_1} = \Delta T \left[\alpha_c + \frac{(\alpha_s - \alpha_c) \cdot \left[\frac{1}{A_c \cdot E_c} + \frac{e \cdot c_1}{E_c \cdot I_c}\right]}{\left[\frac{1}{A_c \cdot E_c} + \frac{e^2}{E_c \cdot I_c} + \frac{1}{A_s \cdot E_s}\right]} \right] \quad \ldots\ldots(23)$$

where $c_1 = \frac{t}{2} + \bar{y}$

at face 2 (away from the steel reinforcement):

$$\varepsilon^u_{c_2} = \Delta T \left[\alpha_c + \frac{(\alpha_s - \alpha_c) \cdot \left[\frac{1}{A_c \cdot E_c} - \frac{e \cdot c_2}{E_c \cdot I_c} \right]}{\left[\frac{1}{A_c \cdot E_c} + \frac{e^2}{E_c \cdot I_c} + \frac{1}{A_s \cdot E_s} \right]} \right] \qquad \ldots\ldots(24)$$

where $c_2 = \frac{t}{2} - \bar{y}$

2.5 SCOPE OF ANALYTICAL EXPRESSIONS:

The analytical expressions (equations 12, 23 and 24) developed in this chapter enable accurate computations of strain and deformation of reinforced concrete structural members. Apart from the geometry of the section, the temperature range and the length of the structure, the factors which affect the computation are the coefficient of expansion and the modulus of elasticity of concrete and steel bar. These properties of concrete are influenced by the type of aggregate used, water-cement ratio, method of curing and age. By carefully controlling these factors the properties (E_c and α_c) of concrete can be varied to keep the strains and deformations of the structures within specified limits.

From the analytical expressions (equations 12, 23 and 24), it is quite evident that the amount and arrangement of the reinforcing steel influence significantly the strain of the slab. The strain increases with the percentage of steel. For unsymmetrically reinforced slabs the strains produced at the face near the steel bars are considerably high. The amount and arrangement of steel reinforcement can be controlled to keep the strain and consequently the deformation of the structure within specified limits.

Many investigators (ref. 14-16) used assumed values of the coefficient of expansion of plain and reinforced concrete. Therefore, their studies lack true deformation and consequently true stress consideration. For future investigation of thermal stress problems, useful values of the coefficient of thermal expansion of reinforced concrete can be obtained by using the analytical expressions (equations 11 and 21) in this thesis.

CHAPTER 3

MATERIALS, FABRICATION AND TESTING

3.1 MATERIALS

(i) Cement:

ASTM designated (ASTM C 150-71) 'Type-1' portland cement (commercial brand - 'Lake Ontario') was used for all slab specimens, control cylinders and prism specimens.

(ii) Fine and Coarse Aggregates:

The fine* and coarse** aggregates used were produced locally and satisfied the ASTM specifications (ASTM C 33-71). The aggregates had been sieved and stored in different bins according to size (sieve size ASTM C 33-71). The petrographic analysis of the aggregates, which was done at the University of Ottawa, Geology Department, is presented in table 3.1.

Both fine and coarse aggregates had been proportioned (according to ASTM C 33-71 specifications) to give the best concrete mix. The sampling percentages of fine and coarse aggregates are given in table 3.2. For fine aggregates the fineness modulus is 2.7. The aggregates had been sieved and recombined in the laboratory in proportions (fig. 3.1) so as to fall in the middle of the ASTM limit (C 33-71) (ref. 22). The maximum size of coarse aggregates used was $\frac{3}{4}$ in., as dictated by the size of the test specimens and clearance requirement of the reinforcing bars.

(iii) Concrete Mixes:

The concrete mixes were designed and chosen to represent

---

* silica sand
** gravel (limestone)

the normal range of mixes used in the construction field. A total of six different concrete mixes was used. The water-cement ratio of the mixes varied from 0.434 to 0.708 with designed 28-day strength varying from 3,000 psi. to 7,000 psi. Table 3.3 and fig. 3.2 show the characteristics of the mixes. The mixes were designed in consultation with the Portland Cement Association Engineering Bulletin (ref. 23).

(iv) Reinforcing Steel:

The reinforcing steel used was U.S.S. deformed steel wire for concrete reinforcement conforming to the ASTM standard specifications for ASTM designate A 496-64 (ref. 24). Eight different sizes of wires were used for reinforcing (table 3.4).

3.2 METHODS OF FABRICATION:

(i) Types of Specimens:

(a) Slab Specimens: A total of one hundred and twenty-five 12 in. x 4 in. x 3 in. slab specimens were made for experimental investigations of deformations. The slabs had varying amounts (0% to 5%) of reinforcement and were made from concrete using different (0.434 to 0.708) water-cement ratios. They were divided into a total of eighteen groups - seventeen groups of seven each and one group of six. Nine of these eighteen groups were symmetrically reinforced. The rest were unsymmetrically reinforced. Out of each of these nine groups (both symmetrical and unsymmetrical) four were wet-cured and five were dry-cured. The amount of longitudinal reinforcement in the slabs of each group varied from 0% to 5% (table 3.5). Table 3.6 shows the designation and characteristics of the different series. Table 3.7 gives the actual number of specimens representing the different variables.

An investigation was carried out on both wet and dry-cured specimens and for both symmetric and unsymmetric reinforcements. The length of the specimens was fixed at 12 in., which enabled the use of a gauge length of 10 in. The 3 in. x 4 in. cross-section allowed for the varying of the steel percentage from 0% to 5% in steps of 1%.

(b) Prism Specimens: Along with each series two prism specimens of 12 in. x 3 in. x 3 in. were also cast. They fitted the special benches prepared specifically to measure the dynamic-E using an SCT-5 machine (plate 3.1). A total of thirty-six prisms was cast.

(ii) Reinforcing, Casting and Curing:

Moulds (plate 3.2) had been specifically designed to be used for 12 in. x 4 in. x 3 in. or 12 in. x 4 in. x 4 in. slab specimens. The end plates of the moulds had small grooves to hold the reinforcing bars during casting. After inserting the reinforcing bars in these grooves, they were held in the centre of the grooves by tiny styrofoam pads. Each mould was used to cast two specimens at a time. Two series, the wet and dry of identical reinforcement, were cast from the same batch of concrete.

A special mould was also prepared for the 12 in. x 3 in. x 3 in. prism specimens. Four prism specimens, two for each series (wet and dry), were cast at the same time along with the slab specimens.

All casting was done in the material behaviour laboratory of the Civil Engineering Department at the University of Ottawa. The casting was done in the shade under normal temperature (68^0F) and humidity (65% to 75% RH). The whole process of casting took approximately 50-60 minutes. The mixing of the concrete was done by using a 3.6 cu. ft. capacity mixer (EIRICH model, type EA-2), capable of 10 to 11 revolutions per minute. All aggregates had been well mixed dry in the mixer, the exact amount of water added and mixing had continued for approximately 2 to 3 minutes. All moulds had been well cleaned and oiled before the casting. The reinforcing bars were kept away from the oil. The three thermocouples (plate 3.3) in each series were inserted in the slab specimens with 0%, 2% and 5% steel. All the specimens were cast in a horizontal position to avoid differential quality of concrete along the length of the specimens. During casting the concrete was consolidated by means of an electrically-driven pencil vibrator (plate 3.4).

Two series, one wet and one dry, i.e. a total of fourteen slab specimens and four prism specimens, were cast in one day. Along with the specimens five control cylinders (6 in. by 12 in.) were cast for each series.

After the casting was completed, the top surfaces of the slab and prism specimens and control cylinders were finished with wooden and steel trowels (plate 3.5).

Immediately after the completion of casting and finishing, the specimens and cylinders were covered with wet burlap and stored in the laboratory for approximately 16 hours. The moulds were then removed. All specimens and cylinders were marked as to the reinforcement type and percentage, curing type specified and date of casting. Both the series (slab and prism specimens and cylinders) were kept immersed in water at temperatures of 68^0 - 70^0F for 7 days. After that the dry series was taken out and kept on a rack inside the laboratory at room temperature. The wet series was kept in the water except during testing time.

The laboratory temperature varied between 68^0F to 72^0F and the relative humidity varied between 65% to 75%.

3.3 EQUIPMENT:

(i) Temperature Measuring Devices:

A Honeywell potentiometer was used to make temperature measurements with the thermocouples. Model number 2736 reads temperature directly from -100^0F to $+200^0$F (accuracy $\pm 0.5^0$F). For better accuracy model 2736 was equipped with a Honeywell Guarded Null Detector model 3970. Plate 3.6 shows the potentiometer. Temperatures read by the potentiometer were checked by the temperatures recorded by a thermometer placed inside and from those indicated by the recorder panel of the Honeywell Control (plate 3.7) mounted on the environmental chamber. Table 4.1 shows the typical temperature data taken in the course of testing.

(ii) Environmental Chamber:

For the purpose of testing the specimens a specially designed Controlled Environmental Chamber (plate 3.8) was used. It was manufactured by the Webber Manufacturing Company (model 43.5, -100 +200). A description of the functioning of the chamber is given below.

The chamber operates through input controllers (Honeywell model 15201316-01-01-2-239-024-00-168 with a range of -100^{0}F to $+200^{0}$F; plate 3.7), motor-driven cycling devices which modulate the cooling and heating capacities. They can be set to select the percentage of a 30-second cycle, during which time the cooling and heating phases are energized. The refrigeration system consists of a high stage and a low stage system which are equipped with discharge pressure switches. The low stage system has a reverse acting pressure control. This switch functions as a control for the high stage unit and is actuated by the discharge pressure of the lower unit. A fan circulates air within the chamber to avoid stratification and to maintain accuracy of temperature.

(iii) Electrodynamic Material Tester:

An SCT-5 type Electrodynamic Material Tester, manufactured by M. Falk & Co., England, was used to determine the dynamic modulus of elasticity of concrete from prism specimens. Shown in plate 3.1, the SCT-5 is a convenient laboratory instrument for measuring the resonant frequency of regularly shaped materials. It is composed of an accurately calibrated oscillator which is coupled to a vibrator for excitation of the specimen, and an amplifier feeding a meter which measures voltage proportional to amplitude from the crystal pick-up in contact with the vibrating specimen. When determining the modulus of elasticity of the prism, vibrations of various frequencies are transmitted to the prism by turning the oscillator dial. The frequency which causes a maximum deflection on the amplitude meter is the resonant or natural frequency. This meter reading is converted into its corresponding frequency by means of a chart supplied by the manufacturers (ref. 25). The dynamic modulus of the concrete prism can be readily obtained according to the ASTM Designation C 215-60 (ref. 22).

The longitudinal resonance modulus of elasticity may be calculated as follows:

$$E_R = DW(n')^2$$

Where:

E_R = longitudinal resonance modulus of elasticity (psi)

W = weight of specimen in lb.

n' = fundamental longitudinal frequency in cps.

$D = 0.1035 \frac{L}{bt}$ for prism in sec^2/sq. in.

L = length of specimen in in.

b, t = dimensions of cross-section of prism in in.

(iv) Cylinder Testing Machine:

A cylinder testing machine (Forny - QC-150-DR) was used for compression and deformation tests of the control cylinders. This apparatus is an electrically operated hydraulic press-type testing machine. Loads are applied by the pressure developed within the hydraulic cylinder. The machine has a capacity of 300,000 lbs. with a minimum gradation of 50 lbs. The testing of a typical cylinder is shown in plate 3.9.

(v) Strain Measuring Devices:

(a) Optical Extensometer: Along the centre line of the slab specimens, deformation measurements were taken at both faces. Considering the 4 in. width of the specimens, it was decided to put one pair of cross hairs in each face. The different equipment used for measuring deformations of the specimens is shown in fig. 3.3. A description of the various components is given below.

A special optical extensometer (plate 3.10) was used to measure strain on the face of the specimens. The particular type used was an SPL Extensometer, manufactured by Gaertner Scientific Corporation.

The extensometer is designed for precision measurement along a vertical line. It consists of two microscopes mounted on an invar bar, which, because of its low coefficient of thermal expansion, retains accuracy of measurement during wide ranges of temperature. The microscopes are capable of travelling on the invar bar independent of each other through a separation of 2 in. to 12 in. A fine motion control can move both the microscopes simultaneously through a one inch range of vertical travel. The 50X microscopes are equipped with calibrated filar micrometer eyepieces capable of measuring to 0.000002 inches. A 16 in. relay bar system is used to extend the mechanical working distance of the scopes to approximately 15.5 in.

This assembly is rigidly mounted on a 4 in. x 6 in. range coordinate motion carriage, which has divided drums to control its movement. One division of the divided drums of the carriage equals 0.001 in. carriage travel. The longitudinal motion travel is 6 in., while the transverse motion is 3 in. The carriage travels on a meehanite cast precision lathe bed type optical bench through a horizontal range of 7.5 ft. Two optical bench assemblies were placed, one on each side of the chamber, to avoid the transferring and re-levelling of the bench from one side to another.

Advance wires of 0.001 in. in diameter were used to mark the targets on both faces of the slab specimens. The sizes of the wires for targets were chosen in accordance with the lowest count of the microscopes, which was 0.000002 in.

The positions for the targets were marked on the specimens. The markings and approximately a one inch square area around them were properly cleaned and a coat of white Gage Kote #1 (made by Wm. T. Beans Inc., Detroit, Michigan; temperature range: -320^0F to $+850^0$F) was then painted over the area to increase the visibility and thereby facilitate the focusing of the microscopes on the targets. When the paint dried, the targets were temporarily fixed over the markings on the specimens by means of cloth tapes. Finally they were firmly fixed in place using Armstrong A-2 adhesive with Activator type A and the cloth tape was then removed. This particular type of adhesive was found to be excellent during temperature changes and kept the targets in position over the test temperature range.

(b) Transducers: In addition to the optical extensometer, displacement transducers (model 7CDT-100 by Hewlett Packard) were used to measure deformations on two specimens in each series, mainly the two without any reinforcement.

A DCDT consists of a coil assembly and a core (plate 3.11). The coil assembly is comprised of a differential transformer coil, a DC-excited solid state oscillator and a phase-sensitive demodulator. When the core is displaced linearly along the axis of the bore of the coil assembly, a voltage charge proportional to displacement occurs in the output; actually, the oscillator converts the DC input to AC, which excites the primary winding, whereas the actual core position fixes the amount of voltage induced in secondary windings. Each of the two secondary circuits contains a secondary winding, a full wave bridge and an RC filter. These secondary circuits are connected in series so that the resultant output is a DC voltage proportional to the core displacement from the electrical centre.

The input of the DCDT's consisted of, in series, a DC power supply unit (Harrison 6204B; table 3.8), mercuty pots as the switching panel and a variable differential transformer. The DCDT's were connected through a switching unit (BLH model 220), voltage to frequency converter (model 2212 A) and finally a frequency counter (model 5212 A). A schematic diagram of deformation measurement using DCDT's is shown in fig. 3.4. Plate 3.12 shows the input and output devices for the DCDT's.

(c) Error Check: To check the errors in the optical extensometer readings due to frequent handling and moving, two specimens (plate 3.13) made from aluminium plates of known characteristics (table 3.9) were used. The DCDT's, as well as targets for the extensometer, were mounted on the aluminium specimens to measure deformation. Therefore, at every stage of testing any discrepancy from the known value could easily be detected and accordingly corrected in the slab specimen readings.

3.4 TEST PROCEDURES:

The two identically reinforced dry and wet series cast from the same concrete (same water-cement ratio) were tested together. Approximately 20 hours prior to the test time the wet specimens (slabs, prisms and cylinders) were taken out of the water and air-dried in the laboratory (temperature 68^0 - 70^0F; 65 - 75% RH). During this time specimens (both wet and dry) were prepared for testing purposes.

Two specially made racks were placed inside the environmental chamber (plate 3.14). Each rack had four shelves. Two SCT-5 sonic testing benches were placed on the two top shelves. The third shelf was made up of a steel plate on which were marked the positions for the slab specimens and the aluminium specimens. When placed in position, the specimen faces were within focusing range of the microscopes mounted on both sides on the coordinate motion carriage resting on the optical bench. The fourth and lowest shelf was used to hold the cylinders during testing.

(i) Slab Specimens:

Before the specimens were put in the chamber they were prepared for testing. First, the two central vertical axes on the two faces were marked. The positions of the targets were marked one inch away from each end, and the distance between was checked by a 10 in. long invar scale pointer. On one face the positions of the aluminium blocks for the DCDT's were marked longitudinally 2 in. on each side from the centre, giving a gauge length of 4 in. This gauge length was used for the purpose of keeping free the line of vision of the extensometer focusing on the two targets on the same face. After marking, the targets and the DCDT's were positioned and fixed in place by Armstrong A-2 adhesive. The specimens were then transferred to the environmental chamber and placed in their previously marked positions on the steel shelf. They were supported underneath by means of very thin metal sheets to make the specimen faces perpendicular to the line of vision of the extensometer. The thermocouple wires and the DCDT's were connected and the lead wires were brought out of the chamber and connected with the appropriate reading instruments.

(ii) Prism Specimens:

For each series of seven slab specimens two prism specimens were cast to determine the dynamic modulus of elasticity. The prisms were 3 in. x 3 in. x 12 in. in dimension. First, the central point of the two ends and a centrally located transverse strip of 1 in. were marked on the prisms; then their individual weights were recorded. Each specimen was mounted on a sonic bench in such a manner that it was centred on the bridge and that both the transmitter and receiver of sonic waves were lightly but constantly touching the central points of the two ends. The SCT-5 electrodynamic material tester apparatus was kept outside the environmental chamber, while the benches were kept inside. This permitted the determination of dynamic modulus values at the various temperatures (-100^0F to $+150^0$F) without disturbing the inside conditions of the chamber. The leads from the benches were then taken out of the chamber through a small hole and connected with the electrodynameter.

Once all adjustments were made and all electrical and sonic connections were checked, the chamber was sealed and the testing begun. A set of initial readings were taken at room temperature. Then the chamber was put into operation. The temperature set pointer was moved to give the desired increments of temperature, and the percentage of cooling and heating was regulated. When the indicator showed that the chamber had reached the desired temperature, the heating and cooling percentage was again regulated and the temperature inside the specimens was checked from time to time until the temperature inside the chamber and inside the specimens was constant. Then another increment of temperature was applied and the process continued for the whole test range of temperature. At each steady state (15^0F interval), deformation, resonant frequency and temperature readings were taken.

(iii) Control Cylinders:

Along with seven slab and two prism specimens, five control cylinders were also cast for each series in order to determine the ultimate concrete strength and the static modulus of elasticity at the test ages (7, 28 and 84 days). All cylinders were subjected to deformation tests. Before testing the cylinders were capped with a standard sulphur compound. For the deformation tests a special steel frame with gauges of 9 in. in length was mounted on the cylinder. The cylinder was put on the loading table and properly centred. This was done by placing a small load on the cylinder and noting the deformation of the two gauges. Once properly positioned, each cylinder was loaded up to 65,000 lbs. in increments of 5,000 lbs. and the deformation of the two gauges was recorded at each increment. The load was then brought down to zero at 5,000 lb. intervals and similar deformation readings were taken. Then the gauges were dismounted and the cylinder was loaded to failure, recording the ultimate load. Data from sonic tests and deformation and compression tests were the input into computer programmes to calculate the dynamic and static modulii of elasticity of concrete.

CHAPTER 4

PRESENTATION OF TEST RESULTS

The test results obtained from the experimental investigations and analytical work are presented in this chapter in concise form. In view of the volume of data involved, it was not considered necessary to record here each reading taken; instead, important data are supplied in the form of tables, graphs and photographic plates. Typical test results are shown in tables 4.1 to 4.6.

4.1 STRESS-STRAIN RELATIONSHIP OF CONCRETE:

(i) Static Tests:

For each series of seven slab specimens and two prism specimens, five 12 in. x 6 in. concrete cylinders were cast, cured and subjected to the same conditions of temperature as those of the test specimens themselves. At each age two deformation and compression tests were carried out on the concrete cylinders. From the load deformation readings the initial tangent modulus of elasticity, E_c, was computed by means of a computer programme (prog. B - appendix D). This programme fitted the experimental points to a straight line by the least square method. The stress-strain curves were plotted in graphical form in figures 4.1 to 4.17. The ultimate cylinder strengths, f'_c, were calculated from the ultimate loads attained in the compression tests. Table 4.7 gives a typical calculation of static compression-deformation tests.

(ii) Dynamic Tests:

The two 12 in. x 3 in. x 3 in. concrete prisms of each series, which were cast, cured and subjected to the same temperature conditions as those of the test series, were tested by the resonance method to determine the dynamic modulus of elasticity of concrete. Readings were taken at room temperature and at each of the various steady state temperatures to which the series was subjected.

The comparative results of the initial tangent modulus of elasticity, the dynamic modulus of elasticity at room temperature and the modulus of elasticity, as obtained by using Ingé-Lyse's equation $E_c = 1800 + 460 f'_c$, are all entered in tabular form, along with the ultimate concrete strengths, f'_c, in tables 4.8 to 4.13.

The sonic test results over the temperature range were analyzed by means of a computer programme (prog. C of appendix D), which converted the frequency readings into the dynamic modulus values and fitted by the least square method a two-part first-degree curve to the temperature-dynamic E plots. Table 4.14 shows the typical dynamic modulus values calculated from sonic resonance readings. Fig. 4.18 shows a typical plot of dynamic modulus values against temperature.

4.2 TEST SPECIMENS:

One hundred and twenty-five slab specimens in eighteen series were tested under various (-100^0F to $+150^0$F) steady state temperature levels. The dimensions of all of the test specimens were the same, whereas six different steel percentages (0% to 5%) with both symmetric and unsymmetric arrangements were considered. Six different concrete mixes, representing a wide range of concrete mix designs, were used.

Finally, two distinct processes of curing - dry and wet - were considered. Fig. 3.1 and table 3.3 show the different mixes used. The variable characteristics, such as curing process, age, type of reinforcement, etc., are reported in table 3.5.

At each steady state temperature during testing, the deformations on both sides of the specimens, as indicated by the optical extensometer, the deformations indicated by transducers fixed on the control specimens, the extensometer and transducer readings on control aluminium blocks, and the temperatures indicated by eight thermocouples inside the chamber and inside the specimens at both the beginning and end of the intervals were recorded (tables 4.1 to 4.6). The temperature interval between each steady state level was approximately 15^0F. All these data were processed with the help of several computer programmes, a detailed description of which is given in the following section.

4.3 COMPUTER PROGRAMMES

(i) Programme A:

Because of the large number of data involved, this programme was written simply to obtain a print out of all the data punched along with differences of temperature and deformation readings at each increment of temperature to detect any error in punching or recording. After all the data were checked thoroughly they were processed with the help of the following computer programmes.

(ii) Programme B:

This was used to process the data of the static-E test.

After the load and deformation readings were converted into stress and strain, the experimental points were fitted to a straight line, from which slope the initial tangent modulus of elasticity for concrete, E_c, was calculated. The cylinder strengths were calculated from the ultimate loads. Table 4.7 gives a typical example of the calculation of static-E by computer.

(iii) Programme C:

The experimental data of the sonic tests were processed with the help of this programme. It was executed in the following steps:

1. From the input values of the weights and cross-sectional dimensions of the specimens and frequency readings taken at each temperature, the values of the dynamic modulus of elasticity were calculated.

2. A two-part first-degree polynomial curve fit subroutine fitted the calculated values above and below the freezing point of water.

3. The point of intersection of these two fitted curves determining the approximate freezing temperature of the specimen was calculated. Table 4.14 gives a typical analysis of sonic resonance readings by computer.

(iv) Programme D:

This programme was devised to analyze the thermal deformation readings of the slab specimens. It has two parts:

(a) The input consisted of deformation and temperature readings of both specimens and control specimens, aluminium blocks, boards, etc.

From the known deformation values of controlling elements, experimental errors were back calculated and consequently the deformation data of the slabs in the experiment were corrected.

(b) Once the data were corrected, they were ready to be analyzed in the following steps:

1. The deformation readings were converted into specimen lengths at each temperature level.

2. The specimen lengths over the temperature range were fitted by a polynomial curve fit subroutine in two parts, both above and below the freezing point. Slopes and intercepts of the fitted curves were found.

3. The standard deviation, the estimate of error (S_{yx}) and the coefficient of correlation (r) for the fitted curves were found. Corrected values of the estimate of error and the coefficient of correlation were found for small data groups.

4. An elaborate plot programme plotted the fitted curve to scale.

5. The experimental points were superimposed on the fitted curve plots.

6. Steps 1 through 5 were repeated for the readings on each face of each specimen.

7. The coefficient of thermal expansion of each specimen at each face was printed out in tabular form.

Tables 4.15-4.16 and figs. 4.19 to 4.32 show the typical output of programme D.

(v) Programme E:

The purpose of this programme was to predict the variations of the thermal deformation of concrete for different percentages of steel reinforcement. The input consisted of the coefficient of expansion of plain concrete, sectional properties of the slabs, the modulus of elasticity of concrete (from dynamic tests) and the modulus of elasticity (fig. 4.33) and the coefficient of steel (ref. 18). The calculation was done in the following steps:

1. The location of the neutral axis was determined from the sectional properties of the section.

2. Independent changes in length of concrete and steel were calculated.

3. The compatibility of deformation and equilibrium of forces were considered. The force developed in steel and concrete was determined. The resulting deformations of both concrete and steel were found. The coefficients of thermal expansion of the reinforced concrete were found for different percentages of steel.

4. The temperature level, the force developed and the coefficient of thermal expansion of reinforced concrete at each temperature level were printed out in tabular vorm. Table 4.17 shows a typical output of programme E.

The flow sheets of the major programmes and printouts of important subroutines are given in appendix D.

CHAPTER 5

DISCUSSION

5.1 COMPRESSION-DEFORMATION RELATIONSHIP:

With the exception of the one year old series (E and N), each series was tested at three different ages. The stress-strain diagrams (figs. 4.1 to 4.17) were obtained from the compresssion-deformation tests on 12 in. x 6 in. concrete cylinders at room temperature. Each curve is an average of two specimens. For each series a general increase in the static modulus of elasticity was observed (tables 4.8 to 4.13) over the age. This trend is fairly regular and is reported in most text books (ref. 26) and relevant papers.

(i) Static-E - Dynamic-E Relationship:

The static modulus of elasticity values were compared with the experimental values of the dynamic modulus of elasticity obtained at room temperature and with Ingé-Lyse's equation of $E_c = 1800 + 460 f'_c$ (tables 4.8 to 4.13). Rasul (ref. 27) reported a similar comparison. The trends in the interrelationship of the different modes of finding the modulus of elasticity are similar in the two investigations.

An effort was made to study the effect of the characteristics of concrete on the modulus of elasticity at room temperature. In figs. 5.1 to 5.5 the modulus of elasticity is plotted against the water-cement ratio for different ages (7, 28 and 84 days dry and wet). The experimental curves at each age for the dynamic-E and static-E tests and for the values computed by Ingé-Lyse's equation are all presented on one figure. The bottom curve represents the ratio E_d/E_c at each point. During the first 7 days the curing was the same for both the dry and wet series. Fig. 5.1 represents both 7 day wet and dry series.

Tables 4.8 to 4.13 and figs. 5.1 to 5.5 show good correlation in the value of the modulus of elasticity with an increase in the water-cement ratio. Noble (ref. 28) as early as 1931 reported such a trend.

The ratio of E_d/E_c varied between 0.975 to 1.20, the 7 day old series having higher ratios. The specimens at greater ages had lower E_d/E_c ratios. It should be pointed out that the actual no-load static-E values are somewhat higher than those reported. A straight line was fitted by the least square method to the experimentally obtained points. The slope of this fitted line was smaller than the initial tangent modulus obtained from the actual stress-strain curve. Therefore, the actual E_d/E_c ratios are lower than those reported. Investigations by Cran (ref. 7) and Whitehurst (ref. 29) show a relationship of the E_d/E_c ratios similar to that which is reported in this thesis. Malhotra (ref. 30) suggested the investigation of frequencies within 15% of fundamental frequency to determine the dynamic modulus of elasticity by the sonic resonant method.

The influence of free moisture on the dynamic modulus of elasticity at the time of testing is shown in figs. 5.6 and 5.7. If the concrete was wet-cured, the modulus of elasticity increased with age (fig. 5.6) and, if the concrete was allowed to dry, the modulus of elasticity decreased with age (fig. 5.7). These findings are very similar to those which Malhotra (ref. 30) and Kesler and Higuchi (ref. 31) have reported.

(ii) Temperature-Modulus Elasticity Relationship:

The variation of the dynamic modulus of elasticity over the temperature range (-100^0F to $+150^0$F) was plotted (fig. 4.18) for a prism specimen. First-degree curves were fitted in parts to the experimentally obtained points by means of the least square method. The slope of the fitted lines gives the rate of change of the modulus of elasticity of concrete both below and above the freezing point of water. It is apparent that the modulus of elasticity changes at a greater rate below the freezing point than above.

Tables 5.1 to 5.6 and Figs. 5.8 to 5.9 show the variation of the slopes of the modulus of elasticity. In figs. 5.8 and 5.9 the slopes above and below freezing points are plotted against the water-cement ratio. A linear variation can easily be observed from these two graphs. At a given age the rate of change is higher for concrete mixes of higher water-cement ratios. This trend was observed for both above and below the freezing point and is in agreement with the theory presented.

In order to study the effects of age and the curing process on the behaviour of modulus of elasticity changes, the slope values were plotted against age. Fig. 5.10 shows the curves representing the changes in slopes for the dry-cured series with age. The below freezing slopes decreased rapidly with age. The rate of change of the slopes became smaller at higher ages. The changes of the slopes above the freezing point showed smaller changes, although decreasing steadily with age. Monfore and Lentz (ref. 6), Berwanger (ref. 8) and Verbeck and Kleiger (ref. 17) reported in their investigations that, for laboratory-cured specimens, the sharp increase in the concrete modulus below freezing was produced by the frozen water. With age, continued hydration and evaporation will drastically reduce the amount of water to be frozen. Obviously the reduction in the amount of water will have a greater effect on the change in the slopes below freezing.

Fig. 5.11 shows the curves representing the changes in the slopes of the dynamic modulus of elasticity (E_d) values with age for the wet-cured series. The behaviour of the wet-cured series below freezing was similar to that of the dry-cured series. Quite logically the change was not as pronounced as in the case of the wet-cured series, when the reduction of available water to be frozen was not as great. But above the freezing temperatures the wet-cured series showed very distinct behaviour from that of the dry-cured series. Instead of decreasing, the specimens of different water-cement ratios showed a slight increase with age. As the temperature of a solid (concrete) increases, the material expands and the particles are subjected to a weaker cohesive force. A given load causes a greater strain at high than at low temperature. The presence of moisture in the solid will also affect this phenomenon. With an increase in temperature the density of water present will decrease and further reduce the stiffness of the solid. At higher ages the increased amount of water causes a faster decrease in stiffness with the result that the rate of change of the modulus of elasticity at these ages increases to some extent over that of the specimens of earlier ages. No previous investigation was reported on the experimental investigation of change of the modulus of elasticity of wet-cured specimens with temperature at different ages.

(iii) Temperature-Freezing of Concrete Relationship:

An attempt was made to establish a possible way of determining if there was any particular pattern followed by the freezing of different mixes of concrete at different ages. For the prism specimens, the variations of the dynamic modulus of elasticity were presented in the form of figures (fig. 4.18). The fitted straight lines showed different slopes below and above the freezing point of water. Therefore, a clear and distinct intersecting point will be obtained if the fitted straight lines are produced to intersect (ref. 8). Since a sharp increase was noticeable in the modulus of elasticity values when the available water in the specimen began to freeze, this point of intersection was logically taken as the probable temperature when the available moisture would start to freeze. The point of intersection of the fitted curves was calculated for each specimen of each water-cement ratio at each age. The average for each water-cement ratio at any given age was plotted. Fig. 5.12 shows the variation of freezing temperatures with water-cement ratios. It shows that, when age is constant, the greater the amount of water the sooner the specimens will freeze. For the 7 day old specimens with a water-cement ratio of 0.672 the freezing point was an average of 30.3^0F, while the water in the 84 day old dry-cured specimens with a 0.445 water-cement ratio froze at an average temperature of 14.6^0F.

Fig. 5.13 shows the probable variations of freezing points with age. With age all specimens froze at lower temperatures, showing a trend of non-linear variation. The wet-cured specimens had a less steep drop in the freezing point temperatures than the dry-cured specimens. This confirmed the theory that at a given age freezing temperatures are directly related to the amount of free water in the specimen.

5.2 TEMPERATURE-COEFFICIENT OF EXPANSION RELATIONSHIP:

Each of the seven specimens of each series was measured on both sides to find the coefficient of expansion of that particular slab over the whole temperature range. The data were processed by a computer programme (prog. D - appendix D). Table 4.15 shows the results obtained from one face of one specimen only. The graphical plots were obtained through the use of a Milgo Plotter, located at the computing centre of the University of Ottawa. For each series the experimentally obtained points were superimposed on the curves, which were fitted to them by means of the least square method (figs. 4.19 to 4.32). The results of fourteen tables (each one similar to table 4.15) for the whole series are summarized in table 4.16.

In the case of each specimen face, the standard deviation, the estimate of error for dependent variables and the coefficient of correlation were calculated for each fitted curve (table 4.15).

These values indicated the goodness of fit and whether there was a good correlation between experimental points and the fitted curves. There was an excellent correlation for all curve fits. The coefficients of correlation varied from 0.8 to 0.97 for most curve fits with occasional low values going down to approximately 0.75. Correction was made for coefficients of correlation and estimates of error values to account for the small group of data in the case of each curve. The corrected values were slightly lower (0.79 to 0.95) but still showed excellent correlation.

(i) Behaviour of Plain Concrete:

In each series the two plain concrete slab specimens served both as a control and as a means to determine the coefficients of thermal expansion of plain concrete. The experimental data were compiled to report a definite trend in the variations of the coefficients of plain concrete with the variables of age, water-cement ratio and curing process. The results of the compilation are reported in table 5.7 and figures 5.14 to 5.17. The numerical values of the coefficient of expansion compare favourably with Mitchell's findings (ref. 2). In this investigation the fine aggregates were predominantly composed of quartz and the coarse aggregates of limestone (table 3.1).

Figs. 5.14 and 5.15 show the variations of the coefficients of expansion with the water-cement ratios for above and below freezing respectively. There are marked similarities among the curves of the two figures, except that the curves for above the freezing point have a greater change in slope. In both above and below the freezing point, the curves show a decrease in the coefficient values with an increase in the water-cement ratio.

Figs. 5.16 and 5.17 show the variations of the coefficients of expansion of plain concrete with age for above and below freezing. A set of nearly parallel curves for the dry series was obtained, as well as another almost parallel set of curves for the wet series. The curves of the wet-cured series are flatter than those of the dry-cured series, indicating that the gain in the coefficient of expansion value is smaller for wet-cured specimens than for dry-cured specimens. When dry-cured, the coefficient of expansion of concrete with a water-cement ratio of 0.445 increased from 4.60×10^{-6} in./in./^{0}F (above freezing) at 7 days to 4.96×10^{-6} in./in./^{0}F (above freezing) at 84 days, whereas, when wet-cured, the coefficient value of the specimen increased only to 4.85×10^{-6} in./in./^{0}F (above freezing) at 84 days. On the average the dry-cured specimens had a 25 to 40% higher increase in the coefficient values than that in the corresponding wet-cured series.

(ii) Behaviour of Reinforced Concrete:

In each series six reinforcement percentages (0% to 5%) were used. Both symmetrical and unsymmetrical reinforcements were used. This enabled the covering of a wide variety of behaviour of concrete coefficients with a number of variables, such as steel percentage, reinforcement type, water-cement ratio, age and curing process. From the two plain concrete specimens the theoretical values of the coefficient of expansion for reinforced concrete were calculated. Tables 5.8 to 5.23 show the theoretical and experimental values of the coefficient of expansion of reinforced concrete for all these variables. It is considered unnecessary to present all of the results in figure form as well; instead, the figures are presented to specifically outline the trends of the general behaviour of the investigation.

Fig. 5.18 shows typical theoretical curves with the corresponding experimental points superimposed on them. The curves show a substantial agreement between experimental and theoretical investigations. To obtain experimental values, slopes of fitted curves (figs. 4.19 to 4.32) were used. There was excellent correlation between the experimental points and the fitted curves. Figs. 5.18 to 5.21 show variations in the coefficient of expansion of reinforced concrete specimens with the percentage of steel. Fig. 5.18 shows the general trends of variation for the unsymmetrically reinforced slabs. Fig. 5.19 shows the variations for symmetrical reinforcements, while figs. 5.20 and 5.21 show the variations due to the position of reinforcement in the unsymmetrical series. In figs. 5.19 to 5.21 the curves are drawn with a larger vertical scale. As predicted by the theoretical investigations (equations 21 to 24), the coefficient of expansion of symmetrically reinforced concrete increased with the percentage of steel. For the unsymmetrically reinforced concrete the coefficient of expansion for the concrete face near the reinforcement increased significantly, while that for the face away from the reinforcement decreased only slightly. Figs. 5.22 and 5.23 show the relative changes of the coefficients of expansion due to the different arrangements of reinforcement.

The effect of the water-cement ratio on the coefficient of expansion of reinforced concrete is very similar to that of plain concrete. Figs. 5.19 to 5.21 show sets of non-linear curves, each representing a particular water-cement ratio. It was apparent that, with the same percentage of steel and the same age, a specimen of a lower water-cement ratio will have a higher coefficient of expansion. This trend remains relatively constant irrespective of the arrangement of reinforcement and the curing method used.

The effect of the curing process on the coefficient of expansion was investigated. Fig. 5.24 and tables 5.8 to 5.23 indicate a general trend that concrete specimens having the same water-cement ratio and the same age but cured differently will have a different coefficient of expansion. The coefficients of expansion of the wet-cured series are lower than those of the dry-cured series. Fig. 5.24 shows identical variations for both above and below the freezing point.

Fig. 5.25 attempts to show the effect of age on the coefficient of expansion values. Curves for the same series (same water-cement ratio and cured similarly) are plotted for different ages. It was apparent that, with age, specimens having the same arrangement and percentage of reinforcement will have a greater coefficient of expansion. This trend is identical for both above and below freezing. Tables 5.8 to 5.23 confirm these results.

Figs. 5.16 and 5.17 and 5.26 to 5.31 summarize the effect of the different variables on the coefficients of expansion of plain and reinforced concrete.

5.3 POSSIBLE ERRORS IN TEST AND ANALYSIS:

Both the theoretical and experimental investigations reported in this thesis were subject to some inadvertent errors. Despite the fact that every precaution was taken, the components of the variables in testing could not be completely controlled and some of the assumptions made for the analytical work may not be correct in their entirety. The possible sources of error are indicated in the following discussion.

1. Two 12 in. x 6 in. control cylinders were used to measure the static modulus of elasticity and the concrete strength, and two 12 in. x 3 in. x 3 in. prism specimens were used to determine the dynamic modulus of elasticity for each series at each age. Although the control cylinders and the prism specimens of each series were cast from the same batch of concrete and cured under identical conditions, they showed some variations in the values of static-E, strength of concrete and dynamic-E and, therefore, the average values of E_c, f'_c and E_d had to be used.

2. Although the gauge length (10 in.) was determined using a special invar scale, it was found to vary up to ±0.01563 in. Errors up to 0.1567% may have been introduced while calculating experimental values of the coefficient of expansion.

3. The positioning of the reinforcing bars might have differed from the intended position due to minor faults in the moulds and casting.

4. For theoretical analysis the known values of E_s (ref. 32) and α_s (ref. 18) were used. Since structural steel varies slightly in

composition within the same ASTM designated type and grade, some minor differences might have been introduced as a result.

5. Three embedded thermocouples were used to measure the temperature of a series during testing. Although the temperature inside the environmental chamber should have been constant, it varied slightly. The three thermocouples showed some variations (up to 1.5°F) in the temperature recorded and therefore the average value of the temperature had to be used.

6. Although the slab specimens were placed in position for testing with extreme care, their faces may not have been exactly perpendicular to the line of view of the optical extensometer.

7. For the controlling aluminium specimens the deformations and temperature were measured at the same instant to avoid any variation due to continuous small changes of temperature in the chamber. It is possible that some time had elapsed between the two measurements.

8. Continuous 24 hour experiments were conducted to maintain the test schedule. For this reason several persons had to work in shifts to set up the apparatus and specimens and take the experimental readings. Thus some inadvertent errors might have occurred.

9. The apparatus used may have had minor mechanical or instrument errors which would have affected the accuracy of the readings.

CHAPTER 6

CONCLUSION

In view of the good agreement of the general trends of behaviour from the experimental and the theoretical investigations, the following conclusions may be drawn:

(i) Elasticity of Modulus of Concrete at Room Temperature:

1. In general, the dynamic modulus of elasticity of concrete is higher than the static modulus of elasticity for the same concrete (figs. 5.1 to 5.5; tables 4.8 to 4.13).

2. The ratio E_d/E_c varies between 0.975 and 1.20. At higher ages the ratio tends to be lower.

3. A general trend shows that, when concrete is wet-cured, the dynamic modulus of elasticity increases with age (fig. 5.6) and, if the concrete is allowed to dry, the dynamic modulus of elasticity decreases with age (fig. 5.7).

4. In general, for the same age, the modulus of elasticity decreases with the increase of the water-cement ratio (figs. 5.1 to 5.5).

(ii) Temperature-Modulus of Elasticity Relationship:

5. The modulus of elasticity of concrete changes at a greater rate below the freezing point than above (fig. 4.18).

6. At a given age the rate of change of the slopes of the modulus of elasticity of concrete with temperature both below and above freezing is greater with a higher water-cement ratio (figs. 5.8 and 5.9; tables 5.1 to 5.6).

7. Below freezing the changes in the slopes of the modulus of elasticity for both the dry-cured and wet-cured concrete specimens are much more pronounced than those above freezing (figs. 5.10-5.11).

8. The below freezing changes in slope of dynamic-E with age for the wet-cured concrete specimens are somewhat less pronounced than those for the dry-cured concrete specimens.

9. The above freezing changes in slope of the modulus of elasticity with age for the wet-cured concrete specimens increase, while those for the dry-cured concrete specimens decrease (figs. 5.10 and 5.11).

(iii) Freezing Temperature in Concrete Slabs:

10. The greater the amount of water in concrete, the higher temperature it will freeze (fig. 5.12). At any given age concrete with a higher water-cement ratio freezes sooner.

11. With age, the freezing point drops for all concrete, the wet-cured specimens showing a lower drop than the dry-cured (fig. 5.13).

(iv) Temperature-Coefficient of Expansion Relationship:

12. The coefficient of expansion of plain concrete both below and above freezing decreases with an increase in the water-cement ratio, the above freezing changes being greater (figs. 5.14 and 5.15).

13. In general, the coefficients of expansion of plain concrete both below and above the freezing point increase with age. The gains in the coefficient values for the dry series are about 25% to 40% higher than those for the wet series (figs. 5.16 and 5.17).

14. The coefficients of expansion of symmetrically reinforced concrete increase with the increase in percentage of steel reinforcement (fig. 5.19). For unsymmetrically reinforced concrete the coefficient of expansion for the concrete face near the reinforcement increases significantly with the increase in percentage of steel, while that for the concrete face away from the reinforcement decreases slightly (figs. 5.20 and 5.21).

15. With the same percentage of steel reinforcement, the coefficient value is higher for the concrete face near the reinforcement of an unsymmetrically reinforced slab than that of a symmetrically reinforced slab. The coefficient value for the concrete face away from the reinforcement is lower than that of the symmetrically reinforced slab (figs. 5.22 and 5.23).

16. With the same percentage of steel and at the same age, a reinforced concrete with a lower water-cement ratio has a higher coefficient of expansion both below and above freezing (figs. 5.19 to 5.21).

17. At any age the wet-cured reinforced concrete specimens of a given water-cement ratio have lower coefficients of expansion than those of the dry-cured specimens (fig. 5.24), both above and below freezing.

18. With age, reinforced concrete slabs of the same water-cement ratio and having undergone the same curing process and having the same arrangement and percentage of reinforcement will have a greater coefficient of expansion both below and above freezing (fig. 5.25 and tables 5.8 to 5.23).

SUGGESTIONS FOR FUTURE RESEARCH:

In light of the experimental and analytical work completed, some suggestions for future investigations may be made.

The analytical expressions developed were verified by a limited number of experimental data. Hence, further experimental work in this direction with an increased range of all the variables, such as temperature, percentage of steel, water-cement ratio and age, would be quite advantageous. In the present study only a particular type of aggregate was used. The fine aggregates were mainly quartz and the gravel mainly limestone. Different types of aggregates and their combinations should be tried to establish a complete behavioural pattern for the entire range of field work.

Different types of curing to represent actual field conditions at construction work sites throughout Canada should also be considered.

REFERENCES

1. Callan, E.J., "Thermal Expansion of Aggregates and Concrete Durability", ACI Journal, Proceedings, V. 48, No. 33, February 1952, pp. 485-504.

2. Mitchell, L.J., "Thermal Expansion Tests on Aggregates, Neat Cements and Concretes", Proceedings, ASTM, V. 53, 1953, pp. 963-977.

3. Saemann, J.C. and Washa, G.W., "Variation of Mortar and Concrete Properties with Temperature", ACI Journal, Proceedings, V. 54, No. 20, November 1957, pp. 385-395.

4. Tokuda, H. and Ito, T., "Some Experimental Results on Thermal Properties of Concrete", Japan Congress on Testing Materials, 7th Proceedings, 1964, pp. 122-123.

5. Dettling, H., "Die Warmedehnung des Zementsteines, der Gesteine und der Betone", Deutscher Ausschuss fuer Stahlbeton, V. 164, 1964, pp. 1-64.

6. Monfore, G.E. and Lentz, A.E., "Physical Properties of Concrete at Very Low Temperature", Journal of the PCA Research and Development Laboratories, V. 4, No. 2, May 1962, pp. 33-39.

7. Cran, J.A., "An Investigation of the Low Temperature Properties of Concrete and Reinforced Concrete Slabs", M.Sc. Thesis, University of Manitoba, Winnipeg, 1963.

8. Berwanger, C., "The Modulus of Concrete and Coefficient of Expansion of Concrete and Reinforced Concrete at Below Normal Temperatures", ACI special paper, Temperature and Concrete, No. SP 25-8, 1971, pp. 192-233.

9. Cruz, R.C., "Elastic Properties of Concrete at High Temperatures", Journal of the PCA Research and Development Laboratories, V. 8, No. 11, January 1966, pp. 37-45.

10. Berdichevskii, A.I. and Svirdov, N.V., "Prochnost Izzibaumykh Zhelezobetonykh Elementove...." (Flexural Strength of Reinforced Concrete Members at very Low Temperatures), Beton i Zhelezobeton, V. 1, January 1965, pp. 16-21.

11. Moskvin, V.M.; Kapkin, M.M. and Anatonov, L.N., "Vliyanie Otriaetelnykh Temperatur na Prochnost i Uprugoplasticheskii Svoista Betona" (Effect of Freezing Temperature on Strength and Elasto-plastic Properties of Concrete), Beton i Zhelezobeton, V. 10, October 1967, pp. 18-21.

12. Hansen, C.T. and Erikson, L., "Temperature Change Effect on Behaviour of Cement Paste, Mortar and Concrete under Load", ACI Journal, Proceedings, V. 63, No. 4, April 1966, pp. 489-504.

13. Berwanger, C., "A Continuous Composite Steel-Concrete Bridge Prestressed by Deformation at the Interior Supports", presented at Second International Symposium on Concrete Bridge Design, ACI Convention, Detroit, Michigan, 1971 and ACI paper No. SP 26-33, 1971, pp. 818-873.

14. Samelson, H. and Tor, A., "Stresses in Reinforced Concrete Sections Subject to Transient Temperature Gradients", ACI Journal, September 1958, V. 30, No. 3, pp. 377-386.

15. Fintel, M. and Khan, F.R., "Effects of Column Exposure in Tall Structures - Temperature Variations and their Effects", ACI Journal, Proceedings, V. 62, No. 85, December 1965, pp. 1533-1556.

16. Sandana, Y.L. and Verma, K.C., "Temperature Effects in Reinforced Concrete Frames", Journal of Institute of Engineers (India), V. 47, No. 5, January 1967, pp. 303-327.

17. Verbeck, G. and Klieger, P., "Calorimeter-Strain Apparatus for Study of Freezing and Thawing Concrete", Bulletin No. 176, Highway Research Board, 1958, pp. 9-22.

18. American Institute of Steel Construction, Inc., "Manual of Steel Construction", 1966.

19. Timoshenko, S.P. and Young, D.H., "Theory of Structures", McGraw-Hill Book Company, New York, 1965, pp. 629.

20. Grinter, L.E., "Elementary Structural Analysis and Design", The MacMillan Company, New York, 1966, pp. 465.

21. Winter, G.; Urquhart, L.C.; O'Rourke, C.E. and Nilson, A.H., "Design of Concrete Structures", 7th Edition, McGraw-Hill Book Company, 1964, pp. 660.

22. "Standard Specifications for Concrete Aggregates", C 33-71, and "Standard Method of Test for Fundamental Transverse, Longitudinal and Torsional Frequencies of Concrete Specimens", C 215-60, ASTM Standards, Part 10, 1971, pp. 14-22 and 134-138 respectively.

23. "Design and Control of Concrete Mixtures", Portland Cement Association Engineering Bulletin, 11th Edition, July 1968, pp. 88.

24. "Standard Specification for Deformed Steel Wire for Concrete Reinforcement", ASTM A 496-64, ASTM Standards, Part 4, 1968, pp. 692-695.

25. Cawkwell, A.E., "The Non-Destructive Testing of Engineering Materials", M. Falk and Company, Ltd., Reigate, England, 24 pp.

26. Troxell, G.E. and Davis, H.E., "Composition and Properties of Concrete", McGraw-Hill Book Company, New York, 1956, 259 pp.

27. Rasul, S.I., "Rectangular Prestressed Concrete Sections under Short Term Loading of Combined Bending and Axial Thrust", M.A.Sc. Thesis, University of Ottawa, 1969.

28. Noble, P.M., "The Effect of Aggregates and other Variables on the Elastic Properties of Concrete", Proceedings, ASTM, V. 31, Part 1, 1931, pp. 399-426.

29. Whitehurst, E.A., "Evaluation of Concrete Properties from Sonic Tests", American Concrete Institute, Monograph No. 2, published jointly by ACI and Iowa State University Press, Ames, Iowa, 1966, 94 pp.

30. Malhotra, V.M., "Non-Destructive Methods for Testing Concrete", Mines Branch Monograph 875, Department of Energy, Mines and Resources, Ottawa, November 1968.

31. Kesler, C.E. and Higuchi, Y., "Determination of Compressive Strength of Concrete by Using its Sonic Properties", Proceedings, ASTM V. 53, 1953, pp. 1044-1051.

32. Day, E.E. and Sevand, A.H., "Characteristics of Electric Strain Gages at Low Temperatures", Proceedings, Society for Experimental Stress Analysis, V. 8, No. 1, 1950, pp. 133-142.

33. Mironov, S.A.; Krylov, B.A. and Ivanova, O.S., "O Srokakh Vyderzhivaniya Betona do Zamerzaniya" (Duration of Concrete Curing Prior to Freezing), Gidrotekhnicheskoe Stroitel'stvo, V. 4, April 1967, pp. 15-19.

34. Slate, F.O. and Matheus, R.E., "Volume Changes on Setting and Curing of Concrete Paste and Concrete from Zero to Seven Days", ACI Journal, V. 64-4, January 1967, pp. 34-39.

35. Malhotra, V.M. and Berwanger, C., "Correlation of Age and Strength with Values Obtained by Dynamic Tests on Concrete", Canada Department of Energy, Mines and Resources, Mines Branch, Investigation Report IR 70-40, June 1970.

36. Whitehurst, E.A. and Parker, W.E., "Dynamic Tests - Significance of Properties of Concrete and Concrete Aggregates", ASTM Special Technical Publication, No. 169, 1956, pp. 104-114.

37. Plowman, J.M., "Concrete Strength near Freezing Point", Engineering, V. 189, January 15, 1960, pp. 78-79.

38. Snedecor, G. and Cochran, W., "Statistical Methods", Iowa State University Press, Ames, Iowa, 1967, 593 pp.

39. Waugh, A.E., "Elements of Statistical Method", 3rd Edition, McGraw-Hill, New York, 1952, 531 pp.

40. Mode, E.B., "Elements of Statistics", Prentice-Hall Inc., New Jersey, 1956, 377 pp.

41. Jones, R., "Non-Destructive Testing of Concrete", Cambridge at the University Press, 1962, 103 pp.

42. Corden, W.A., "Freezing and Thawing of Concrete - Mechanism and Control", American Concrete Institute, Monograph 3, Iowa State University Press, Ames, Iowa, 1966, 99 pp.

43. Czernin, W., "Cement Chemistry and Physics for Civil Engineers", Chemical Publishing Co. Inc., New York, 1962, 139 pp.

44. Spiegel, M.R., "Theory and Problem of Statistics", Schaum Publishing Co., New York, 1961, 359 pp.

APPENDIX A: FIGURES

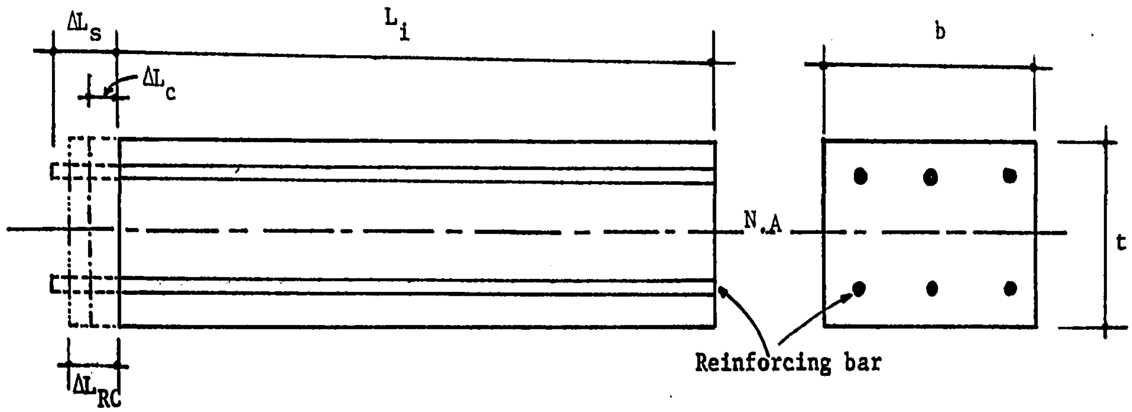

FIG. 2.1 - SYMMETRICALLY REINFORCED CONCRETE SLAB

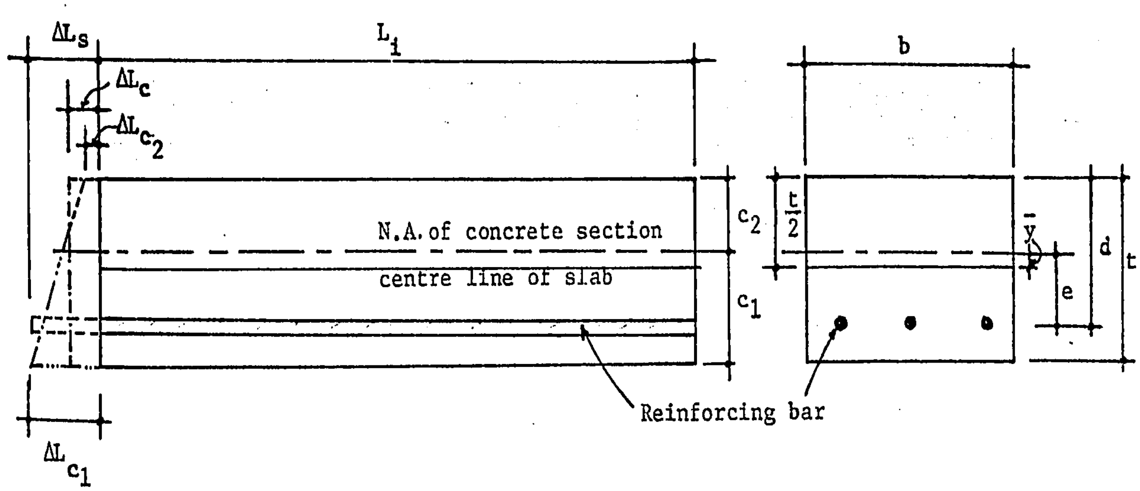

FIG. 2.2 - UNSYMMETRICALLY REINFORCED CONCRETE SLAB

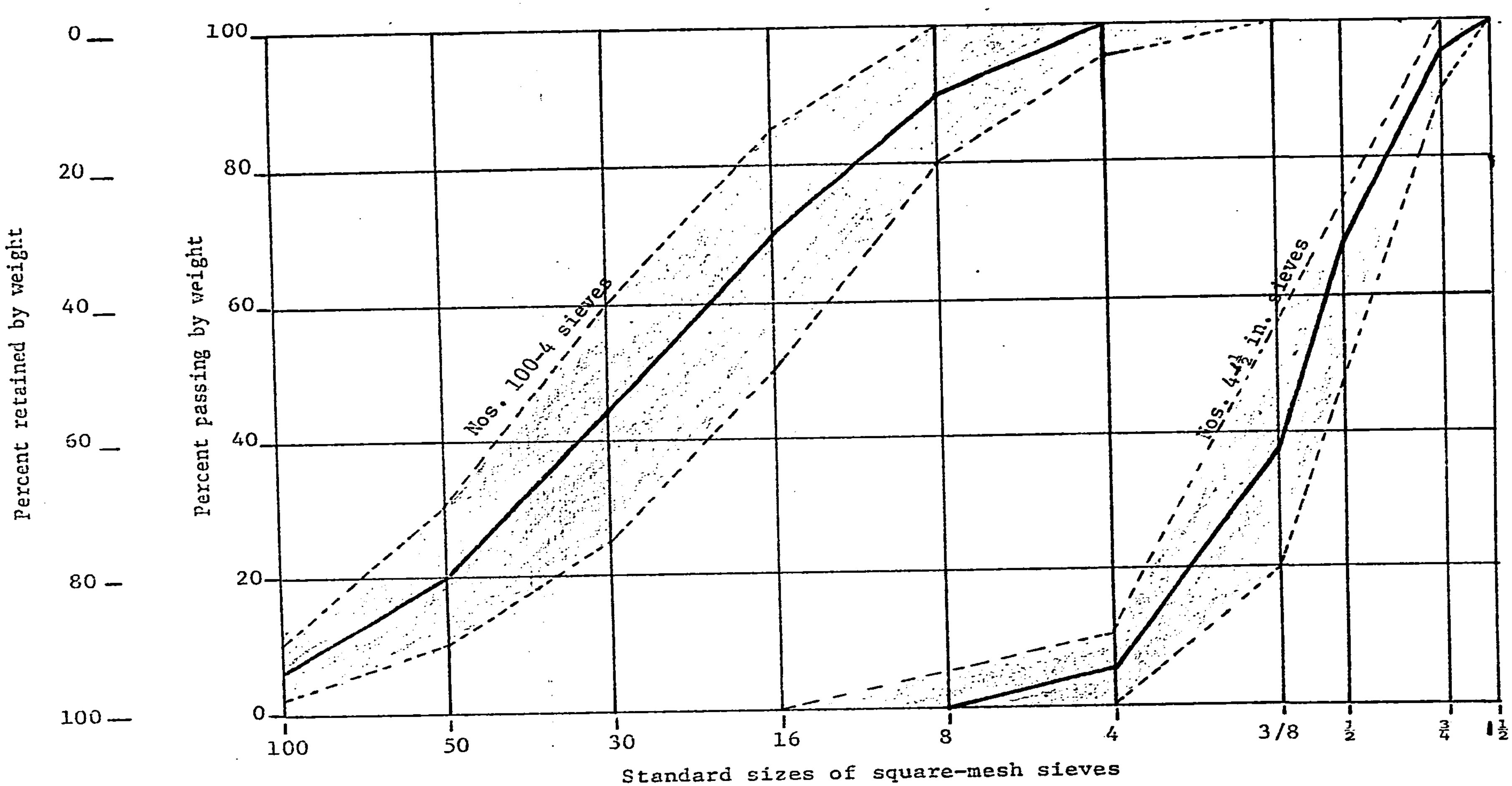

FIG. 3.1: GRADING CURVE OF THE DESIGNED MIX IS SUPERIMPOSED UPON LIMITS (SHADED AREA) SPECIFIED IN ASTM C 33

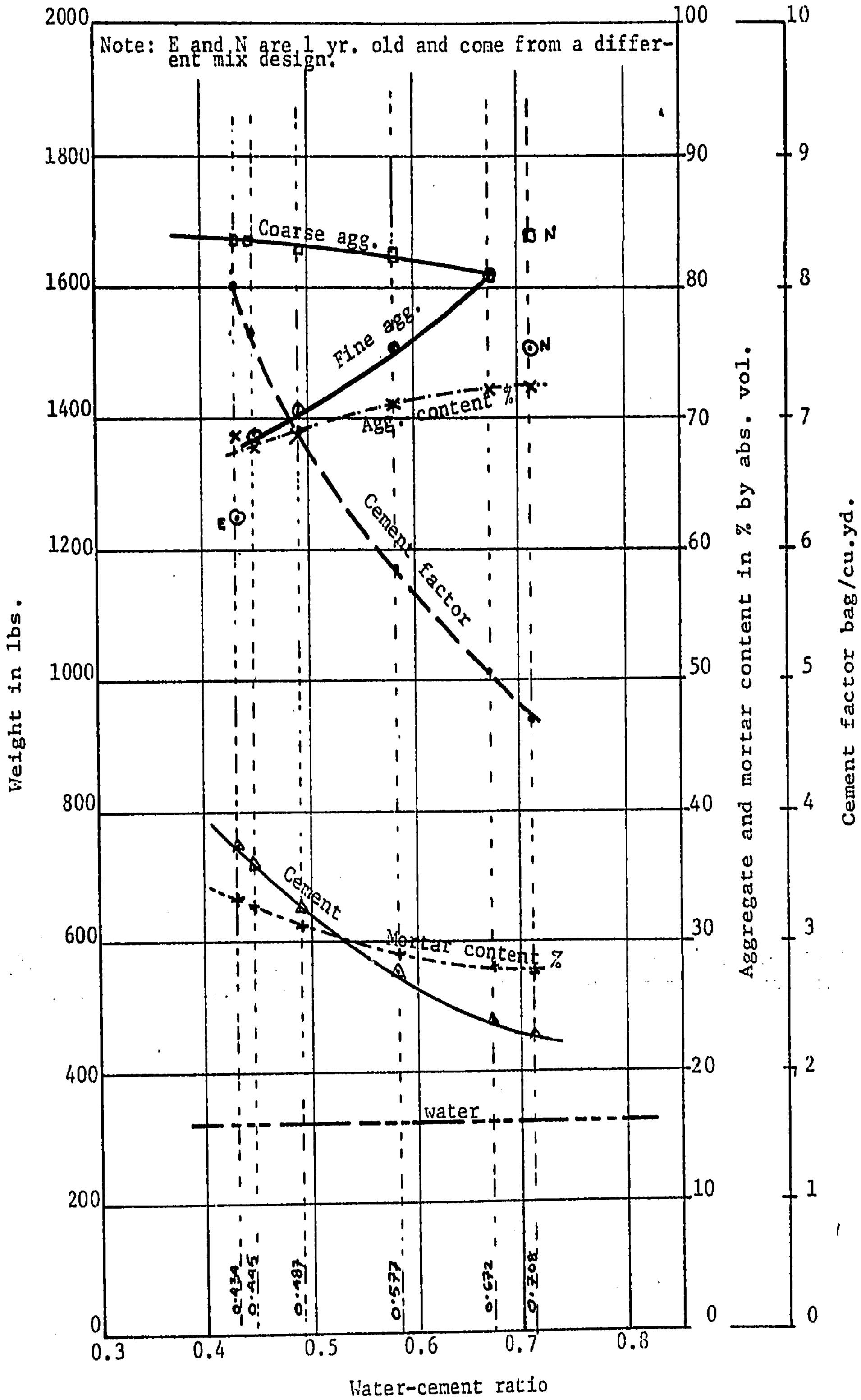

FIG. 3.2: CONCRETE MIX PROPERTIES

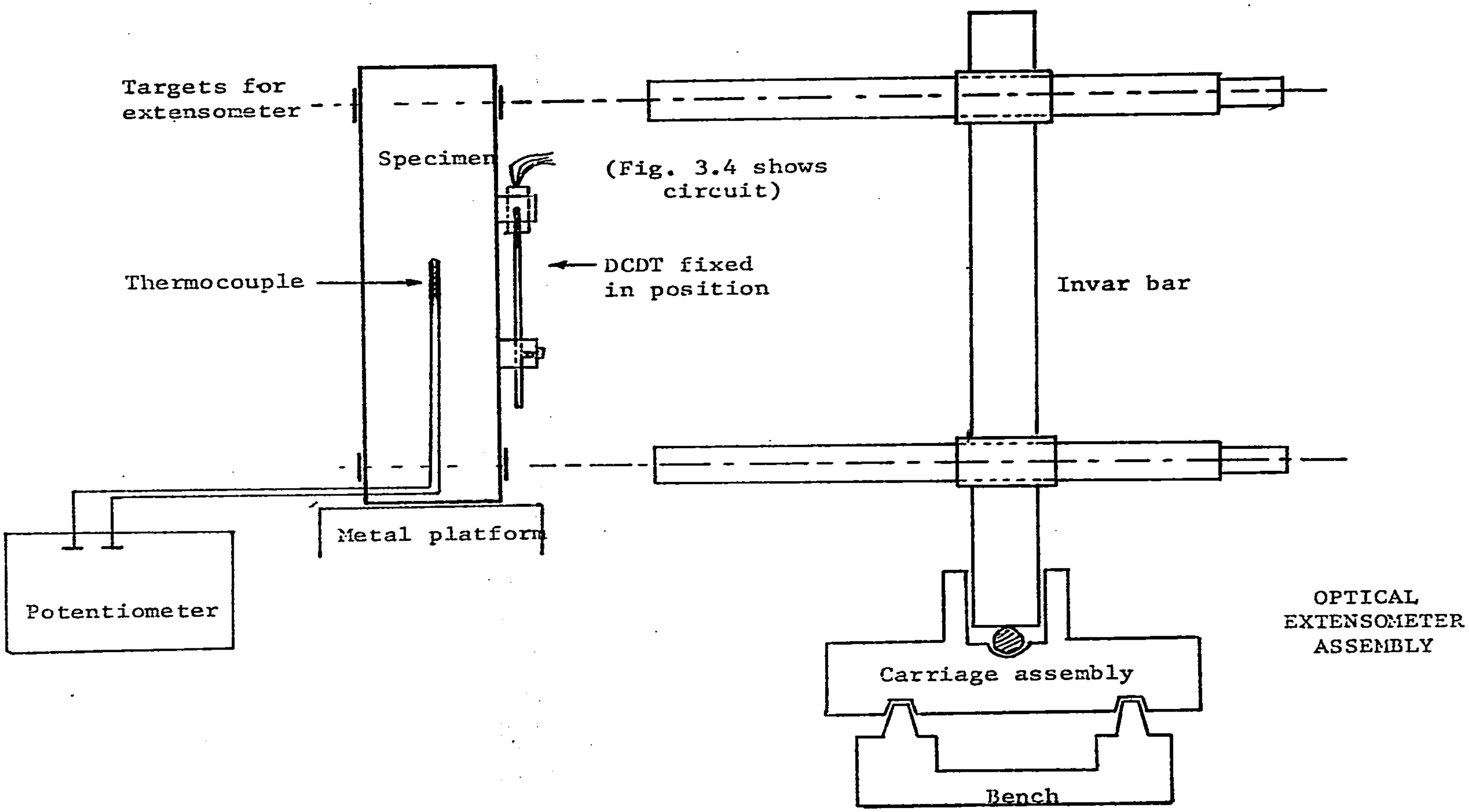

FIG. 3.3: EXPERIMENTAL DISPOSITION OF TEMPERATURE AND DEFORMATION MEASUREMENT OF CONCRETE SLABS

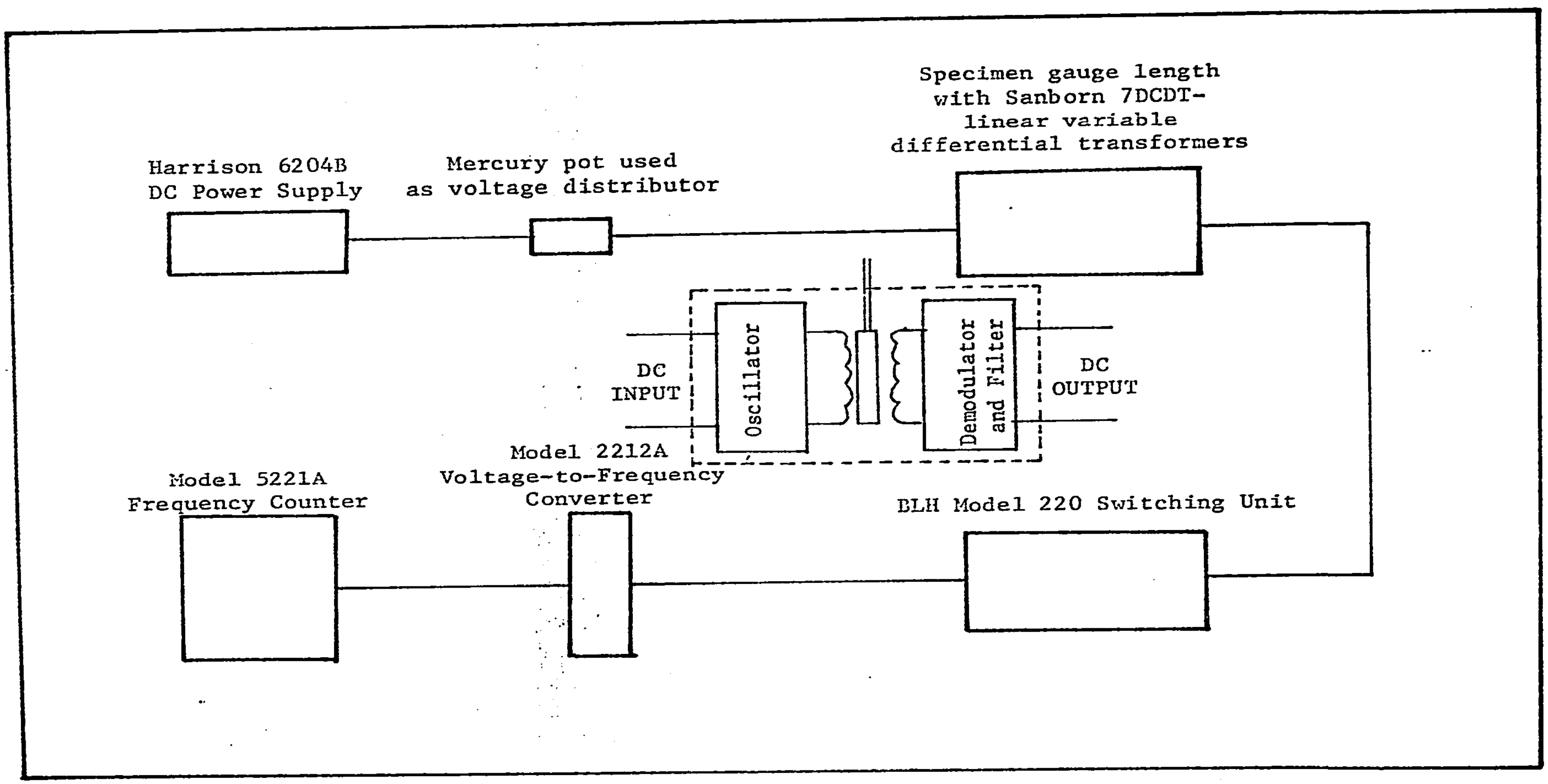

FIG. 3.4: SCHEMATIC DIAGRAM SHOWING STRAIN MEASUREMENT BY USING DCDT'S

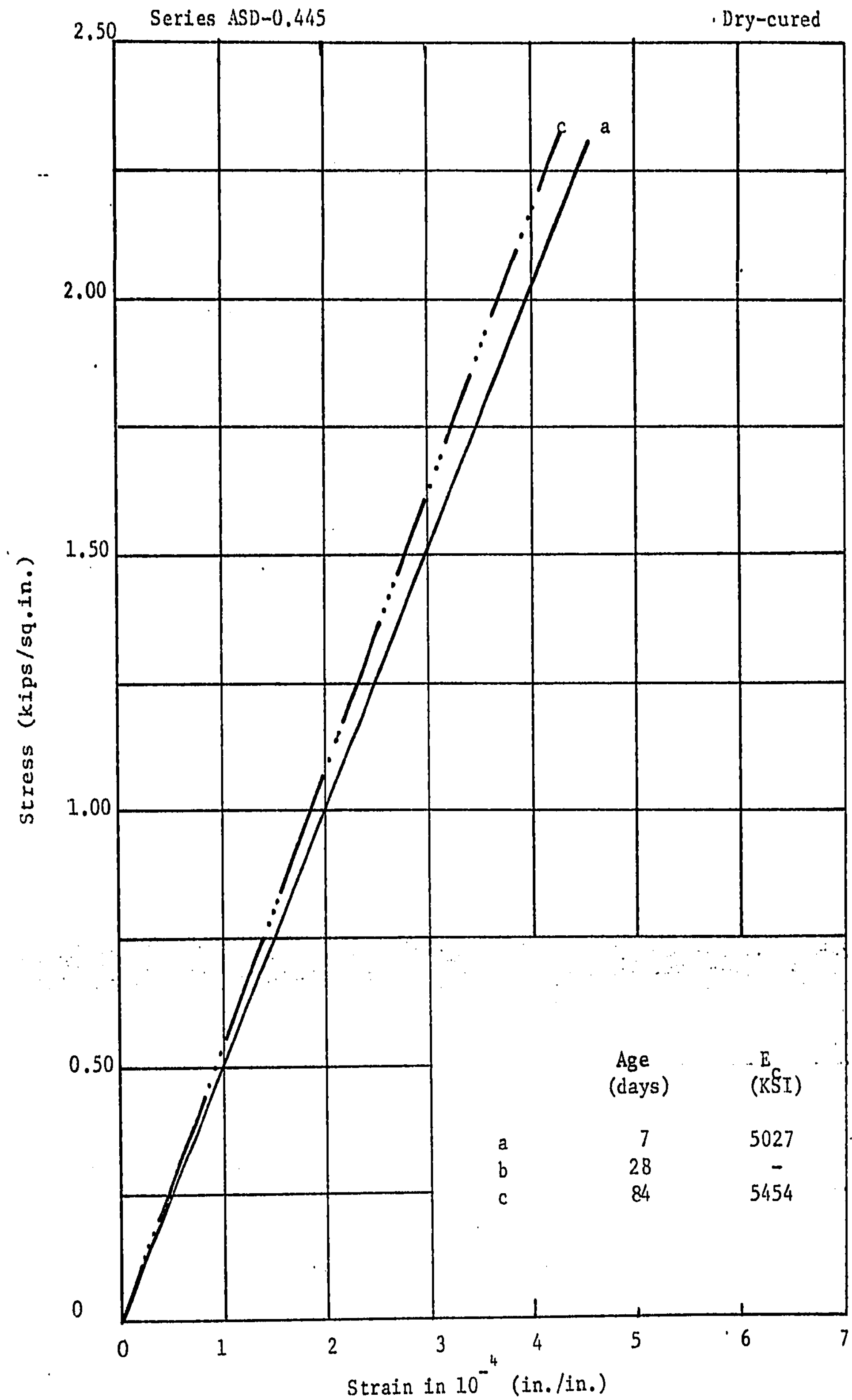

FIG. 4.1: STRESS-STRAIN CURVE FOR CONCRETE

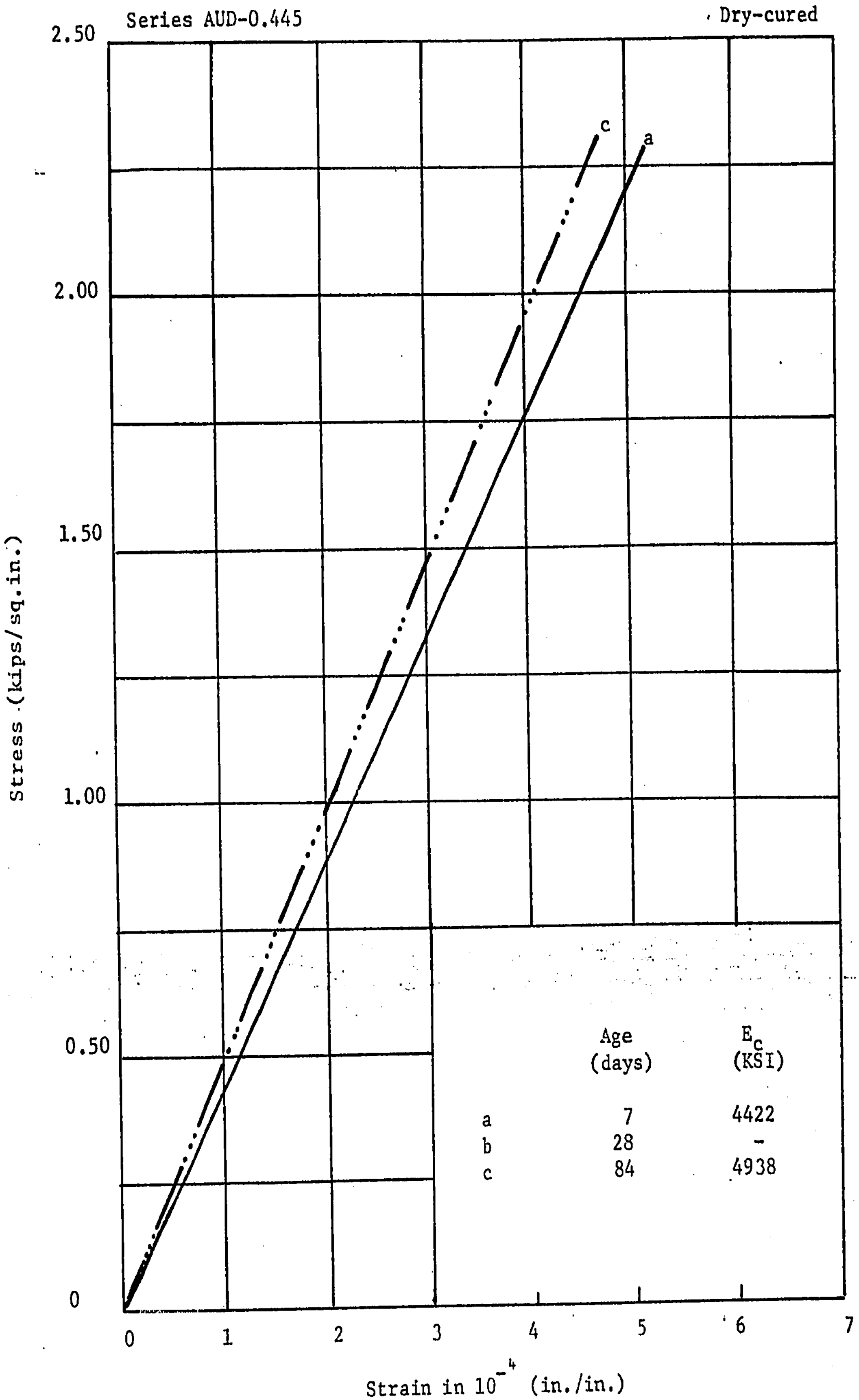

FIG. 4.2: STRESS-STRAIN CURVE FOR CONCRETE

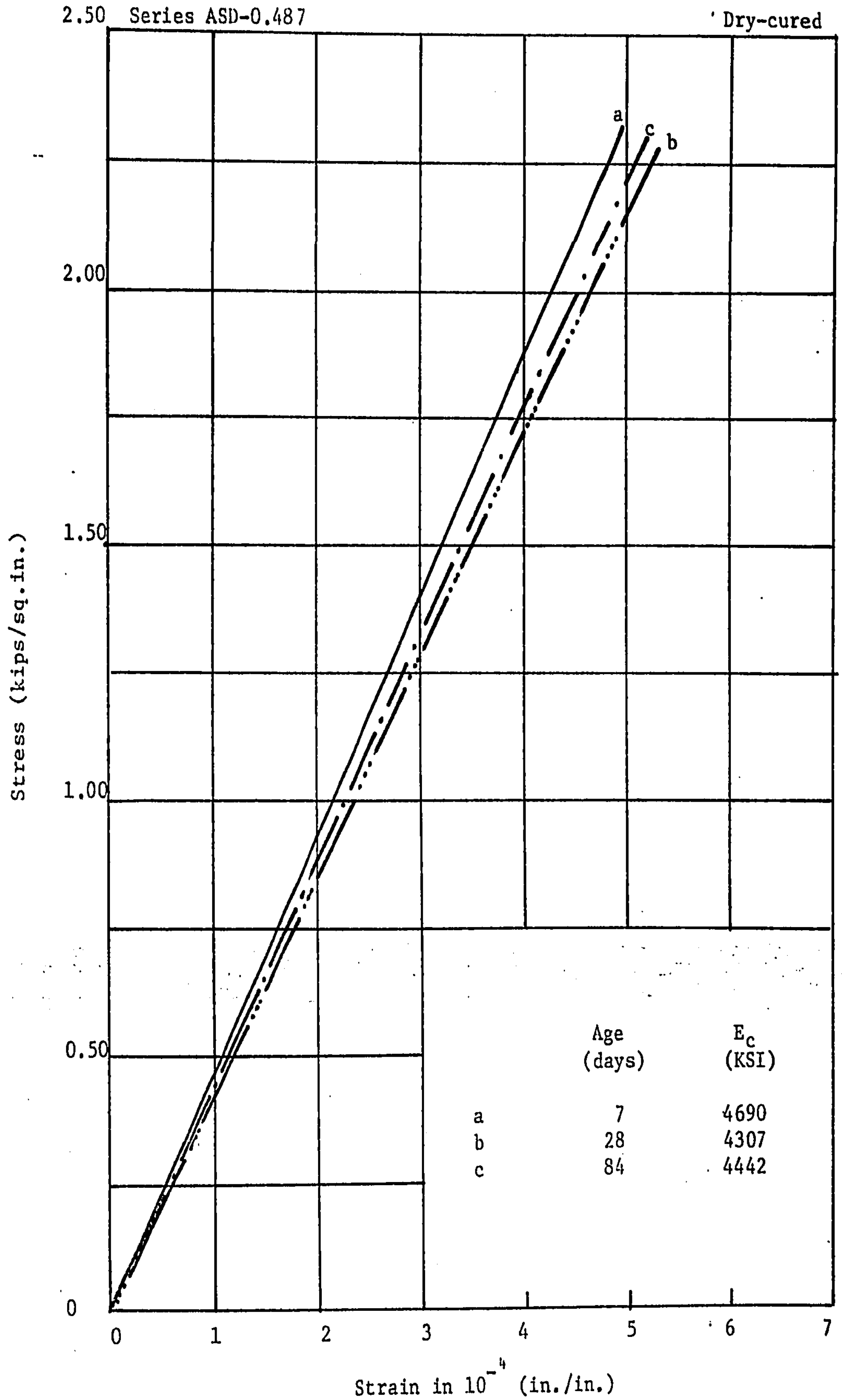

FIG. 4.3: STRESS-STRAIN CURVE FOR CONCRETE

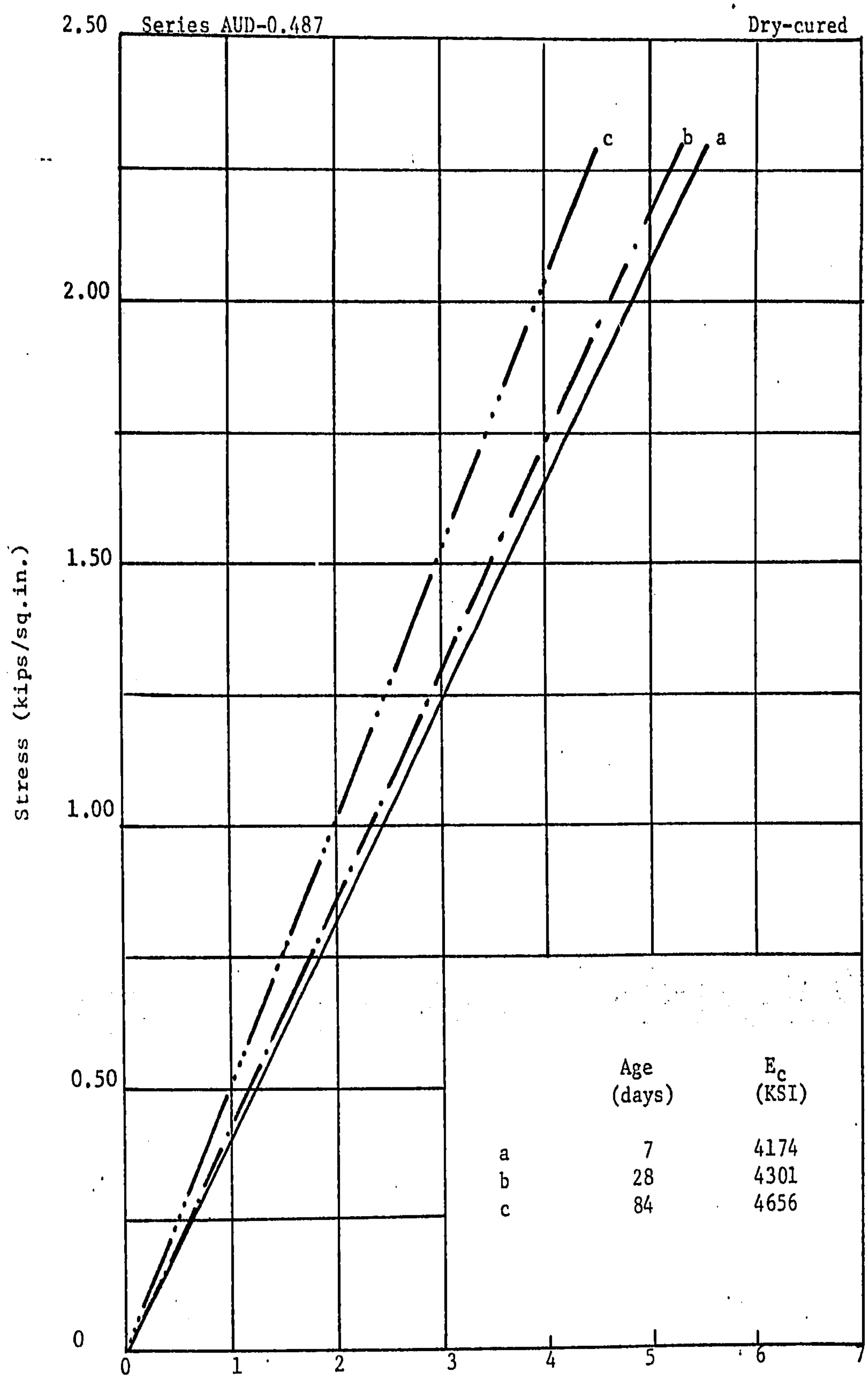

Strain in 10^{-4} (in./in.)

FIG. 4.4: STRESS-STRAIN CURVE FOR CONCRETE

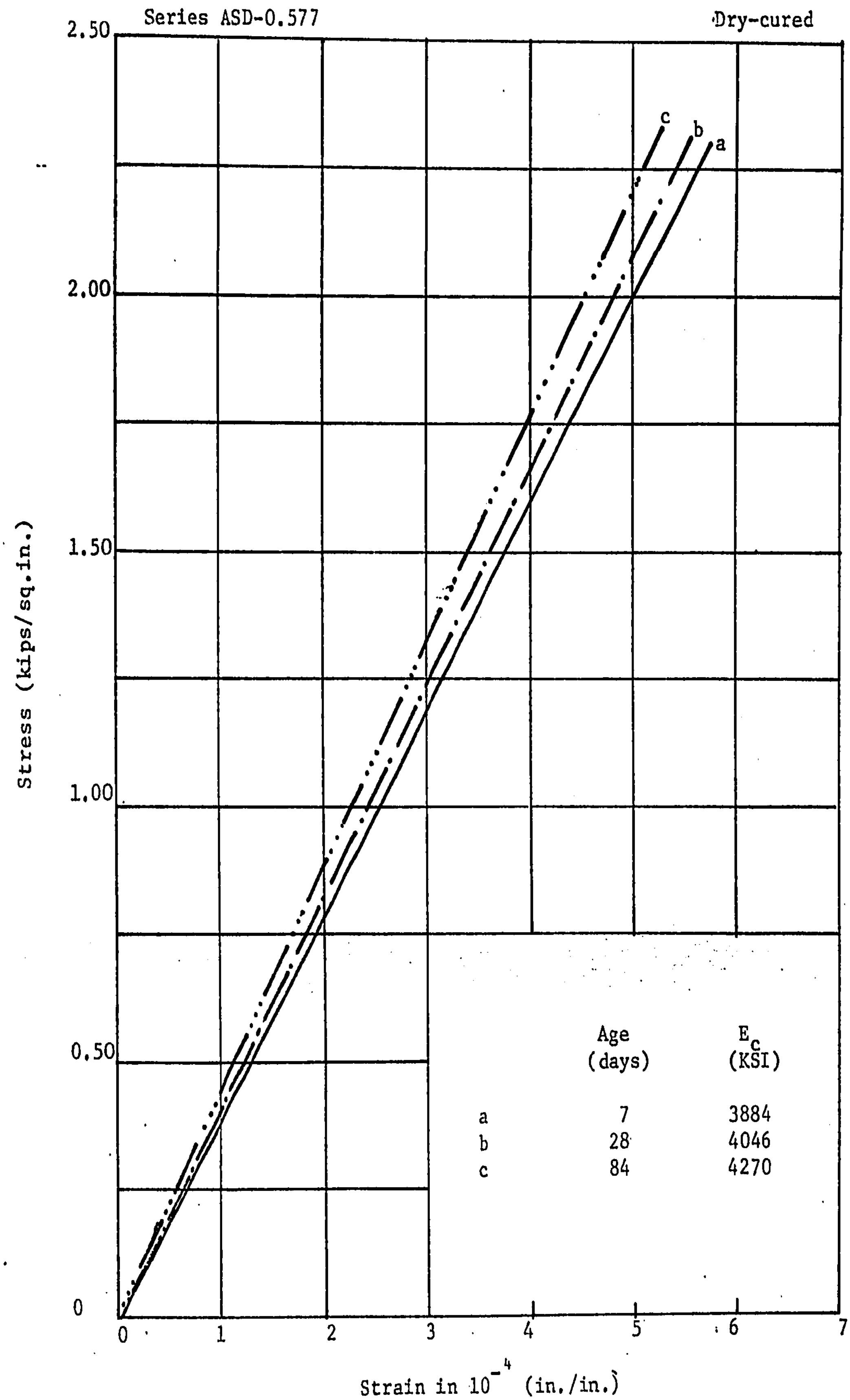

FIG. 4.5: STRESS-STRAIN CURVE FOR CONCRETE

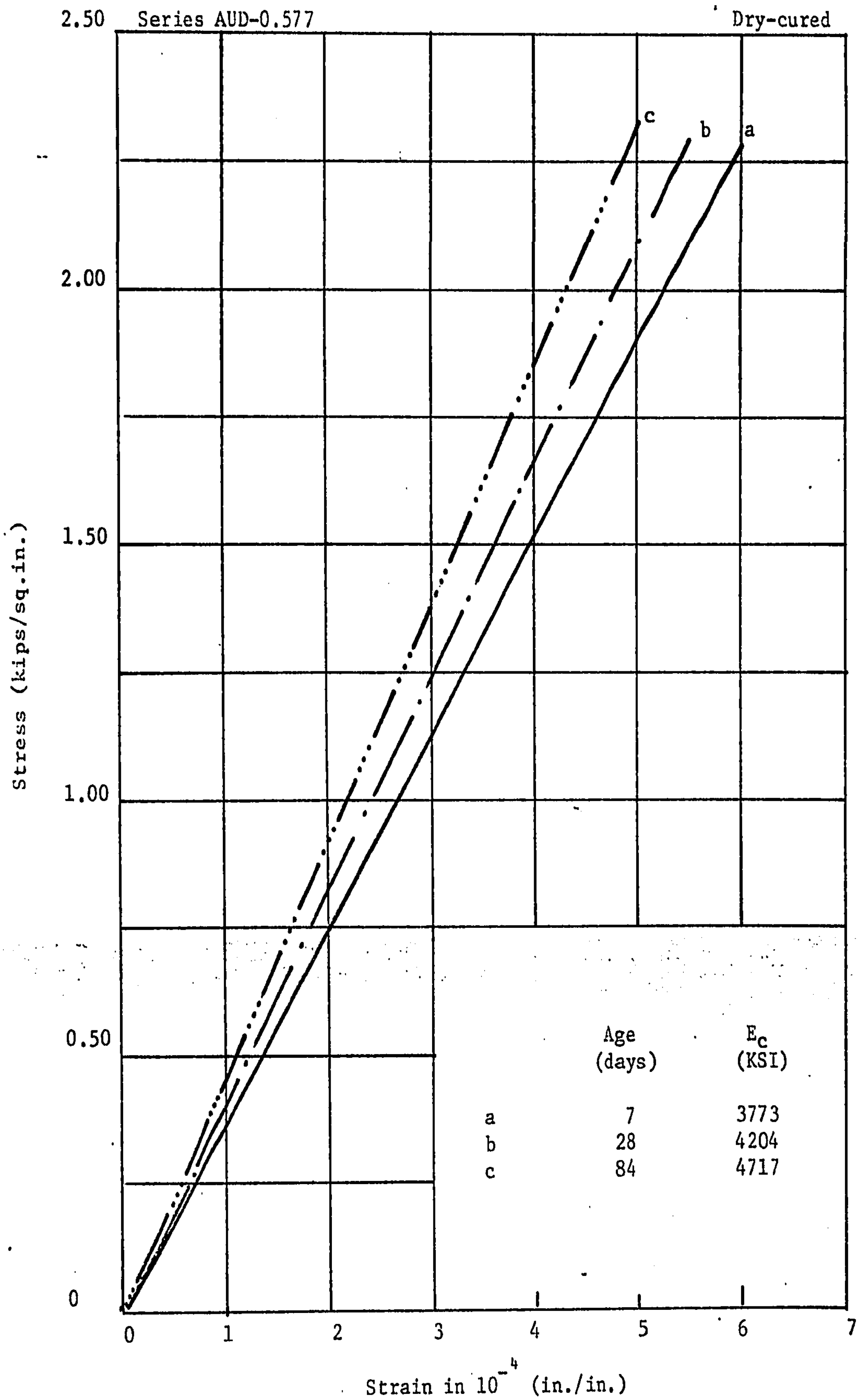

FIG. 4.6: STRESS-STRAIN CURVE FOR CONCRETE

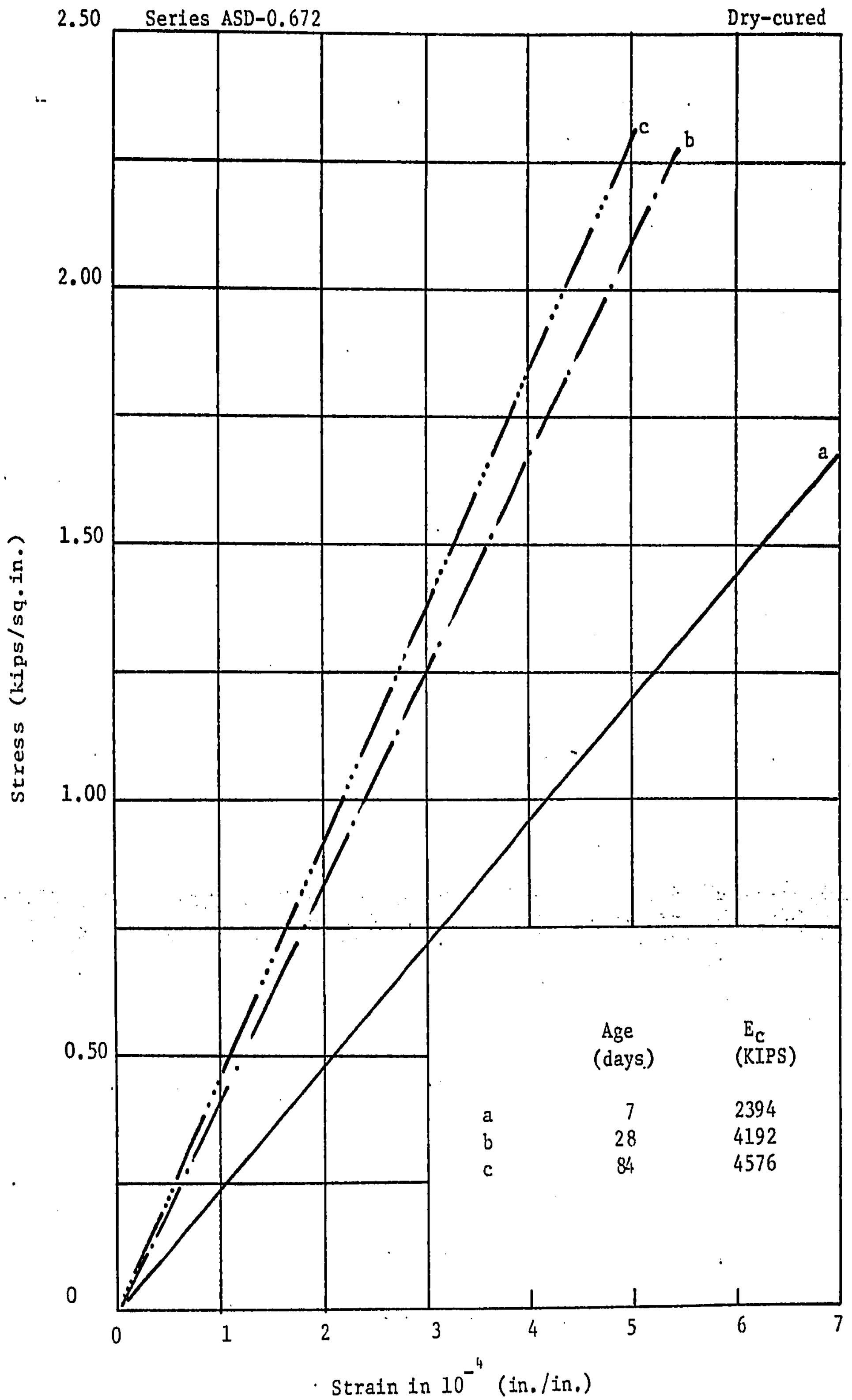

FIG. 4.7: STRESS-STRAIN CURVE FOR CONCRETE

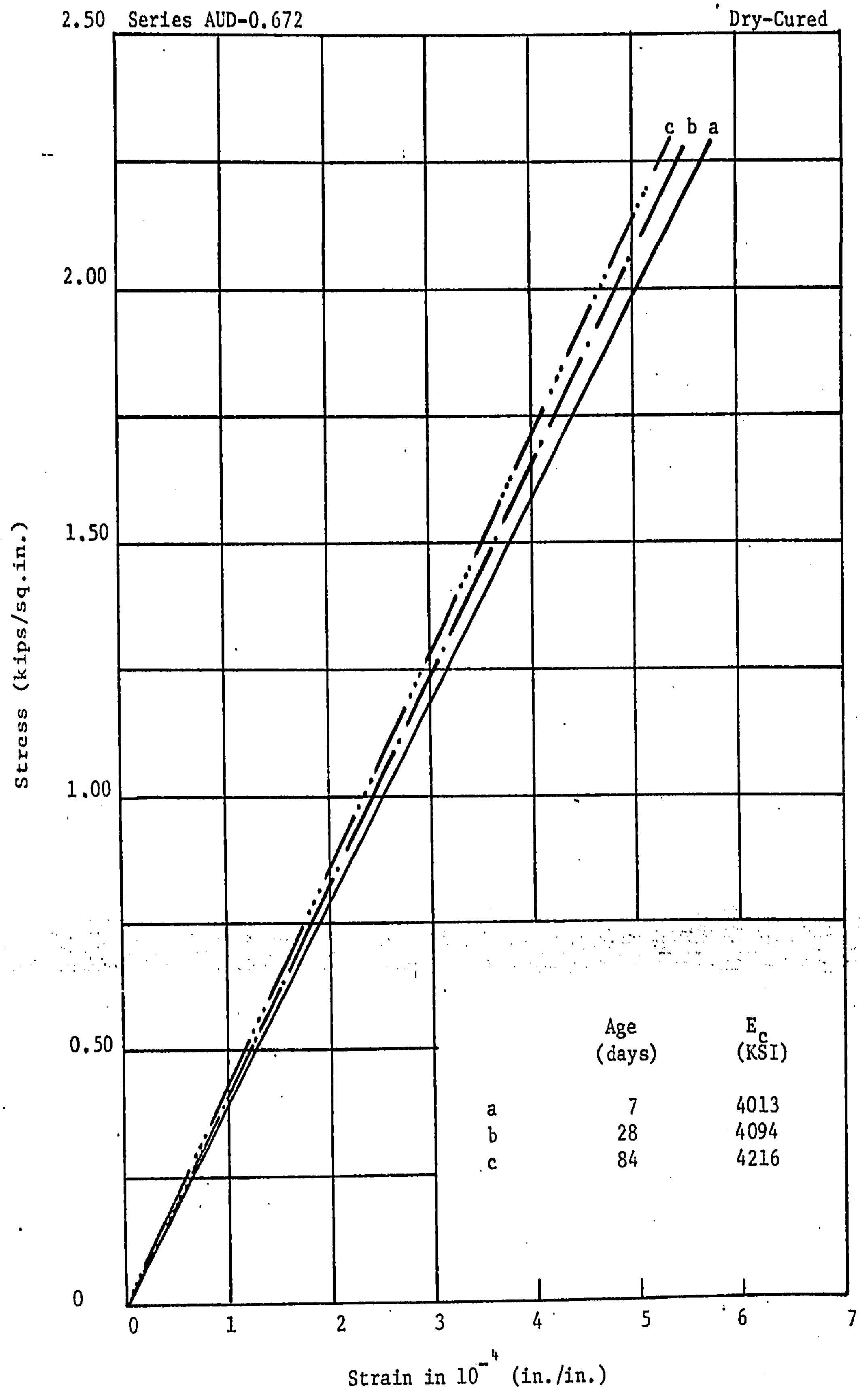

FIG. 4.8: STRESS-STRAIN CURVE FOR CONCRETE

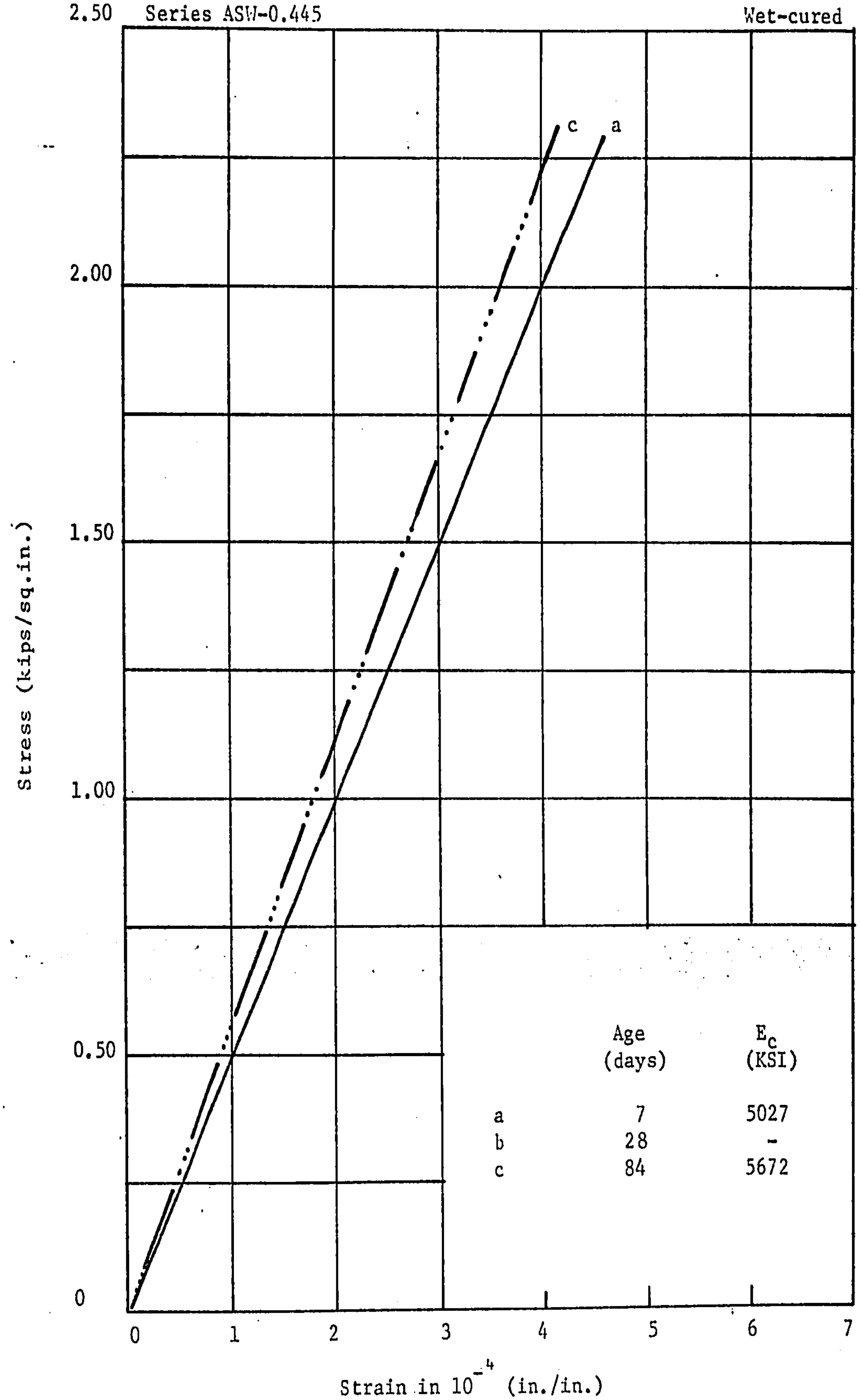

	Age (days)	E_c (KSI)
a	7	5027
b	28	-
c	84	5672

FIG. 4.9: STRESS-STRAIN CURVE FOR CONCRETE

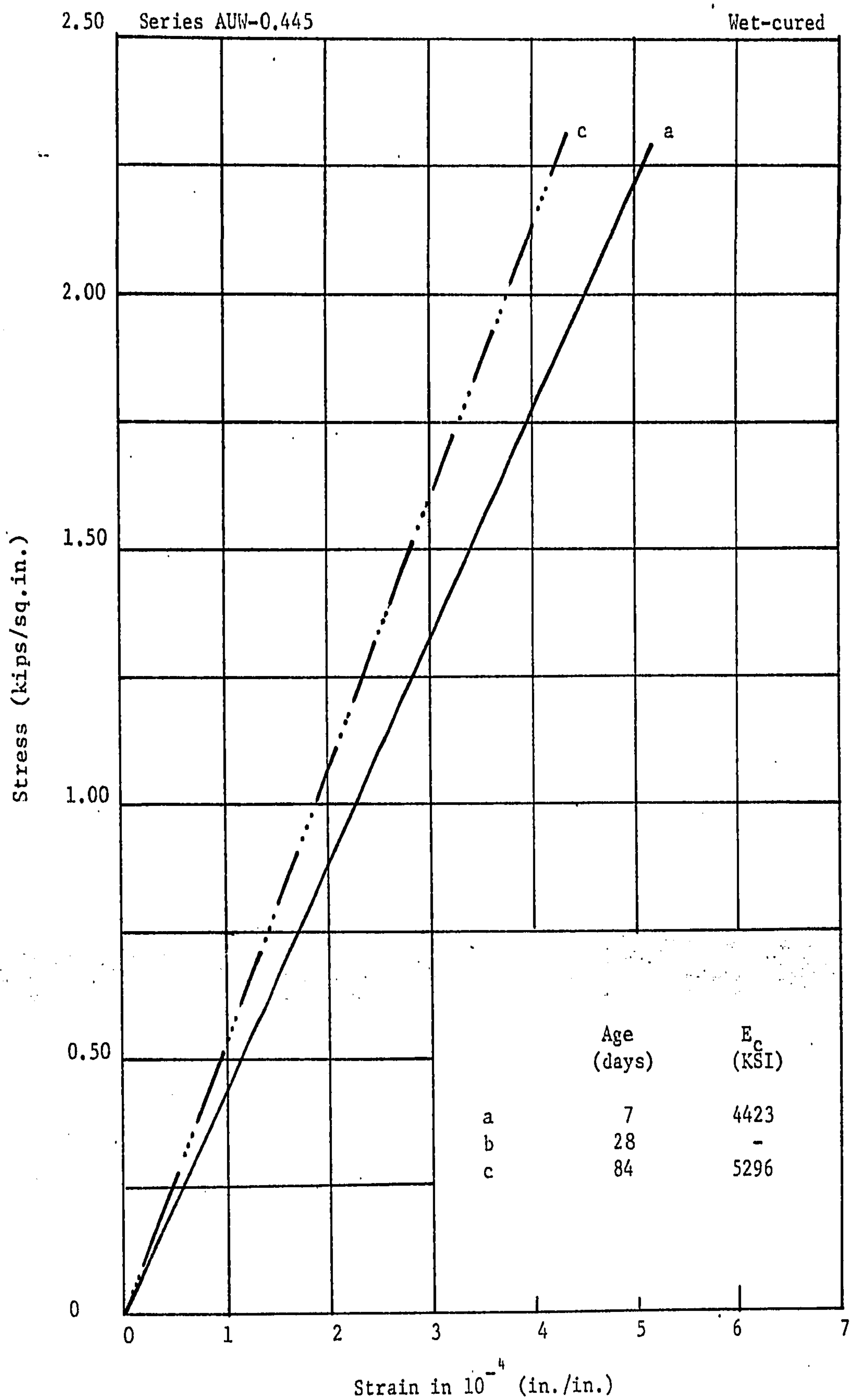

	Age (days)	E_c (KSI)
a	7	4423
b	28	-
c	84	5296

FIG. 4.10: STRESS-STRAIN CURVE FOR CONCRETE

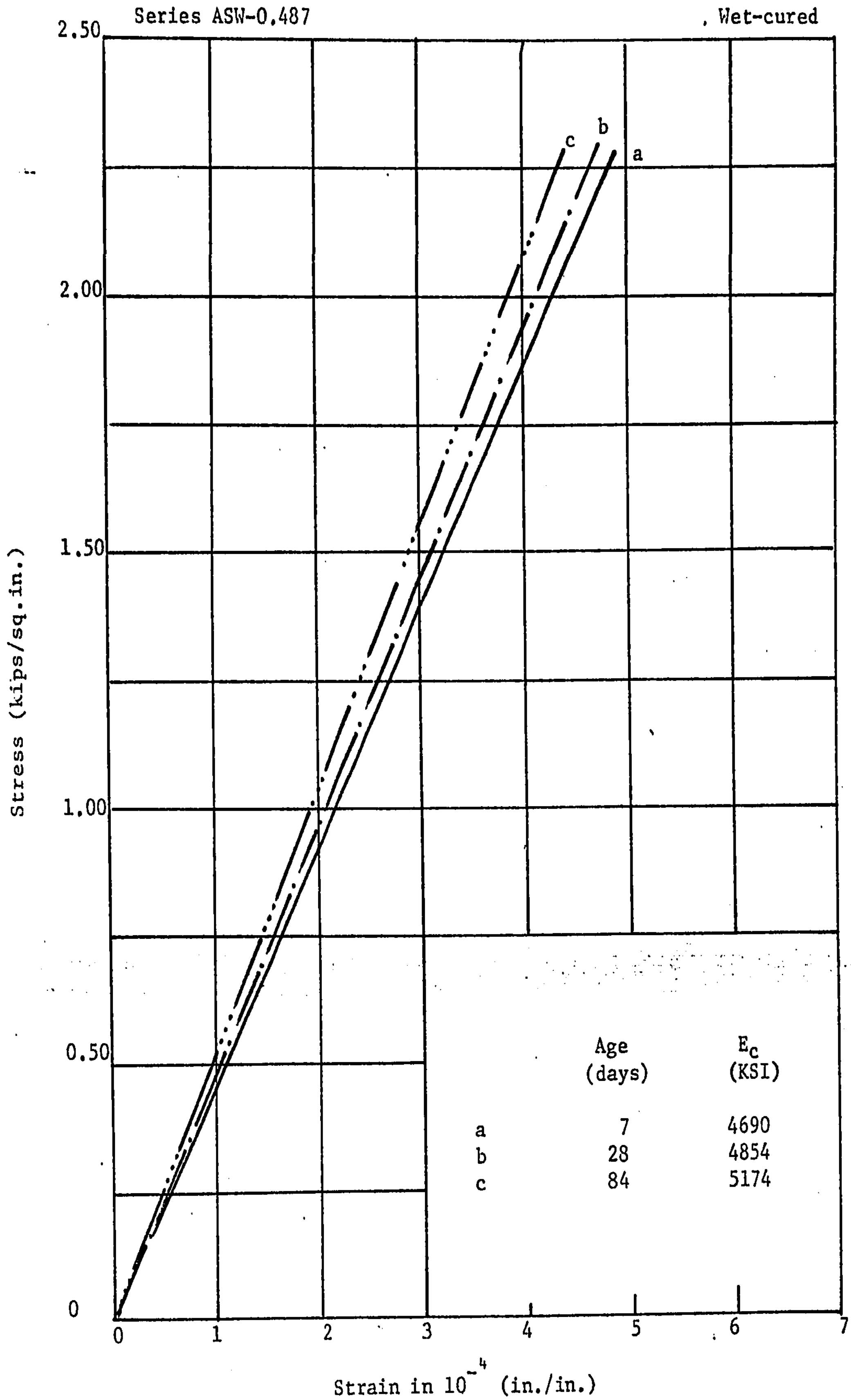

FIG. 4.11: STRESS-STRAIN CURVE FOR CONCRETE

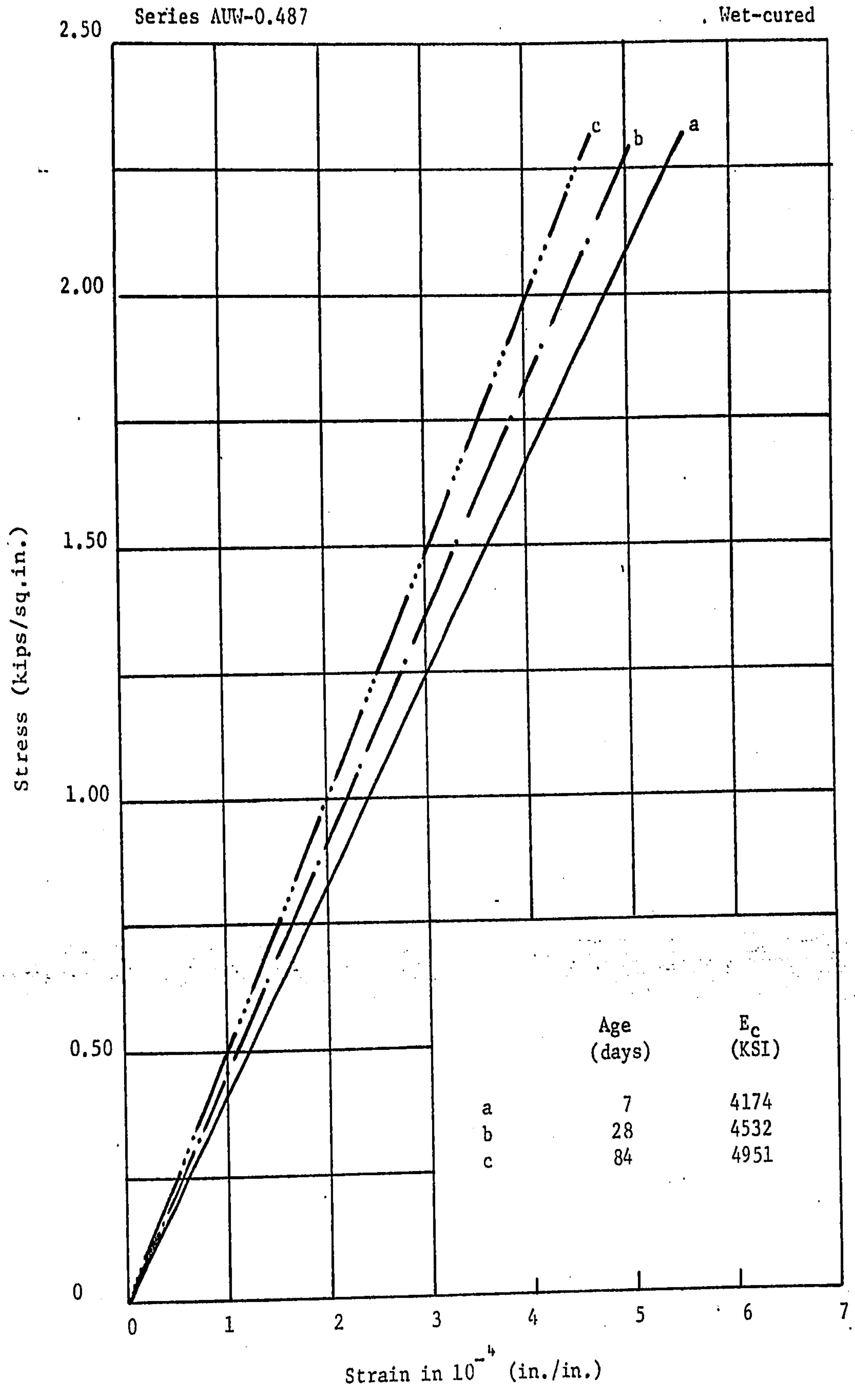

FIG. 4.12: STRESS-STRAIN CURVE FOR CONCRETE

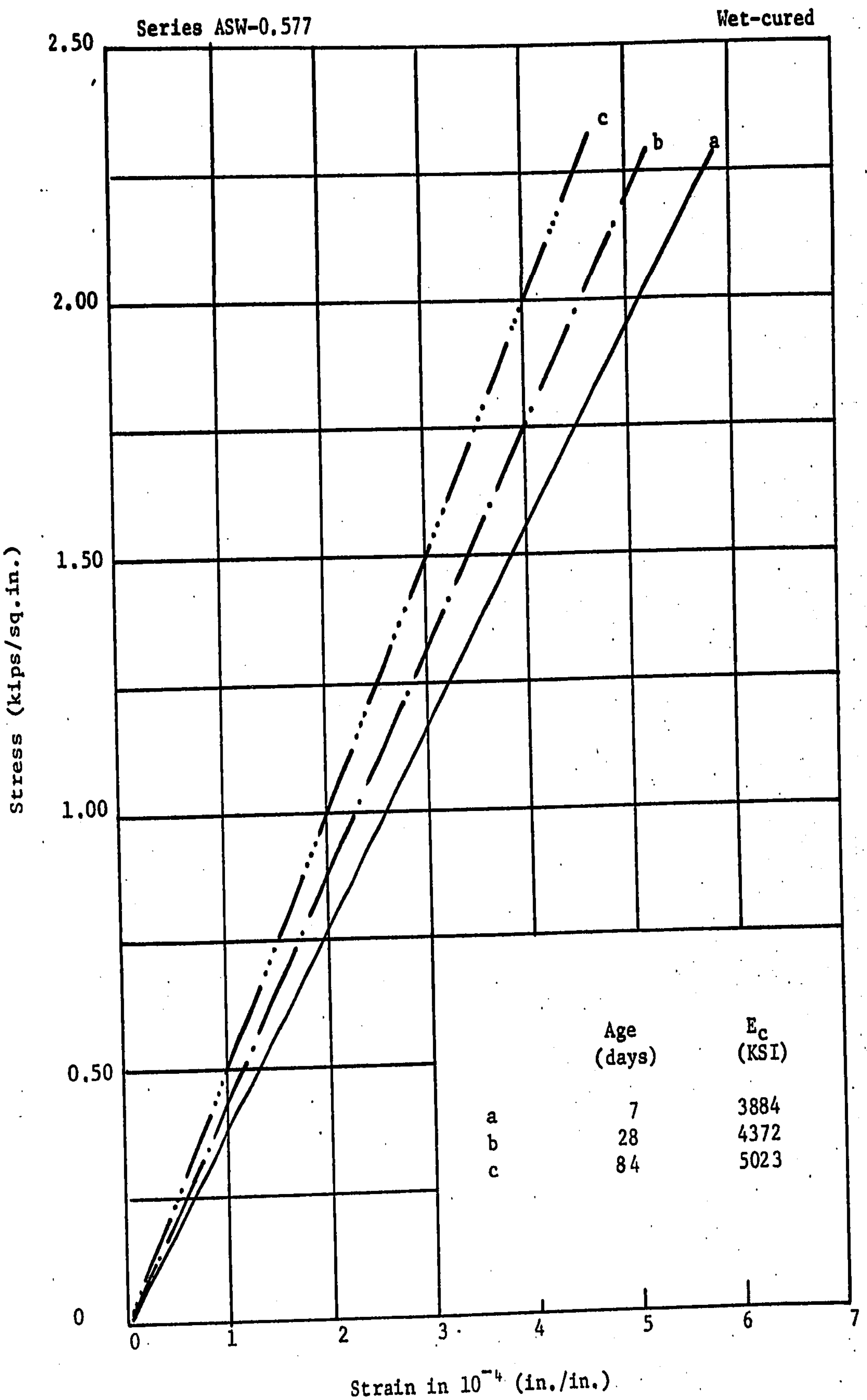

FIG. 4.13: STRESS-STRAIN CURVE FOR CONCRETE

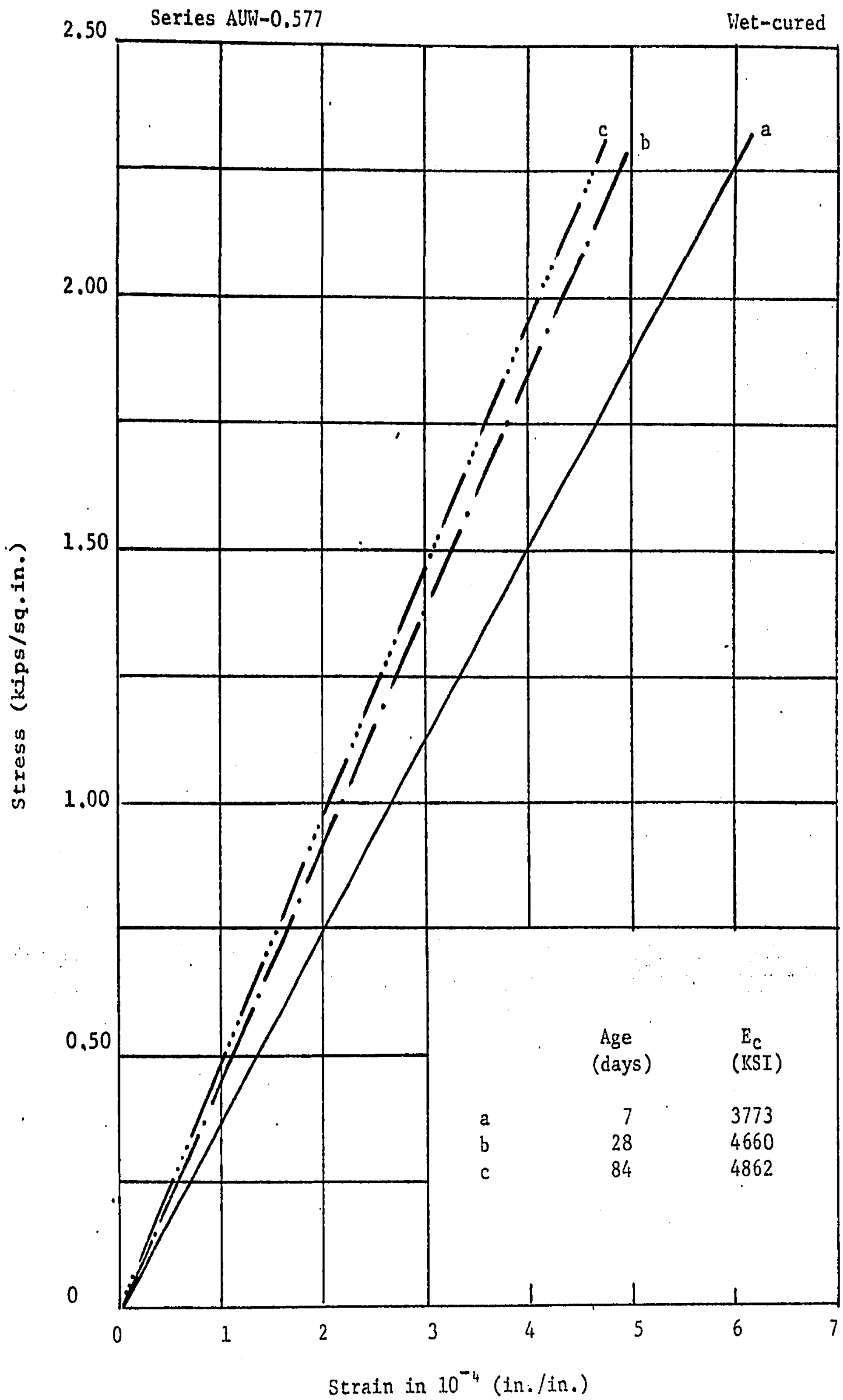

FIG. 4.14: STRESS-STRAIN CURVE FOR CONCRETE

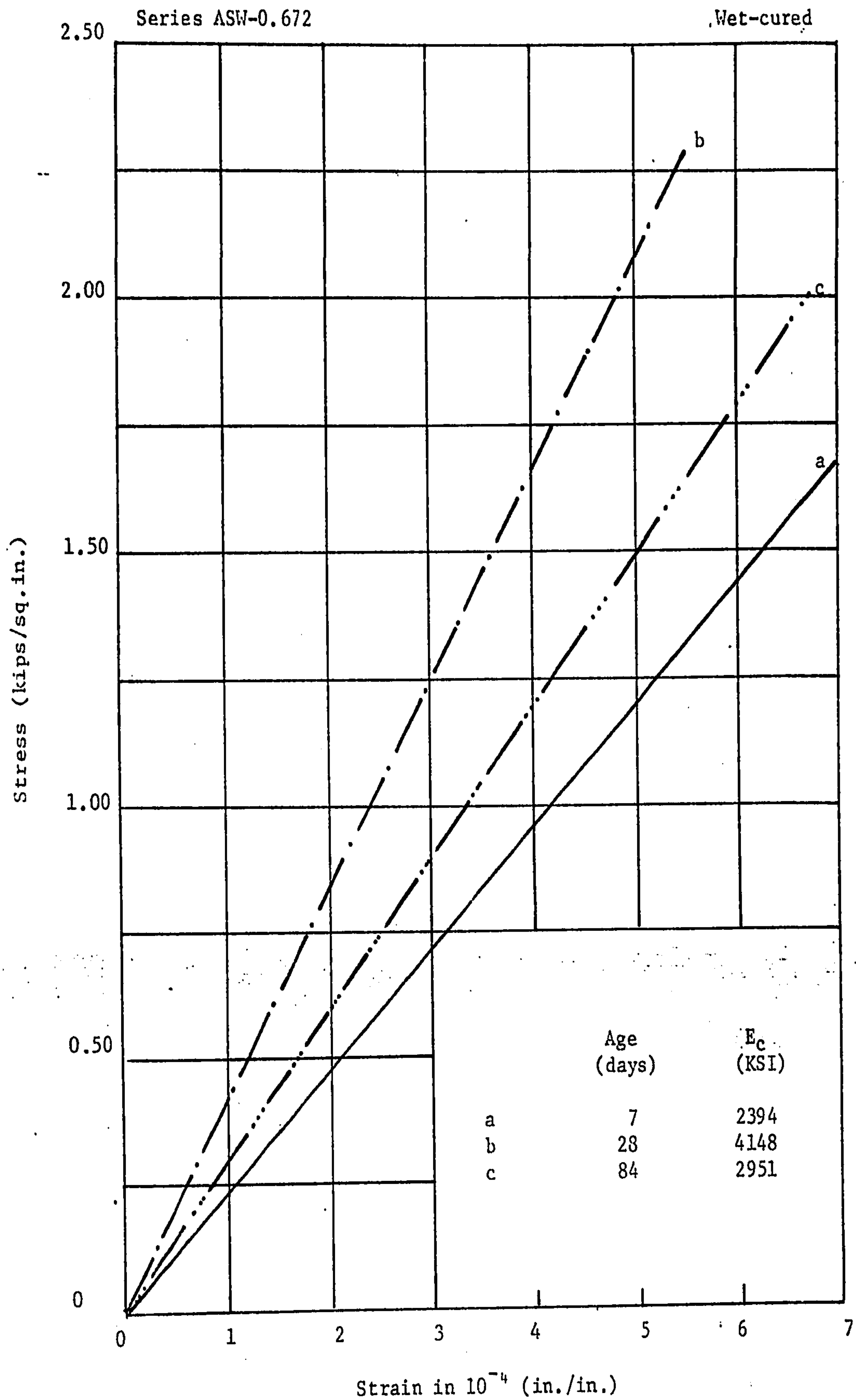

	Age (days)	E_c (KSI)
a	7	2394
b	28	4148
c	84	2951

FIG. 4.15: STRESS-STRAIN CURVE FOR CONCRETE

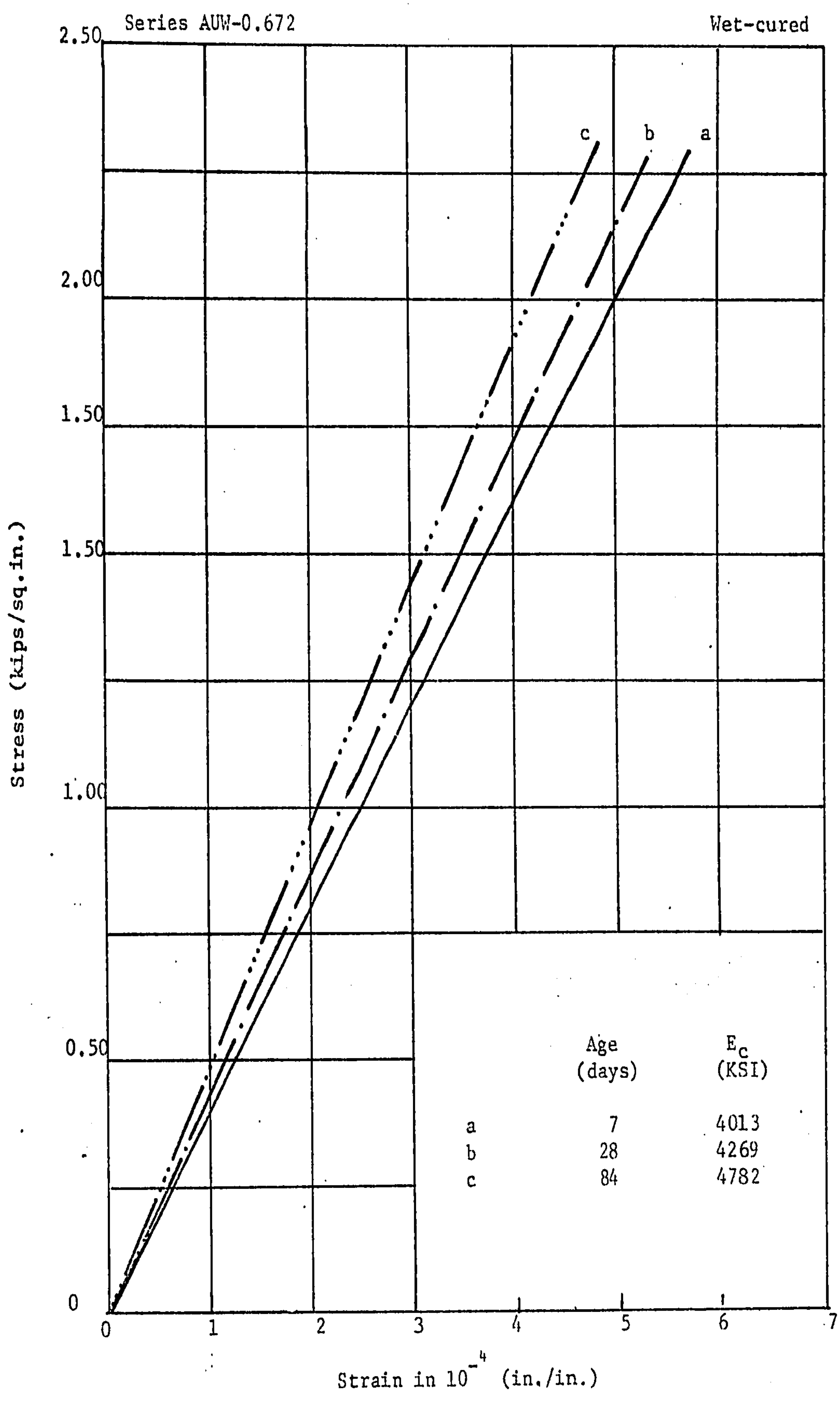

	Age (days)	E_c (KSI)
a	7	4013
b	28	4269
c	84	4782

FIG. 4.16: STRESS-STRAIN CURVE FOR CONCRETE

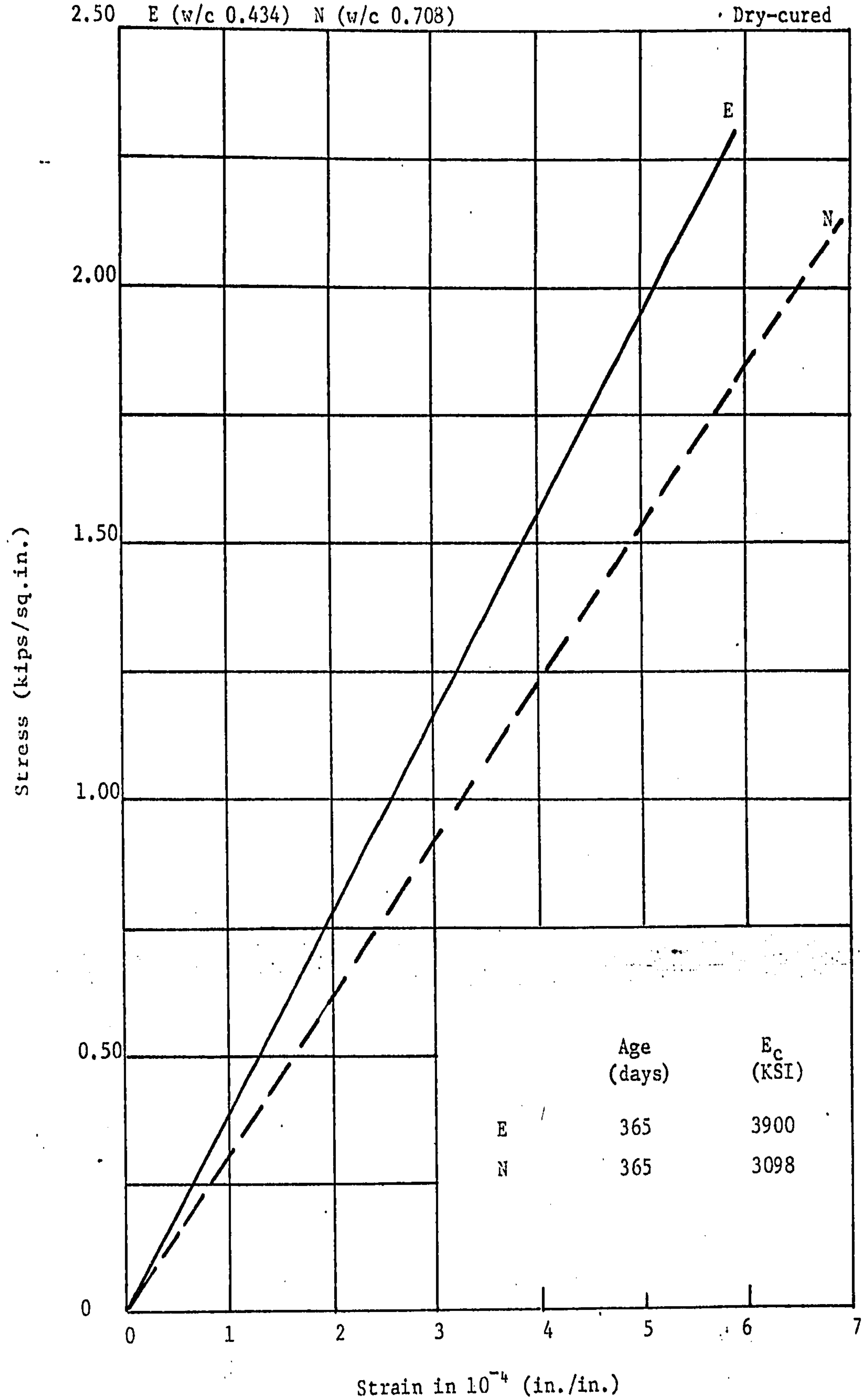

FIG. 4.17: STRESS-STRAIN CURVE FOR CONCRETE

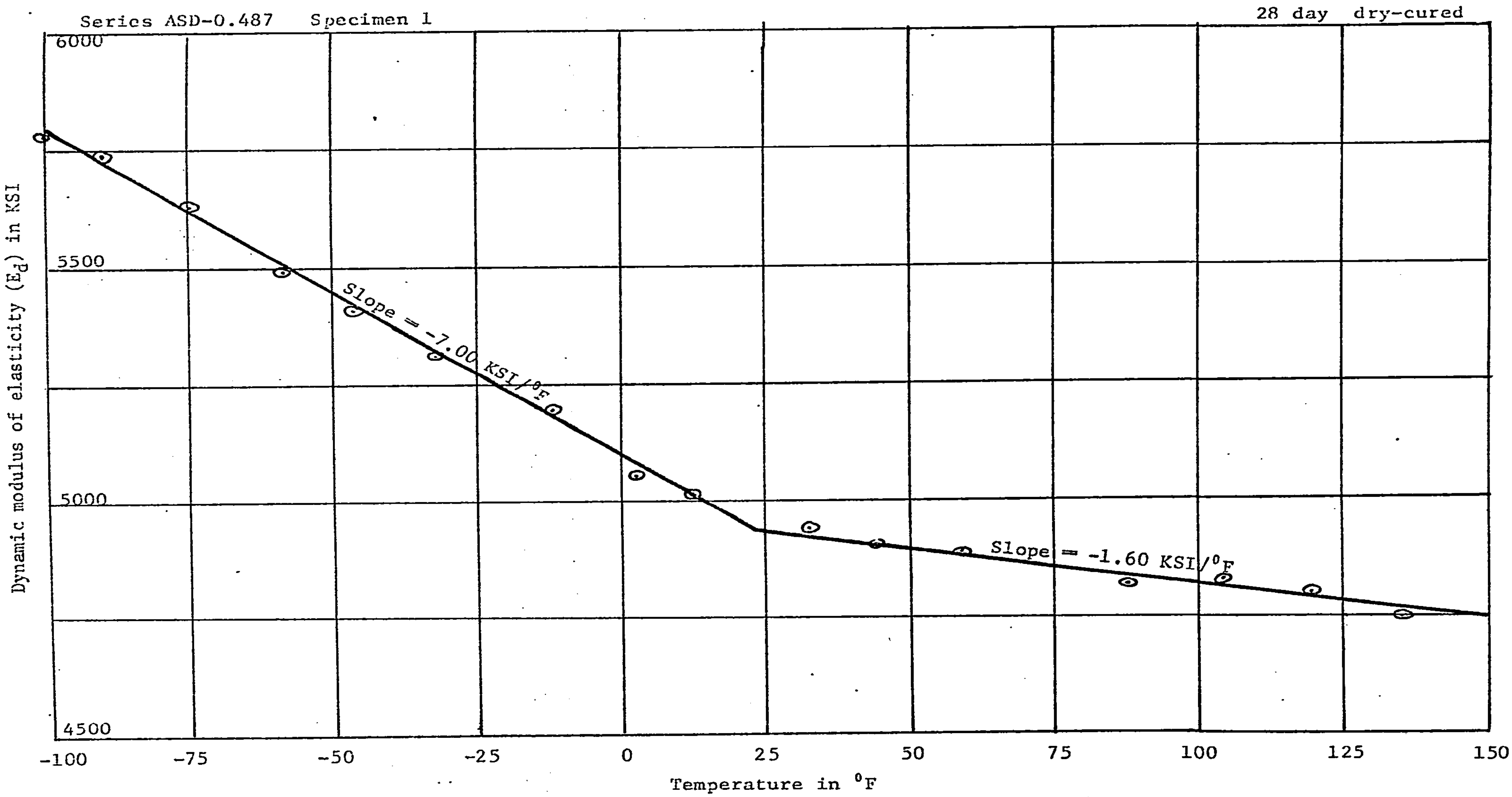

FIG. 4.18: EFFECT OF TEMPERATURE ON DYNAMIC MODULUS OF ELASTICITY

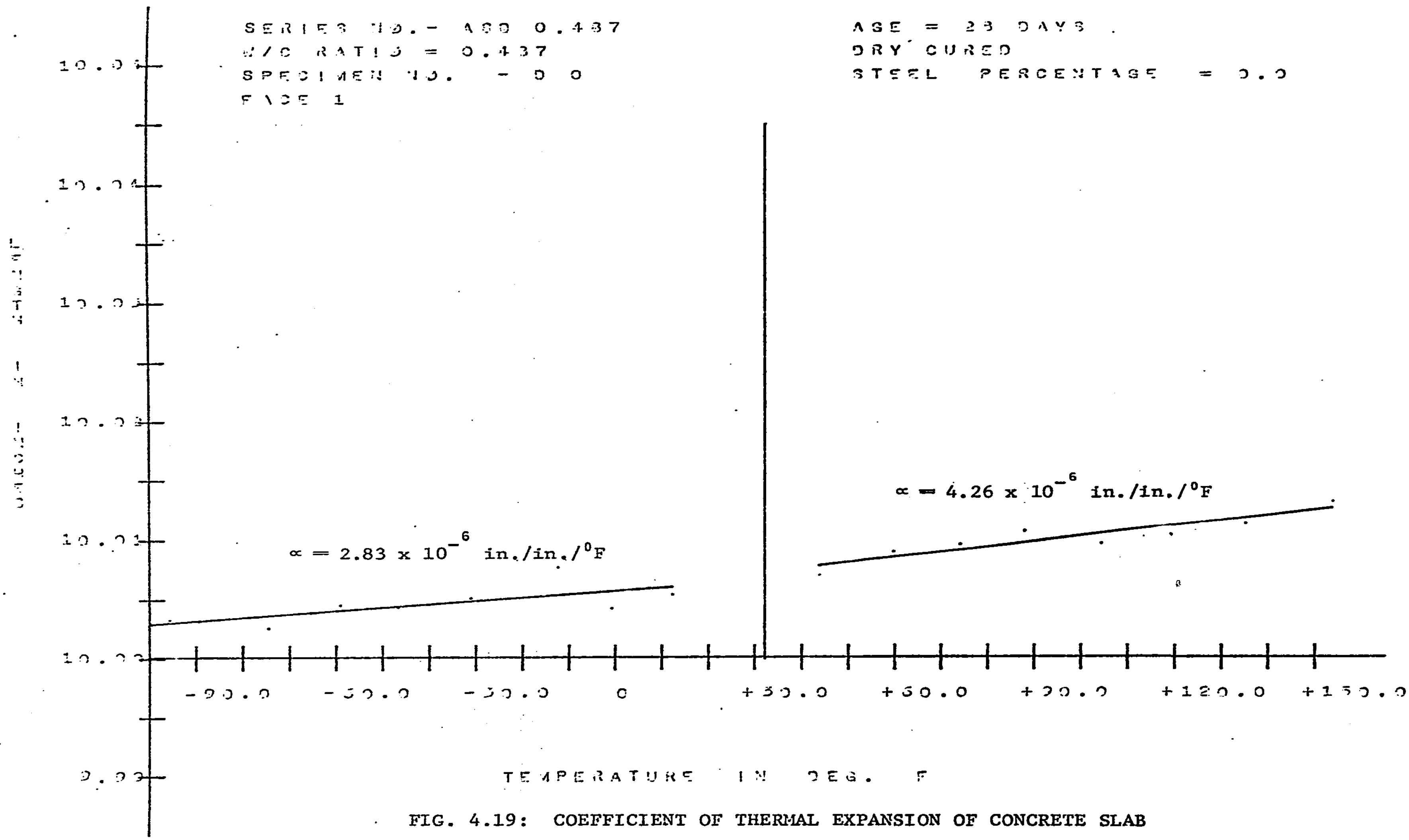

FIG. 4.19: COEFFICIENT OF THERMAL EXPANSION OF CONCRETE SLAB

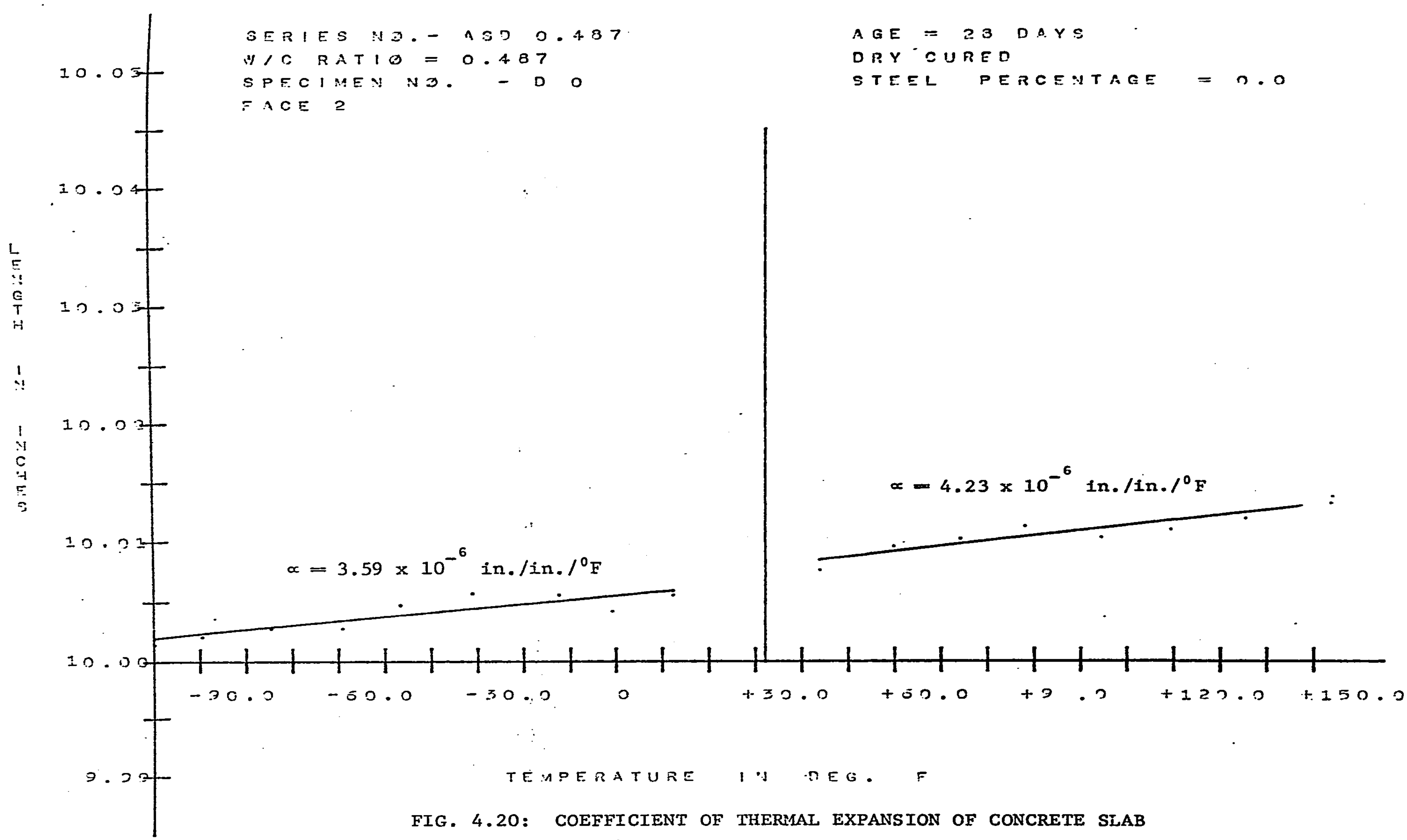

FIG. 4.20: COEFFICIENT OF THERMAL EXPANSION OF CONCRETE SLAB

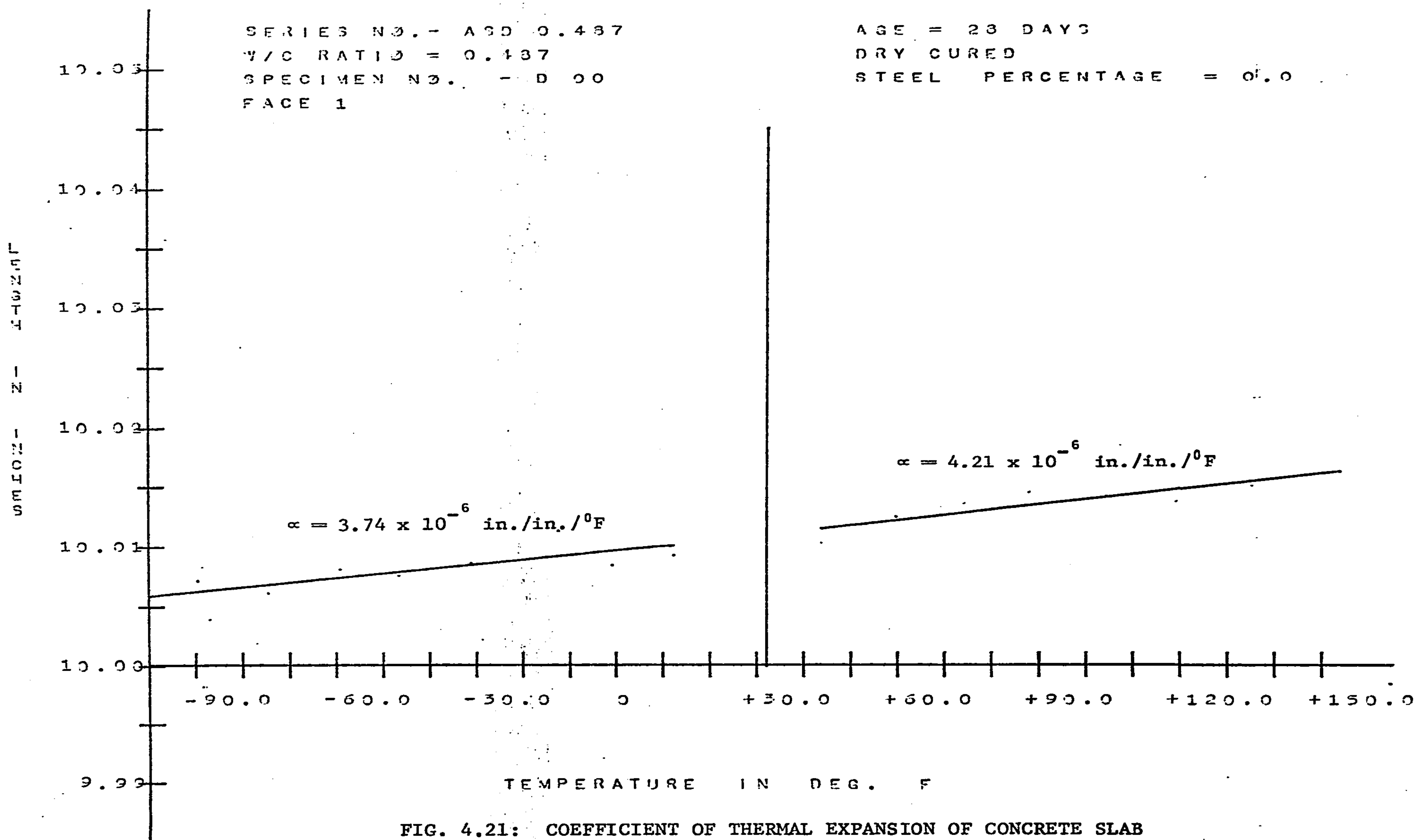

FIG. 4.21: COEFFICIENT OF THERMAL EXPANSION OF CONCRETE SLAB

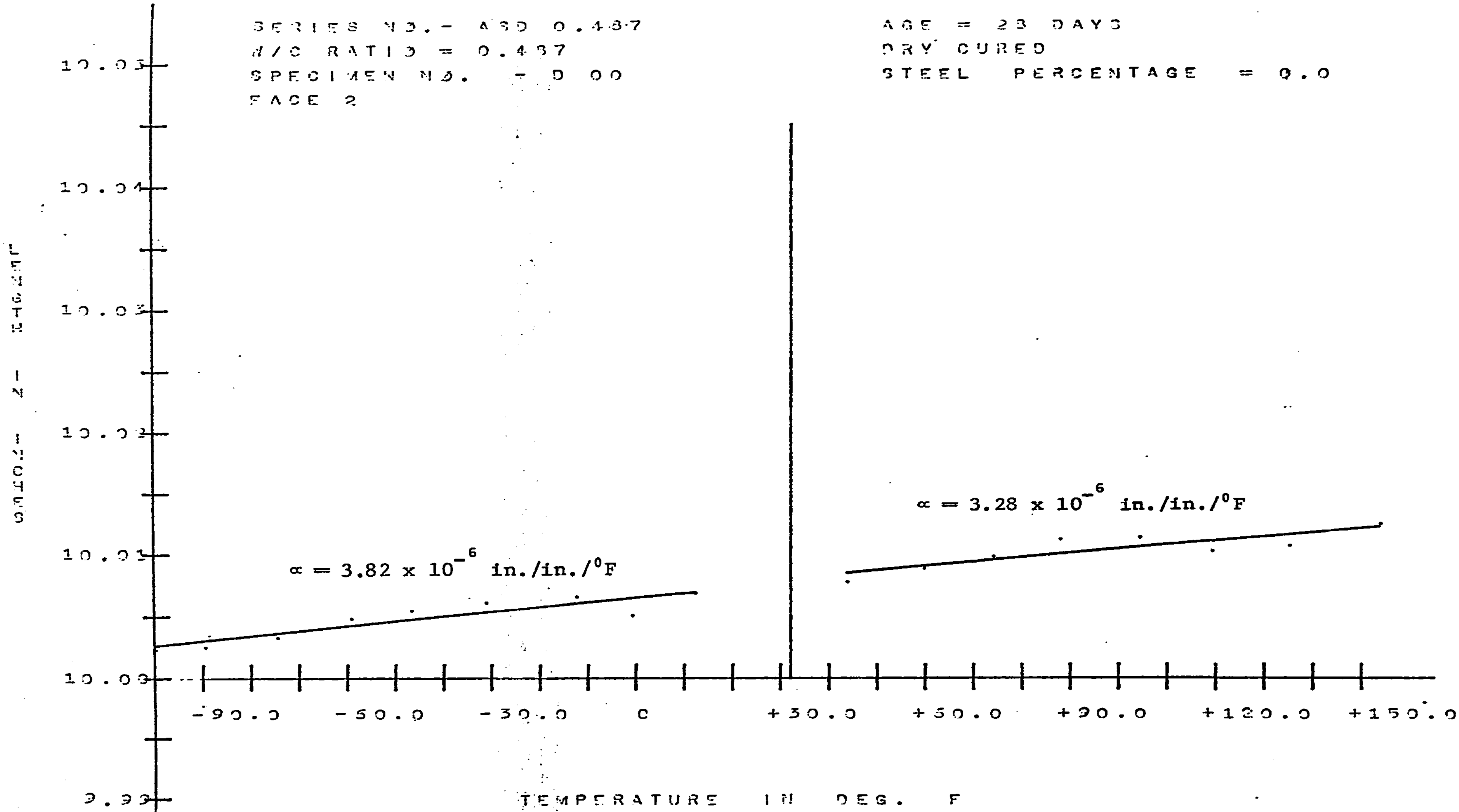

FIG. 4.22: COEFFICIENT OF THERMAL EXPANSION OF CONCRETE SLAB

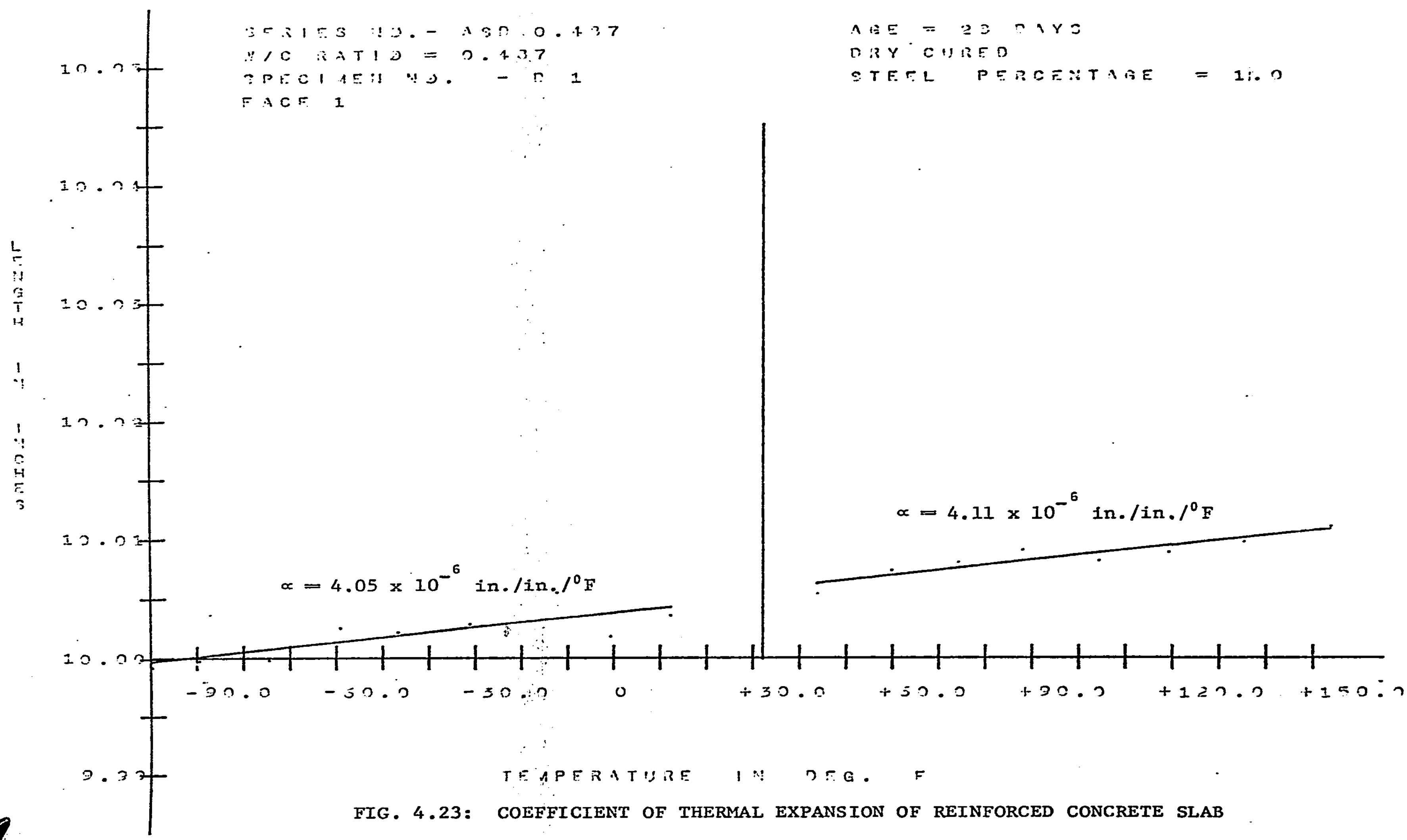

FIG. 4.23: COEFFICIENT OF THERMAL EXPANSION OF REINFORCED CONCRETE SLAB

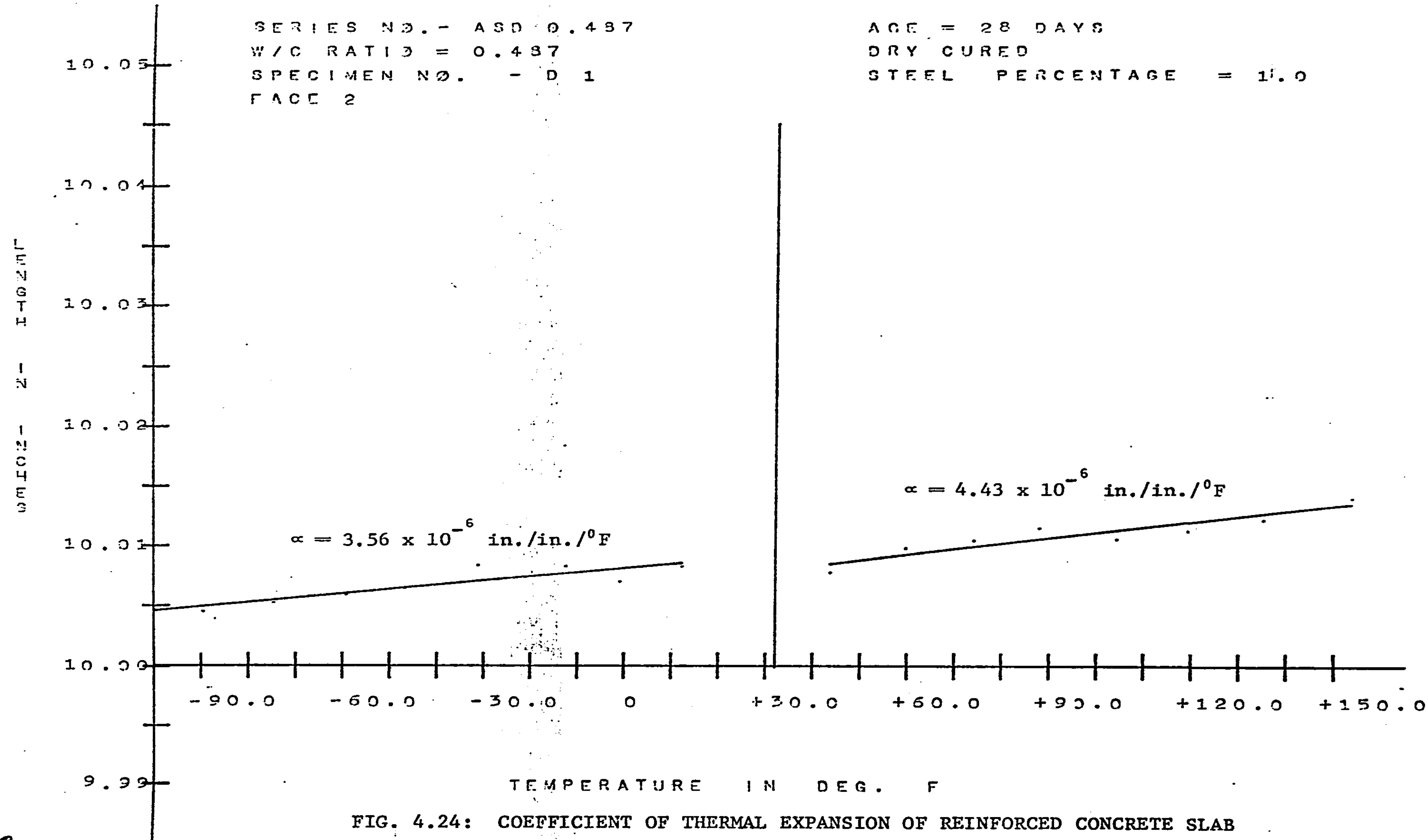

FIG. 4.24: COEFFICIENT OF THERMAL EXPANSION OF REINFORCED CONCRETE SLAB

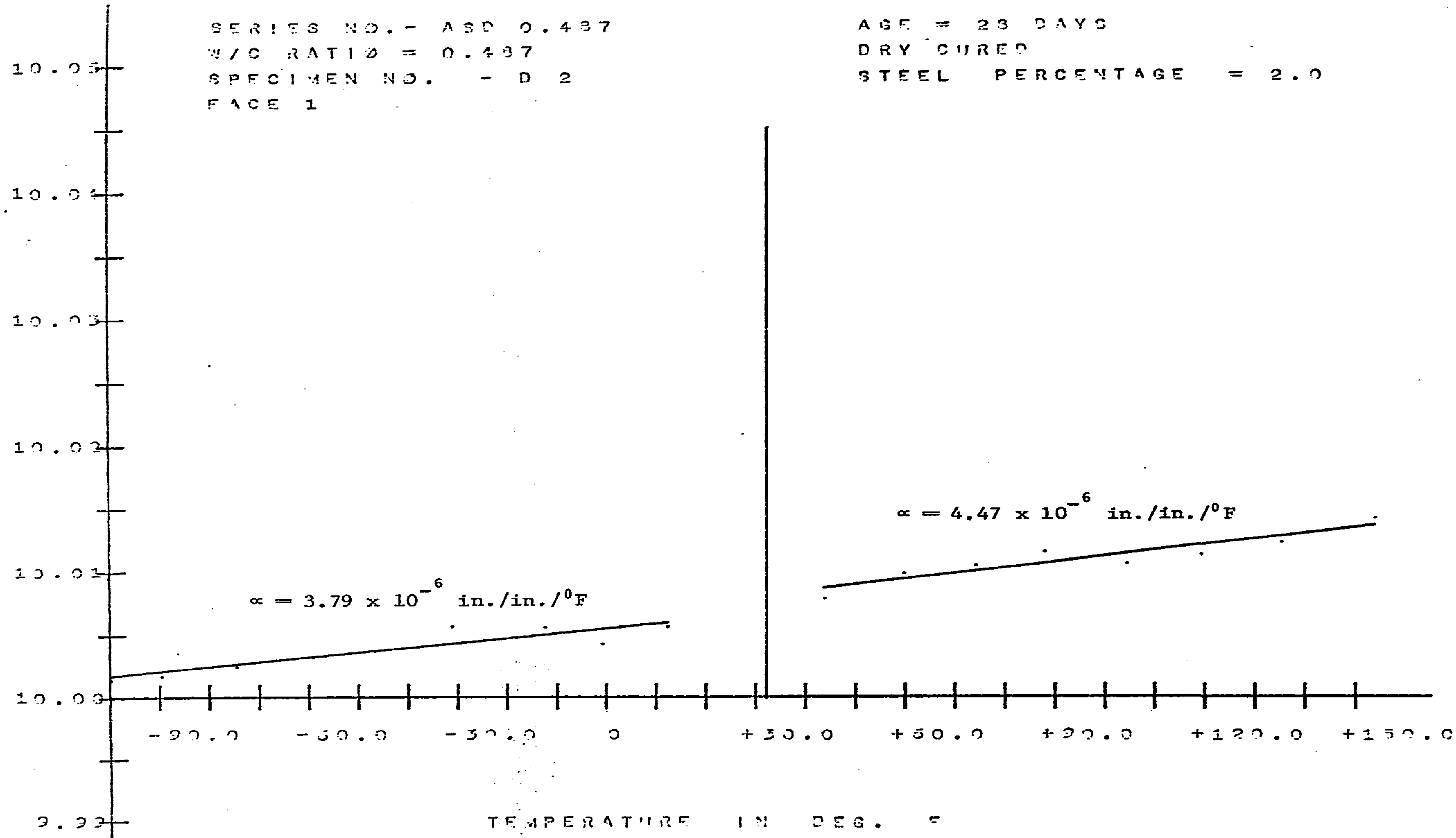

FIG. 4.25: COEFFICIENT OF THERMAL EXPANSION OF REINFORCED CONCRETE SLAB

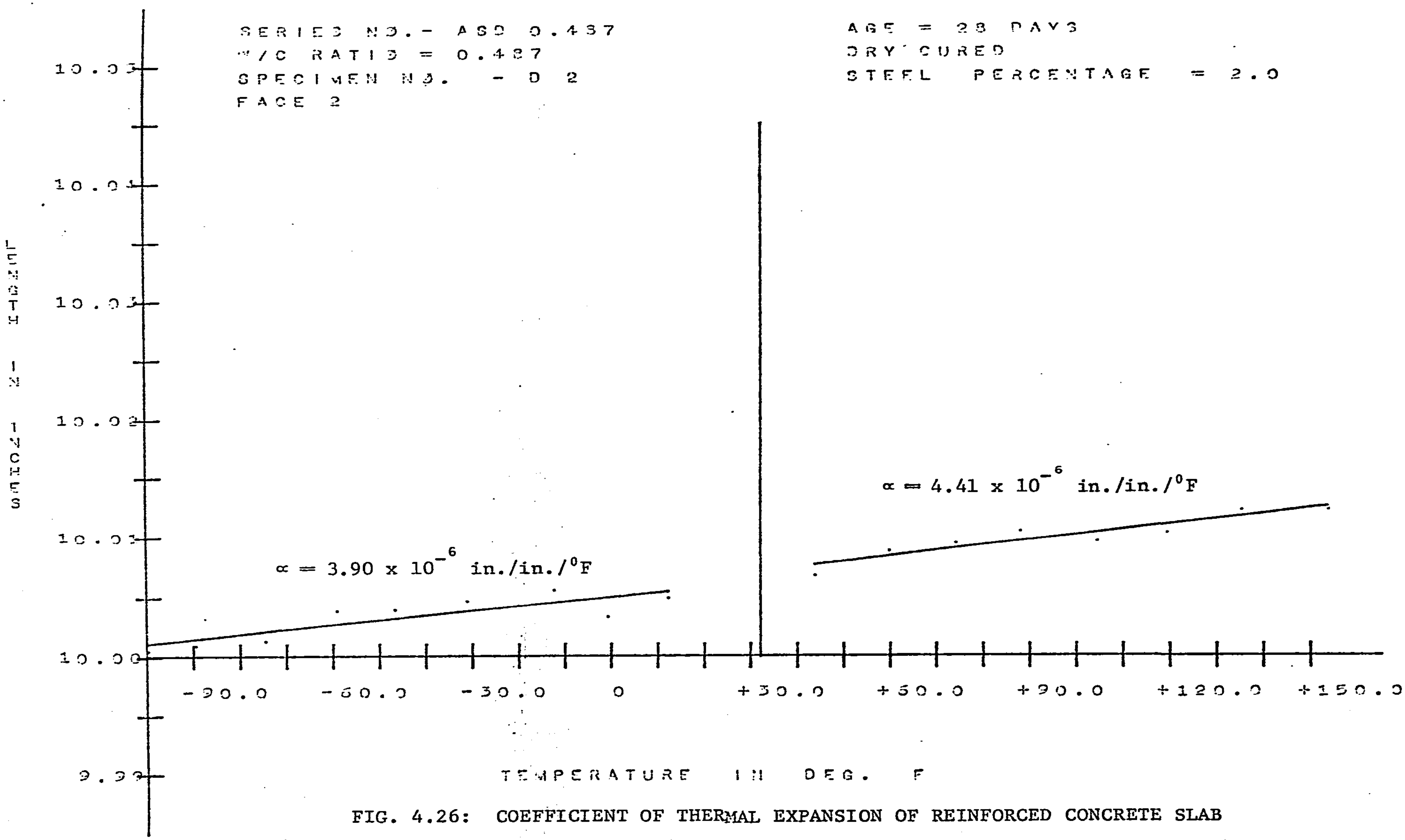

FIG. 4.26: COEFFICIENT OF THERMAL EXPANSION OF REINFORCED CONCRETE SLAB

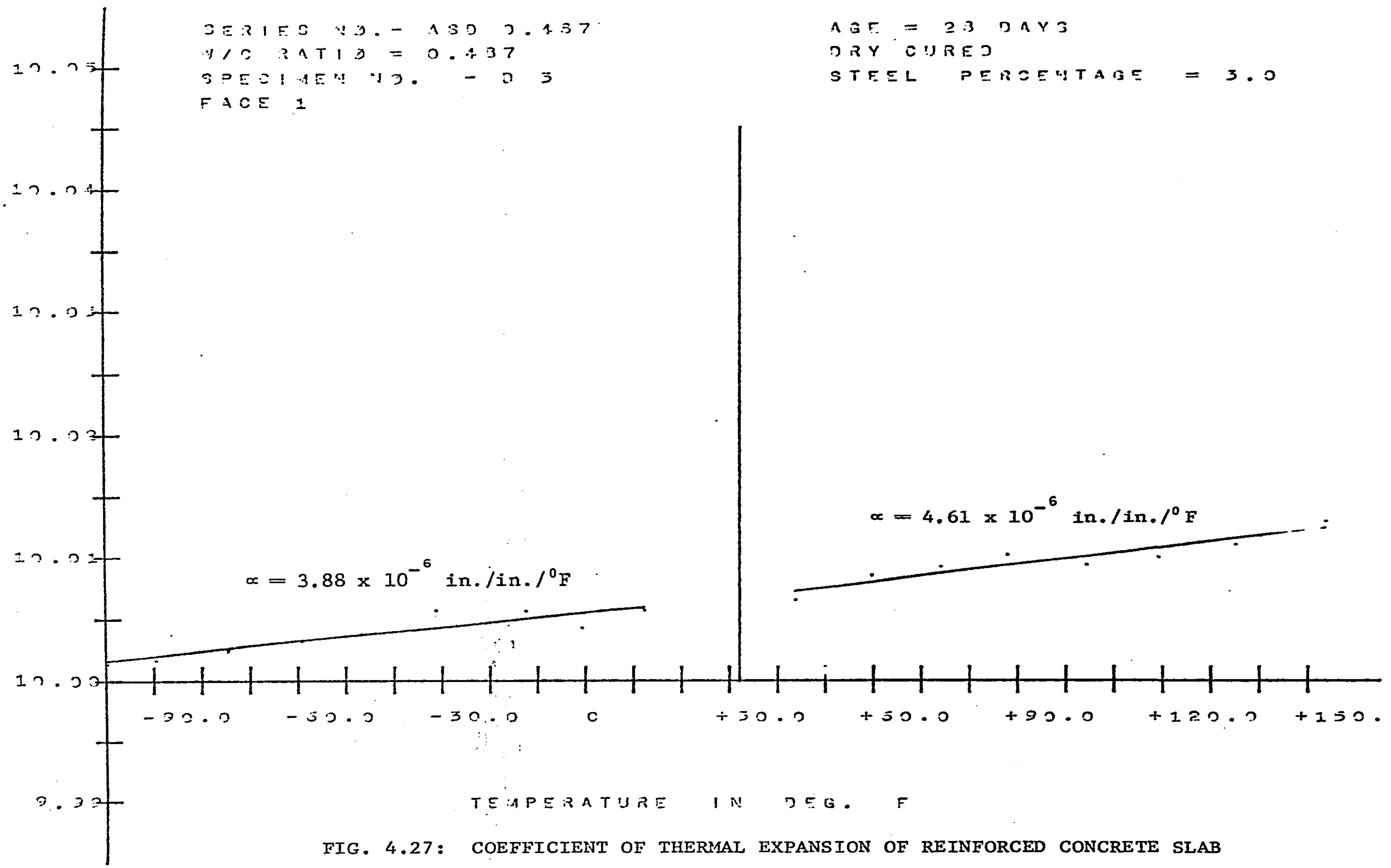

FIG. 4.27: COEFFICIENT OF THERMAL EXPANSION OF REINFORCED CONCRETE SLAB

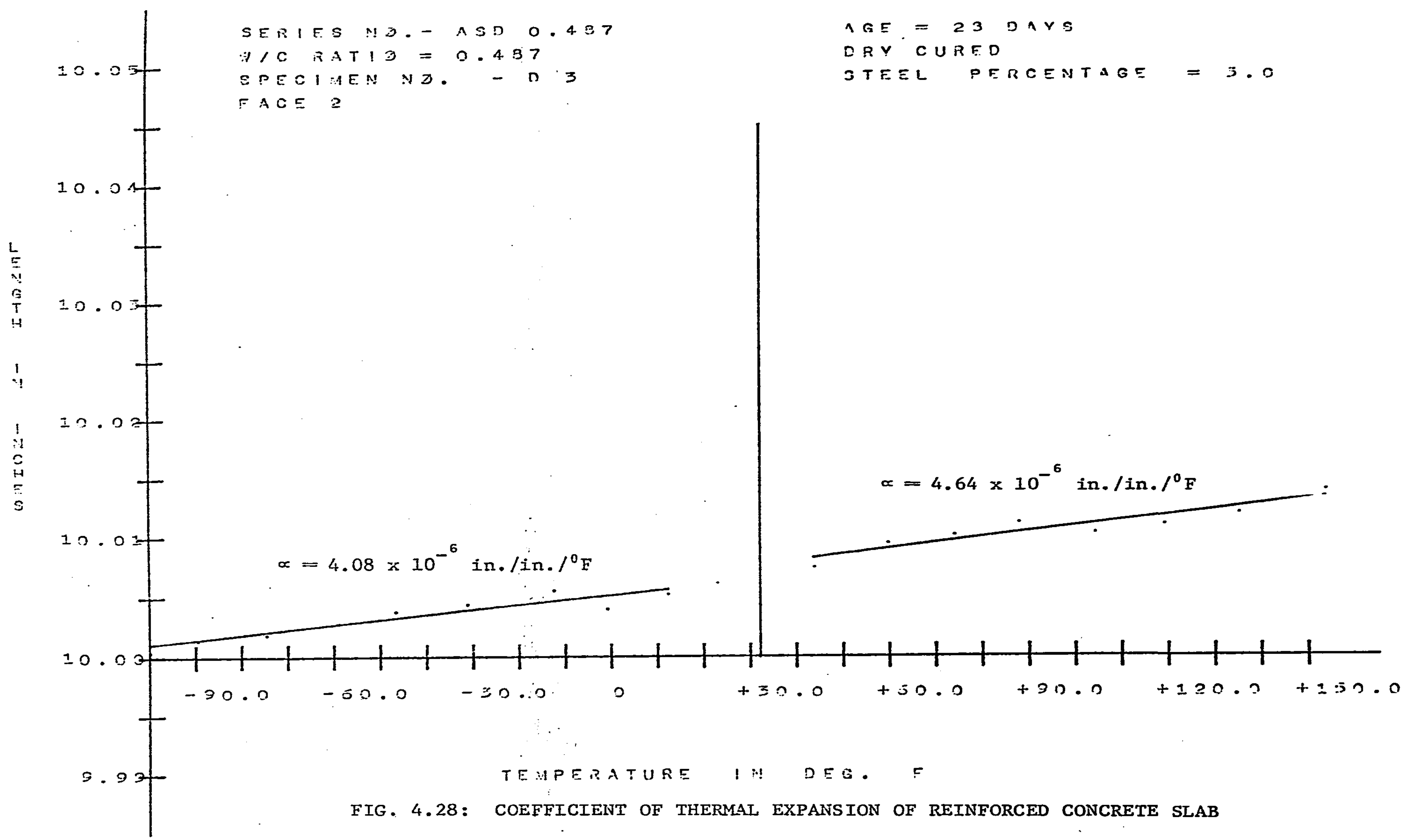

FIG. 4.28: COEFFICIENT OF THERMAL EXPANSION OF REINFORCED CONCRETE SLAB

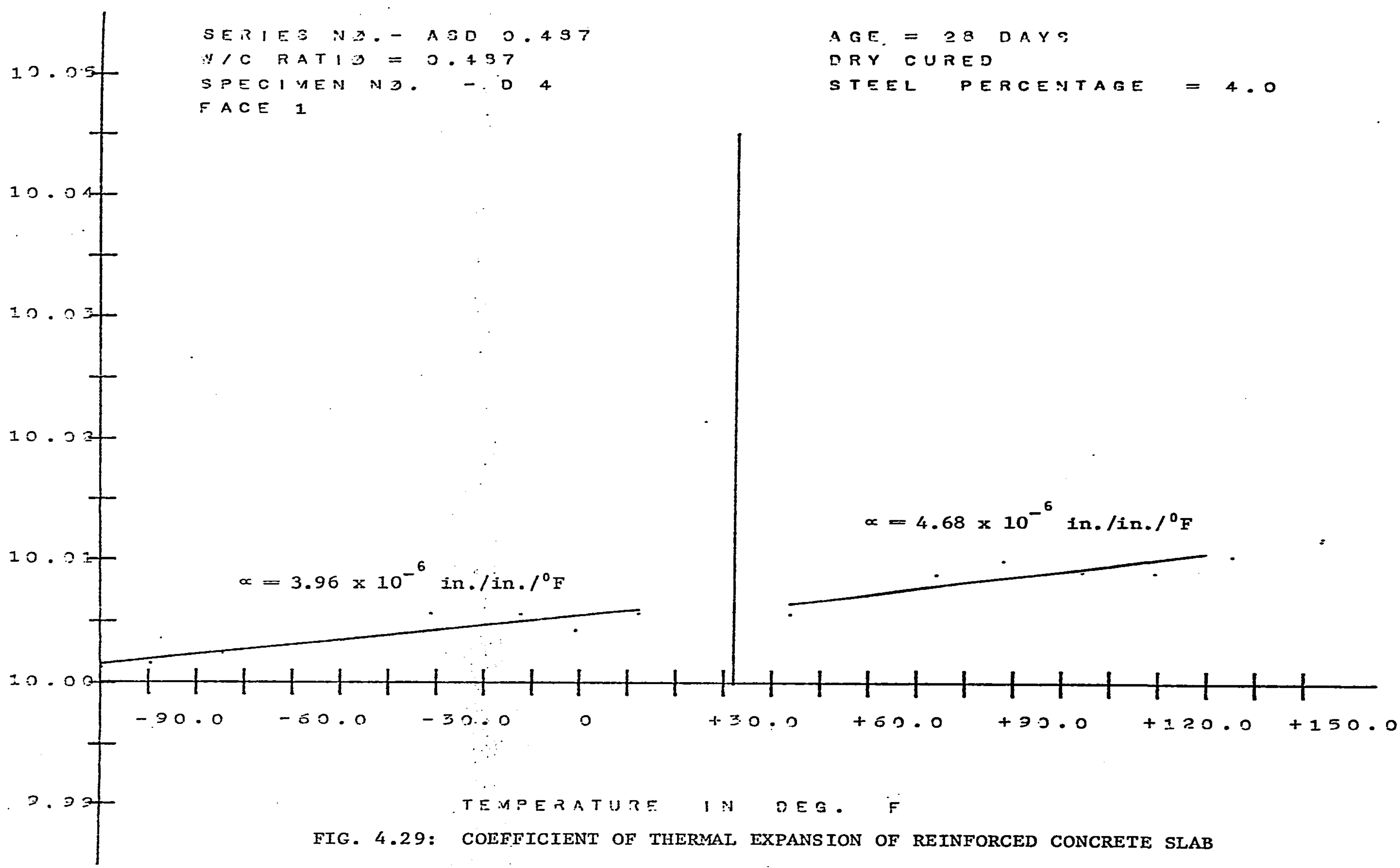

FIG. 4.29: COEFFICIENT OF THERMAL EXPANSION OF REINFORCED CONCRETE SLAB

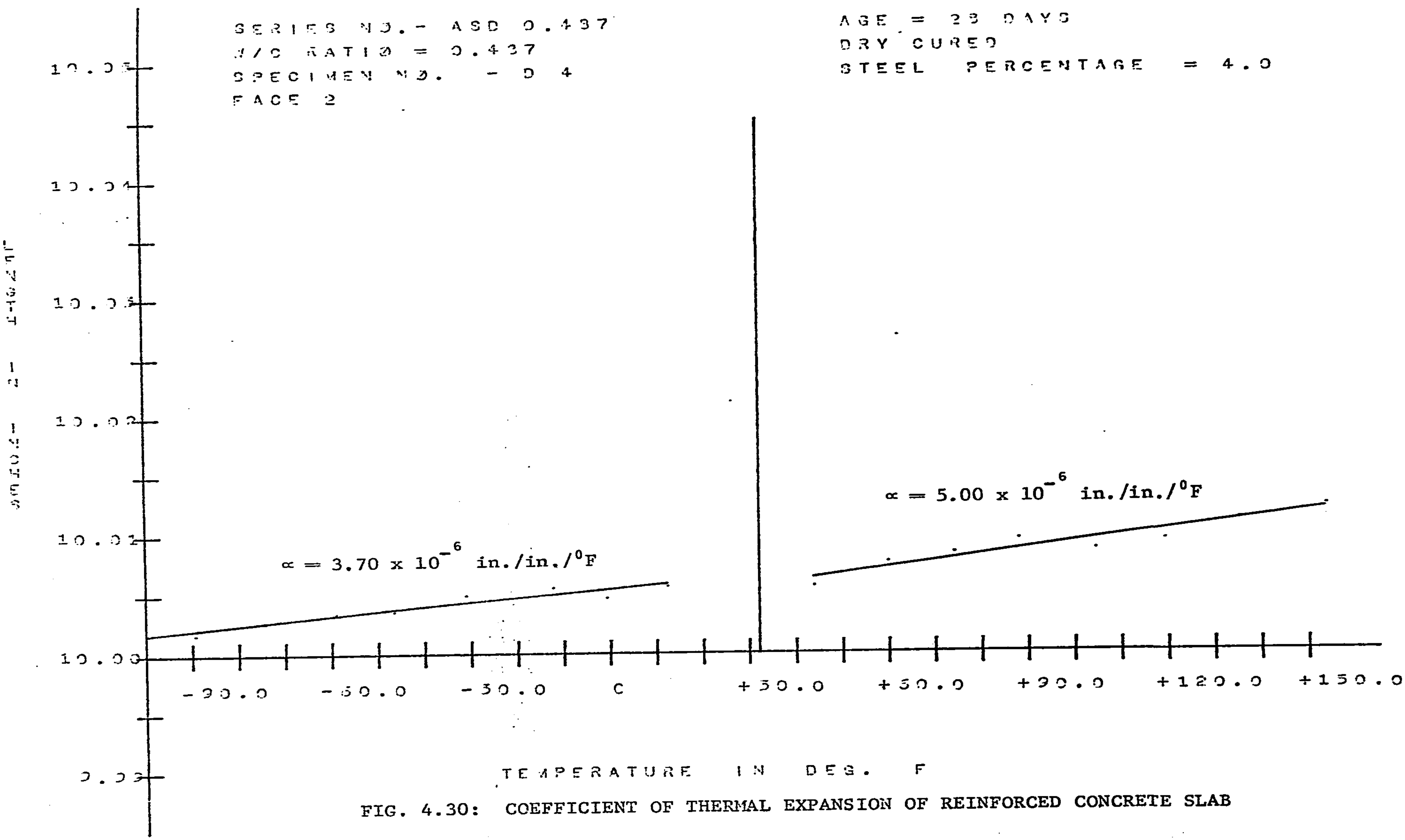

FIG. 4.30: COEFFICIENT OF THERMAL EXPANSION OF REINFORCED CONCRETE SLAB

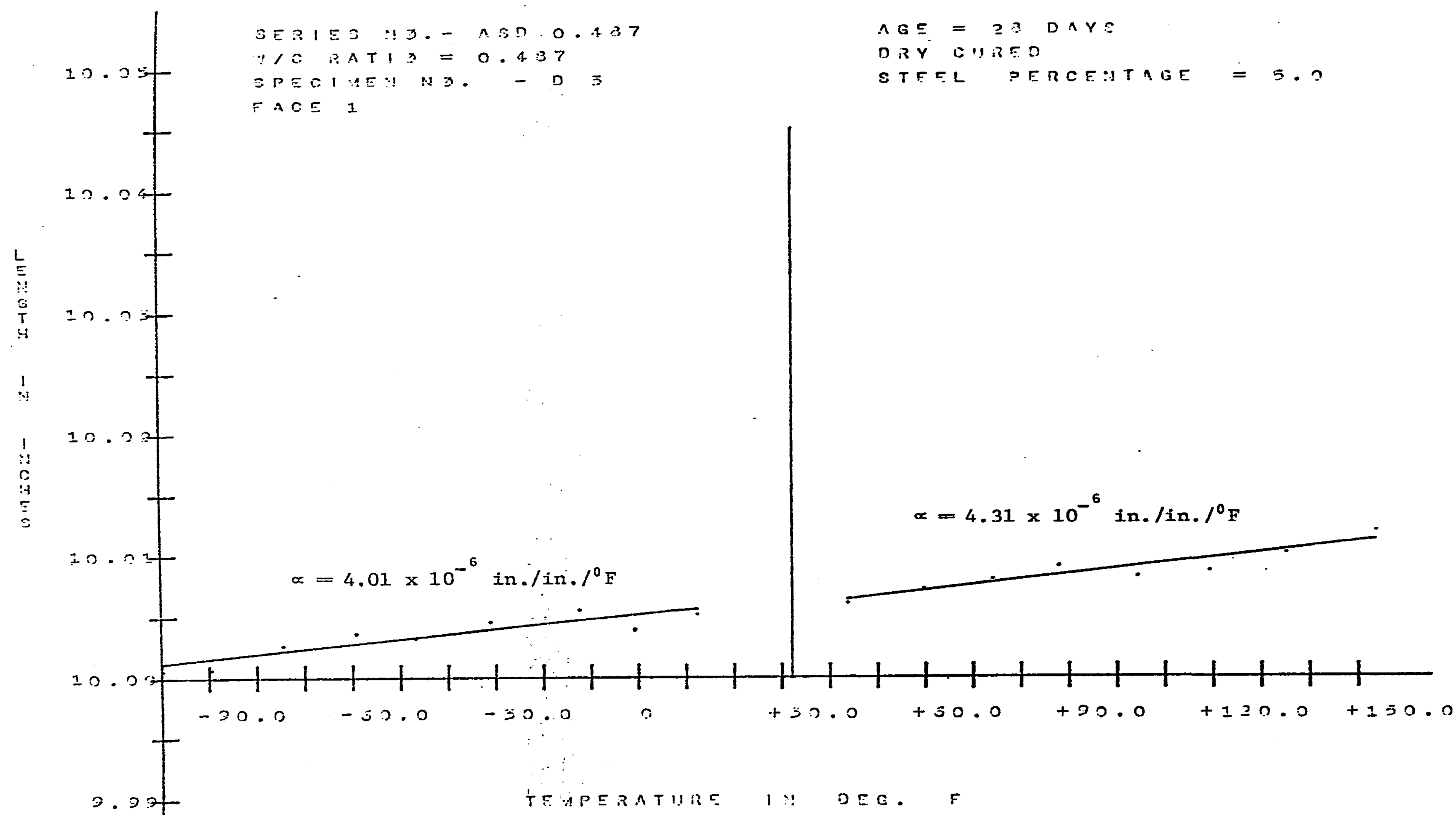

FIG. 4.31: COEFFICIENT OF THERMAL EXPANSION OF REINFORCED CONCRETE SLAB

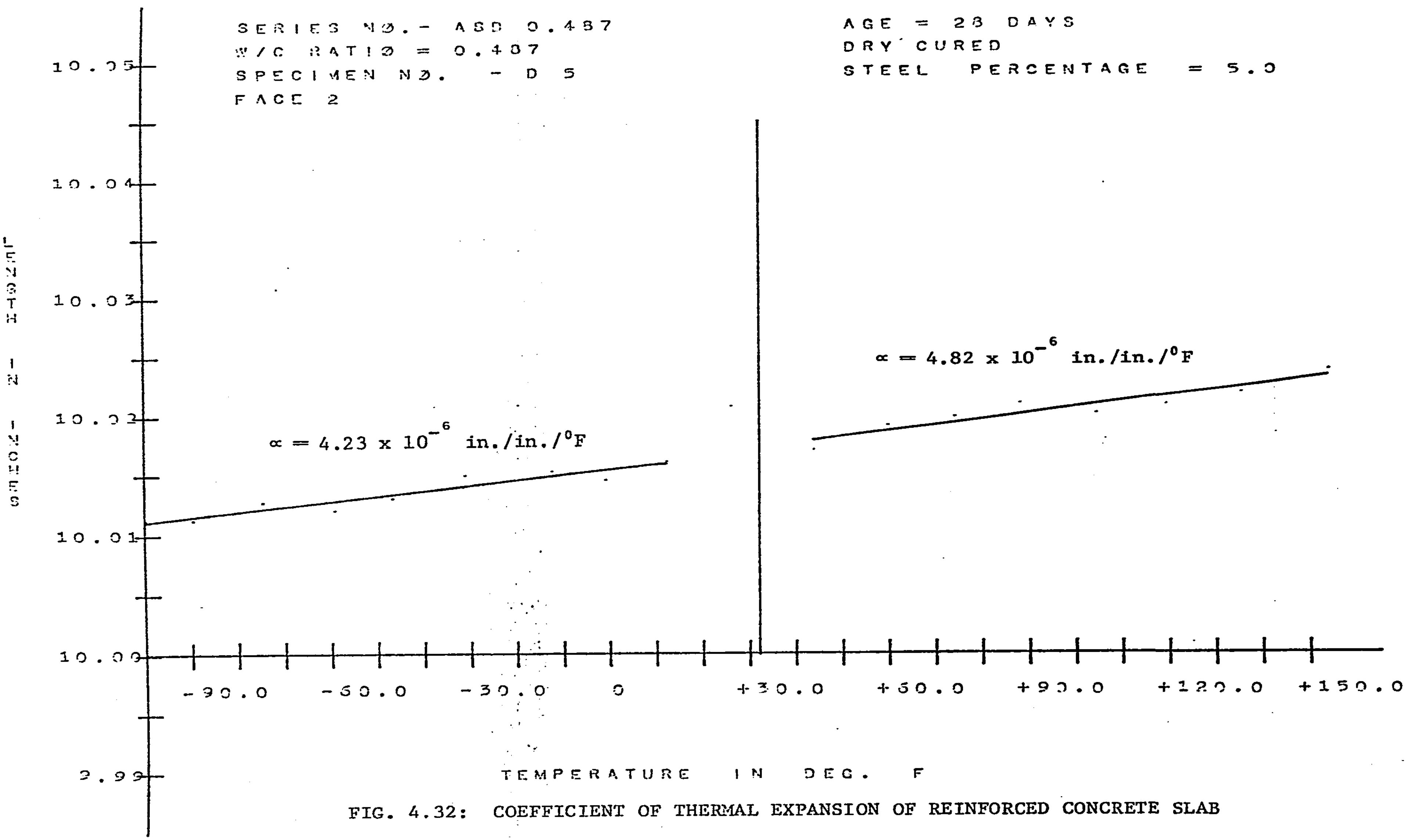

FIG. 4.32: COEFFICIENT OF THERMAL EXPANSION OF REINFORCED CONCRETE SLAB

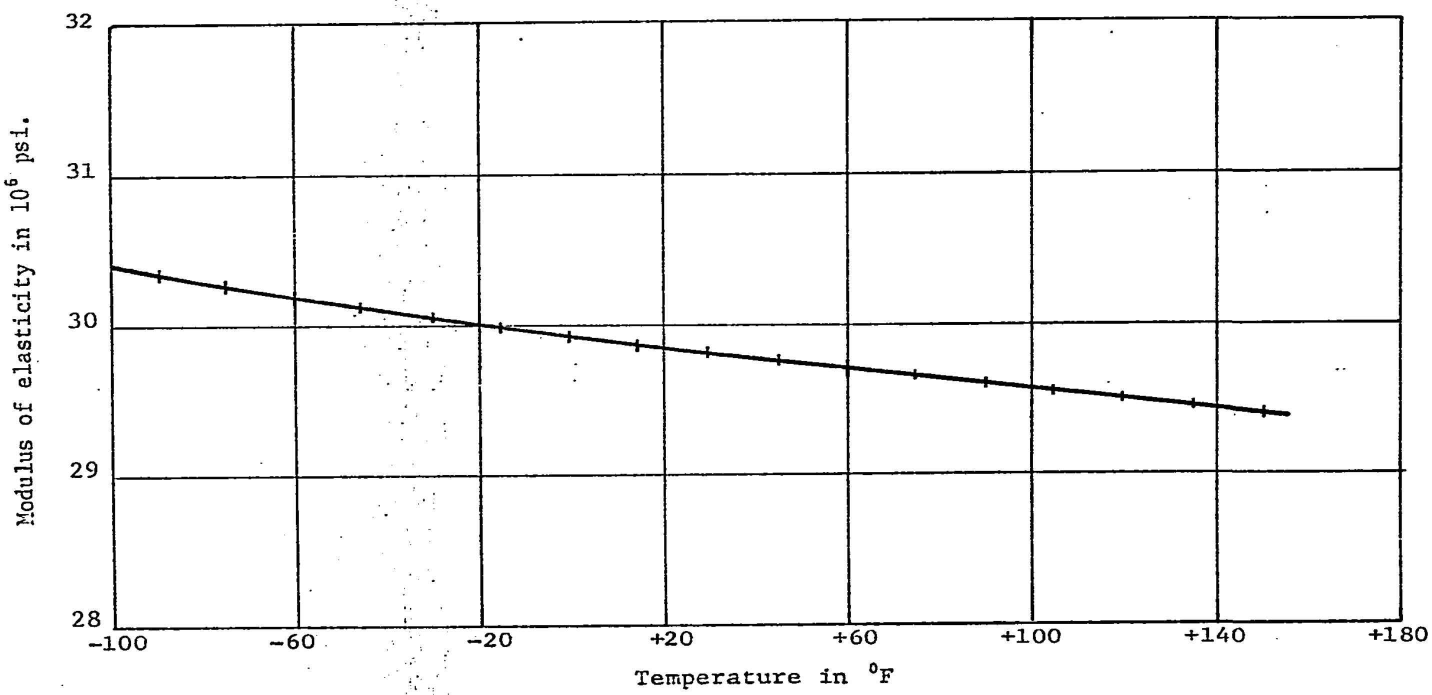

FIG. 4.33: MODULUS OF ELASTICITY OF STEEL USED IN THE THEORETICAL ANALYSIS OF COEFFICIENT OF LINEAR EXPANSION OF REINFORCED CONCRETE (ACCORDING TO REF. 32)

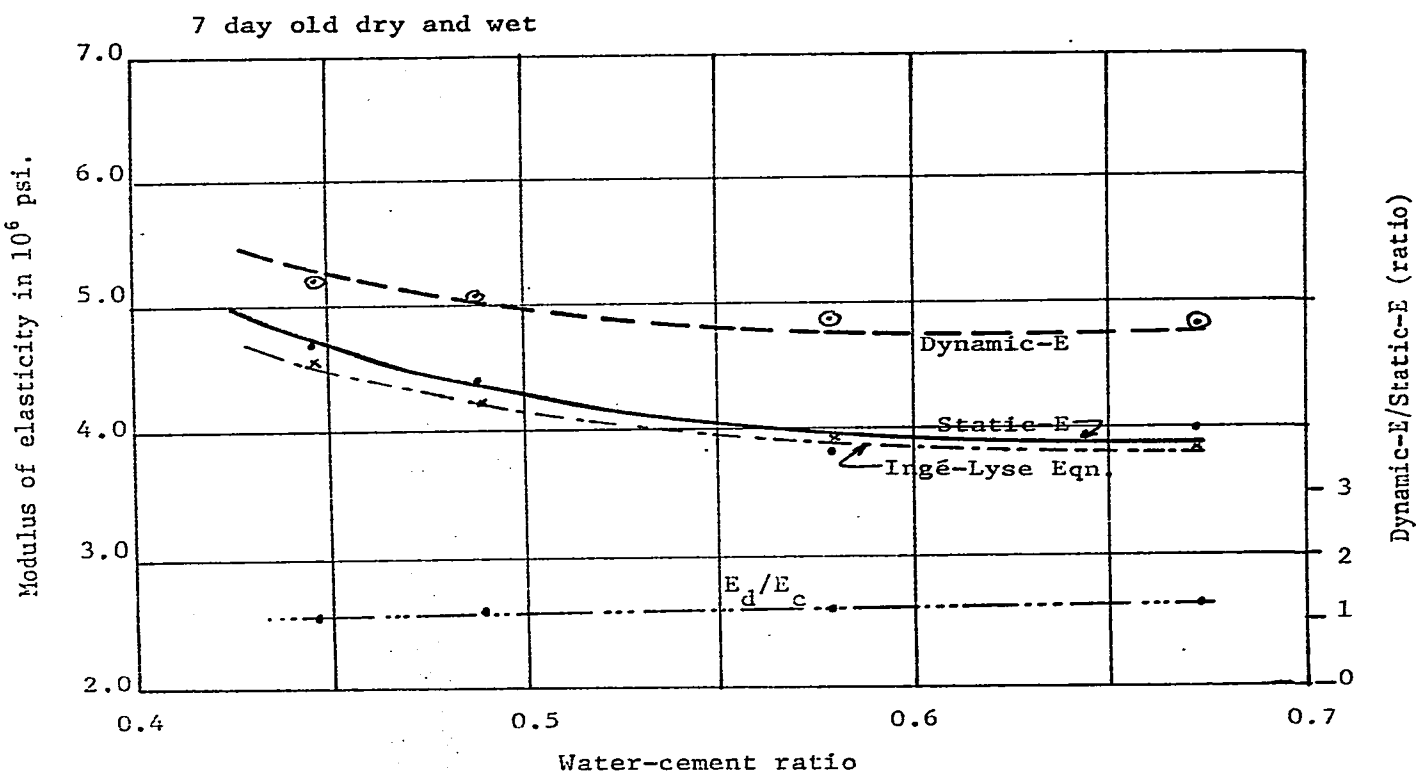

FIG. 5.1: VARIATION OF STATIC-E AND DYNAMIC-E VALUES (7 DAY OLD)

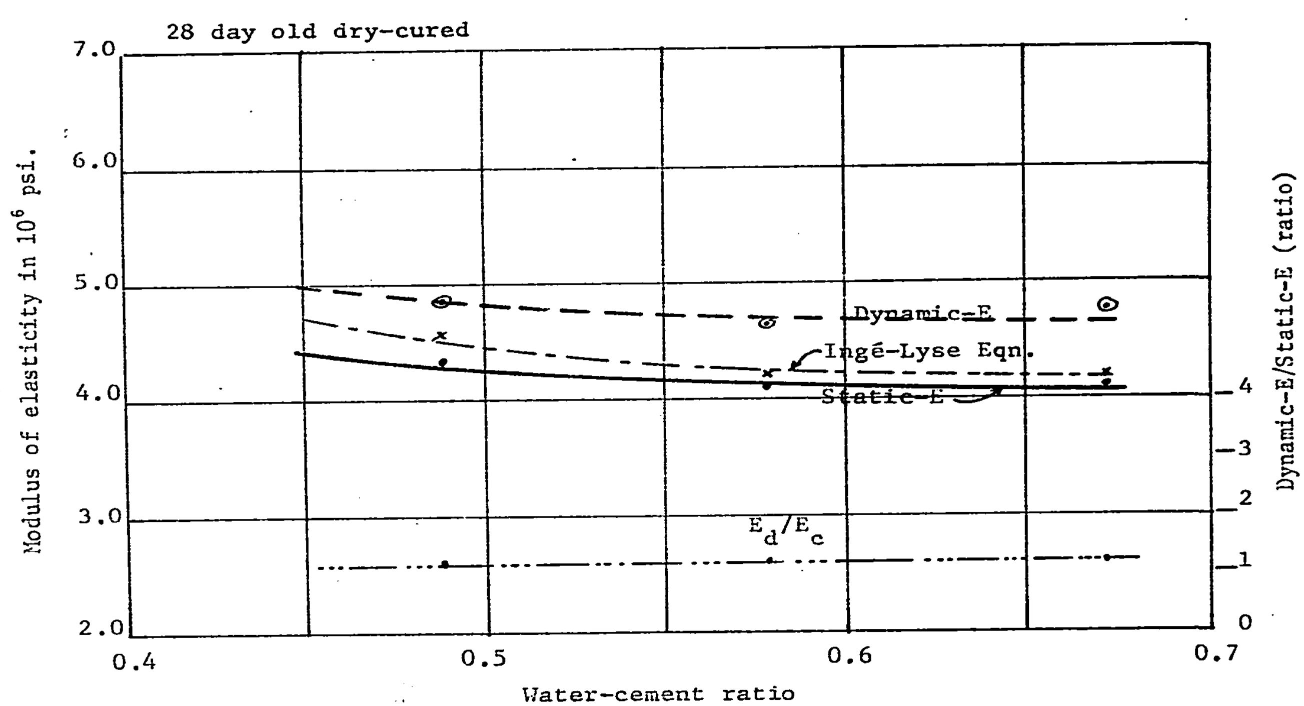

FIG. 5.2: VARIATION OF STATIC-E AND DYNAMIC-E VALUES

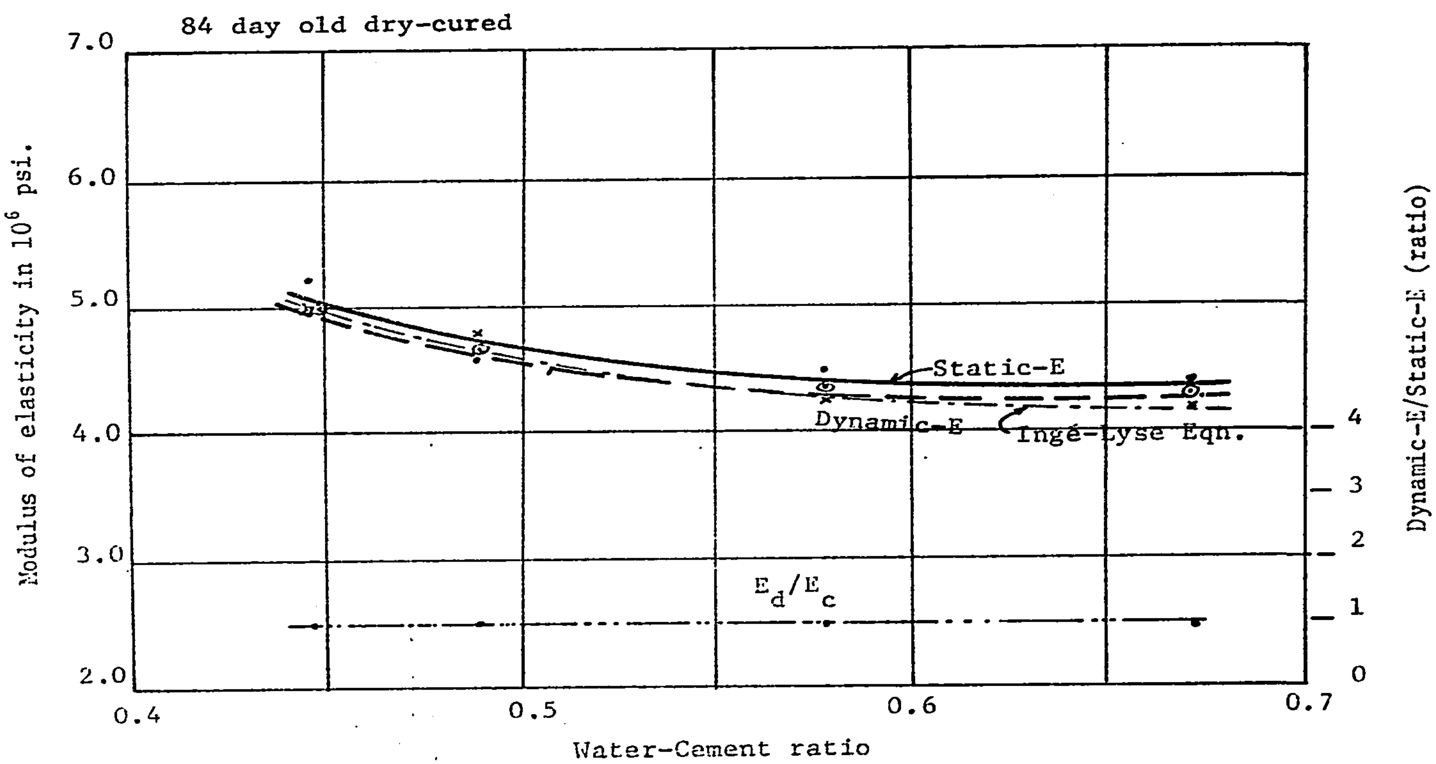

FIG. 5.3: VARIATION OF STATIC-E AND DYNAMIC-E VALUES

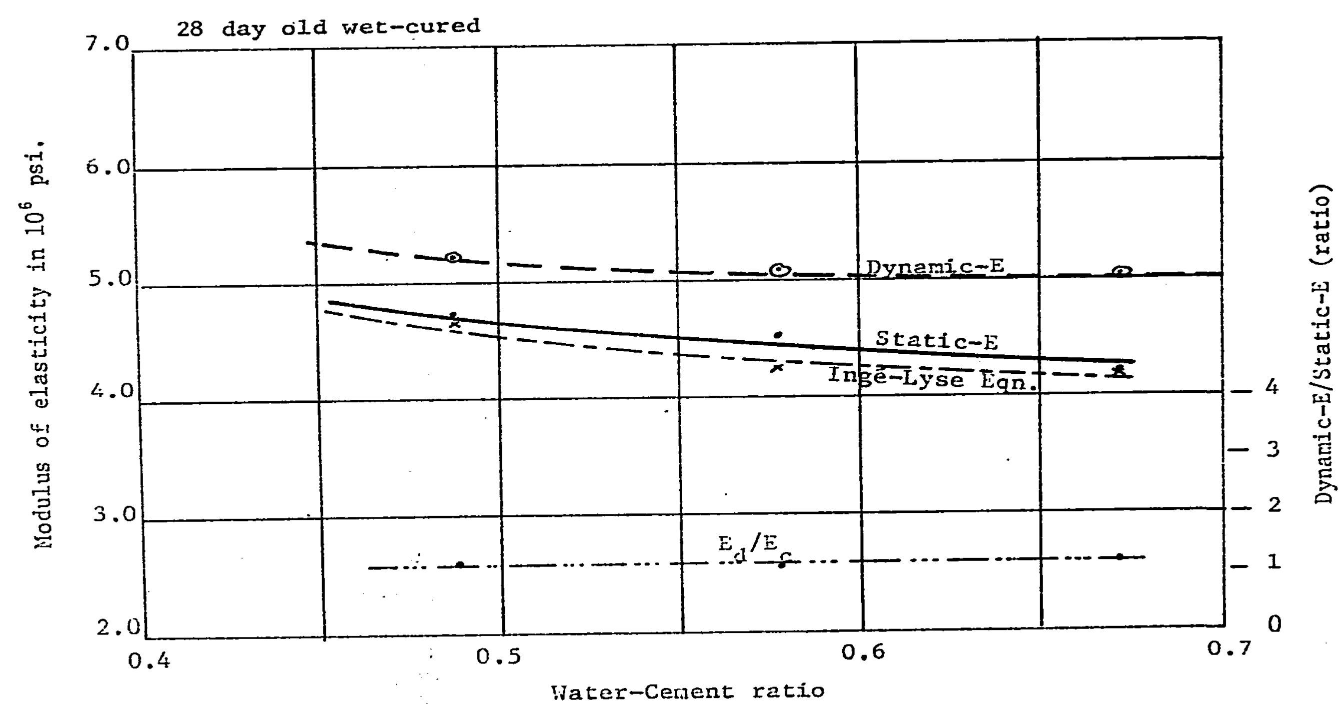

FIG. 5.4: VARIATION OF STATIC-E AND DYNAMIC-E VALUES

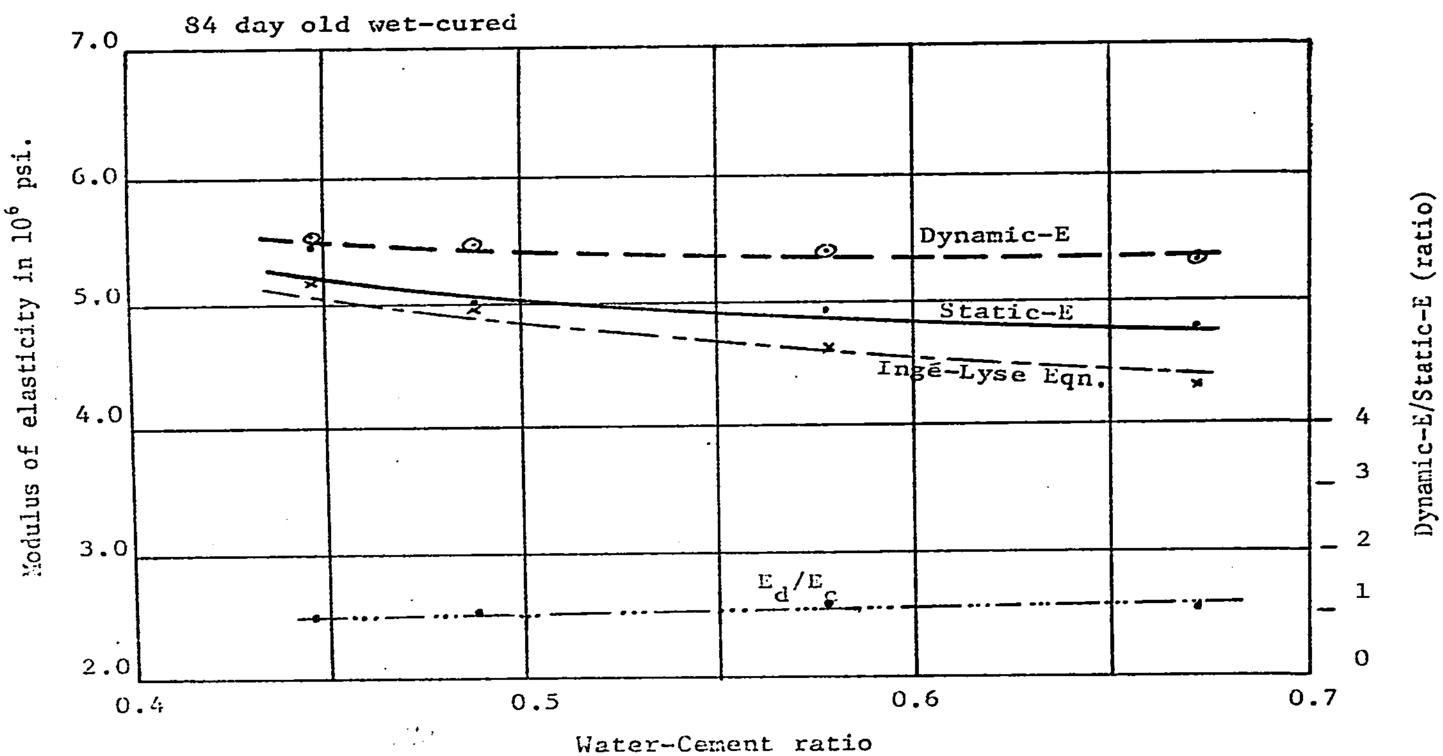

FIG. 5.5: VARIATION OF STATIC-E AND DYNAMIC-E VALUES

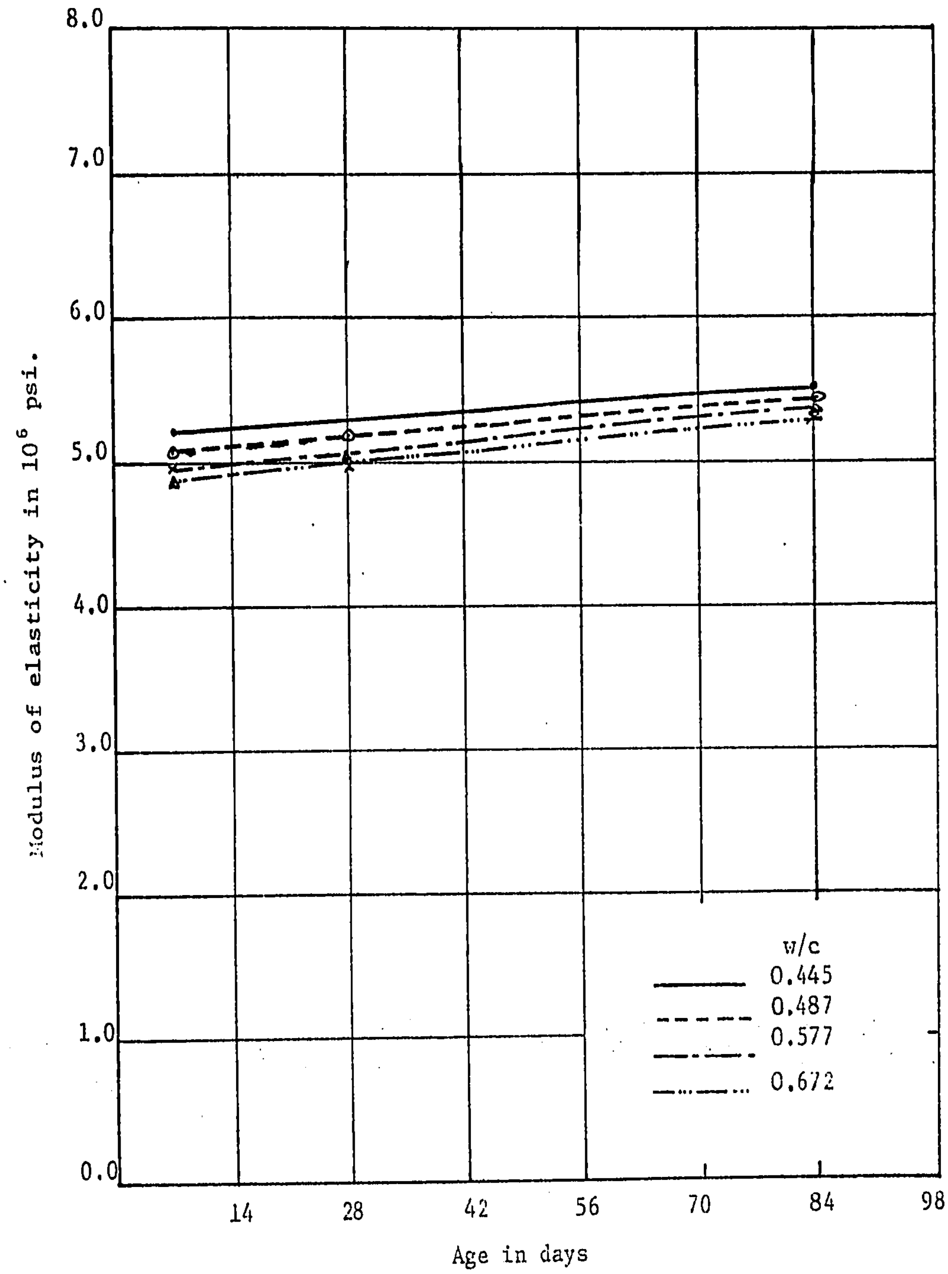

FIG. 5.6: EFFECT OF AGE ON MODULUS OF ELASTICITY (E_d) OF WET-CURED SPECIMENS AT ROOM TEMPERATURE

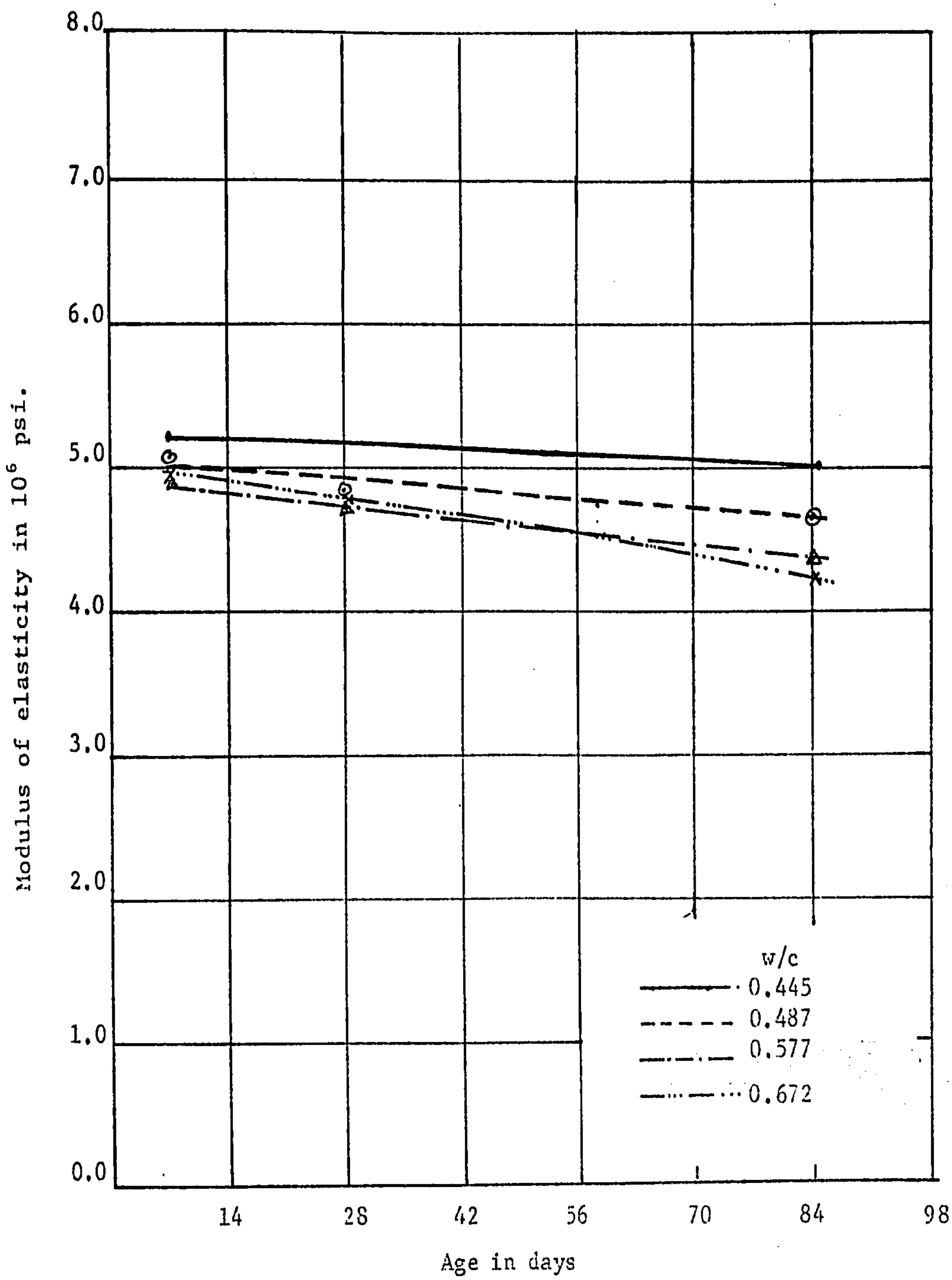

FIG. 5.7: EFFECT OF AGE ON MODULUS OF ELASTICITY (E_d) OF DRY-CURED SPECIMENS AT ROOM TEMPERATURE

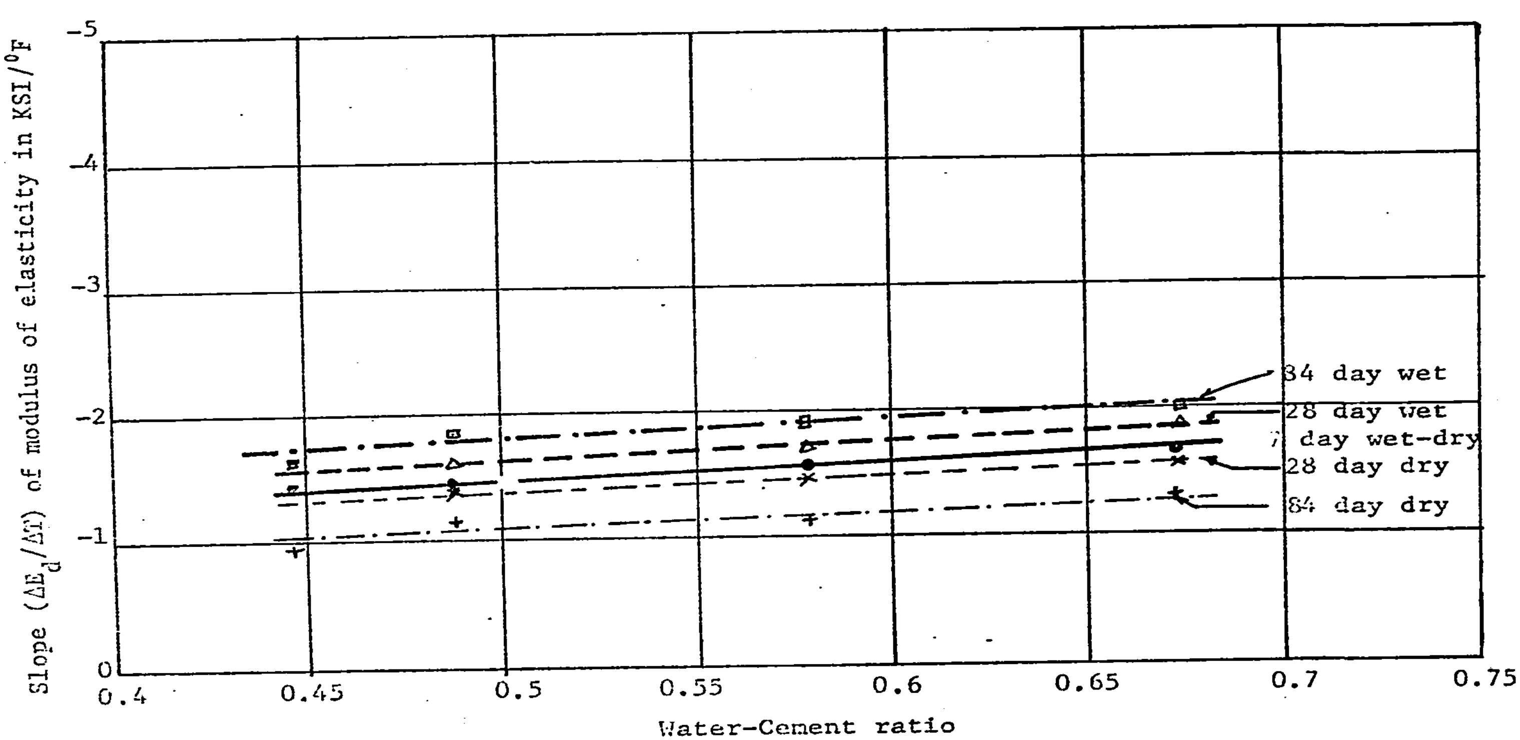

FIG. 5.8: EFFECT OF WATER-CEMENT RATIO ON ABOVE FREEZING SLOPE ($\Delta E_d/\Delta T$) OF MODULUS OF ELASTICITY

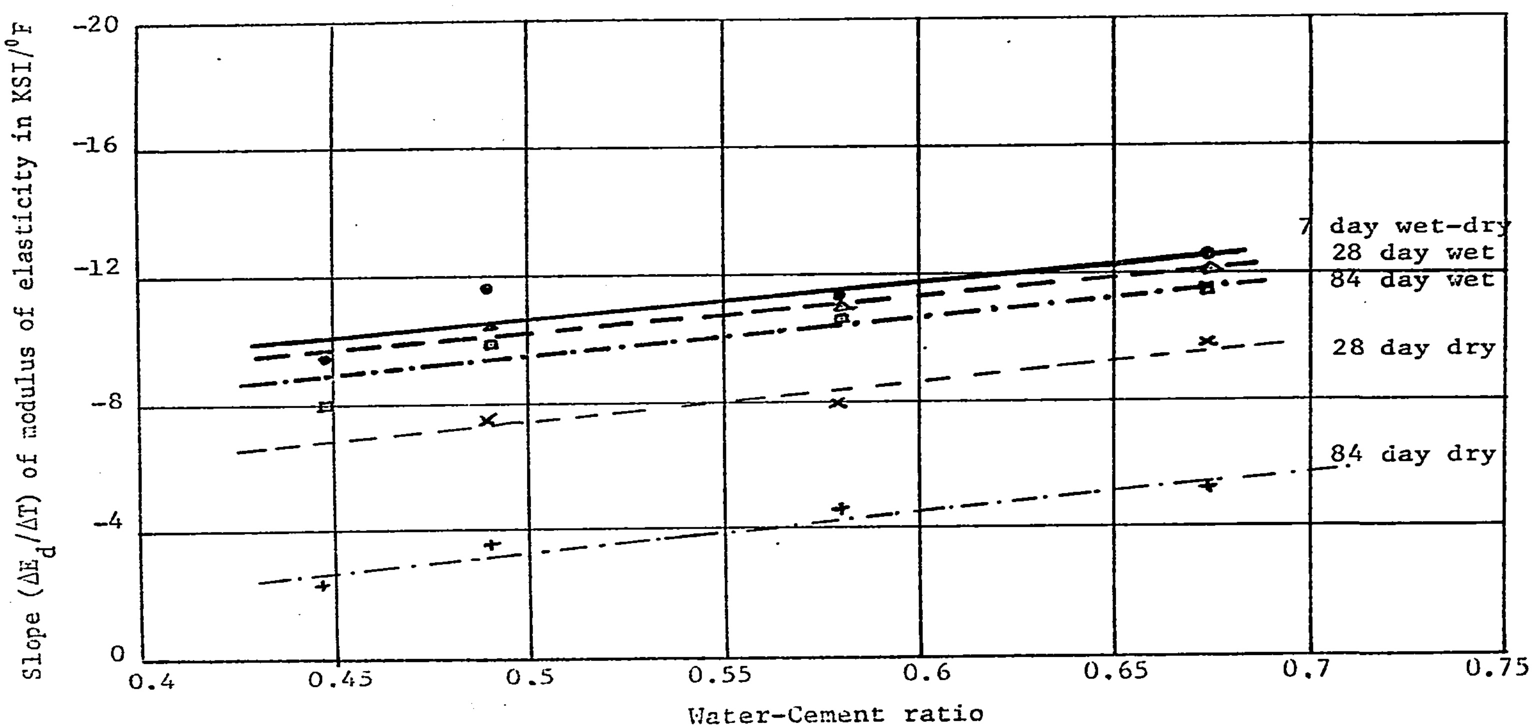

FIG. 5.9: EFFECT OF WATER-CEMENT RATIO ON BELOW FREEZING SLOPE ($\Delta E_d/\Delta T$) OF MODULUS OF ELASTICITY

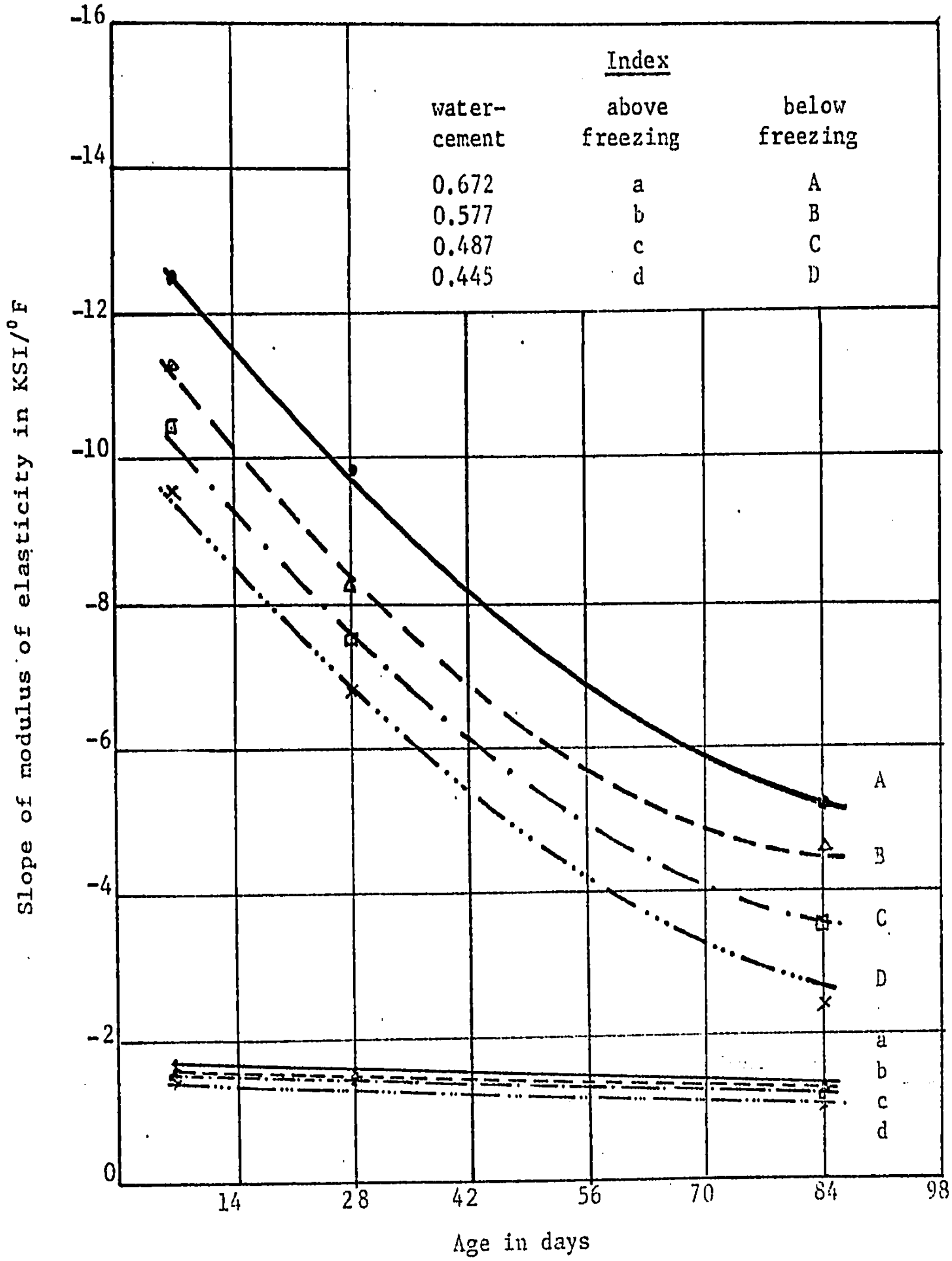

FIG. 5.10: EFFECT OF AGE ON SLOPE ($\Delta E_d/\Delta T$) OF MODULUS OF ELASTICITY OF DRY-CURED CONCRETE SPECIMENS

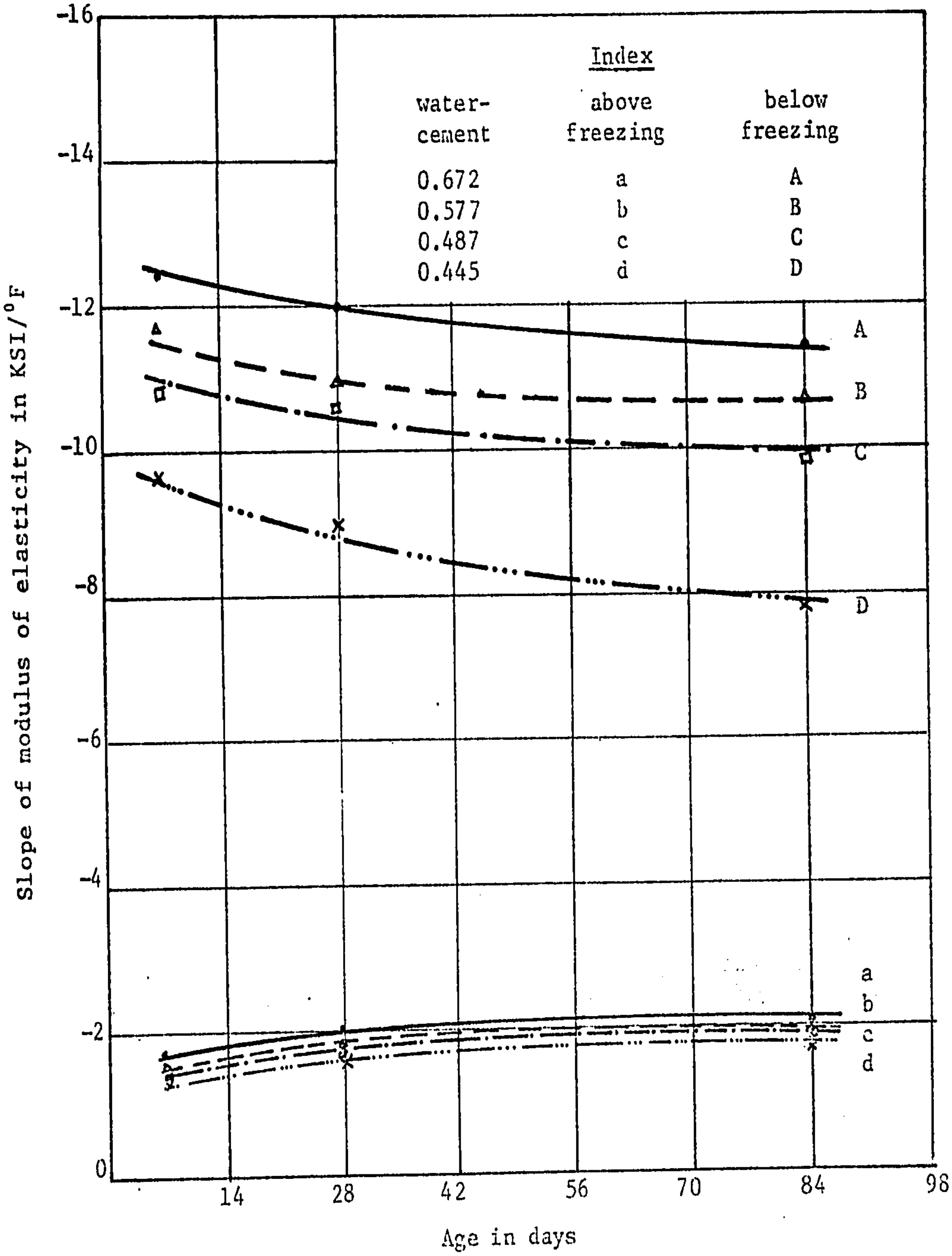

FIG. 5.11: EFFECT OF AGE ON SLOPE ($\Delta E_d/\Delta T$) OF MODULUS OF ELASTICITY OF WET-CURED CONCRETE SPECIMENS

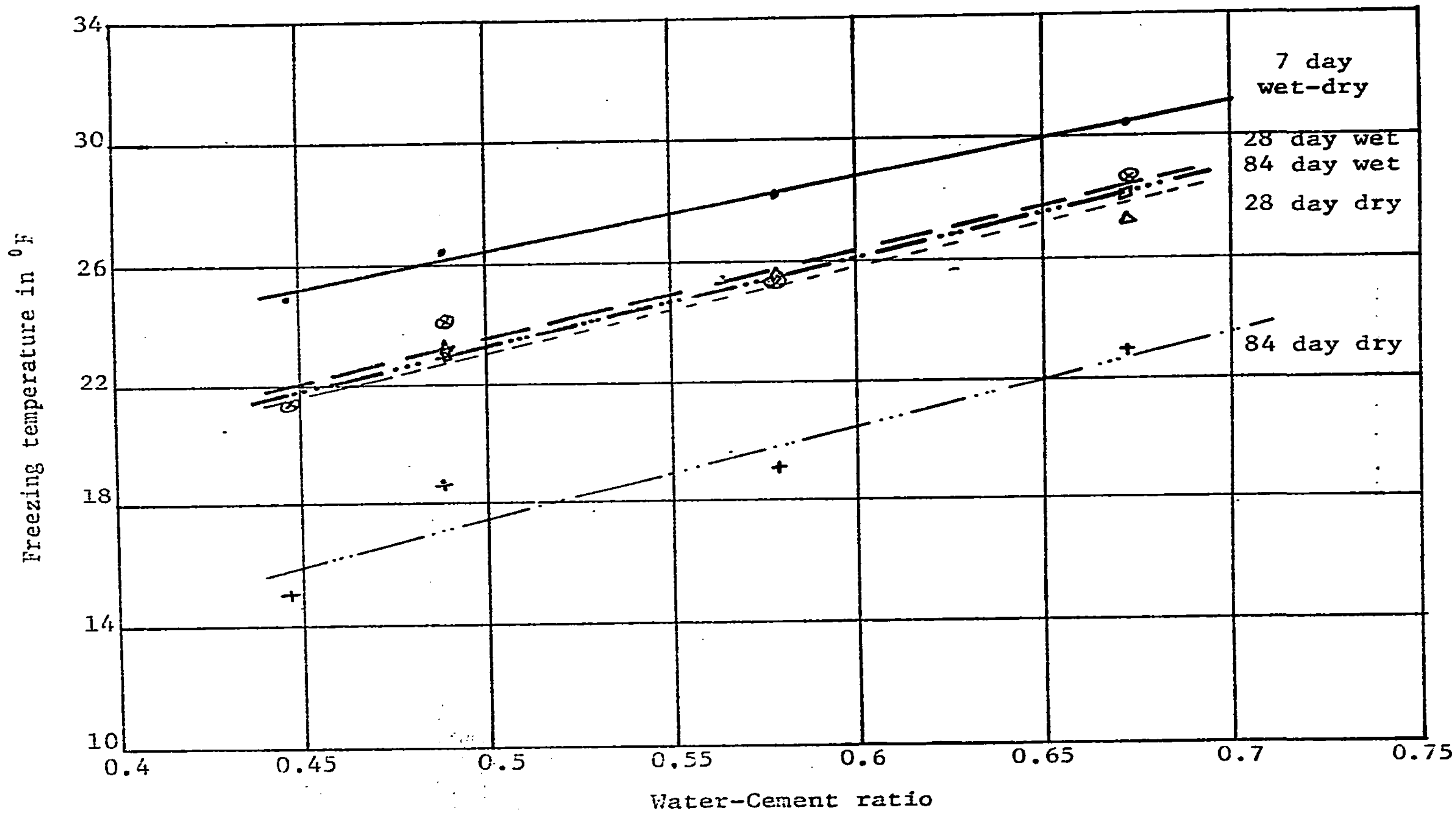

FIG. 5.12: PROBABLE VARIATION OF FREEZING POINT OF WATER WITH WATER-CEMENT RATIO OF THE CONCRETE MIXES

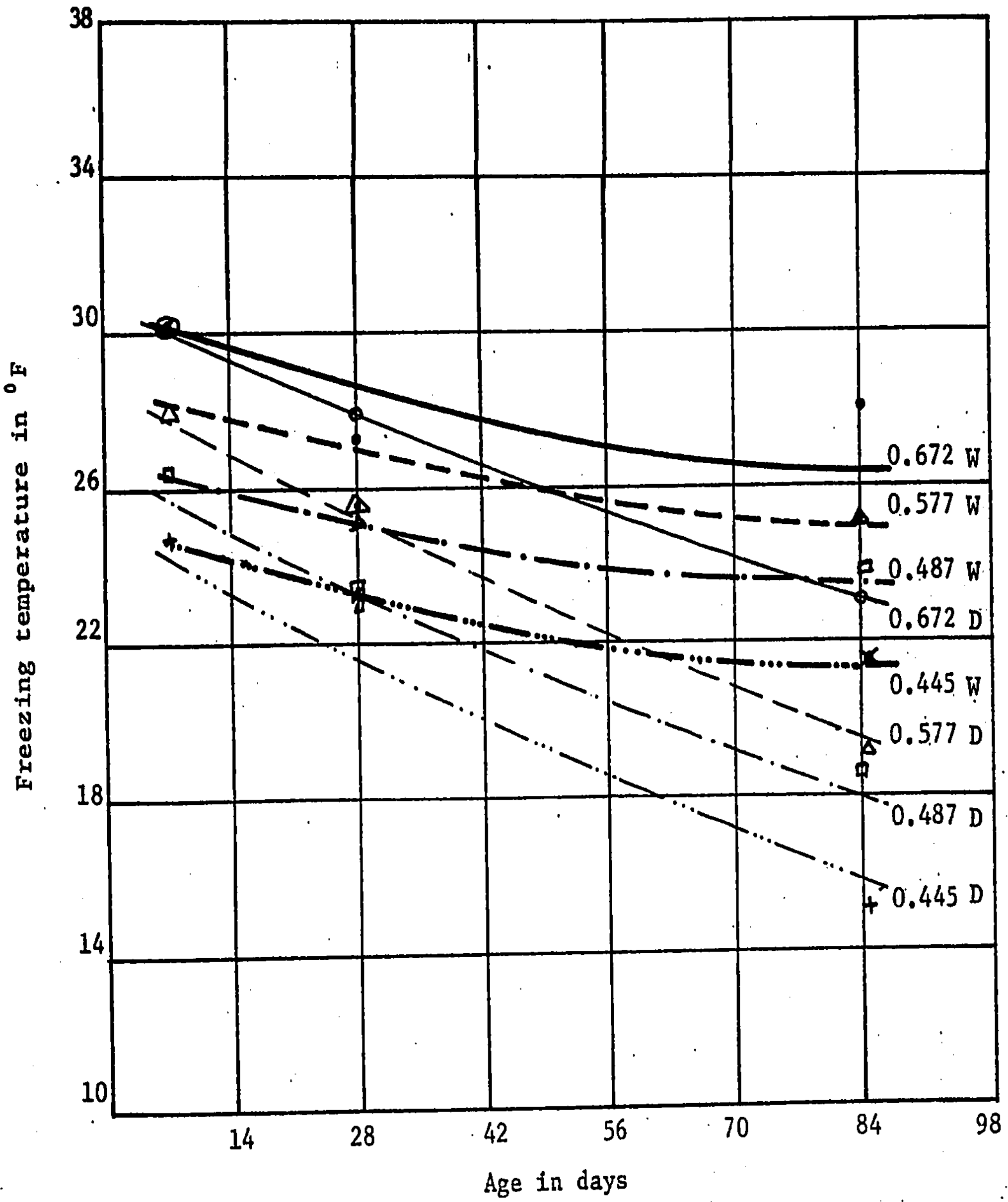

FIG. 5.13: PROBABLE VARIATION OF FREEZING POINT WITH AGE OF CONCRETE MIXES AND TYPE OF CURING

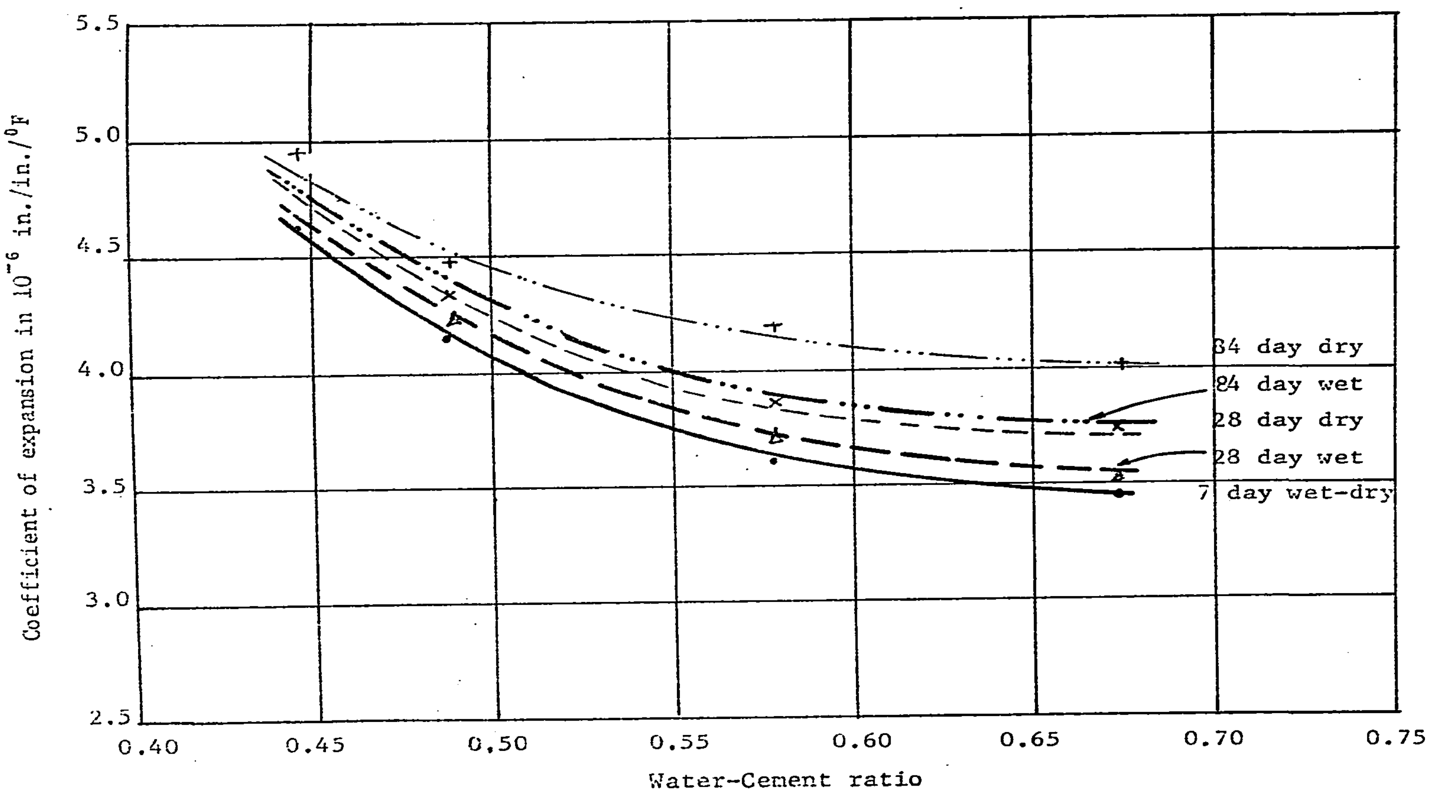

FIG. 5.14: EFFECT OF WATER-CEMENT RATIO ON ABOVE FREEZING COEFFICIENT OF THERMAL EXPANSION OF PLAIN CONCRETE

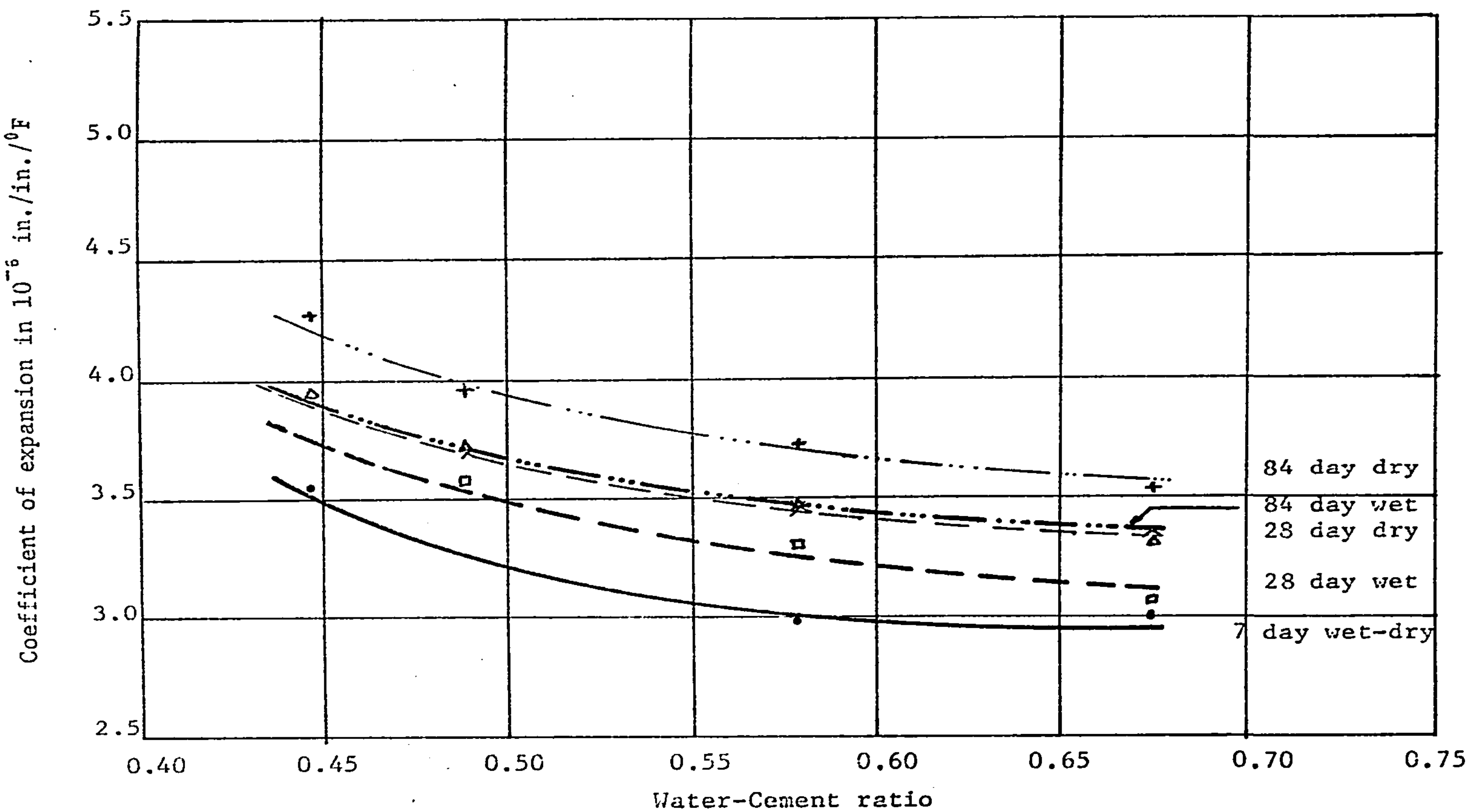

FIG. 5.15: EFFECT OF WATER-CEMENT RATIO ON BELOW FREEZING COEFFICIENT OF THERMAL EXPANSION OF PLAIN CONCRETE

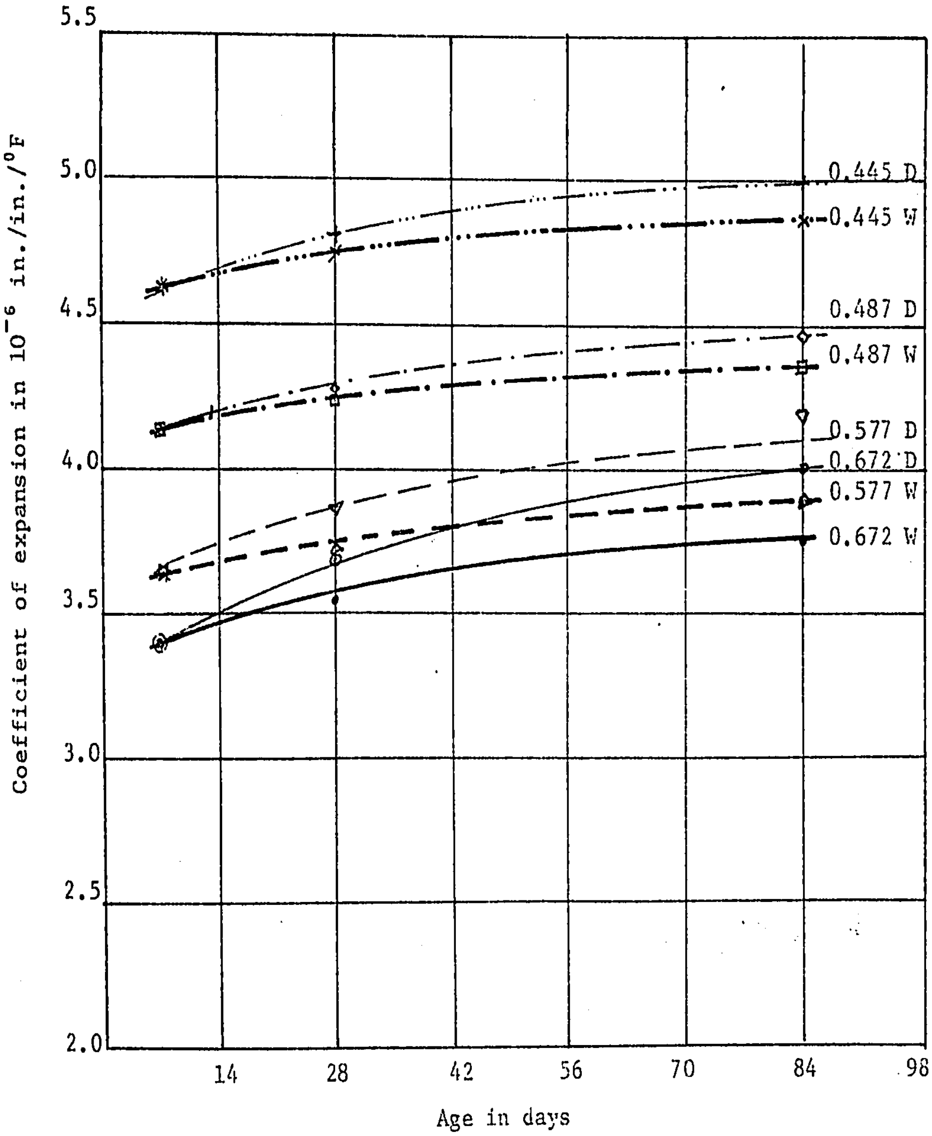

FIG. 5.16: EFFECT OF AGE ON ABOVE FREEZING COEFFICIENT OF EXPANSION OF PLAIN CONCRETE

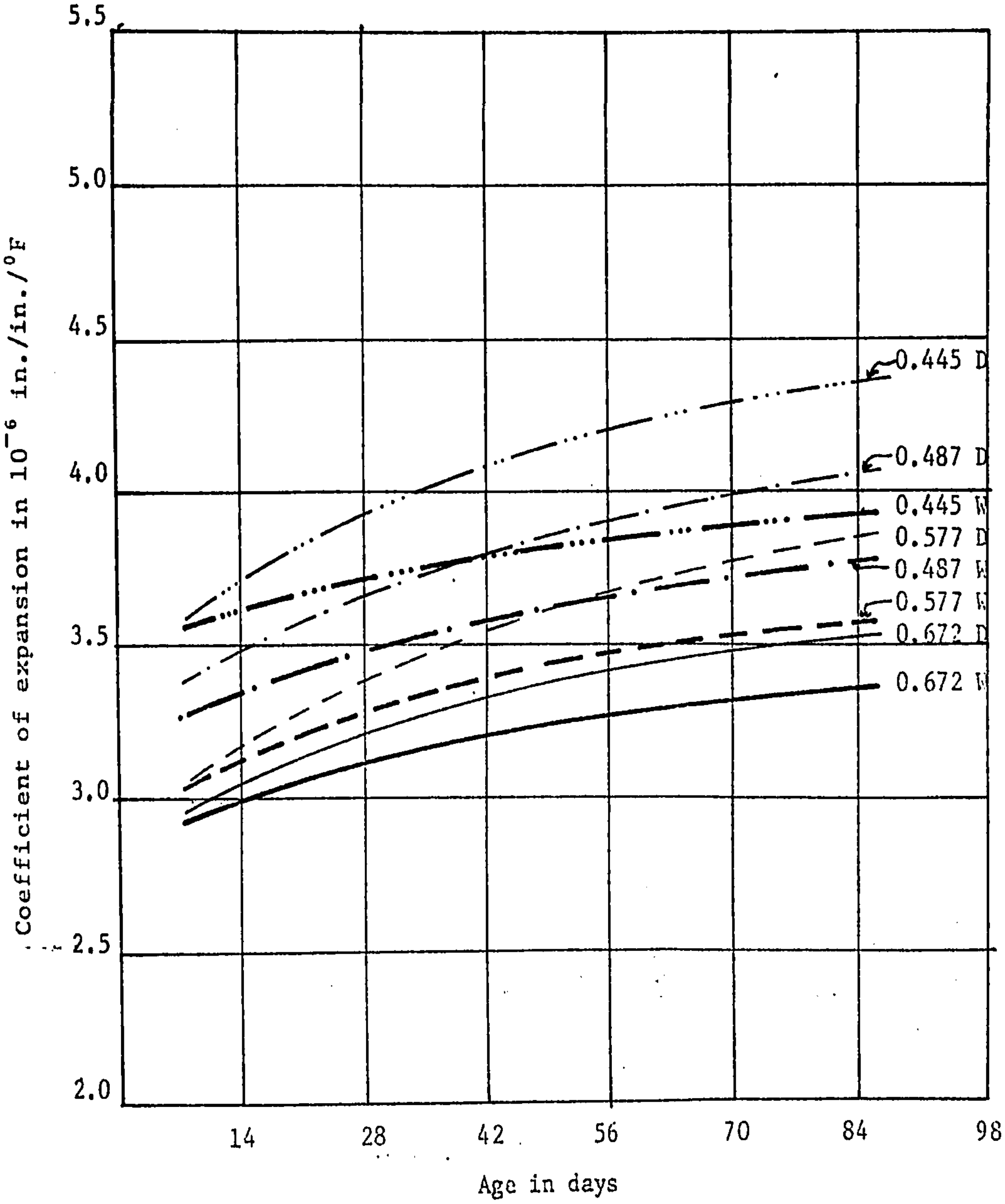

FIG. 5.17: EFFECT OF AGE ON BELOW FREEZING COEFFICIENT OF EXPANSION OF PLAIN CONCRETE

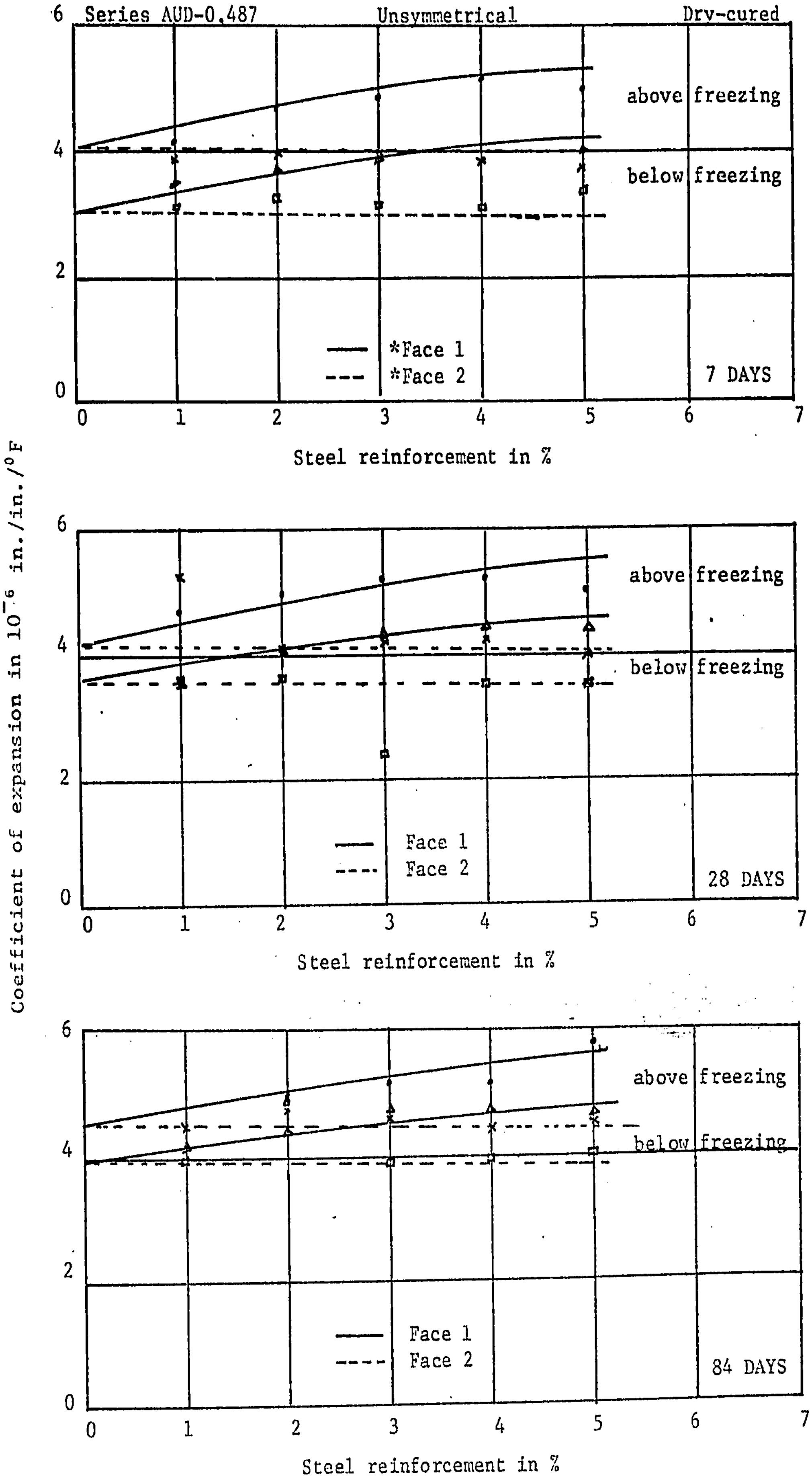

*Face 1: near the steel reinforcement
Face 2: away from the steel reinforcement

FIG. 5.18: EFFECT OF STEEL RATIO ON COEFFICIENT OF THERMAL EXPANSION OF REINFORCED CONCRETE

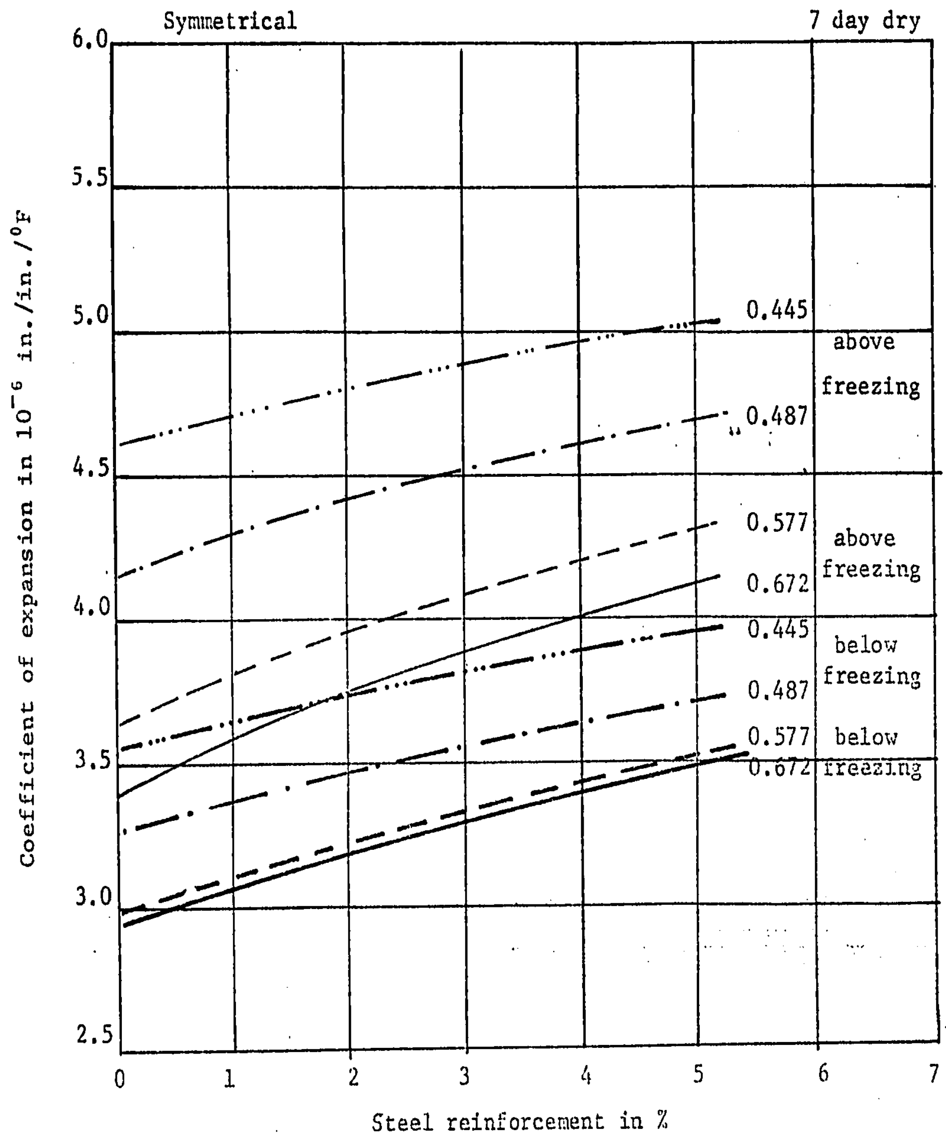

FIG. 5.19: EFFECT OF STEEL PERCENTAGE AND WATER-CEMENT RATIO ON COEFFICIENT OF THERMAL EXPANSION OF REINFORCED CONCRETE

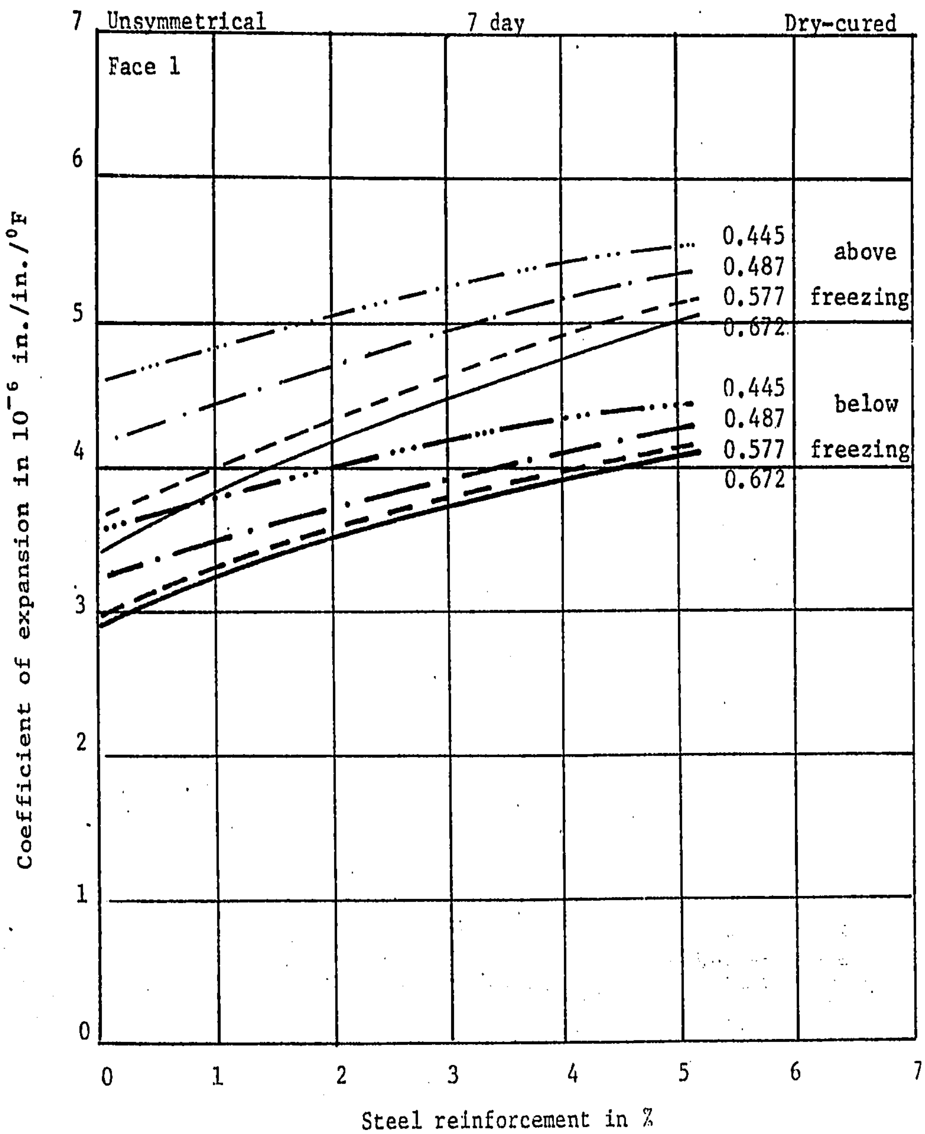

FIG. 5.20: EFFECT OF PERCENTAGE OF STEEL AND WATER-CEMENT RATIO ON COEFFICIENT OF EXPANSION OF CONCRETE

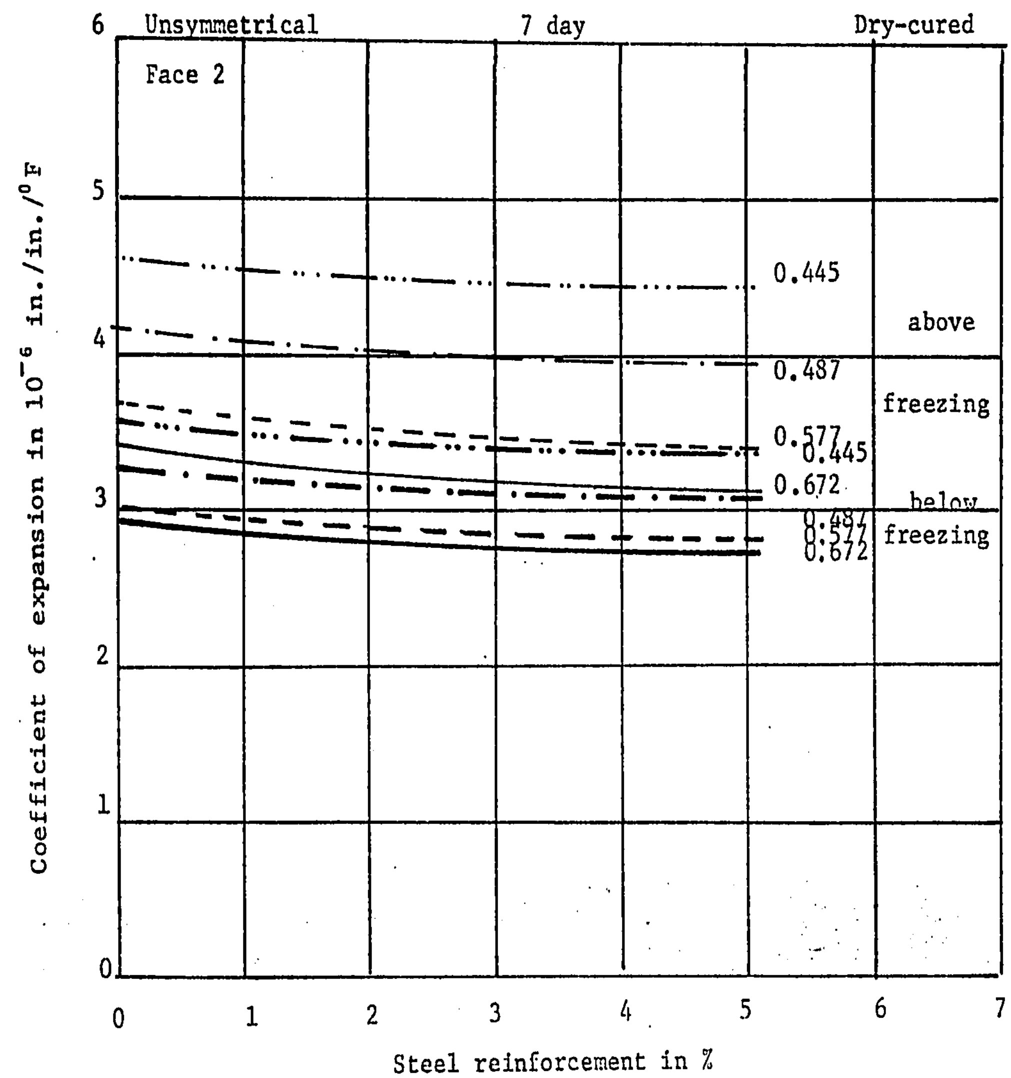

FIG. 5.21: EFFECT OF PERCENTAGE OF STEEL AND WATER-CEMENT RATIO ON COEFFICIENT OF EXPANSION OF CONCRETE

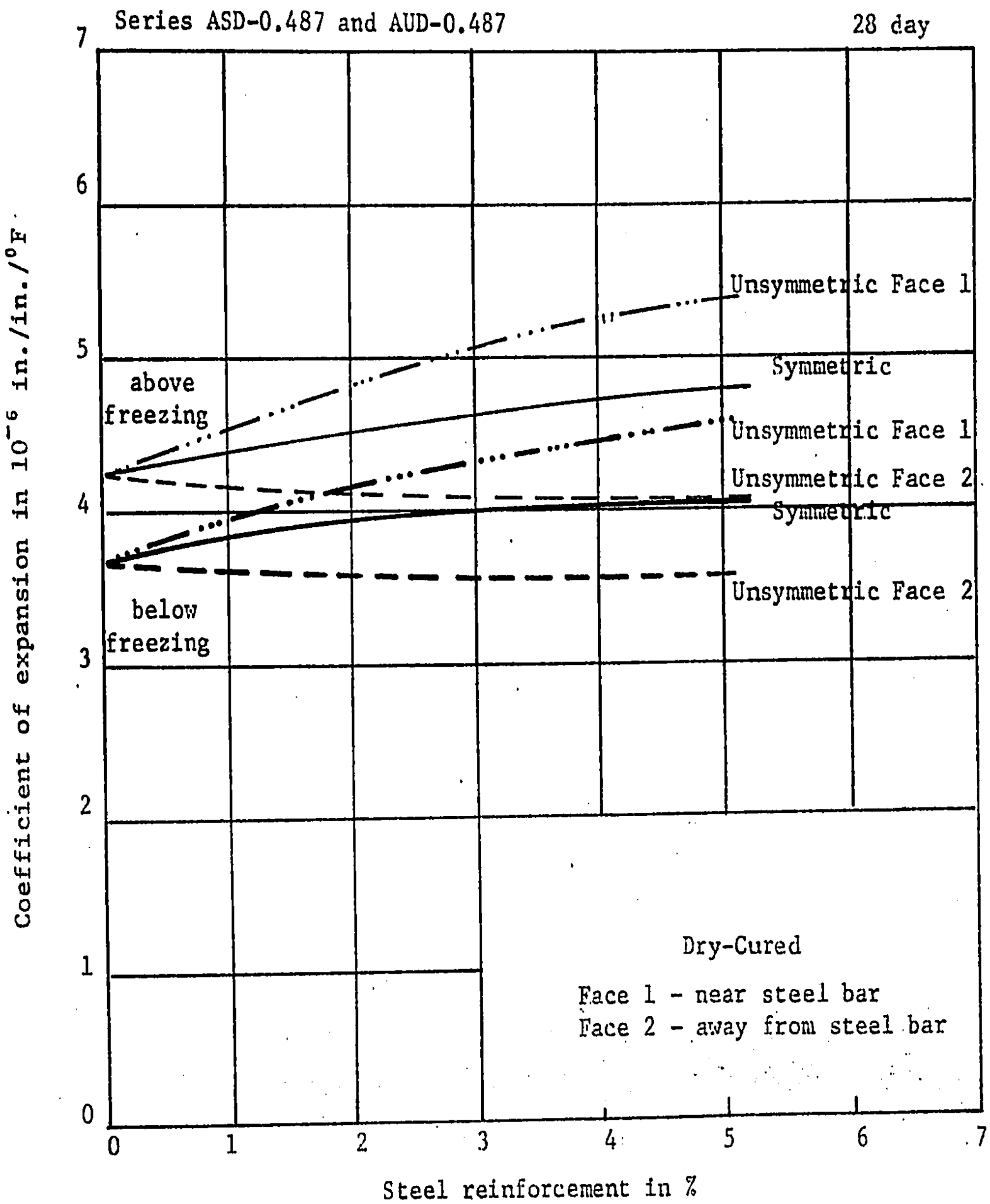

FIG. 5.22: EFFECT OF REINFORCEMENT TYPE ON VARIATION OF COEFFICIENT OF EXPANSION OF REINFORCED CONCRETE

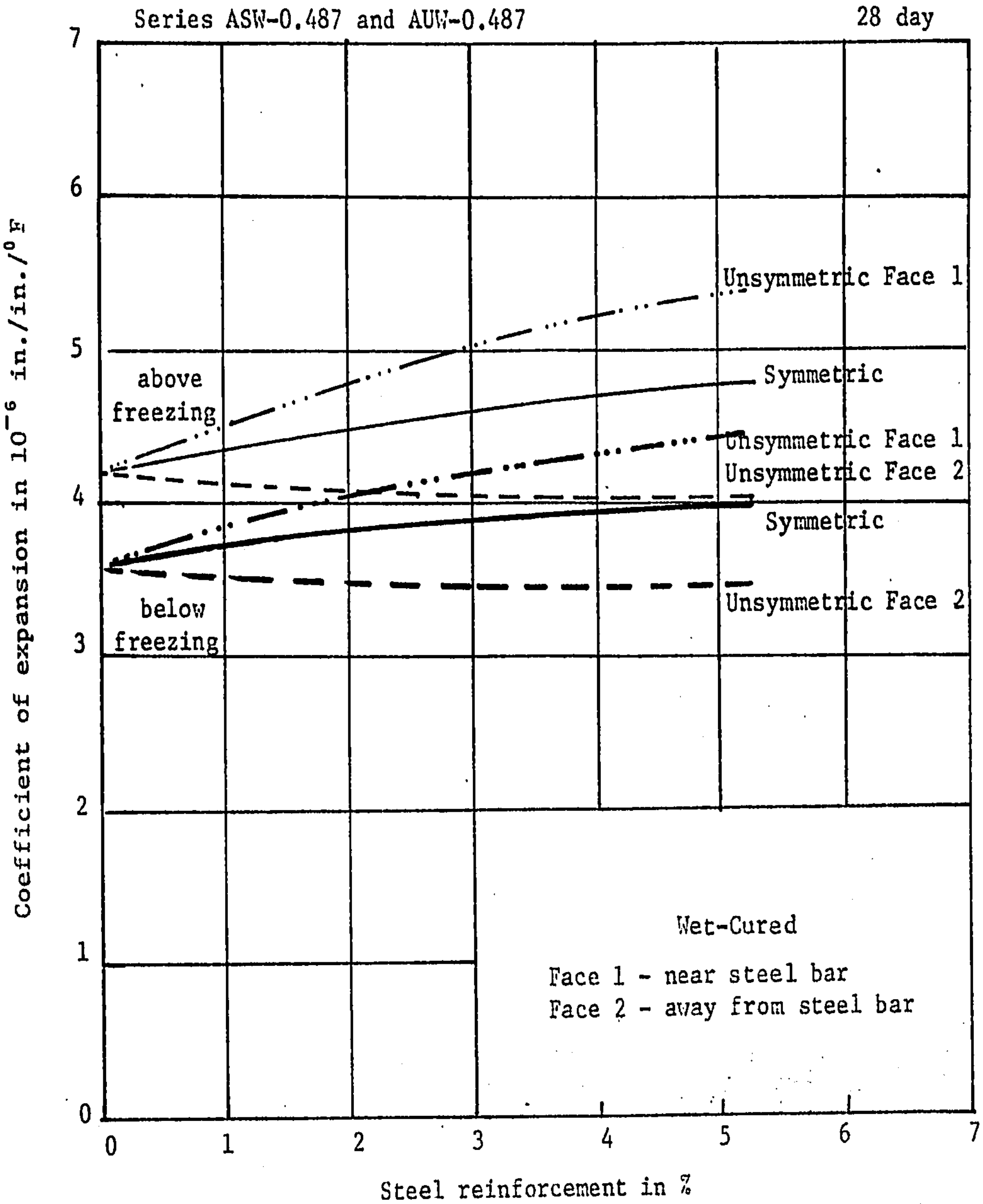

FIG. 5.23: EFFECT OF REINFORCEMENT TYPE ON VARIATION OF COEFFICIENT OF EXPANSION OF REINFORCED CONCRETE

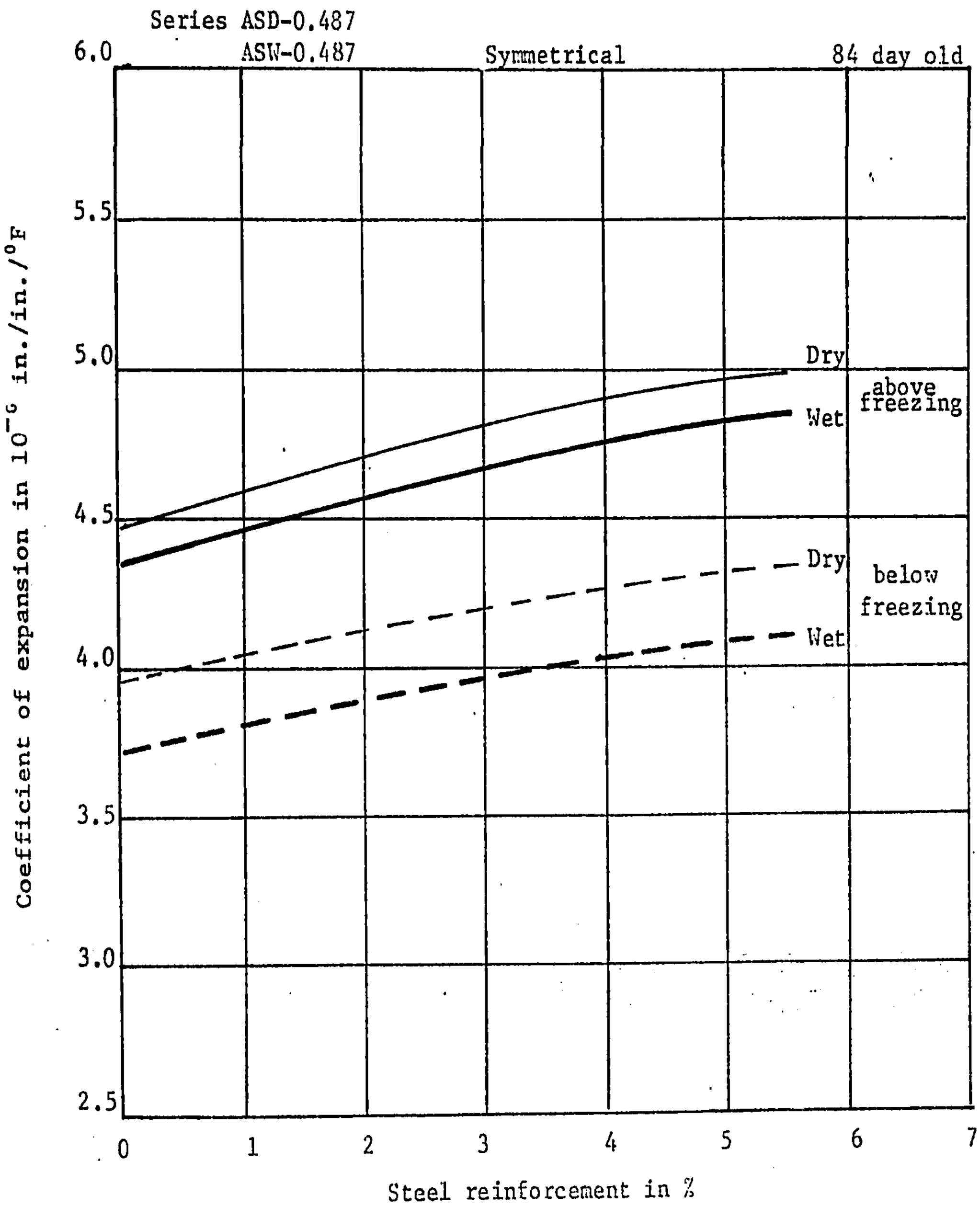

FIG. 5.24: EFFECT OF CURING ON VARIATION OF COEFFICIENT OF THERMAL EXPANSION OF REINFORCED CONCRETE

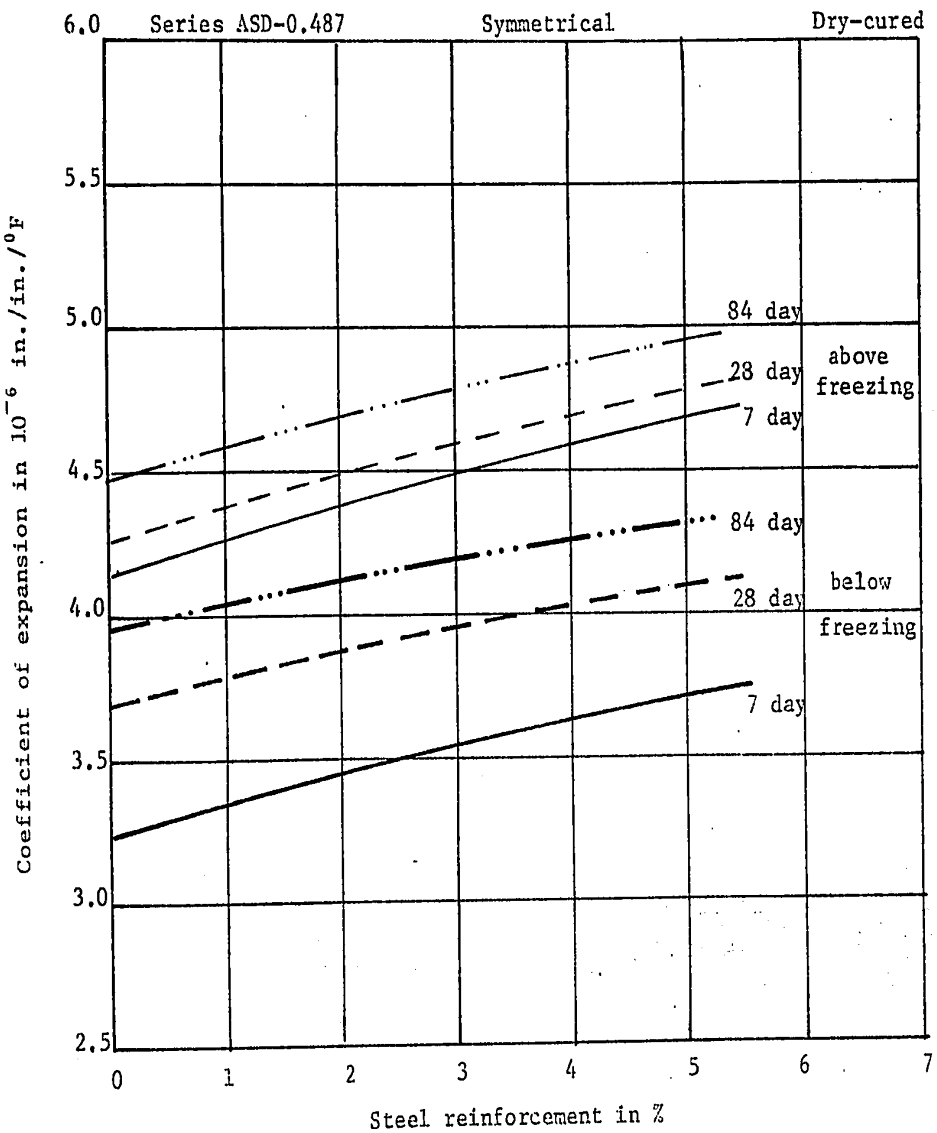

FIG. 5.25: VARIATION OF COEFFICIENT OF EXPANSION OF REINFORCED CONCRETE WITH AGE AND PERCENTAGE OF STEEL

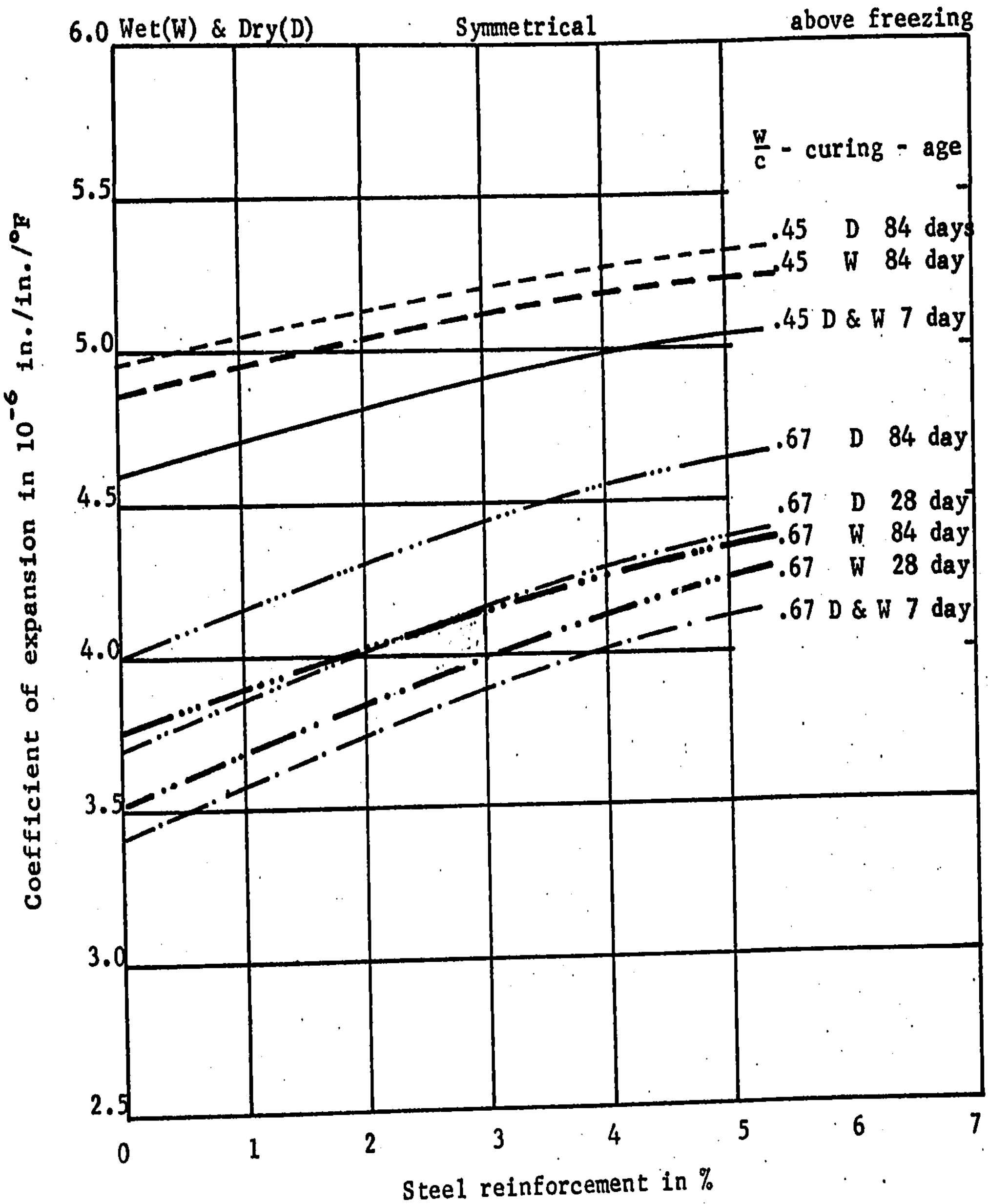

FIG. 5.26: ABOVE FREEZING COEFFICIENTS OF THERMAL EXPANSION OF SYMMETRICALLY REINFORCED CONCRETE SLAB

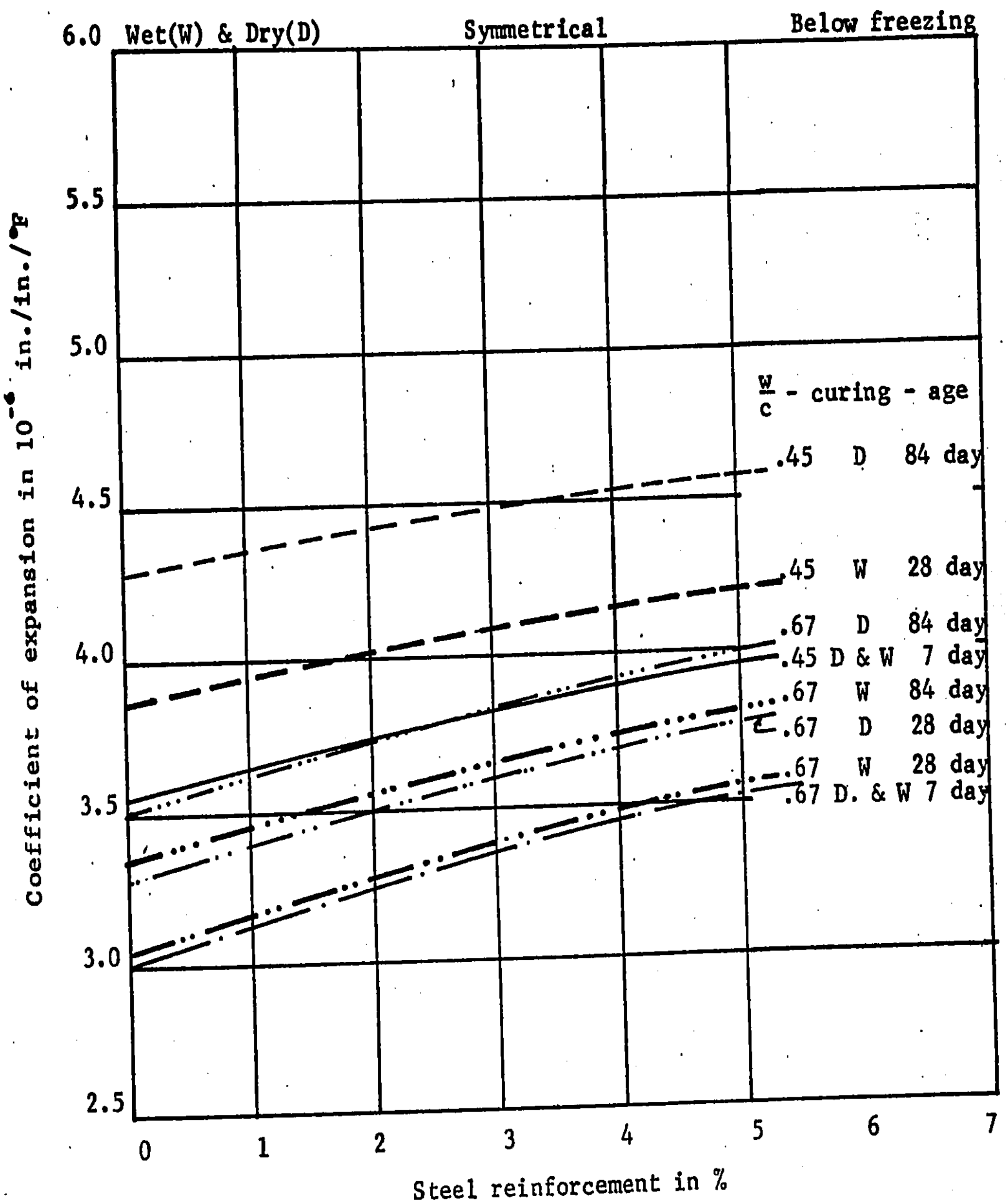

FIG. 5.27: BELOW FREEZING COEFFICIENTS OF THERMAL EXPANSION OF SYMMETRICALLY REINFORCED CONCRETE SLAB

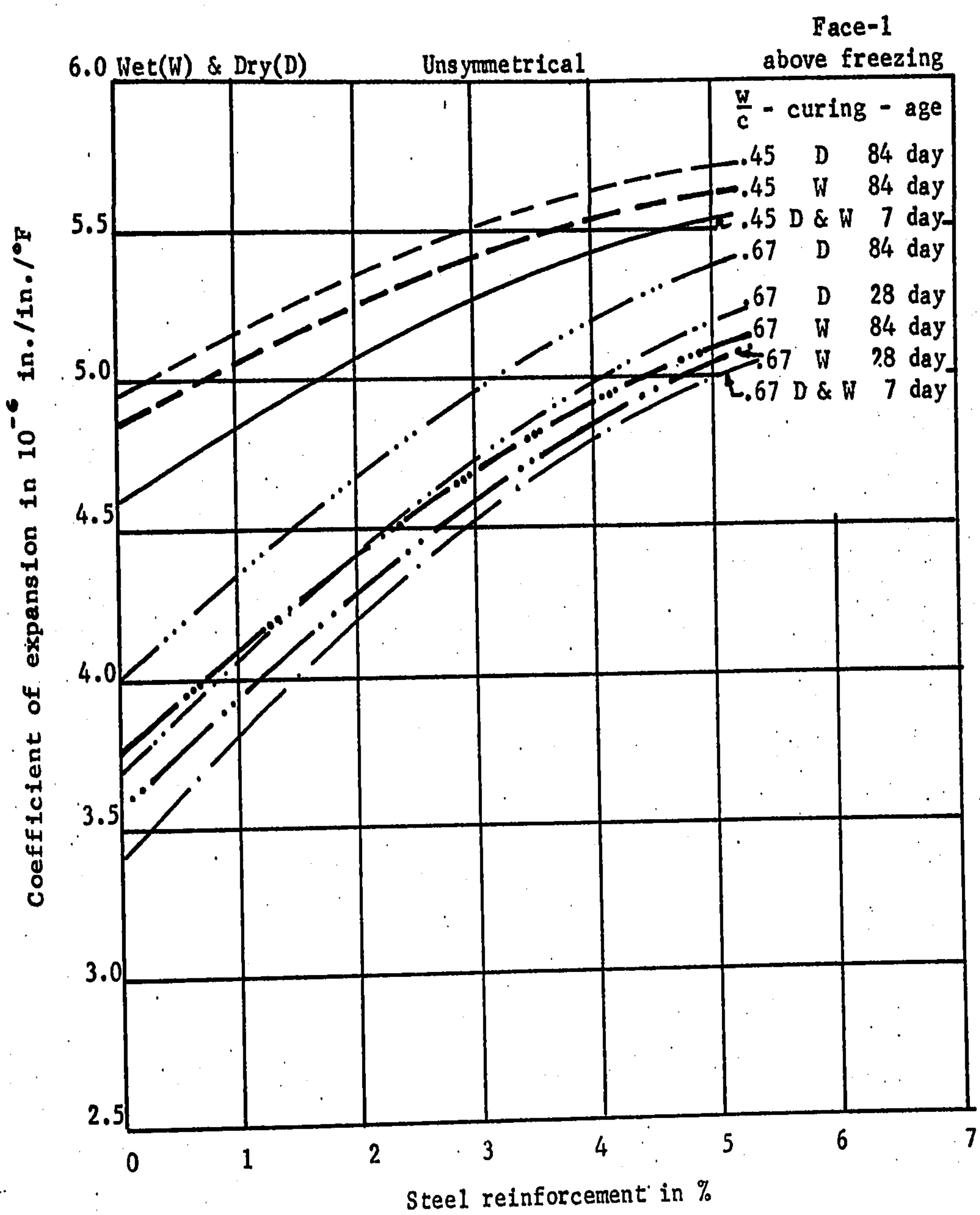

FIG. 5.28: ABOVE FREEZING COEFFICIENTS OF THERMAL EXPANSION OF UNSYMMETRICALLY REINFORCED CONCRETE SLAB (FACE NEAR STEEL)

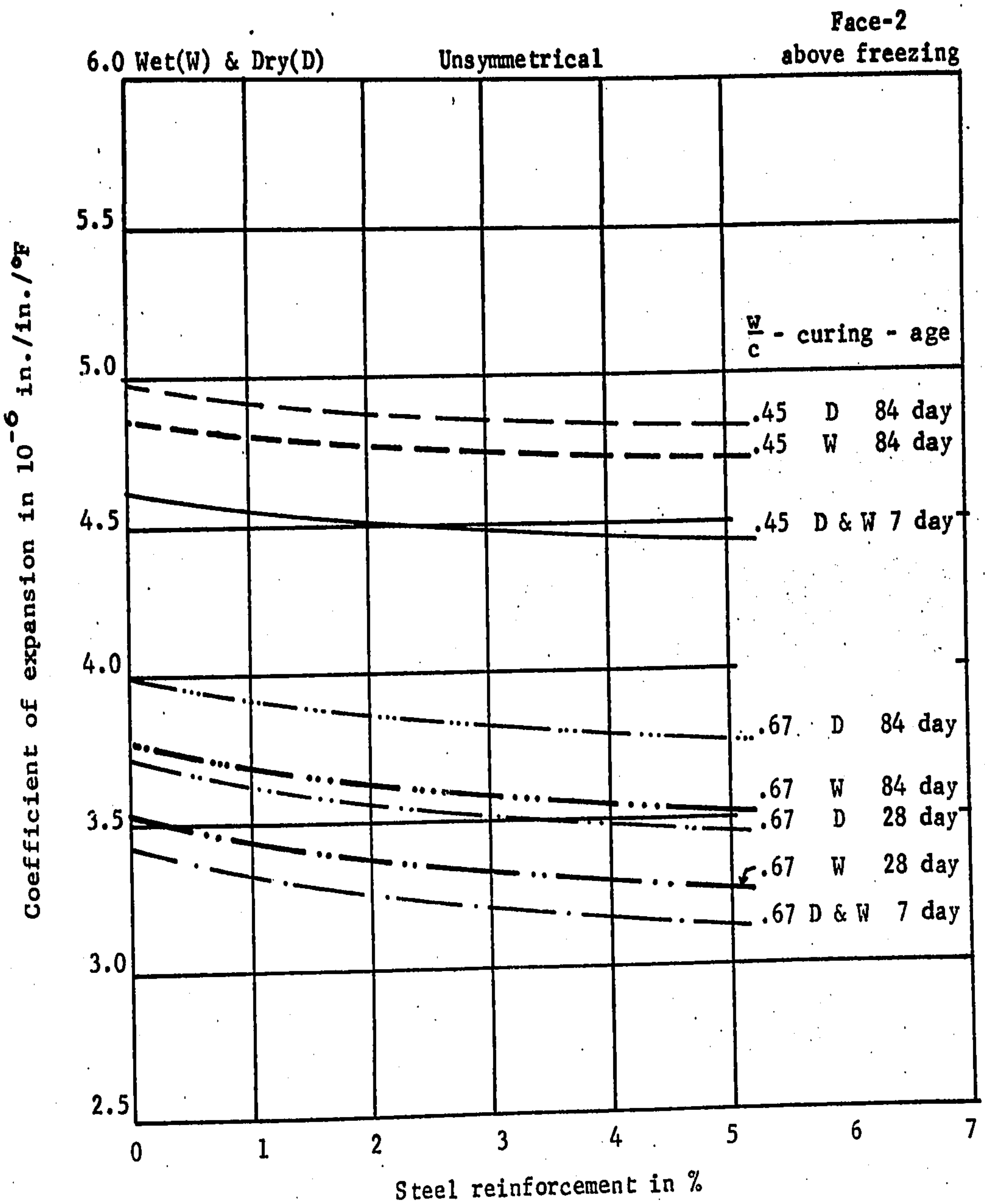

FIG. 5.29: ABOVE FREEZING COEFFICIENTS OF THERMAL EXPANSION OF UNSYMMETRICALLY REINFORCED CONCRETE SLAB (FACE AWAY FROM STEEL)

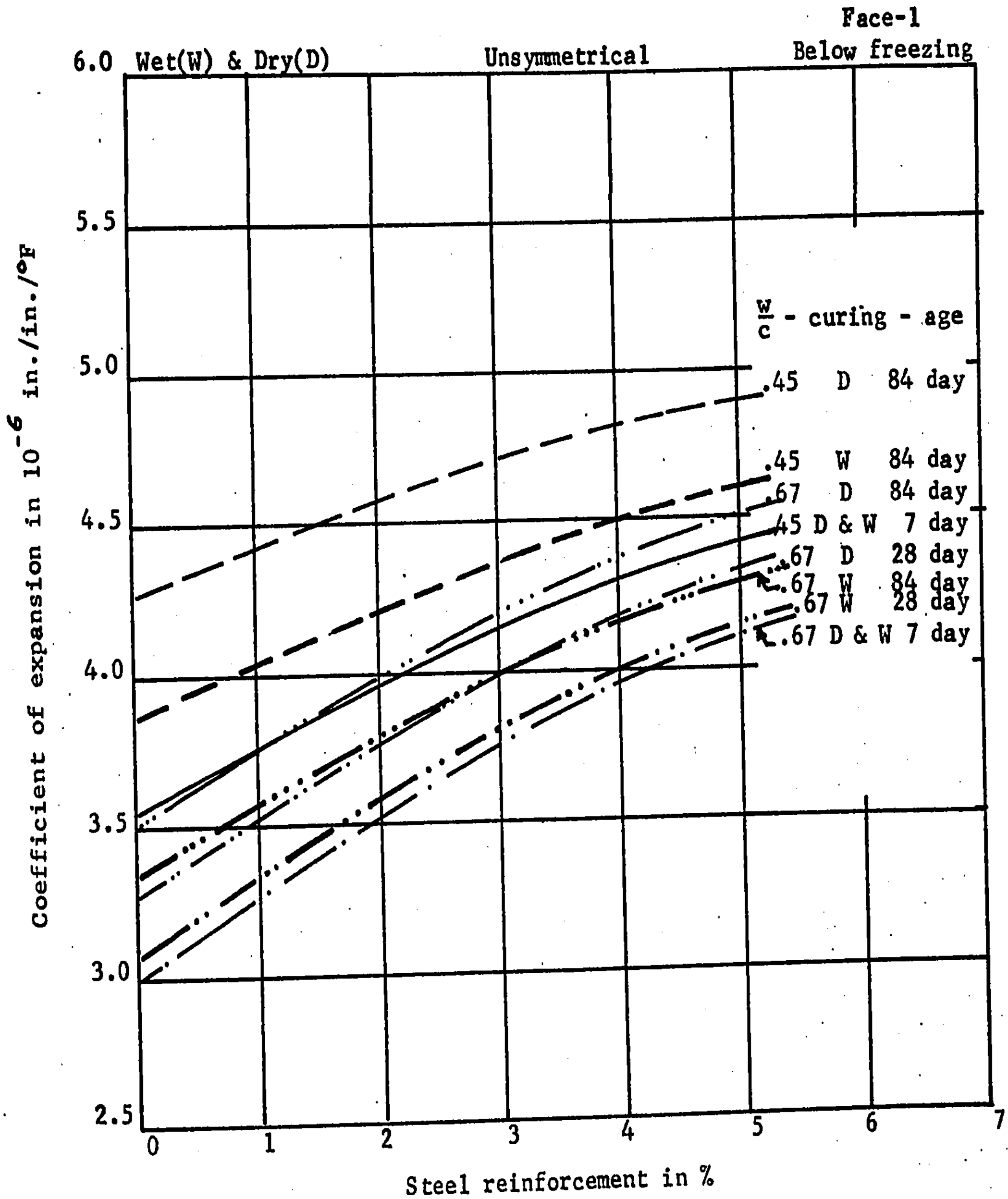

FIG. 5.30: BELOW FREEZING COEFFICIENTS OF EXPANSION OF UNSYMMETRICALLY REINFORCED CONCRETE SLAB (FACE NEAR STEEL)

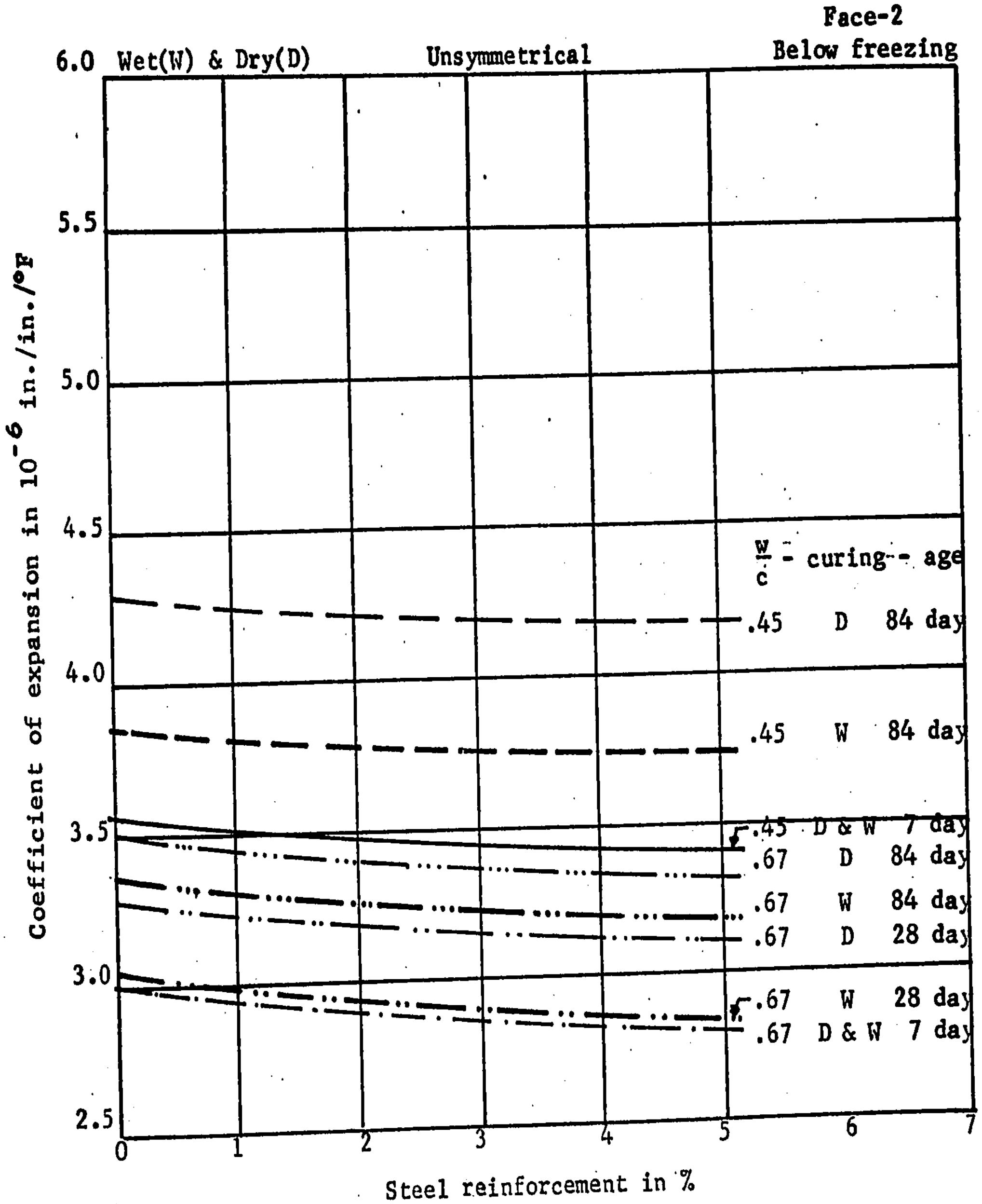

FIG. 5.31 BELOW FREEZING COEFFICIENTS OF EXPANSION OF UNSYMMETRICALLY REINFORCED CONCRETE SLAB (FACE AWAY FROM STEEL)

APPENDIX B: TABLES

TABLE 3.1: PETROGRAPHIC ANALYSIS OF AGGREGATES USED IN CONCRETE

MINERALS	MINERAL CONTENT (%) IN THE AGGREGATES								
	COARSE AGG.				SILICA SAND				
	¾"	½"	3/8"	#4	#8	#16	#30	#50	#100
Quartz	2.0	1.7	8.0	9.0	16.3	16.0	24.0	45.00	71.20
Carbonate (Calcite)	60.0	65.0	75.0	55.0	35.0	40.0	30.0	31.00	8.00
Amphibole (Hornblende)	trace	0.4	trace	trace	trace	trace	1.5	2.00	2.00
Garnet	-	-	-	0.5	-	-	-	0.86	1.75
Magnetite	-	-	-	-	-	-	-	0.70	2.02
Pyroxene(Augite, Diopside, Hyperstine)	trace	-	1.0	0.5	3.2	1.0	3.5	0.96	0.40
Feldspar (K-feldspar, Plagioclase)	34.0	29.5	12.0	31.5	36.0	35.0	35.0	3.61	8.00
Mica (Biotite, Muscovite, Phlogopite)	4.0	3.5	1.5	1.5	5.0	3.0	0.5	1.37	trace
Rock fragments (Schist, granite, Syenite, Quartzite)	-	-	-	-	3.0	1.5	3.5	3.61	6.60
Accessory Minerals	trace (*1)	trace (*2)	2.0 (*3)	1.0 (*4)	0.5 (*5)	3.5 (*6)	1.5 (*7)	0.50 (*8)	0.10 (*9)

*1: Amphibole, pyroxene, iron oxides
*2: Iron oxides, sphene, sulphides
*3: Iron oxides, apatite, tourmaline, amphibole
*4: Chlorite, iron oxide, amphibole
*5: Hornblende, amphibole
*6: Hornblende, diopside, amphibole
*7: Cordierite, apatite, magnetite
*8: Apatite, pyrite
*9: Mica, apatite, pyrite

TABLE 3.2: GRADING OF COARSE AND FINE AGGREGATES

Sieve Size	% Passing by Weight	% Retained by Cumulative Weight	% Retained on each Sieve by Weight	% Proportion used by Weight
		FINE AGGREGATE		
No. 4	100	0	0	0
No. 8	90	10	10	10
No. 16	70	30	20	20
No. 30	44	56	26	30
No. 50	20	80	24	25
No. 100	6	94	14	15
		270 F.M. = 2.7	94	100
		COARSE AGGREGATE		
$\frac{3}{4}$"	95	5	5	5
$\frac{1}{2}$"	67	33	28	30
3/8"	27	63	30	30
No. 4	5	95	32	35
No. 8	0	100	0	0
			95	100

TABLE 3.3: CHARACTERISTICS OF DIFFERENT MIXES

MIX NO.	WATER-CEMENT RATIO	WEIGHT OF CONTENTS (LBS) (For 1 yd.^{3}) Cement	Fine Aggregate (F.M=2.7)	Coarse Aggregate	Water	CEMENT FACTOR bag/cu.yd.	MORTAR CONTENT %	AGGREGATE CONTENT	DESIGN SLUMP
1	0.672	477	1610	1610	317	5.08	27.82	0.722	3"
2	0.577	550	1505	1650	317	5.85	29.2	0.71	3"
3	0.487	650	1415	1655	317	6.92	31.1	0.689	3"
4	0.445	714	1370	1670	317	7.6	32.4	0.676	3"
5	0.434	740	1240	1675	322	7.86	33.1	0.689	3"
6	0.708	456	1500	1675	322	4.86	27.7	0.723	3"

TABLE 3.4: PROPERTIES OF REINFORCING BARS

Designation No.	Diameter (in.)	Area (sq.in.)
D-3	0.195	0.03
D-4	0.225	0.04
D-5.2	0.257	0.052
D-7.2	0.303	0.072
D-8.5	0.329	0.085
D-11	0.374	0.110
D-15	0.437	0.150
D-20	0.504	0.200

Tensile strength min. psi. = 85,000

Yield strength min. psi. = 75,000

TABLE 3.5: VARIATION OF LONGITUDINAL REINFORCEMENT IN THE SLAB SPECIMENS

SPECIMEN NO.	CURING TYPE	ARRANGEMENT OF REINFORCEMENT	DESIGN % OF STEEL	REINFORCEMENT PROVIDED	ACTUAL Area of Steel (in.^{2})	ACTUAL % of Steel
D-0 W-0	Dry Wet	Symmetric	0	0	0	0
D-00 W-00	Dry Wet	Symmetric	0	0	0	0
D-1 W-1	Dry Wet	Symmetric	1	4D3	0.12	1
D-2 W-2	Dry Wet	Symmetric	2	4D4+2D3	0.22	1.84
D-3 W-3	Dry Wet	Symmetric	3	4D7.2+2D3	0.348	2.9
D-4 W-4	Dry Wet	Symmetric	4	4D8.5+2D7.2	0.484	4.03
D-5 W-5	Dry Wet	Symmetric	5	4D11+2D8.5	0.61	5.07
D-0 W-0	Dry Wet	Unsymmetric	0	0	0	0
D-00 W-00	Dry Wet	Unsymmetric	0	0	0	0
D-1 W-1	Dry Wet	Unsymmetric	1	2D4+1D3	0.11	0.92
D-2 W-2	Dry Wet	Unsymmetric	2	2D8.5+1D7.2	0.242	2.02
D-3 W-3	Dry Wet	Unsymmetric	3	1D15+2D11	0.37	3.08
D-4 W-4	Dry Wet	Unsymmetric	4	3D15	0.45	3.75
D-5 W-5	Dry Wet	Unsymmetric	5	3D20	0.60	5.0

Note: Steel bars used are deformed wire gauges (ASTM A 496).

TABLE 3.6: CHARACTERISTICS OF DIFFERENT SERIES

SERIES	WATER-CEMENT RATIO	ARRANGEMENT OF REINFORCEMENT	TEST AGE (days)	CURING Type	In Water $70^0 \pm$	In Air $68-72^0F$ 65-75%RH
ASD	0.672	Symmetric	7,28,84	Dry	7	Until test
ASD	0.577	Symmetric	7,28,84	Dry	7	Until test
ASD	0.487	Symmetric	7,28,84	Dry	7	Until test
ASD	0.445	Symmetric	7, 84	Dry	7	Until test
ASW	0.672	Symmetric	7,28,84	Wet	Until test	-
ASW	0.577	Symmetric	7,28,84	Wet	Until test	-
ASW	0.487	Symmetric	7,28,84	Wet	Until test	-
ASW	0.445	Symmetric	7, 84	Wet	Until test	-
AUD	0.672	Unsymmetric	7,28,84	Dry	7	Until test
AUD	0.577	Unsymmetric	7,28,84	Dry	7	Until test
AUD	0.487	Unsymmetric	7,28,84	Dry	7	Until test
AUD	0.445	Unsymmetric	7, 84	Dry	7	Until test
AUW	0.672	Unsymmetric	7,28,84	Wet	Until test	-
AUW	0.577	Unsymmetric	7,28,84	Wet	Until test	-
AUW	0.487	Unsymmetric	7,28,84	Wet	Until test	-
AUW	0.445	Unsymmetric	7, 84	Wet	Until test	-
N	0.708	Unsymmetric	365	Dry	7	Until test
E	0.434	Symmetric	365	Dry	7	Until test

Note: In each series the steel percentage varied from 0 to 5.

TABLE 3.7: FABRICATION PLAN FOR SPECIMENS AND CYLINDERS FOR DIFFERENT VARIABLES

VARIABLES		NUMBERS FABRICATED AND TESTED		
		Slab Specimens 12" x 4" x 3"	Prism Specimens 12" x 3" x 3"	Cylinders 12" x 6"
AGE	7 day	112	32	16
	28 day	112/84*	32/24*	32/24*
	84 day	112	32	32
	365 day	13	4	4
W/C RATIO	.434	7	2	2
	.445	28	8	20
	.487	28	8	20
	.577	28	8	20
	.672	28	8	20
	.708	6	2	2
METHOD OF CURING	Wet	56	16	40
	Dry	69	20	44
TEMPERATURE RANGE	Above Freezing	125	36	-
	Below Freezing	125	36	-
ARRANGEMENT OF STEEL	Symmetrical	63	-	-
	Unsymmetrical	62	-	-
REINFORCEMENT PERCENTAGE	0	35	-	-
	1	18	-	-
	2	18	-	-
	3	18	-	-
	4	18	-	-
	5	18	-	-
TOTAL NO. CAST		125	36	84

* Actually tested differed from No. prepared

TABLE 3.8 : FEATURES OF MODEL 6204B DC POWER SUPPLY

OUTPUT		INPUT	LOAD REGULATION	LINE REGULATION	TEMP. COEFF.	STABILITY	METER RANGES
D C VOLTAGE	D C CURRENT		CONST. VOLTAGE	CONST. VOLTAGE	CONST. VOLTAGE	CONST. VOLTAGE	
0-20V 0-40V	0-0.6A 0-0.3A	105-125/ 210-250 VAC 50-400 Hz 0.40A, 24W	0.01% PLUS 4 MV	0.01% PLUS 4 MV	0.02% PLUS 1 MV/^{0}C	0.1% PLUS 5 MV	0-5V, 0-50V, 0-.075A, 0-.75A

TABLE 3.9: PROPERTIES OF CONTROL ALUMINIUM PLATE

DIMENSION - ¼ in. x 12 in. x 3 in.

COMMERCIAL IDENTITY - 6351-T6

MANUFACTURER - Alcan

COMPOSITION:

Elements	Percentage
Cu	0.1
Fe	0.5
Mg	0.4 to 0.80
Mn	0.4 to 0.80
Si	0.7 to 1.3
Pipenium	0.20
Other elements	0.05
Aluminium	rest

THERMAL PROPERTIES:

Conductivity (at 25^{0}C) - 104.8 BTU

Coefficient of Expansion - 0.00001322 in./in./^{0}F

0.0000239 in./in./^{0}C

TABLE 4.1: SUMMARY OF TEMPERATURE READINGS (^{0}F)
(IN DECREASING ORDER)

Series - AUD 0.445 | Age - 84 days | Dry-Cured

TEMPERATURE CONTROL INDICATED BY			TEMPERATURE OF EMBEDDED THERMOCOUPLES						Average (for series) of Embedded Thermocouples
			D-0		D-2		D-5		
Temp. Set	Pointer	Pen	Before Reading	After Reading	Before Reading	After Reading	Before Reading	After Reading	
150	152→155	154	155.0	153.2	155.0	154.0	155.2	153.6	154.3
135	136→138	137	138.0	138.0	138.2	138.7	138.0	139.0	138.3
120	125→127	125	125.8	125.1	126.0	125.0	125.8	125.0	125.5
105	108→110	109	109.8	109.4	109.9	110.1	108.2	109.5	109.5
90	90→ 92	91	90.0	91.0	91.8	91.0	90.0	92.0	91.0
75	72→ 75	73	73.5	74.0	74.5	74.5	73.2	72.6	73.7
60	59→ 62	60	60.5	61.5	60.2	60.7	59.5	61.1	60.6
45	45→ 47	46	45.5	46.7	46.0	46.8	45.5	47.0	46.3
30	29→ 31	30	31.2	31.3	29.8	30.0	29.0	29.0	30.5
15	15→ 17	15	15.9	16.3	15.1	15.9	15.0	15.5	15.6
0	2→ 3	3	3.0	2.5	2.5	2.0	2.4	3.0	2.6
-15	-12→-14	-13	-13.0	-13.0	-14.0	-12.9	-13.9	-13.0	-13.3
-30	-26→-29	-27	-28.5	-28.5	-26.1	-27.8	-28.0	-28.0	-27.8
-45	-44→-46	-44	-45.0	-46.0	-44.0	-45.0	-44.3	-45.0	-44.9
-60	-60→-62	-61	-60.0	-60.8	-61.0	-62.0	-60.0	-60.5	-60.7
-75	-74→-77	-75	-76.0	-74.9	-75.9	-76.0	-76.0	-77.0	-76.0
-90	-88→-91	-90	-91.0	-89.0	-89.1	-88.0	-88.2	-89.0	-89.1
-100	-99→-101	-100	-100.0	-100.5	-101.5	-99.7	-101.5	-98.2	-100.2
30	30→ 38	31	31.0	31.8	30.7	31.3	30.5	31.3	31.1

TABLE 4.2: COMPRESSION AND DEFORMATION READINGS IN 10^{-5} IN.

Series - AUD 0.445 Dry-Cured
Age - 84 days Gauge Length = 9 in.

LOAD IN KIPS	CYLINDER NO. D4				CYLINDER NO. D5			
	LOADING		UNLOADING		LOADING		UNLOADING	
	Dial 1	Dial 2	Dial 1	Dial 2	Dial 1	Dial 2	Dial 1	Dial 2
0	0	0	40	5	0	0	20	20
5	35	20	75	40	48	20	65	40
10	70	45	120	73	75	35	105	90
15	105	75	160	108	111	65	140	110
20	140	105	195	140	142	87	175	142
25	170	135	232	172	170	127	190	175
30	205	165	268	203	200	160	237	207
35	240	195	300	235	230	187	270	242
40	275	230	330	263	260	220	300	270
45	310	260	360	295	290	255	325	302
50	350	295	393	325	320	295	355	340
55	383	327	418	350	350	330	380	360
60	420	360	443	375	385	370	400	395
65	460	397	460	397	420	405	420	405
ULT. LOAD	197.5 KIPS				191.5 KIPS			

TABLE 4.3: DEFORMATION READINGS OF CONTROL ELEMENTS BY TRANSDUCERS

Series - AUD 0.445
Age - 84 days

Dry-Cured
Gauge Length = 4 in.

DEFORMATION READINGS

TEMPERATURE (^{0}F)	CONTROL ALUMINIUM BLOCK		CONTROL SPECIMENS			
	AL-1	AL-2	D-0	D-00	W-0	W-00
120	68420	76040	55850	66980	69000	57890
105	67816	75970	55514	66960	68541	58242
90	67458	75164	55748	67120	67961	58320
75	66626	74134	55639	67817	66990	58661
60	67201	74676	56325	68549	67674	59298
45	64827	72009	54647	67193	65470	57870
30	64371	71126	54267	67533	64639	58109
15	63473	70216	53718	67476	63940	58076
0	61591	68602	51974	66883	62493	57654
-15	59445	67928	50105	67330	61769	57778
-30	55781	65931	46704	66958	60846	57653
-45	51556	63156	43362	65889	59484	56604
-60	45584	58000	38238	63363	56649	54125
-75	40495	53197	34127	61822	54082	51583
-90	35414	49071	28022	59573	51617	48559
-100	29321	45692	21920	56656	49800	45600
30	63233	71229	54250	67200	63500	55080
TRANSDUCER #	3	4	5	6	9	1

Range Reading - IV
Vernier Reading - 5

Gate Opening - 1 sec.
Sensitivity - 0.1 volt

TABLE 4.4: TEMPERATURE AND DEFORMATION READINGS OF CONTROL ALUMINIUM BLOCK BY OPTICAL EXTENSOMETER

Series - AUD 0.445
Age - 84 days

Dry-Cured
Gauge Length = 10"

CONTROL BLOCK 1		CONTROL BLOCK 2	
Temperature at time of Reading ^0F	Deformation Reading in 0.002 in.	Temperature at time of Reading ^0F	Deformation Reading in 0.002 in.
156.0	-2.45	155.2	-2.75
137.6	-1.50	138.4	-1.16
123.0	0.00	122.8	0.17
109.0	0.56	109.9	1.57
98.0	1.98	97.2	2.38
80.5	3.16	79.2	3.75
59.2	4.80	61.2	4.56
45.7	5.30	47.0	5.90
31.0	5.71	33.5	5.93
15.8	6.91	17.0	7.27
-4.0	7.78	3.0	8.02
-12.5	8.42	-13.0	8.73
-28.0	9.54	-25.5	9.62
-45.2	10.44	-41.0	10.70
-62.9	11.07	-59.0	11.48
-79.0	11.81	-74.8	12.27
-90.2	12.65	-87.0	12.86
-105.0	13.45	-99.1	13.88
30.0	6.22	37.0	6.19

TABLE 4.5: DEFORMATION READINGS OF CONCRETE SLABS BY OPTICAL EXTENSOMETER

Series - ASD 0.487
Age - 28 days

Face 1

Dry-Cured
Gauge length = 10 in.

EXTENSOMETER READING IN 2 x 10^{-3} IN.

TEMP. (^{0}F)	D-0	D-00	D-1	D-2	D-3	D-4	D-5
153.6	-6.53	-8.05	6.16	16.02	3.43	4.56	3.44
134.7	-5.58	-7.48	6.83	16.99	4.41	5.38	4.39
118.8	-5.14	-6.82	7.27	17.45	4.88	6.01	5.09
103.9	-4.82	-7.07	7.60	17.78	5.22	5.98	5.30
87.5	-5.28	-7.20	7.16	17.35	4.79	5.56	4.89
73.7	-4.78	-6.76	7.66	17.85	5.31	6.10	5.40
59.3	-4.48	-6.21	7.97	18.17	5.64	6.93	5.77
43.3	-3.49	-5.11	8.97	19.18	6.65	7.74	6.35
31.7	-3.53	-4.92	8.94	19.15	6.63	7.64	6.56
12.1	-2.70	-4.62	9.87	20.26	7.02	7.68	6.78
-1.3	-2.07	-4.21	10.77	20.96	7.74	8.40	7.43
-12.8	-3.87	-5.66	8.77	20.29	7.06	7.73	6.59
-31.6	-2.50	-4.26	10.30	20.25	7.03	7.71	7.11
-47.1	-2.14	-3.77	10.58	21.25	8.04	8.72	7.76
-59.6	-2.22	-4.02	10.43	21.49	8.29	8.97	7.57
-75.0	-1.23	-3.03	11.75	21.84	8.64	9.33	8.04
-90.0	-1.54	-3.58	11.77	22.22	9.03	9.73	9.06
-100.2	-1.46	-2.42	12.02	22.37	9.19	9.89	9.09
30.0	-3.60	-5.39	9.14	20.56	7.33	8.00	6.86

TABLE 4.6: SONIC RESONANCE TEST READINGS

Series - AUD 0.445 | Age - 84 days | Dry-Cured

	SPECIMEN 1		SPECIMEN 2	
TEMP. (^{0}F)	Sonic Test Reading	Resonant Frequency	Sonic Test Reading	Resonant Frequency
75.0	1964.8	6222	1976.0	6334
154.3	1961.6	6191	1964.6	6222
138.3	1961.5	6190	1964.6	6222
128.5	1964.2	6217	1965.5	6229
109.5	1965.5	6230	1966.5	6240
91.0	1964.5	6220	1969.5	6266
73.7	1966.0	6235	1968.0	6255
60.6	1967.0	6245	1969.0	6262
46.3	1968.0	6253	1970.8	6278
30.5	1970.0	6269	1970.4	6274
2.6	1971.7	6287	1974.0	6313
-13.3	1974.7	6317	1975.3	6323
-27.8	1976.5	6338	1977.4	6346
-44.9	1980.0	6373	1969.0	6364
-60.7	1980.5	6380	1981.0	6388
-76.0	1982.0	6398	1983.5	6415
-89.1	1985.0	6435	1983.0	6413
-100.2	1986.5	6453	1985.0	6434
31.1	1961.2	6237	1973.0	6297
WEIGHT	9.39 lbs.		9.43 lbs.	

TABLE 4.7: COMPRESSION DEFORMATION TEST RESULTS

Series - ASD 0.487
Age - 28 days

Dry-Cured
Symmetrical

TEST ONE			TEST TWO		
STRESS KIPS/SQ.IN.	STRAIN 10^{-4} IN./IN.		STRESS KIPS/SQ.IN.	STRAIN 10^{-4} IN./IN.	
	Actual	Fitted		Actual	Fitted
0.0	0.0	0.0	0.0	0.0	0.0
0.177	0.3222	0.4222	0.177	0.3500	0.3996
0.354	0.6833	0.8444	0.354	0.7833	0.7991
0.531	1.0667	1.2667	0.531	1.2167	1.1987
0.707	1.4556	1.6889	0.707	1.6444	1.5982
0.884	1.8611	2.1111	0.884	2.0333	1.9978
1.061	2.2389	2.5333	1.061	2.4111	2.3974
1.238	2.5889	2.9556	1.238	2.7833	2.7969
1.415	2.9444	3.3778	1.415	3.1722	3.1965
1.592	3.3833	3.8000	1.592	3.5611	3.5960
1.768	3.7944	4.2222	1.768	3.9722	3.9956
1.945	5.8944	4.6444	1.945	4.3722	4.3952
2.122	4.6222	5.0667	2.122	4.8000	4.7947
2.299	5.0444	5.4889	2.299	5.2222	5.1943

Fitted values of Modulus of Elasticity:

$E_{c_1} = 4188.29$ kips/sq.in.

$E_{c_2} = 4425.83$ kips/sq.in.

Av. $E_c = 4307.06$ kips/sq.in.

Ultimate Concrete Stresses:

$f'_{c1} = 6.3662$ kips/sq.in.

$f'_{c2} = 6.3308$ kips/sq.in.

Av. $f'_c = 6.3485$ kips/sq.in.

TABLE 4.8: CONCRETE STRENGTH AND MODULUS OF ELASTICITY OF DRY-CURED SERIES AT 7 DAYS OF AGE (AT ROOM TEMP.)

Series No.	Ultimate Cylinder Strength (f'_c) (KSI)	Av. Ultimate Cylinder Strength (Av. f'_c) (KSI)	Initial Modulus of Elasticity (E_c) (KSI)	Av. Initial Modulus of Elasticity (Av. E_c) (KSI)	Dynamic Modulus of Elasticity (E_{cd}) (KSI)	Av. Dynamic Modulus of Elasticity (Av. E_{cd}) (KSI)	Ingé-Lyse's Equation $E_c = 1800 + 460f'_c$ (KSI)
ASD 0.445	6.437 5.146	5.792	5102 4952	5027	5328 5317	5322	4464
AUD 0.445	6.083 6.366	6.225	4521 4325	4423	5308 5268	5288	4664
ASD 0.487	5.411 5.305	5.358	4836 4545	4690	5100 5318	5209	4260
AUD 0.487	5.429 5.288	5.358	4268 4079	4174	5107 5042	5074	4264
ASD 0.577	4.633 4.792	4.713	3841 3927	3884	4980 4811	4896	3968
AUD 0.577	4.633 4.792	4.713	3965 3580	3773	4673 4756	4714	3968
ASD 0.672	3.926* 3.926*	3.926	2394* 2394*	2394	4920 4982	4951	3606
AUD 0.672	4.386 4.350	4.368	3919 4107	4013	4967 4964	4966	3809

*One specimen only

TABLE 4.9: CONCRETE STRENGTH AND MODULUS OF ELASTICITY OF DRY-CURED SERIES AT 28 DAYS OF AGE (AT ROOM TEMP.)

Series No.	Ultimate Cylinder Strength (f'_c) (KSI)	Av. Ultimate Cylinder Strength (Av. f'_c) (KSI)	Initial Modulus of Elasticity (E_c) (KSI)	Av. Initial Modulus of Elasticity (Av. E_c) (KSI)	Dynamic Modulus of Elasticity (E_{cd}) (KSI)	Av. Dynamic Modulus of Elasticity (Av. E_{cd}) (KSI)	Ingé-Lyse's Equation $E_c = 1800 + 460f'_c$ (KSI)
ASD 0 .445							
AUD 0 .445							
ASD 0.487	6.366 6.331	6.34	4188 4426	4307	4843 4776	4809	4716
AUD 0.487	5.659 5.960	5.809	4285 4318	4301	4900 4839	4869	4472
ASD 0.577	5.712 5.358	5.535	4135 3957	4046	4636 4798	4717	4346
AUD 0.577	5.234 4.421	4.828	3948 4460	4204	4697 4579	4638	4021
ASD 0.672	5.111 5.164	5.137	4168 4216	4192	4848 4794	4811	4163
AUD 0.672	5.305 4.810	5.058	3940 4247	4094	4777 4920	4849	4127

TABLE 4.10: CONCRETE STRENGTH AND MODULUS OF ELASTICITY OF DRY-CURED SERIES AT 84 DAYS OF AGE AND E AND N SERIES AT 365 DAYS (AT ROOM TEMP.)

Series No.	Ultimate Cylinder Strength (f'_c) (KSI)	Av. Ultimate Cylinder Strength (Av. f'_c) (KSI)	Initial Modulus of Elasticity (E_c) (KSI)	Av. Initial Modulus of Elasticity (Av. E_c) (KSI)	Dynamic Modulus of Elasticity (E_{cd}) (KSI)	Av. Dynamic Modulus of Elasticity (Av. E_{cd}) (KSI)	Ingé-Lyse's Equation $E_c = 1800 + .460f'_c$ (KSI)
ASD 0.445	6.525 7.180	6.853	5206 5703	5455	4887 4710	4798	4952
AUD 0.445	6.985 6.773	6.879	4825 5051	4938	5022 5231	5126	4964
ASD 0 .487	6.384 6.384	6.384	4461 4423	4442	4569 4702	4635	4737
AUD 0.487	6.578 6.826	6.702	4144 5167	4656	4619 4540	4580	4883
ASD 0.577	5.358 6.083	5.721	4291 4250	4270	4398 4467	4433	4432
AUD 0.577	4.987 4.810	4.898	4066 5367	4717	4226 4172	4199	4053
ASD 0.672	5.429 5.429	5.429	4576 4576	4576	4342 4269	4305	4297
AUD 0.672	5.394 5.482	5.438	4303 4129	4216	4585 4149	4367	4301
E 0.434	6.844 6.525	6.685	4089 3711	3900	4077 7072	4074	4875
N 0.708	4.456 4.332	4.394	3324 2871	3098	3605 3562	3584	3821

TABLE 4.11: CONCRETE STRENGTH AND MODULUS OF ELASTICITY OF WET-CURED SERIES AT 7 DAYS OF AGE (AT ROOM TEMP.)

Series No.	Ultimate Cylinder Strength (f'_c) (KSI)	Av. Ultimate Cylinder Strength (Av. f'_c) (KSI)	Initial Modulus of Elasticity (E_c) (KSI)	Av. Initial Modulus of Elasticity (Av. E_c) (KSI)	Dynamic Modulus of Elasticity (E_{cd}) (KSI)	Av. Dynamic Modulus of Elasticity (Av. E_{cd}) (KSI)	Ingé-Lyse's Equation $E_c = 1800 + 460f'_c$ (KSI)
ASW 0.445	6.437 5.146	5.792	5102 4952	5027	5188 5026	5107	4464
AUW 0.445	6.083 6.366	6.225	4521 4325	4423	4979 5265	5122	4664
ASW 0.487	5.411 5.305	5.358	4836 4545	4690	5078 5080	5079	4264
AUW 0.487	5.429 5.288	5.358	4268 4079	4174	5013 4955	4984	4264
ASW 0.577	4.633 4.792	4.713	3841 3927	3884	4946 4873	4909	3968
AUW 0.577	4.633 4.792	4.713	3965 3580	3773	4994 5036	5015	3968
ASW 0.672	3.926 3.926	3.926	2394 2394	2394	4889 4982	4936	3606
AUW 0.672	4.386 4.350	4.368	3919 4107	4013	5046 4968	5007	3809

TABLE 4.12: CONCRETE STRENGTH AND MODULUS OF ELASTICITY OF WET-CURED SERIES AT 28 DAYS OF AGE (AT ROOM TEMP.)

Series No.	Ultimate Cylinder Strength (f'_c) (KSI)	Av. Ultimate Cylinder Strength (Av. f'_c) (KSI)	Initial Modulus of Elasticity (E_c) (KSI)	Av. Initial Modulus of Elasticity (Av. E_c) (KSI)	Dynamic Modulus of Elasticity (E_{cd}) (KSI)	Av. Dynamic Modulus of Elasticity (Av. E_{cd}) (KSI)	Ingé-Lyse's Equation $E_c = 1800 + 460f'_c$ (KSI)
ASW 0.445							
AUW 0.445							
ASW 0.487	6.525 5.677	6.101	4937 4772	4854	5309 5325	5317	4606
AUW 0.487	5.641 5.889	5.765	4474 4589	4532	5147 5129	5138	4452
ASW 0.577	5.783 5.181	5.482	4214 4530	4372	5220 5142	5181	4322
AUW 0.577	5.146 5.234	5.190	5008 4313	4660	5052 5002	5027	4187
ASW 0.672	4.704 5.146	4.925	4222 4074	4148	4813 5011	4912	4066
AUW 0.672	5.517 5.429	5.473	4202 4332	4269	5175 5000	5087	4317

TABLE 4.13: CONCRETE STRENGTH AND MODULUS OF ELASTICITY OF WET-CURED SERIES AT 84 DAYS OF AGE (AT ROOM TEMP.)

Series No.	Ultimate Cylinder Strength (f'_c) (KSI)	Av. Ultimate Cylinder Strength (Av. f'_c) (KSI)	Initial Modulus of Elasticity (E_c) (KSI)	Av. Initial Modulus of Elasticity (Av. E_c) (KSI)	Dynamic Modulus of Elasticity (E_{cd}) (KSI)	Av. Dynamic Modulus of Elasticity (Av. E_{cd}) (KSI)	Ingē-Lyse's Equation $E_c = 1800 + 460f'_c$ (KSI)
ASW 0.445	6.614 7.693	7.153	6001 5342	5672	5511 5430	5470	5090
AUW 0.445	7.905 7.94	7.922	5215 5376	5296	5551 5727	5639	5444
ASW 0.487	7.021 6.897	6.959	5341 5007	5174	5295 5711	5503	5010
AUW 0.487	7.215 7.074	7.144	5003 4900	4951	5472 5459	5466	5086
ASW 0.577	6.119 6.561	6.340	5323 4723	5023	5796 5505	5650	4716
AUW 0.577	5.783 6.083	5.933	4931 4795	4863	5460 5125	5293	4529
ASW 0.672	2.122 2.122	2.122	2952 2952	2952	5221 5454	5338	2776
AUW 0.672	5.641 5.164	5.402	4651 4917	4782	5602 5217	5410	4285

TABLE 4.14: TYPICAL ANALYSIS OF SONIC RESONANT TEST READINGS

Series - ASD 0.487
Specimen 1

Age - 28 days
Dry-Cured

TEMP. (^{0}F)	SONIC RESONANT FREQUENCY	DYNAMIC-E Experimental (KSI)	DYNAMIC-E Fitted (KSI)
74.9	6107	4847	-
153.6	6032	4729	4729
134.7	6040	4742	4759
118.8	6076	4798	4785
103.9	6095	4828	4808
87.5	6092	4824	4835
73.7	6110	4852	4857
59.3	6127	4879	4880
43.3	6145	4906	4900
31.7	6162	4935	4920
12.1	6208	5008	-
-1.3	6270	5110	5100
-12.8	6319	5190	5188
-31.6	6408	5335	5320
-47.1	6455	5416	5428
-59.6	6503	5495	5516
-75.0	6583	5633	5624
-90.0	6646	5741	5729
-100.2	6678	5796	5800
30.0	6148	4913	-

TABLE 4.14: TYPICAL ANALYSIS OF SONIC RESONANT TEST READINGS

Series - ASD 0.487
Specimen 1

Age - 28 days
Dry-Cured

TEMP. (^{0}F)	SONIC RESONANT FREQUENCY	DYNAMIC-E Experimental (KSI)	DYNAMIC-E Fitted (KSI)
74.9	6107	4847	-
153.6	6032	4729	4729
134.7	6040	4742	4759
118.8	6076	4798	4785
103.9	6095	4828	4808
87.5	6092	4824	4835
73.7	6110	4852	4857
59.3	6127	4879	4880
43.3	6145	4906	4900
31.7	6162	4935	4920
12.1	6208	5008	-
-1.3	6270	5110	5100
-12.8	6319	5190	5188
-31.6	6408	5335	5320
-47.1	6455	5416	5428
-59.6	6503	5495	5516
-75.0	6583	5633	5624
-90.0	6646	5741	5729
-100.2	6678	5796	5800
30.0	6148	4913	-

TABLE 4.15: TYPICAL ANALYSIS OF EXPERIMENTAL DEFORMATION READINGS OF CONCRETE SLABS

ASD 0.487 28.00 DAYS

SPECIMEN NO. D5 FACE 2

TEMPERATURE	SPECIMEN LENGTH CORRECTED	SPECIMEN LENGTH FITTED
153.60	10.0237	10.0231
134.70	10.0217	10.0222
118.80	10.0207	10.0214
103.90	10.0200	10.0207
87.50	10.0208	10.0199
73.70	10.0198	10.0192
59.30	10.0191	10.0185
43.30	10.0170	10.0177

AFT1 = 10.01566029 BFT1 = 0.00004822

CHECK -VE VALUES RSQ= 0.86712378 RRSQ= 0.84497786

ESTIMATE OF ERR IN Y-DIRECTION
UNCORRECTED = 0.0007CORRECTED = 0.0007

STANDARD DEVIATION = 0.0018

COEFF. OF CORRELATIONS*
CALCULATED = 0.9312CORRECTED = 0.9192

TABLE 4.15: TYPICAL ANALYSIS OF EXPERIMENTAL DEFORMATION READINGS OF CONCRETE SLABS (CON'D)

ASD 0.487 28.00 DAYS

SPECIMEN NO. D5 FACE 2

TEMPERATURE	SPECIMEN LENGTH CORRECTED	SPECIMEN LENGTH FITTED
12.10	10.0160	10.0158
-1.30	10.0144	10.0152
-12.80	10.0152	10.0148
-31.60	10.0149	10.0140
-47.10	10.0130	10.0133
-59.60	10.0120	10.0128
-75.00	10.0127	10.0121
-90.00	10.0112	10.0115
-100.20	10.0112	10.0111

AFT1 = 10.01529884 BFT1 = 0.00004231

CHECK -VE VALUES RSQ= 0.89023346 RRSQ= 0.87455261

ESTIMATE OF ERR IN Y-DIRECTION
UNCORRECTED = 0.0006CORRECTED = 0.0006

STANDARD DEVIATION = 0.0017

COEFF. OF CORRELATIONS*
CALCULATED = 0.9435CORRECTED = 0.9352

TABLE 4.16: SUMMARY OF EXPERIMENTAL RESULTS FOR A SERIES

ASD 0.487 28.00 DAYS

TABLE OF CO-EFFICIENT VALUES

SPECIMEN NO	TEMPERATURE RANGE ABOVE-FREEZING FACE-1	ABOVE-FREEZING FACE-2	BELOW-FREEZING FACE-1	BELOW-FREEZING FACE-2
D0	4.2652	4.2265	2.8334	3.5893
D00	4.2120	3.2824	3.7377	3.8170
D1	4.1103	4.4250	4.0517	3.5616
D2	4.4685	4.4105	3.7929	3.8999
D3	4.6089	4.6428	3.8792	4.0828
D4	4.6816	5.0011	3.9551	3.6997
D5	4.3088	4.8220	4.0138	4.2312

TABLE 4.17: TYPICAL RESULT OF THEORETICAL ANALYSIS

SERIES NO.-ASD 0.4970 28.0000DAYS
****

THEORETICAL VALUES OF CO-EFFICIENT OF THERMAL EXPANSION
REINFORCED CONCRETE WITH 5% STEEL REINFORCEMENT
TYPE OF REINFORCEMENT- SYMMETRICAL
****

TEMPERATURE IN DEG. F. INITIAL	FINAL	DIFFERENCE	FORCE DEVELOPED IN CONCRETE	THERMAL-COEFF. OF REINFORCED CONCRETE
150.00	135.00	-15.00	-455.342773	0.0000048091
135.00	120.00	-15.00	-456.683594	0.0000048081
120.00	105.00	-15.00	-457.439697	0.0000048065
105.00	90.00	-15.00	-458.894531	0.0000048057
90.00	75.00	-15.00	-459.881104	0.0000048043
75.00	60.00	-15.00	-461.100098	0.0000048032
60.00	45.00	-15.00	-462.317871	0.0000048022
45.00	30.00	-15.00	-257.388672	0.0000045560
30.00	15.00	-15.00	-372.471924	0.0000041367
15.00	0.0	-15.00	-374.848633	0.0000041299
0.0	-15.00	-15.00	-377.455811	0.0000041236
-15.00	-30.00	-15.00	-380.013428	0.0000041175
-30.00	-45.00	-15.00	-382.621826	0.0000041117
-45.00	-60.00	-15.00	-385.186523	0.0000041061
-60.00	-75.00	-15.00	-387.709961	0.0000041006
-75.00	-90.00	-15.00	-390.093750	0.0000040953
-90.00	-100.00	-10.00	-261.129883	0.0000040918

AVERAGE VALUES OF CO-EFFICIENTS ARE:

ABOVE FREEZING POINT:-

0.0000048061

BELOW FREEZING POINT:-

0.0000041095

****

TABLE 5.1: VARIATION OF RATE OF CHANGE OF MODULUS OF ELASTICITY WITH TEMPERATURE. DRY-CURED SERIES AT 7 DAYS OF AGE

SERIES	SPECIMEN NO.	SLOPE OF DYNAMIC-E ($KSI/^0F$) above freezing	SLOPE OF DYNAMIC-E ($KSI/^0F$) below freezing	APPROX. FREEZING POINT (^0F)	AVERAGE DYNAMIC-E AT ROOM TEMP. (KSI)
ASD 0.445	1	-1.55	- 9.65	24.57	5322
	2	-1.47	-10.03	24.81	
AUD 0.445	1	-1.46	- 9.81	28.32	5288
	2	-1.20	- 8.86	23.98	
ASD 0.487	1	-1.283	-11.15	26.62	5209
	2	-1.37	-11.78	26.10	
AUD 0.487	1	-1.40	-11.15	26.40	5074
	2	-1.37	-12.29	26.50	
ASD 0.577	1	-1.704	-12.357	28.31	4896
	2	-1.68	-12.2	27.81	
AUD 0.577	1	-1.47	-10.70	27.8	4714
	2	-1.385	-10.673	28.10	
ASD 0.672	1	-1.74	-12.48	30.33	4951
	2	-1.732	-12.42	29.9	
AUD 0.672	1	-1.69	-11.95	31.04	4966
	2	-1.69	-11.94	30.73	

TABLE 5.2: VARIATION OF RATE OF CHANGE OF MODULUS OF ELASTICITY WITH TEMPERATURE. DRY-CURED SERIES AT 28 DAYS OF AGE

SERIES	SPECIMEN NO.	SLOPE OF DYNAMIC-E ($KSI/^0F$) above freezing	SLOPE OF DYNAMIC-E ($KSI/^0F$) below freezing	APPROX. FREEZING POINT (^0F)	AVERAGE DYNAMIC-E AT ROOM TEMP. (KSI)
ASD 0.445	1				
	2				
AUD 0.445	1				
	2				
ASD 0.487	1	-1.59	-7.00	22.87	4809
	2	-1.47	-7.69	23.63	
AUD 0.487	1	-1.46	-8.59	22.09	4869
	2	-1.38	-6.60	23.047	
ASD 0.577	1	-1.65	-8.20	25.104	4717
	2	-1.57	-8.21	25.25	
AUD 0.577	1	-1.37	-7.71	25.0	4638
	2	-1.36	-7.66	24.78	
ASD 0.672	1	-1.599	-9.89	27.0	4811
	2	-1.60	-9.80	27.15	
AUD 0.672	1	-1.51	-9.58	30.14	4849
	2	-1.495	-9.42	27.34	

TABLE 5.3: VARIATION OF RATE OF CHANGE OF MODULUS OF ELASTICITY WITH TEMPERATURE. DRY-CURED SERIES AT 84 DAYS OF AGE

SERIES	SPECIMEN NO.	SLOPE OF DYNAMIC-E ($KSI/^0F$) above freezing	SLOPE OF DYNAMIC-E ($KSI/^0F$) below freezing	APPROX. FREEZING POINT (^0F)	AVERAGE DYNAMIC-E AT ROOM TEMP. (KSI)
ASD 0.445	1	-1.00	-2.50	14.61	4798
	2	-1.08	-1.87	15.5	
AUD 0.445	1	-0.92	-2.48	16.78	5126
	2	-0.81	-2.13	20.13	
ASD 0.487	1	-1.028	-3.99	18.18	4635
	2	-1.07	-3.095	18.17	
AUD 0.487	1	-1.15	-3.31	20.12	4580
	2	-1.427	-3.63	18.4	
ASD 0.577	1	-1.21	-4.71	20.38	4433
	2	-1.28	-4.60	29.24	
AUD 0.577	1	-1.11	-4.38	18.61	4199
	2	-0.97	-4.59	18.67	
ASD 0.672	1	-1.50	-5.51	21.29	4305
	2	-1.14	-5.21	20.43	
AUD 0.672	1	-1.23	-4.96	23.40	4367
	2	-1.27	-5.07	24.02	

TABLE 5.4: VARIATION OF RATE OF CHANGE OF MODULUS OF ELASTICITY WITH TEMPERATURE. WET-CURED SERIES AT 7 DAYS OF AGE

SERIES	SPECIMEN NO.	SLOPE OF DYNAMIC-E ($KSI/^0F$) above freezing	SLOPE OF DYNAMIC-E ($KSI/^0F$) below freezing	APPROX. FREEZING POINT (^0F)	AVERAGE DYNAMIC-E AT ROOM TEMP. (KSI)
ASW 0.445	1	-1.535	- 9.497	23.83	5107
	2	-1.49	-10.03	24.52	
AUW 0.445	1	-1.41	- 8.73	24.27	5122
	2	-1.40	- 9.17	24.10	
ASW 0.487	1	-1.545	-12.18	25.76	5079
	2	-1.537	-12.25	26.21	
AUW 0.487	1	-1.60	-11.80	26.83	4984
	2	-1.56	-11.70	26.4	
ASW 0.577	1	-1.739	-11.936	28.06	4909
	2	-1.72	-11.76	27.65	
AUW 0.577	1	-1.43	-10.303	28.26	5015
	2	-1.43	-10.25	28.39	
ASW 0.672	1	-1.736	-12.466	30.02	4936
	2	-1.728	-12.42	30.33	
AUW 0.672	1	-1.592	-12.99	29.94	5007
	2	-1.57	-12.9	30.17	

TABLE 5.5: VARIATION OF RATE OF CHANGE OF MODULUS OF ELASTICITY WITH TEMPERATURE. WET-CURED SERIES AT 28 DAYS OF AGE

SERIES	SPECIMEN NO.	SLOPE OF DYNAMIC-E ($KSI/^0F$) above freezing	SLOPE OF DYNAMIC-E ($KSI/^0F$) below freezing	APPROX. FREEZING POINT (^0F)	AVERAGE DYNAMIC-E AT ROOM TEMP. (KSI)
ASW 0.445	1				
	2				
AUW 0.445	1				
	2				
ASW 0.487	1	-1.69	-10.50	23.3	4606
	2	-1.64	-11.11	26.87	
AUW 0.487	1	-1.58	-10.59	18.95	4452
	2	-1.60	-10.59	23.82	
ASW 0.577	1	-1.81	-11.39	25.96	4322
	2	-1.73	-11.115	24.18	
AUW 0.577	1	-1.66	-10.88	28.26	4187
	2	-1.67	-10.715	23.89	
ASW 0.672	1	-1.80	-11.297	27.2	4066
	2	-1.846	-11.41	26.80	
AUW 0.672	1	-1.91	-12.80	27.40	4317
	2	-1.86	-12.35	27.10	

TABLE 5.6: VARIATION OF RATE OF CHANGE OF MODULUS OF ELASTICITY WITH TEMPERATURE. WET-CURED SERIES AT 84 DAYS OF AGE

SERIES	SPECIMEN NO.	SLOPE OF DYNAMIC-E (KSI/^{0}F) above freezing	SLOPE OF DYNAMIC-E (KSI/^{0}F) below freezing	APPROX. FREEZING POINT (^{0}F)	AVERAGE DYNAMIC-E AT ROOM TEMP. (KSI)
ASW 0.445	1	-1.357	- 7.99	21.98	5470
	2	-1.59	- 8.42	22.24	
AUW 0.445	1	-1.64	- 7.29	19.67	5639
	2	-1.68	- 7.76	21.51	
ASW 0.487	1	-1.81	-10.20	23.94	5503
	2	-1.83	-10.51	27.11	
AUW 0.487	1	-1.996	- 9.34	21.304	5466
	2	-1.88	- 9.7	24.04	
ASW 0.577	1	-1.759	-11.19	23.25	5650
	2	-1.91	-10.60	25.75	
AUW 0.577	1	-1.92	- 9.89	35.13	5293
	2	-1.93	-10.81	26.25	
ASW 0.672	1	-2.25	-12.0	29.83	5338
	2	-2.09	-11.90	29.1	
AUW 0.672	1	-1.809	-10.89	27.7	5410
	2	-1.81	-10.83	26.37	

TABLE 5.7: VARIATION OF COEFFICIENT OF EXPANSION OF PLAIN CONCRETE WITH AGE, WATER-CEMENT RATIO AND CURING PROCESS

CURING TYPE	WATER-CEMENT RATIO	AGE IN DAYS 7 above freezing	7 below freezing	28 above freezing	28 below freezing	84 above freezing	84 below freezing
DRY	0.445	4.60*	3.55	4.80	3.94	4.96	4.27
	0.487	4.15	3.25	4.25	3.70	4.47	3.95
	0.577	3.64	2.99	3.85	3.46	4.20	3.71
	0.672	3.41	3.00	3.70	3.28	4.00	3.50
WET	0.445	4.60	3.55	4.73	3.72	4.85	3.86
	0.487	4.15	3.25	4.22	3.60	4.35	3.72
	0.577	3.64	2.99	3.71	3.30	3.87	3.49
	0.672	3.41	3.0	3.524	3.03	3.75	3.34

*All values in 10^{-6} in./in./^{0}F

NOTE: Values for the 28 day old specimens of 0.445 water-cement ratio are interpolated.

TABLE 5.8: THEORETICAL AND EXPERIMENTAL VALUES OF COEFFICIENT OF EXPANSION OF REINFORCED CONCRETE. VARIATION WITH AGE AND STEEL PERCENTAGE (IN 10^6 IN./IN./^{0}F)

Series - ASD 0.445 Symmetrical Dry-Cured

AGE IN DAYS	% OF STEEL	THEORETICAL above freezing	THEORETICAL below freezing	EXPERIMENTAL above freezing Face 1	EXPERIMENTAL above freezing Face 2	EXPERIMENTAL below freezing Face 1	EXPERIMENTAL below freezing Face 2
7	0	4.60	3.55	4.41	4.48	3.53	3.25
	1	4.70	3.64	4.61	4.29	3.63	3.39
	2	4.78	3.72	4.55	5.17	3.70	3.88
	3	4.87	3.80	4.70	4.86	4.04	3.59
	4	4.96	3.88	4.80	4.83	3.87	3.68
	5	5.03	3.95	4.89	4.67	3.93	4.80
28	0						
	1						
	2						
	3						
	4						
	5						
84	0	4.96	4.27	5.00	4.77	4.00	4.17
	1	5.05	4.38	5.33	4.68	3.77	4.24
	2	5.11	4.39	5.10	4.57	4.26	4.29
	3	5.18	4.45	5.59	5.24	4.34	4.35
	4	5.26	4.51	5.63	5.83	4.38	4.40
	5	5.32	4.55	5.31	5.34	4.60	4.69

Face 1 - near steel
Face 2 - away from steel

TABLE 5.9: THEORETICAL AND EXPERIMENTAL VALUES OF COEFFICIENT OF EXPANSION OF REINFORCED CONCRETE. VARIATION WITH AGE AND STEEL PERCENTAGE (IN 10^6 IN./IN./^{0}F)

Series - ASD 0.487 Symmetrical Dry-Cured

AGE IN DAYS	% OF STEEL	THEORETICAL above freezing	THEORETICAL below freezing	EXPERIMENTAL above freezing Face 1	EXPERIMENTAL above freezing Face 2	EXPERIMENTAL below freezing Face 1	EXPERIMENTAL below freezing Face 2
7	0	4.15	3.25	4.29	3.65	3.18	3.33
	1	4.28	3.36	4.70	4.59	3.38	3.19
	2	4.38	3.44	4.42	4.49	3.46	3.73
	3	4.49	3.53	4.54	4.60	3.09	3.56
	4	4.60	3.63	4.66	3.58	3.66	3.84
	5	4.69	3.70	4.81	4.88	3.72	3.74
28	0	4.25	3.70	4.24	3.75	3.29	3.70
	1	4.38	3.79	4.11	4.42	4.05	3.56
	2	4.48	3.86	4.47	4.41	3.79	3.90
	3	4.59	3.95	4.61	4.64	3.88	4.08
	4	4.69	4.03	4.68	5.00	3.96	3.70
	5	4.78	4.09	4.31	4.82	4.01	4.23
84	0	4.47	3.95	4.46	3.98	3.83	3.53
	1	4.59	4.04	5.46	4.61	4.05	4.05
	2	4.68	4.12	4.69	4.19	4.11	3.81
	3	4.79	4.18	4.42	4.85	4.16	3.87
	4	4.89	4.26	5.15	4.35	4.26	4.54
	5	4.97	4.32	4.65	5.33	4.32	4.34

Face 1 - near steel
Face 2 - away from steel

TABLE 5.10: THEORETICAL AND EXPERIMENTAL VALUES OF COEFFICIENT OF EXPANSION OF REINFORCED CONCRETE. VARIATION WITH AGE AND STEEL PERCENTAGE (IN 10^6 IN./IN./^{0}F)

Series - ASD 0.577 Symmetrical Dry-Cured

AGE IN DAYS	% OF STEEL	THEORETICAL above freezing	THEORETICAL below freezing	EXPERIMENTAL above freezing Face 1	EXPERIMENTAL above freezing Face 2	EXPERIMENTAL below freezing Face 1	EXPERIMENTAL below freezing Face 2
7	0	3.64	2.99	3.65	3.09	2.83	2.86
	1	3.80	3.11	3.22	3.28	2.96	2.98
	2	3.93	3.21	3.83	3.38	3.83	3.08
	3	4.07	3.32	3.49	3.44	3.17	3.19
	4	4.20	3.42	3.65	3.68	3.27	3.28
	5	4.32	3.51	3.70	3.66	3.36	3.01
28	0	3.85	3.46	3.24	4.10	3.48	3.32
	1	4.01	3.57	4.24	4.24	3.59	3.61
	2	4.13	3.65	4.64	4.42	3.30	3.68
	3	4.26	3.74	4.43	4.53	3.77	3.78
	4	4.39	3.84	4.72	4.48	3.85	3.52
	5	4.49	3.91	4.63	4.88	3.95	3.69
84	0	4.20	3.71	4.20	4.38	3.89	3.64
	1	4.35	3.82	4.16	4.47	3.81	3.82
	2	4.46	3.90	4.32	4.01	3.89	3.91
	3	4.58	3.99	4.46	4.09	3.99	4.01
	4	4.70	4.08	4.53	4.60	4.06	4.28
	5	4.79	4.15	4.40	4.64	4.47	4.15

Face 1 - near steel
Face 2 - away from steel

TABLE 5.11: THEORETICAL AND EXPERIMENTAL VALUES OF COEFFICIENT OF EXPANSION OF REINFORCED CONCRETE. VARIATION WITH AGE AND STEEL PERCENTAGE (IN 10^6 IN./IN./^{0}F)

Series - ASD 0.672 Symmetrical Dry-Cured

AGE IN DAYS	% OF STEEL	THEORETICAL above freezing	THEORETICAL below freezing	EXPERIMENTAL above freezing Face 1	EXPERIMENTAL above freezing Face 2	EXPERIMENTAL below freezing Face 1	EXPERIMENTAL below freezing Face 2
7	0	3.41	3.00	3.41	4.19	2.63	2.76
	1	3.59	3.12	2.75	3.27	3.02	2.86
	2	3.72	3.21	3.34	3.41	2.94	3.32
	3	3.87	3.32	3.54	3.93	3.05	3.07
	4	4.01	3.42	3.34	3.74	3.15	3.07
	5	4.13	3.51	3.80	4.06	3.08	3.27
28	0	3.70	3.28	3.31	3.37	3.02	3.22
	1	3.86	3.39	3.47	3.49	3.32	3.33
	2	3.98	3.48	3.59	3.53	3.40	3.41
	3	4.13	3.58	3.70	3.71	3.84	3.28
	4	4.26	3.67	3.53	3.85	3.32	3.75
	5	4.37	3.75	4.01	3.83	3.67	3.70
84	0	4.00	3.50	3.74	3.90	3.51	3.40
	1	4.16	3.62	4.13	4.18	3.53	3.53
	2	4.28	3.71	4.29	4.26	3.76	3.45
	3	4.42	3.81	4.31	4.41	3.48	4.06
	4	4.54	3.91	4.02	4.73	3.81	3.82
	5	4.65	3.99	4.61	4.14	3.87	3.63

Face 1 - near steel
Face 2 - away from steel

TABLE 5.12: THEORETICAL AND EXPERIMENTAL VALUES OF COEFFICIENT OF EXPANSION OF REINFORCED CONCRETE. VARIATION WITH AGE AND STEEL PERCENTAGE (IN 10^6 IN./IN./^{0}F)

Series - ASW 0.445 Symmetrical Wet-Cured

AGE IN DAYS	% OF STEEL	THEORETICAL above freezing	THEORETICAL below freezing	EXPERIMENTAL above freezing Face 1	EXPERIMENTAL above freezing Face 2	EXPERIMENTAL below freezing Face 1	EXPERIMENTAL below freezing Face 2
7	0	4.60	3.55	4.71	4.46	3.65	3.51
	1	4.70	3.64	4.45	5.27	3.67	3.61
	2	4.78	3.72	4.90	4.94	3.75	3.70
	3	4.87	3.80	4.97	5.02	3.63	3.91
	4	4.96	3.88	4.61	5.10	3.90	3.57
	5	5.03	3.95	5.13	4.94	3.96	3.98
28	0						
	1						
	2						
	3						
	4						
	5						
84	0	4.85	3.86	4.77	5.02	3.71	3.57
	1	4.93	3.94	4.91	5.40	3.85	3.62
	2	5.00	3.99	4.44	5.15	3.92	3.68
	3	5.07	4.06	5.21	5.53	4.54	3.73
	4	5.14	4.13	5.52	5.64	3.72	3.67
	5	5.20	4.19	5.20	5.63	4.11	3.86

Face 1 - near steel
Face 2 - away from steel

TABLE 5.13: THEORETICAL AND EXPERIMENTAL VALUES OF COEFFICIENT OF EXPANSION OF REINFORCED CONCRETE. VARIATION WITH AGE AND STEEL PERCENTAGE (IN 10^6 IN./IN./^{0}F)

Series - ASW 0.487 Symmetrical Wet-Cured

AGE IN DAYS	% OF STEEL	THEORETICAL above freezing	THEORETICAL below freezing	EXPERIMENTAL above freezing Face 1	EXPERIMENTAL above freezing Face 2	EXPERIMENTAL below freezing Face 1	EXPERIMENTAL below freezing Face 2
7	0	4.15	3.25	4.27	4.29	3.21	3.29
	1	4.28	3.36	4.48	4.46	3.38	3.40
	2	4.38	3.44	4.50	4.86	3.45	3.43
	3	4.49	3.53	4.77	4.69	3.93	3.34
	4	4.59	3.63	4.79	4.80	3.43	3.95
	5	4.69	3.70	4.73	4.91	3.72	3.76
28	0	4.22	3.60	3.93	3.98	3.41	3.79
	1	4.34	3.69	4.19	3.86	3.78	3.69
	2	4.44	3.76	4.30	4.33	3.75	3.48
	3	4.54	3.84	4.47	4.48	3.82	3.85
	4	4.65	3.92	4.48	4.53	4.13	3.92
	5	4.73	3.98	4.61	5.10	3.97	3.68
84	0	4.35	3.72	4.29	4.18	3.62	3.45
	1	4.46	3.80	4.40	4.26	3.26	3.52
	2	4.54	3.86	4.47	4.50	4.07	3.55
	3	4.64	3.94	5.42	4.62	3.81	4.05
	4	4.74	4.01	4.75	4.79	3.95	4.36
	5	4.81	4.07	4.94	4.17	4.35	3.89

Face 1 - near steel
Face 2 - away from steel

TABLE 5.14: THEORETICAL AND EXPERIMENTAL VALUES OF COEFFICIENT OF EXPANSION OF REINFORCED CONCRETE. VARIATION WITH AGE AND STEEL PERCENTAGE (IN 10^6 IN./IN./^{0}F)

Series - ASW 0.577 Symmetrical Wet-Cured

AGE IN DAYS	% OF STEEL	THEORETICAL above freezing	THEORETICAL below freezing	EXPERIMENTAL above freezing Face 1	EXPERIMENTAL above freezing Face 2	EXPERIMENTAL below freezing Face 1	EXPERIMENTAL below freezing Face 2
7	0	3.64	2.99	3.45	2.72	3.05	2.98
	1	3.80	3.11	3.19	3.17	3.12	3.27
	2	3.93	3.21	2.78	3.29	3.36	3.06
	3	4.07	3.32	3.39	3.48	3.45	3.48
	4	4.20	3.42	3.97	3.55	3.32	3.81
	5	4.32	3.51	3.70	2.94	3.66	3.66
28	0	3.71	3.30	3.18	3.48	3.07	3.44
	1	3.86	3.40	3.94	3.85	3.17	3.38
	2	3.98	3.48	4.00	4.05	3.43	3.23
	3	4.11	3.58	4.48	4.25	3.18	3.54
	4	4.24	3.67	4.29	4.01	3.61	3.63
	5	4.35	3.74	4.43	4.48	3.69	3.72
84	0	3.87	3.49	3.90	4.02	3.53	3.76
	1	4.01	3.58	3.99	4.19	3.70	3.72
	2	4.11	3.65	4.14	4.34	3.78	3.79
	3	4.23	3.73	4.58	4.24	3.14	3.68
	4	4.34	3.81	4.62	4.61	3.93	3.95
	5	4.44	3.88	4.42	4.17	4.00	3.76

Face 1 - near steel
Face 2 - away from steel

TABLE 5.15: THEORETICAL AND EXPERIMENTAL VALUES OF COEFFICIENT OF EXPANSION OF REINFORCED CONCRETE. VARIATION WITH AGE AND STEEL PERCENTAGE (IN 10^6 IN./IN./^{0}F)

Series - ASW 0.672 Symmetrical Wet-Cured

AGE IN DAYS	% OF STEEL	THEORETICAL		EXPERIMENTAL			
		above freezing	below freezing	above freezing		below freezing	
				Face 1	Face 2	Face 1	Face 2
7	0	3.41	3.00	3.47	3.05	2.82	3.40
	1	3.59	3.12	2.95	3.47	3.00	3.17
	2	3.72	3.21	3.60	3.67	3.23	3.26
	3	3.87	3.32	3.74	4.65	3.34	3.39
	4	4.01	3.42	4.00	3.93	3.02	3.60
	5	4.13	3.51	4.00	4.13	3.54	3.56
28	0	3.52	3.03	2.81	2.92	3.18	3.55
	1	3.69	3.15	3.10	3.10	3.48	3.49
	2	3.82	3.24	3.20	3.17	3.57	3.91
	3	3.96	3.34	2.76	2.83	3.33	3.68
	4	4.10	3.45	3.50	3.49	3.77	3.56
	5	4.22	3.53	3.51	3.55	3.85	4.56
84	0	3.75	3.34	3.21	3.89	3.39	3.50
	1	3.90	3.44	3.77	3.89	3.07	3.51
	2	4.01	3.51	3.86	3.94	3.41	3.77
	3	4.13	3.60	3.79	4.32	3.65	3.67
	4	4.25	3.69	4.12	4.20	4.14	3.96
	5	4.36	3.76	4.09	4.26	3.80	3.83

Face 1 - near steel
Face 2 - away from steel

TABLE 5.16: THEORETICAL AND EXPERIMENTAL VALUES OF COEFFICIENT OF EXPANSION OF REINFORCED CONCRETE. VARIATION WITH AGE AND STEEL PERCENTAGE (IN 10^6 IN./IN./^{0}F

Series - AUD 0.445 Unsymmetrical Dry-Cured

AGE IN DAYS	% OF STEEL	THEORETICAL				EXPERIMENTAL			
		above freezing		below freezing		above freezing		below freezing	
		Face 1	Face 2	Face 1	Face 2	Face 1	Face 2	Face 1	Face 2
7	0	4.60	4.60	3.55	3.55	4.48	5.07	3.46	3.27
	1	4.83	4.55	3.76	3.51	4.72	4.62	3.47	3.43
	2	5.06	4.51	3.98	3.47	5.05	4.39	4.04	3.42
	3	5.26	4.48	4.16	3.44	5.71	4.44	4.00	3.26
	4	5.36	4.46	4.26	3.42	4.60	4.02	4.13	3.41
	5	5.54	4.43	4.43	3.39	5.64	4.73	4.34	7.72
28	0								
	1								
	2								
	3								
	4								
	5								
84	0	4.96	4.96	4.27	4.27	4.20	4.87	4.65	4.24
	1	5.16	4.92	4.42	4.24	4.82	4.73	4.40	4.38
	2	5.35	4.89	4.57	4.21	4.30	4.92	4.62	4.33
	3	5.51	4.86	4.70	4.19	5.44	4.81	4.62	4.31
	4	5.60	4.84	4.77	4.19	5.65	6.81	4.81	4.22
	5	5.74	4.82	4.89	4.16	5.61	4.74	4.87	4.27

Face 1 - near steel
Face 2 - away from steel

TABLE 5.17: THEORETICAL AND EXPERIMENTAL VALUES OF COEFFICIENT OF EXPANSION OF REINFORCED CONCRETE. VARIATION WITH AGE AND STEEL PERCENTAGE (IN 10^6 IN./IN./^{0}F

Series - AUD 0.487 Unsymmetrical Dry-Cured

AGE IN DAYS	% OF STEEL	THEORETICAL				EXPERIMENTAL			
		above freezing		below freezing		above freezing		below freezing	
		Face 1	Face 2	Face 1	Face 2	Face 1	Face 2	Face 1	Face 2
7	0	4.15	4.15	3.25	3.25	3.53	4.17	2.92	3.86
	1	4.44	4.09	3.49	3.20	4.10	3.80	3.57	3.16
	2	4.73	4.04	3.74	3.16	4.62	3.82	3.69	3.33
	3	4.98	4.00	3.95	3.12	4.77	3.94	3.90	3.11
	4	5.11	3.98	4.07	3.10	5.13	3.78	6.19	3.13
	5	5.33	3.94	4.26	3.07	4.90	3.66	3.99	3.40
28	0	4.25	4.25	3.70	3.70	3.97	4.37	3.48	3.72
	1	4.54	4.19	3.91	3.66	4.70	5.37	3.41	3.57
	2	4.83	4.14	4.13	3.62	5.00	4.09	4.04	3.57
	3	5.07	4.10	4.30	3.59	5.19	4.26	4.28	2.29
	4	5.20	4.08	4.40	3.57	5.24	4.20	4.49	3.48
	5	5.41	4.04	4.57	3.55	5.00	4.07	4.36	3.50
84	0	4.47	4.47	3.95	3.95	4.70	5.08	3.87	4.29
	1	4.74	4.41	4.15	3.91	4.21	4.49	4.28	4.06
	2	5.02	4.36	4.35	3.87	5.46	4.97	4.48	4.99
	3	5.24	4.33	4.52	3.84	5.53	4.70	4.78	3.97
	4	5.36	4.31	4.60	3.83	4.91	4.42	4.65	3.93
	5	5.55	4.28	4.75	3.81	5.87	4.63	4.69	4.04

Face 1 - near steel
Face 2 - away from steel

TABLE 5.18: THEORETICAL AND EXPERIMENTAL VALUES OF COEFFICIENT OF EXPANSION OF REINFORCED CONCRETE. VARIATION WITH AGE AND STEEL PERCENTAGE (IN 10^6 IN./IN./^{0}F)

Series - AUD 0.577 Unsymmetrical Dry-Cured

AGE IN DAYS	% OF STEEL	THEORETICAL above freezing Face 1	THEORETICAL above freezing Face 2	THEORETICAL below freezing Face 1	THEORETICAL below freezing Face 2	EXPERIMENTAL above freezing Face 1	EXPERIMENTAL above freezing Face 2	EXPERIMENTAL below freezing Face 1	EXPERIMENTAL below freezing Face 2
7	0	3.64	3.64	2.99	2.99	3.48	3.10	2.86	3.25
	1	4.01	3.57	3.27	2.94	4.10	3.63	3.46	2.99
	2	4.38	3.50	3.55	2.88	4.21	3.46	3.55	2.81
	3	4.68	3.45	3.79	2.84	4.76	3.54	3.48	3.33
	4	4.84	3.42	3.92	2.82	4.25	3.07	4.15	2.80
	5	5.11	3.38	4.15	2.79	5.25	4.10	4.18	2.90
28	0	3.85	3.85	3.46	3.46	3.00	3.42	3.19	3.62
	1	4.20	3.78	3.70	3.41	4.02	3.64	3.56	3.32
	2	4.56	3.72	3.95	3.37	4.92	3.55	4.33	3.88
	3	4.84	3.67	4.16	3.33	4.71	3.19	4.03	2.23
	4	5.00	3.64	4.27	3.31	4.84	3.73	4.21	3.42
	5	5.25	3.60	4.46	3.28	4.41	3.41	3.40	3.39
84	0	4.20	4.20	3.71	3.71	3.91	4.28	3.40	3.85
	1	4.53	4.13	3.95	3.66	4.56	4.23	3.82	3.54
	2	4.85	4.07	4.19	3.62	4.78	3.95	3.75	3.52
	3	5.11	4.03	4.38	3.59	5.12	4.14	4.41	3.55
	4	5.25	4.01	4.49	3.57	5.05	4.24	4.27	3.66
	5	5.48	3.98	4.66	3.54	5.34	4.07	4.51	3.50

Face 1 - near steel
Face 2 - away from steel

TABLE 5.19: THEORETICAL AND EXPERIMENTAL VALUES OF COEFFICIENT OF EXPANSION OF REINFORCED CONCRETE. VARIATION WITH AGE AND STEEL PERCENTAGE (IN 10^6 IN./IN./^{0}F

Series - AUD 0.672 Unsymmetrical Dry-Cured

AGE IN DAYS	% OF STEEL	THEORETICAL				EXPERIMENTAL			
		above freezing		below freezing		above freezing		below freezing	
		Face 1	Face 2	Face 1	Face 2	Face 1	Face 2	Face 1	Face 2
7	0	3.41	3.41	3.00	3.00	3.32	3.76	3.33	2.89
	1	3.80	3.33	3.27	2.95	3.59	3.25	3.13	3.27
	2	4.19	3.26	3.54	2.90	3.87	3.06	3.46	2.53
	3	4.52	3.20	3.78	2.86	4.30	3.50	3.66	2.42
	4	4.69	3.18	3.91	2.83	5.18	3.13	3.77	2.92
	5	4.98	3.13	4.13	2.80	4.69	3.10	3.90	2.75
28	0	3.70	3.70	3.28	3.28	4.50	3.74	3.03	3.15
	1	4.06	3.63	3.53	3.23	4.25	3.96	3.57	3.38
	2	4.43	3.56	3.79	3.18	4.60	3.74	3.66	3.15
	3	4.72	3.51	4.00	3.14	4.80	3.79	4.16	3.16
	4	4.89	3.48	4.13	3.12	5.15	3.69	4.13	3.32
	5	5.15	3.44	4.33	3.10	5.07	3.72	4.34	3.05
84	0	4.00	4.00	3.50	3.50	3.22	4.18	3.38	3.68
	1	4.36	3.93	3.76	3.45	4.51	3.42	3.32	3.62
	2	4.71	3.86	4.03	3.40	4.04	3.04	3.93	3.18
	3	5.00	3.82	4.24	3.36	5.06	3.60	3.84	3.28
	4	5.14	3.79	4.36	3.34	4.96	3.64	4.58	3.27
	5	5.39	3.75	4.55	3.31	5.56	4.45	4.64	3.62

Face 1 - near steel
Face 2 - away from steel

TABLE 5.20: THEORETICAL AND EXPERIMENTAL VALUES OF COEFFICIENT OF EXPANSION OF REINFORCED CONCRETE. VARIATION WITH AGE AND STEEL PERCENTAGE (IN 10^6 IN./IN./^{0}F

Series - AUW 0.445 Unsymmetrical Wet-Cured

AGE IN DAYS	% OF STEEL	THEORETICAL				EXPERIMENTAL			
		above freezing		below freezing		above freezing		below freezing	
		Face 1	Face 2	Face 1	Face 2	Face 1	Face 2	Face 1	Face 2
7	0	4.60	4.60	3.55	3.55	4.49	5.37	3.74	3.68
	1	4.83	4.55	3.76	3.51	4.64	4.76	3.82	3.56
	2	5.06	4.51	3.98	3.47	5.19	5.06	3.86	3.31
	3	5.26	4.48	4.16	3.44	4.95	4.62	3.93	3.51
	4	5.36	4.46	4.26	3.42	5.60	4.50	4.09	3.31
	5	5.54	4.43	4.43	3.39	5.77	4.71	4.62	3.53
28	0								
	1								
	2								
	3								
	4								
	5								
84	0	4.85	4.85	3.86	3.86	5.49	4.66	4.01	4.17
	1	5.04	4.81	4.03	3.82	5.03	4.85	4.11	3.93
	2	5.23	4.78	4.21	3.79	5.12	5.06	4.20	3.87
	3	5.39	4.75	4.36	3.77	5.47	4.73	4.35	3.83
	4	5.48	4.73	4.44	3.75	5.15	4.49	4.34	3.65
	5	5.63	4.71	4.59	3.73	5.73	4.85	4.65	3.84

Face 1 - near steel
Face 2 - away from steel

TABLE 5.21: THEORETICAL AND EXPERIMENTAL VALUES OF COEFFICIENT OF EXPANSION OF REINFORCED CONCRETE. VARIATION WITH AGE AND STEEL PERCENTAGE (IN 10^6 IN./IN./^{0}F)

Series - AUW 0.487 | Unsymmetrical | Wet-Cured

AGE IN DAYS	% OF STEEL	THEORETICAL above freezing Face 1	THEORETICAL above freezing Face 2	THEORETICAL below freezing Face 1	THEORETICAL below freezing Face 2	EXPERIMENTAL above freezing Face 1	EXPERIMENTAL above freezing Face 2	EXPERIMENTAL below freezing Face 1	EXPERIMENTAL below freezing Face 2
7	0	4.15	4.15	3.25	3.25	4.14	4.67	2.95	3.35
	1	4.44	4.09	3.49	3.20	4.56	4.34	3.34	3.04
	2	4.73	4.04	3.74	3.16	5.35	4.58	3.62	3.01
	3	4.98	4.00	3.95	3.12	5.31	4.46	4.12	3.10
	4	5.11	3.98	4.07	3.10	5.56	3.95	3.71	2.95
	5	5.33	3.94	4.26	3.07	5.97	4.27	8.30	3.17
28	0	4.22	4.22	3.60	3.60	3.63	4.35	3.91	3.83
	1	4.50	4.17	3.80	3.56	4.79	4.44	4.23	3.68
	2	4.78	4.11	4.01	3.52	5.06	4.39	4.15	3.46
	3	5.01	4.07	4.19	3.49	5.04	4.12	4.32	3.66
	4	5.14	4.05	4.29	3.47	5.43	4.40	4.22	3.49
	5	5.35	4.02	4.45	3.45	5.57	5.04	4.96	3.69
84	0	4.35	4.35	3.72	3.72	3.79	4.52	2.98	3.43
	1	4.60	4.30	3.90	3.69	4.52	4.18	3.16	3.11
	2	4.85	4.25	4.09	3.65	4.73	4.18	3.60	3.27
	3	5.06	4.22	4.26	3.62	5.22	4.38	4.02	3.40
	4	5.18	4.20	4.35	3.61	4.80	4.10	4.05	2.80
	5	5.38	4.17	4.50	3.58	5.36	4.18	4.03	3.23

Face 1 - near steel
Face 2 - away from steel

TABLE 5.22: THEORETICAL AND EXPERIMENTAL VALUES OF COEFFICIENT OF EXPANSION OF REINFORCED CONCRETE. VARIATION WITH AGE AND STEEL PERCENTAGE (IN 10^6 IN./IN./^{0}F)

Series - AUW 0.577 Unsymmetrical Wet-Cured

AGE IN DAYS	% OF STEEL	THEORETICAL				EXPERIMENTAL			
		above freezing		below freezing		above freezing		below freezing	
		Face 1	Face 2	Face 1	Face 2	Face 1	Face 2	Face 1	Face 2
7	0	3.64	3.64	2.99	2.99	3.58	3.60	3.15	2.93
	1	4.01	3.57	3.27	2.94	3.79	3.32	3.09	2.77
	2	4.38	3.50	3.55	2.88	2.66	3.36	2.27	2.81
	3	4.68	3.45	3.79	2.84	4.55	3.30	3.80	3.00
	4	4.84	3.42	3.92	2.82	4.89	3.11	4.02	2.89
	5	5.11	3.38	4.15	2.79	4.98	3.28	4.33	2.78
28	0	3.71	3.71	3.30	3.30	3.42	3.52	2.96	3.38
	1	4.05	3.64	3.53	3.25	3.35	3.35	3.39	3.12
	2	4.44	3.57	3.78	3.21	4.15	3.34	3.69	3.20
	3	4.69	3.53	3.40	3.17	4.81	3.50	4.22	3.01
	4	4.85	3.50	4.10	3.15	4.73	3.42	4.09	3.19
	5	5.11	3.46	4.29	3.12	5.16	3.34	4.49	3.12
84	0	3.87	3.87	3.49	3.49	3.63	4.47	2.96	3.51
	1	4.18	3.81	3.69	3.45	4.33	3.59	3.74	3.56
	2	4.49	3.75	3.91	3.41	4.54	3.84	3.59	3.51
	3	4.75	3.71	4.92	3.39	4.74	3.88	4.11	3.48
	4	4.89	3.68	4.19	3.36	4.78	3.49	3.73	3.26
	5	5.13	3.65	4.37	3.33	5.52	3.84	4.10	3.40

Face 1 - near steel
Face 2 - away from steel

TABLE 5.23: THEORETICAL AND EXPERIMENTAL VALUES OF COEFFICIENT OF EXPANSION OF REINFORCED CONCRETE. VARIATION WITH AGE AND STEEL PERCENTAGE (IN 10^6 IN./IN./^{0}F)

Series - AUW 0.672 Unsymmetrical Wet-Cured

AGE IN DAYS	% OF STEEL	THEORETICAL				EXPERIMENTAL			
		above freezing		below freezing		above freezing		below freezing	
		Face 1	Face 2	Face 1	Face 2	Face 1	Face 2	Face 1	Face 2
7	0	3.41	3.41	3.00	3.00	3.70	2.99	2.43	2.78
	1	3.80	3.33	3.27	2.95	3.45	3.69	1.93	2.61
	2	4.19	3.26	3.54	2.90	4.46	3.57	2.60	2.48
	3	4.52	3.20	3.78	2.86	5.06	3.00	3.45	2.69
	4	4.69	3.18	3.91	2.83	4.91	3.14	3.77	2.60
	5	4.98	3.13	4.13	2.80	5.16	4.33	4.09	2.40
28	0	3.52	3.52	3.03	3.03	3.54	3.33	3.14	2.70
	1	3.90	3.45	3.30	2.98	3.98	3.73	2.82	2.95
	2	4.28	3.38	3.57	2.93	4.62	3.42	3.69	2.61
	3	4.58	3.33	3.80	2.89	4.76	3.34	3.64	2.78
	4	4.76	3.30	3.93	2.86	5.04	3.29	3.83	2.72
	5	5.04	3.26	4.15	2.83	5.17	3.34	4.16	2.85
84	0	3.75	3.75	3.34	3.34	3.37	3.78	3.01	3.45
	1	4.07	3.69	3.56	3.30	3.81	3.57	3.41	3.44
	2	4.41	3.62	3.79	3.25	4.03	3.34	3.84	3.34
	3	4.68	3.58	3.99	3.22	4.84	3.47	3.99	3.19
	4	4.83	3.55	4.10	3.20	3.80	3.50	3.09	3.38
	5	5.08	3.51	4.28	3.17	4.98	3.37	4.58	3.25

Face 1 - near steel
Face 2 - away from steel

APPENDIX C: PHOTOGRAPHS

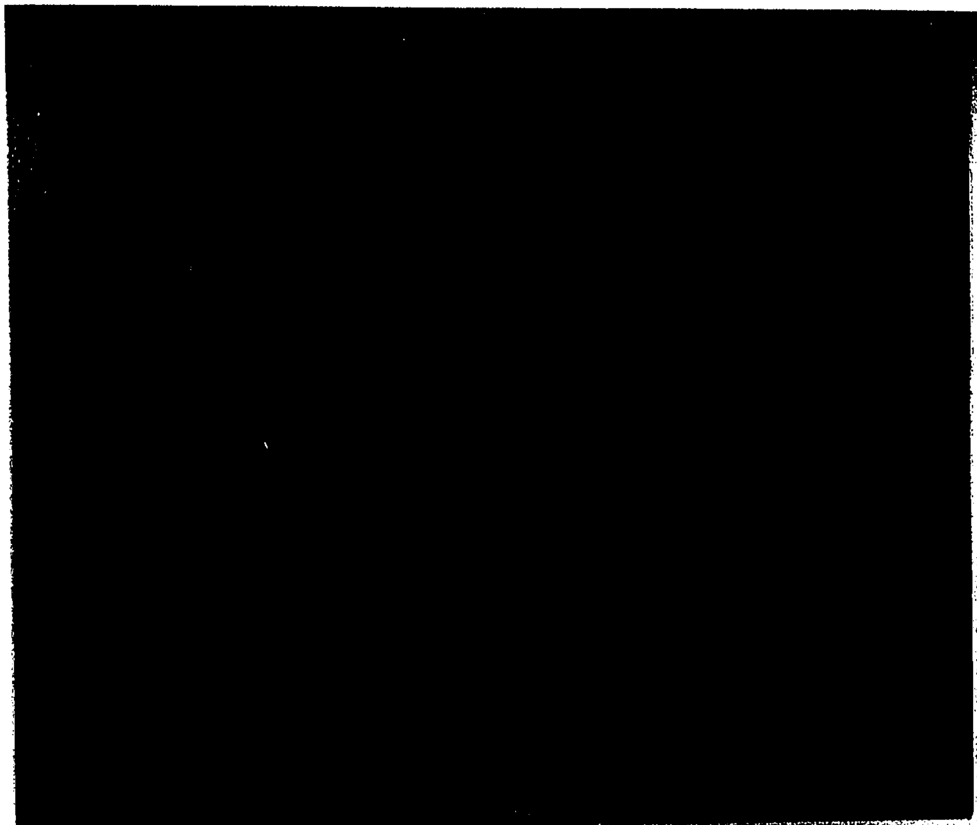

PLATE [illegible]

[illegible] (rear).

PLATE 3.2 - MOULDS FOR SLAB SPECIMENS

The grooves are welded to the end plates (front and rear). Styrofoam pads (left rear) in the grooves hold reinforcements in place.

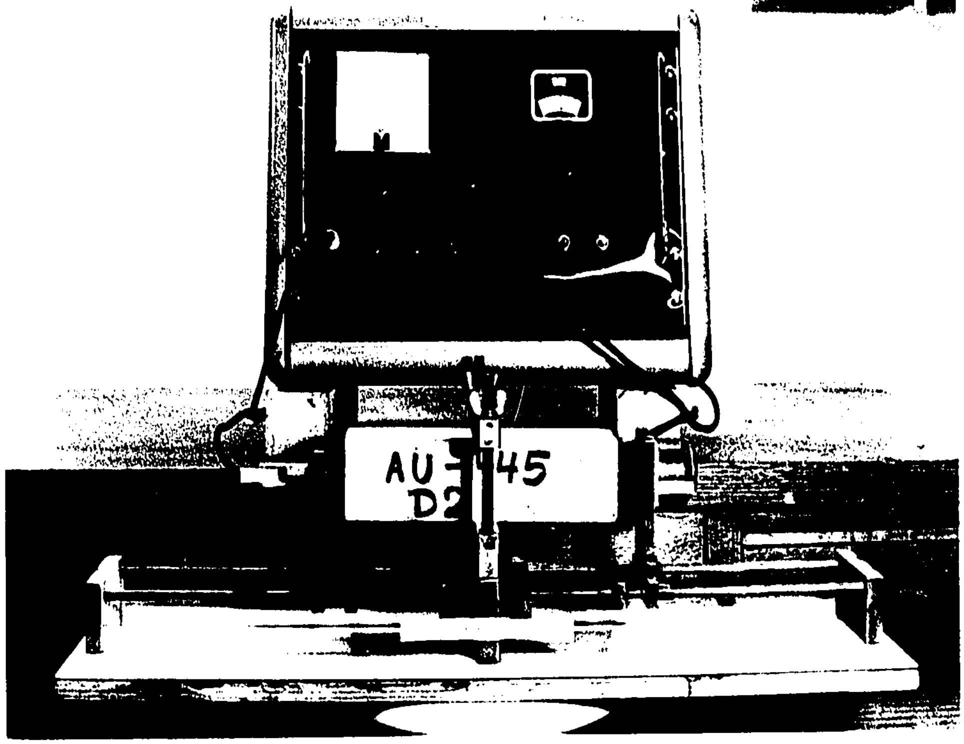

PLATE 3.1 - SONIC RESONANT TEST

The pick-up and the vibrator attached to the ends of the specimen (front) in the bench are connected to the SCT-5 (rear).

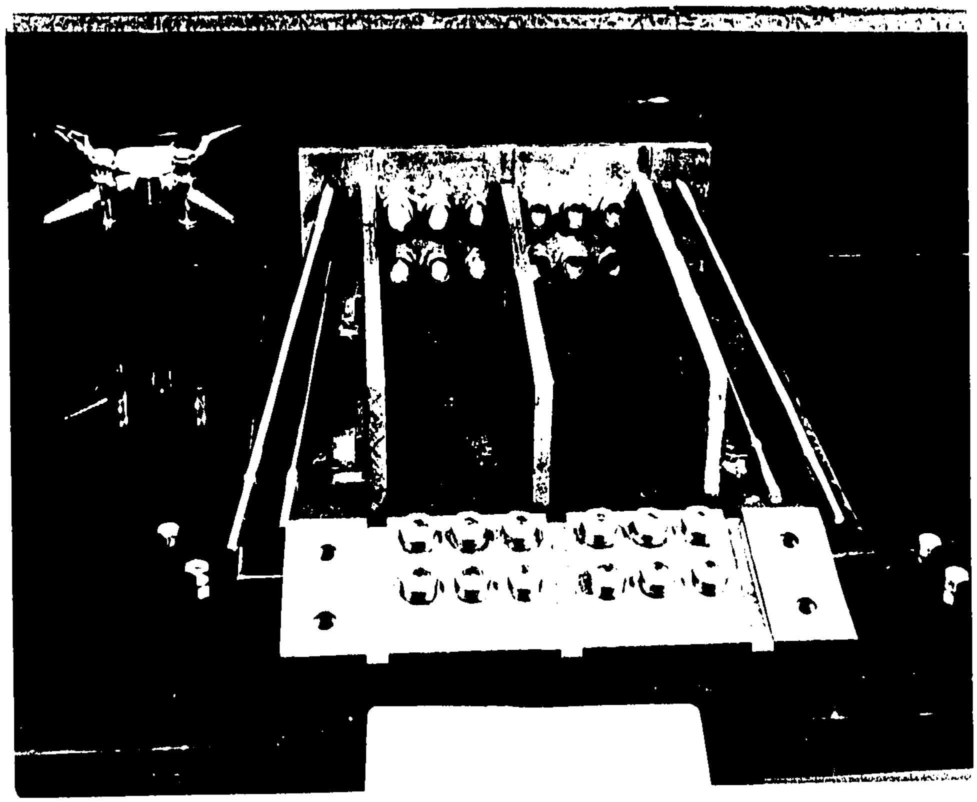

[illegible]

PLATE 3.3 - THERMOCOUPLE

The two metallic wires (left) are soldered to form the thermocouple.

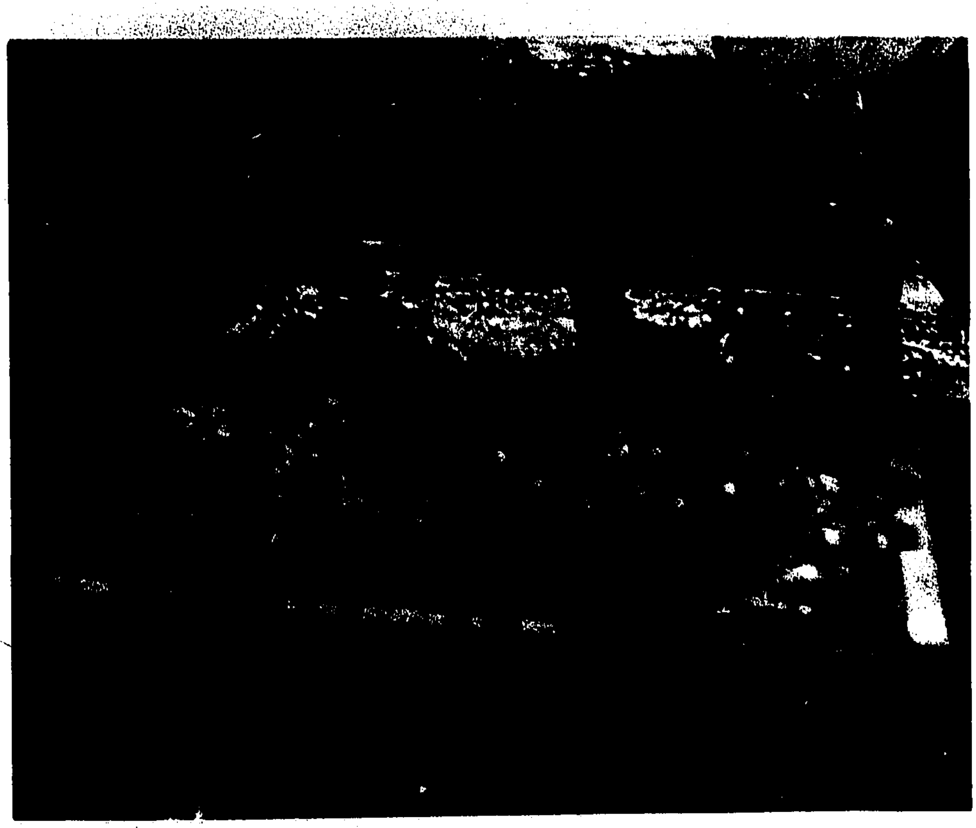

PLATE 3.4 - CONSOLIDATION OF CONCRETE DURING CASTING

Concrete being consolidated by Pencil Vibrator (top). Ends of thermocouple wires can be seen (front and rear).

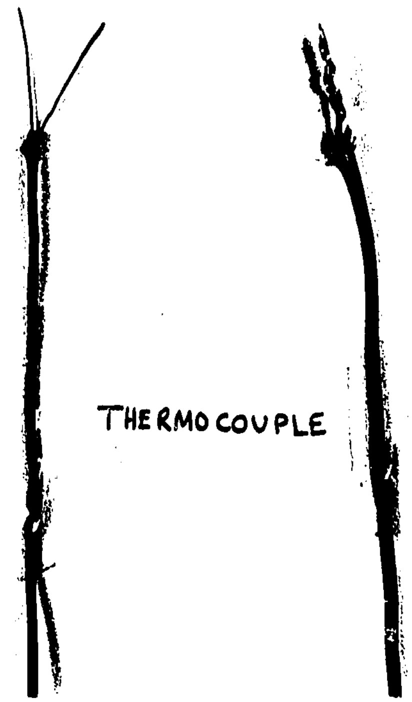

PLATE 3.3 - THERMOCOUPLE

The two metallic wires (left) are soldered to form the thermocouple.

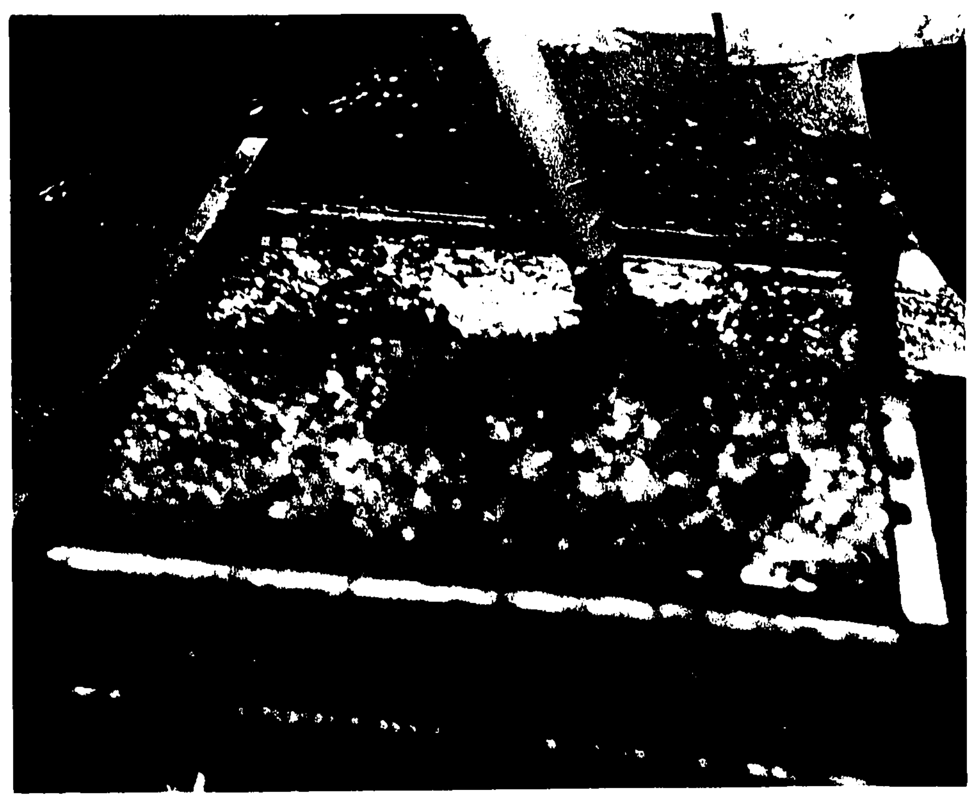

PLATE 3.4 - CONSOLIDATION OF CONCRETE DURING CASTING

Concrete being consolidated by Pencil Vibrator (top). Ends of thermocouple wires can be seen (front and rear).

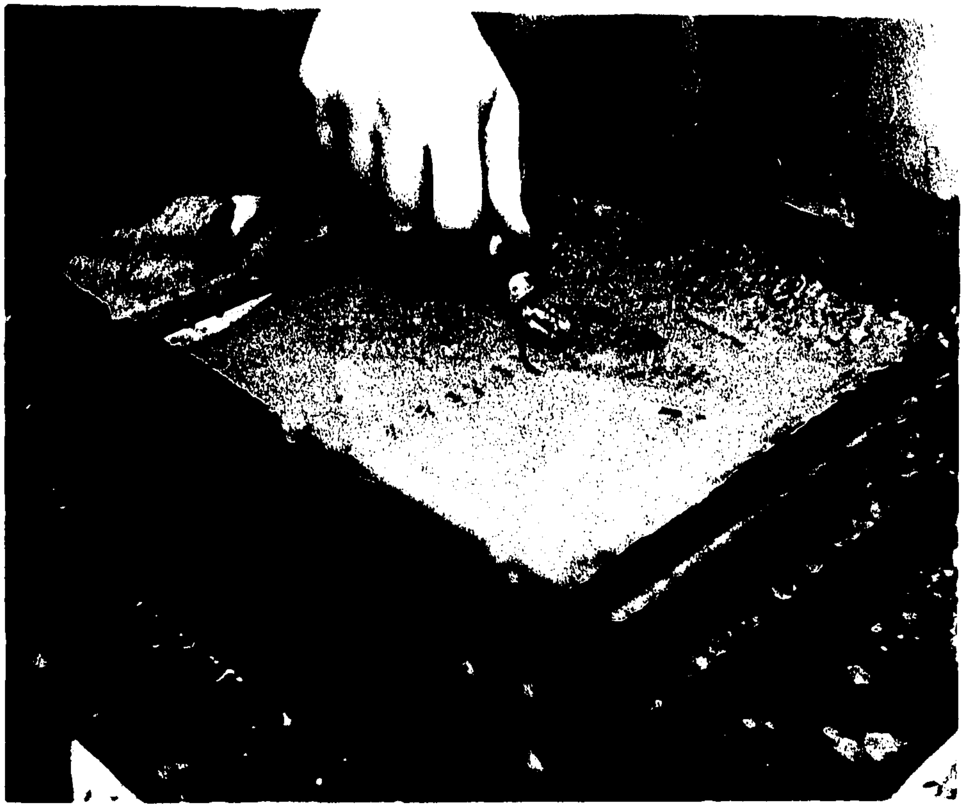

PLATE 3.5 - TROWEL FINISH OF CONCRETE SLABS

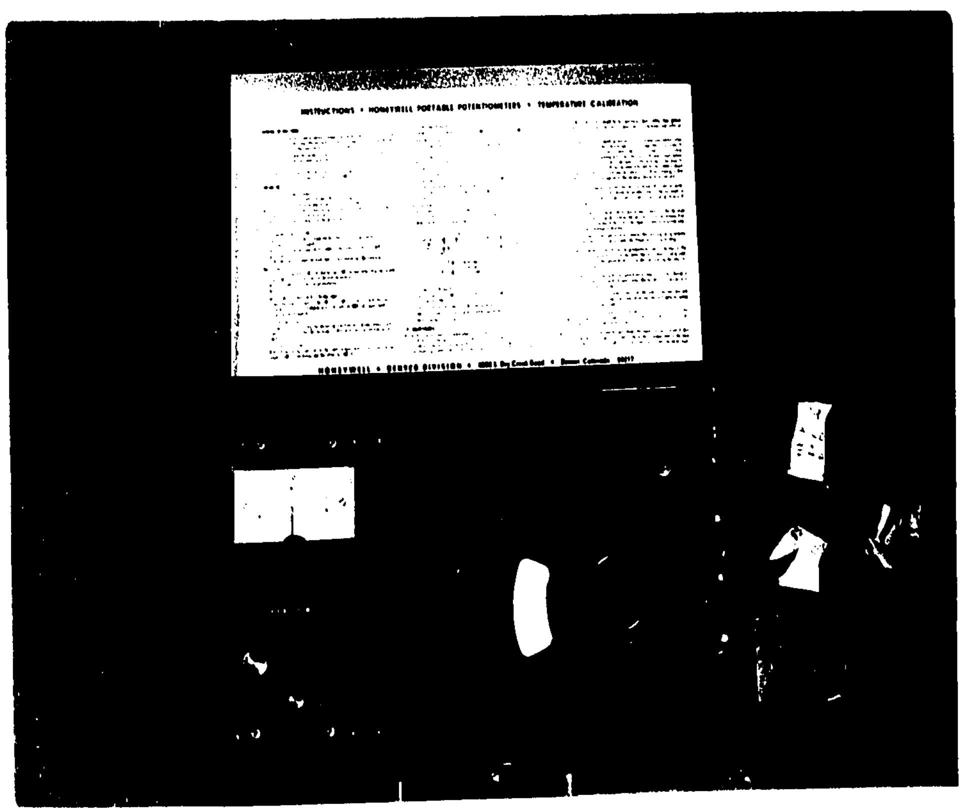

PLATE 3.6 - TEMPERATURE MEASUREMENT OF POTENTIOMETER

Guarded null detector (left), temperature scale (centre) and two thermocouples connected for temperature measurement are shown.

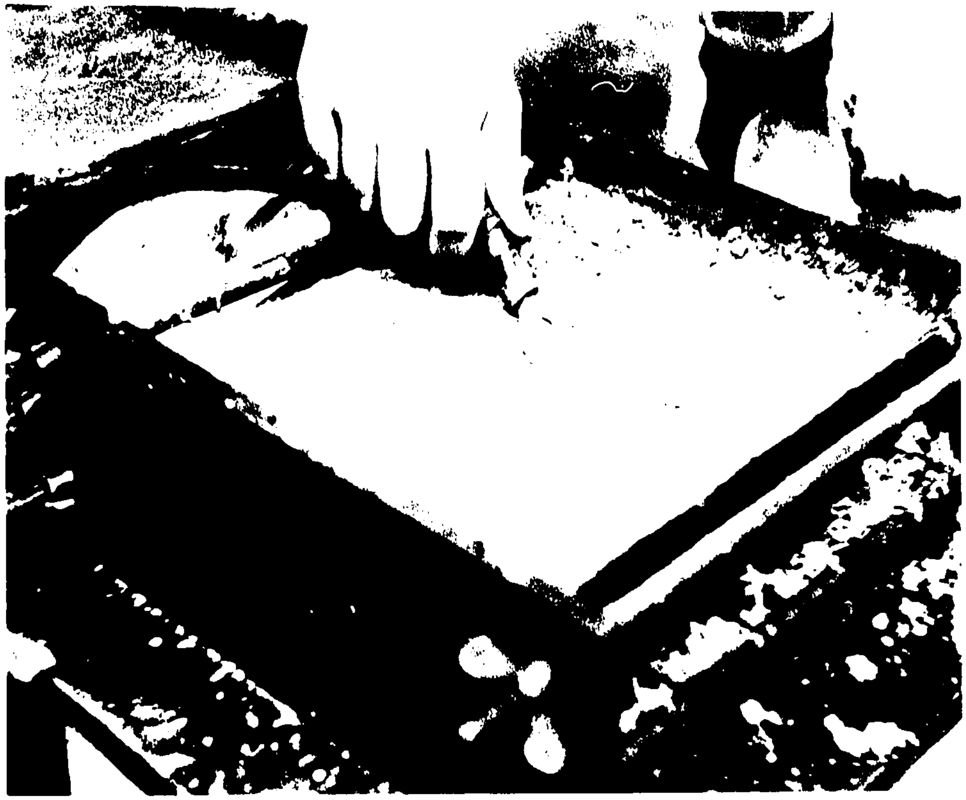

[illegible] OF CONCRETE SLAB

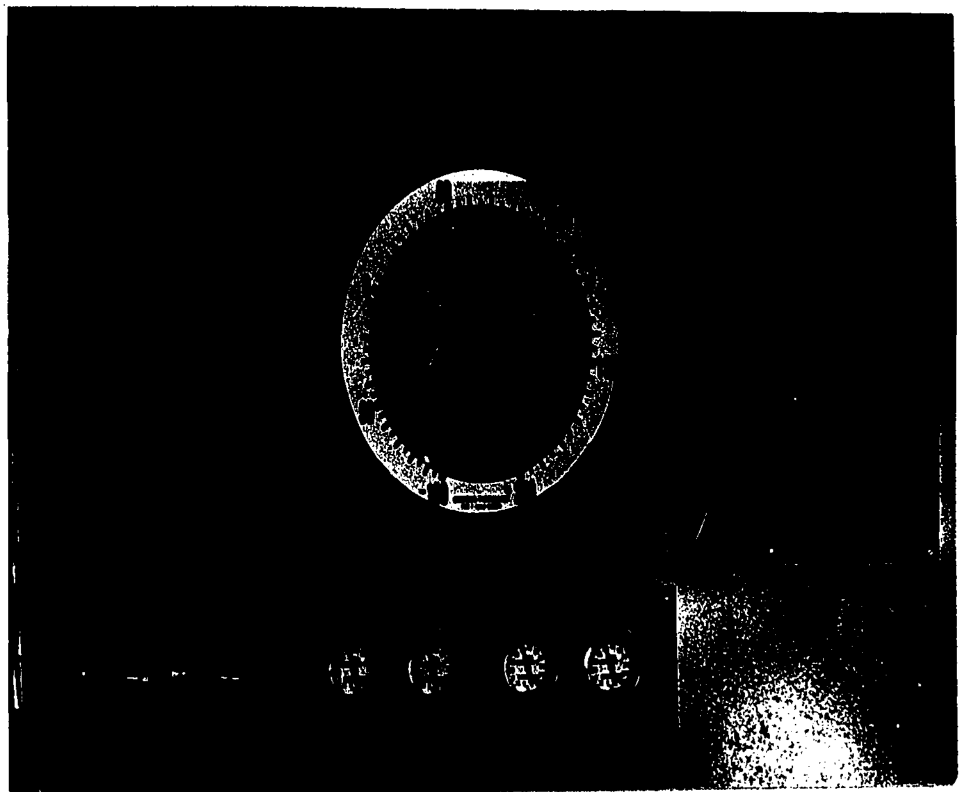

PLATE 3.7 - HONEYWELL CONTROL FOR ENVIRONMENTAL CHAMBER

The temperature recorder panel (top centre) has an instant pointer, a setter and a pen marking on a 24-hour circular scale.

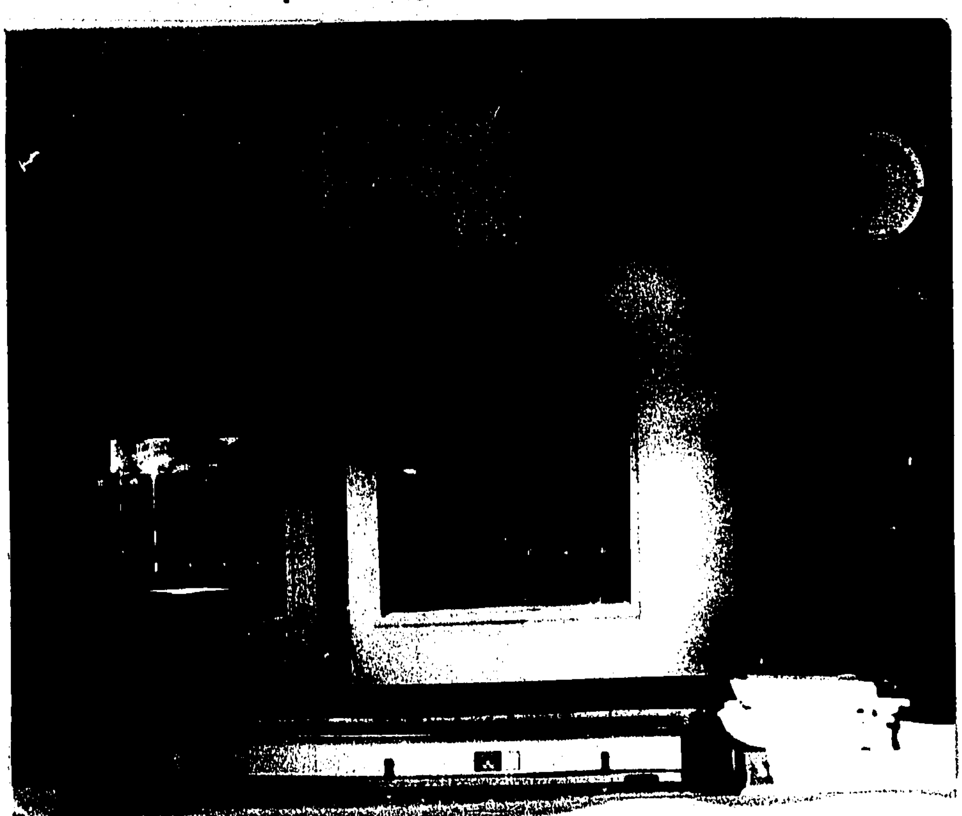

PLATE 3.8 - OUTER VIEW OF ENVIRONMENTAL CHAMBER

The slab specimens (through the window), the potentiometer (bottom right) and the control panel (top left) are seen.

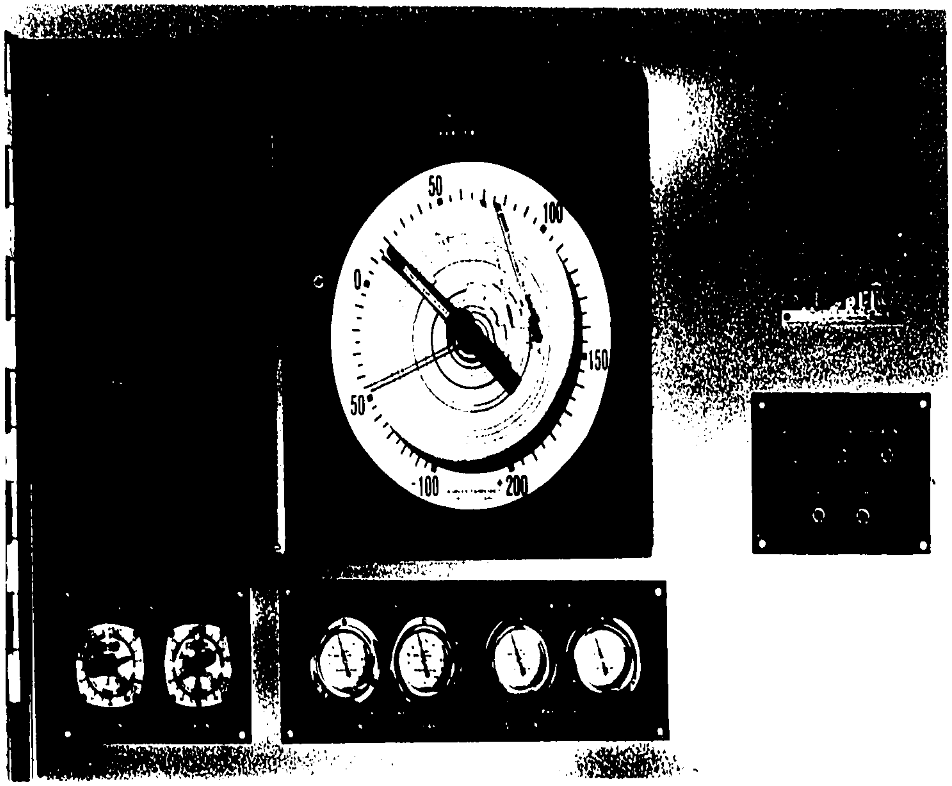

PLATE 3.7 - HONEYWELL CONTROL FOR ENVIRONMENTAL CHAMBER

The temperature recorder panel (top centre) has an instant pointer, a setter and a pen marking on a 24-hour circular scale.

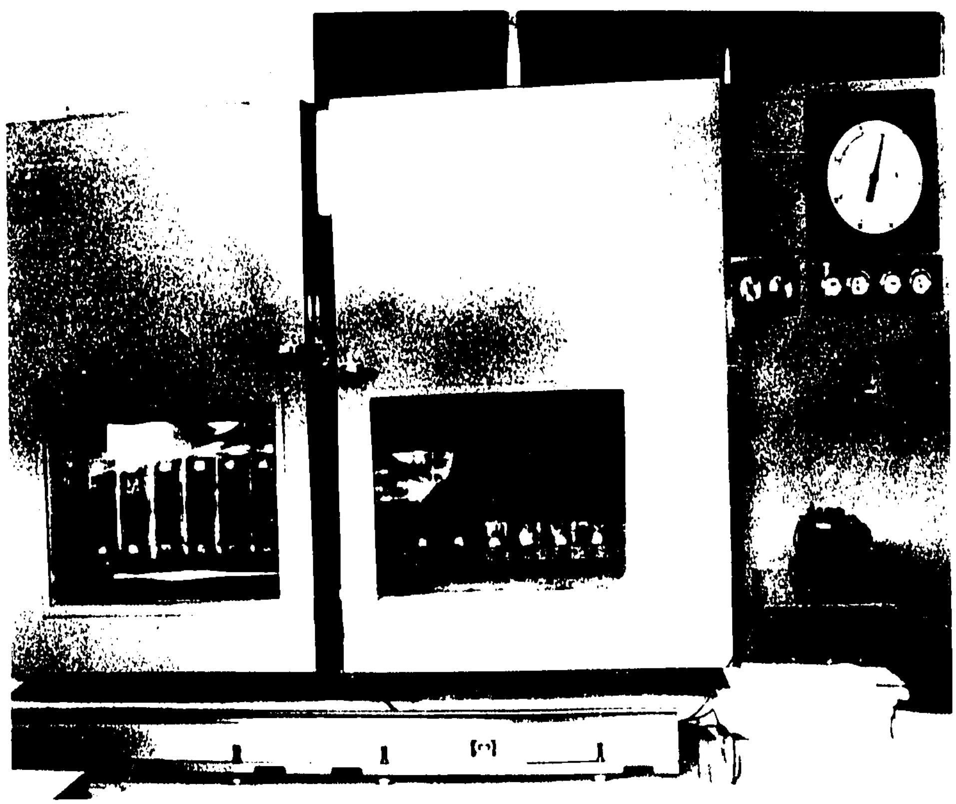

PLATE 3.8 - OUTER VIEW OF ENVIRONMENTAL CHAMBER

The slab specimens (through the window), the potentiometer (bottom right) and the control panel (top left) are seen.

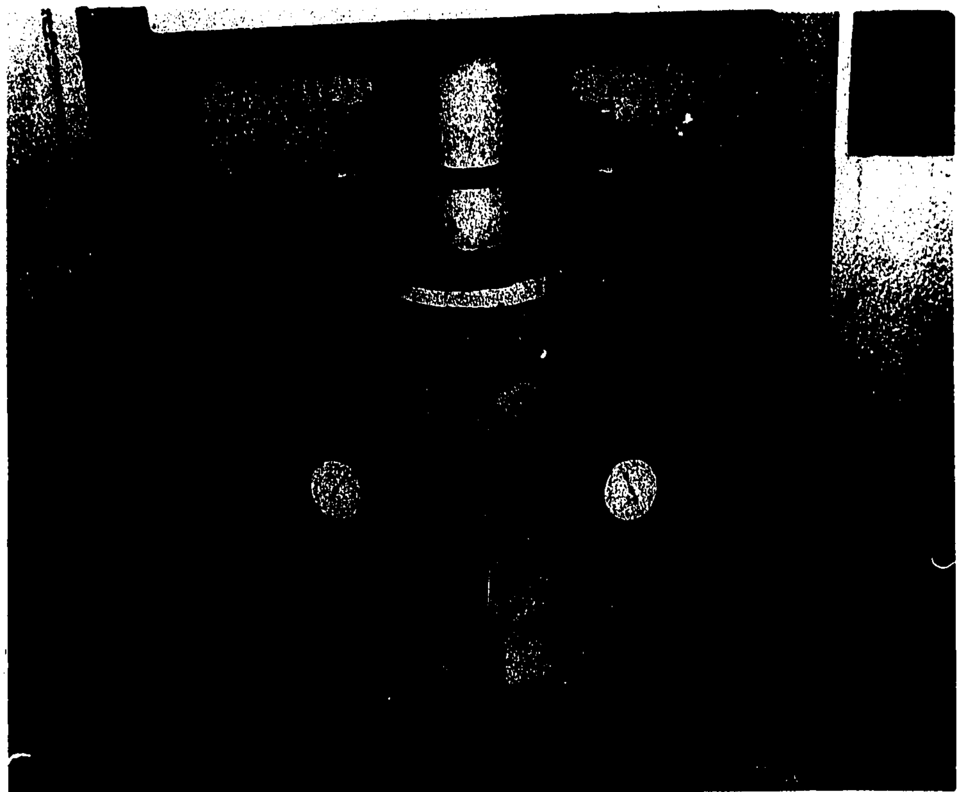

PLATE 3.9 - DEFORMATION TEST FOR CONTROL CYLINDERS

Gauges (left and right) are mounted on the frame attached to the cylinder. Load cell is on top.

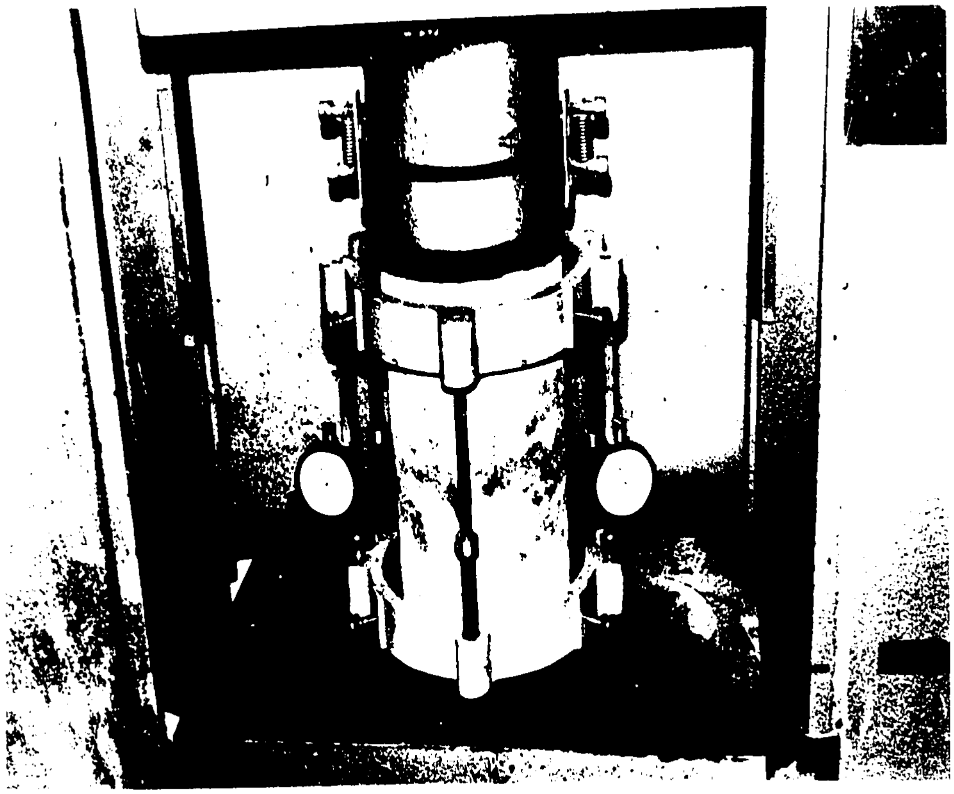

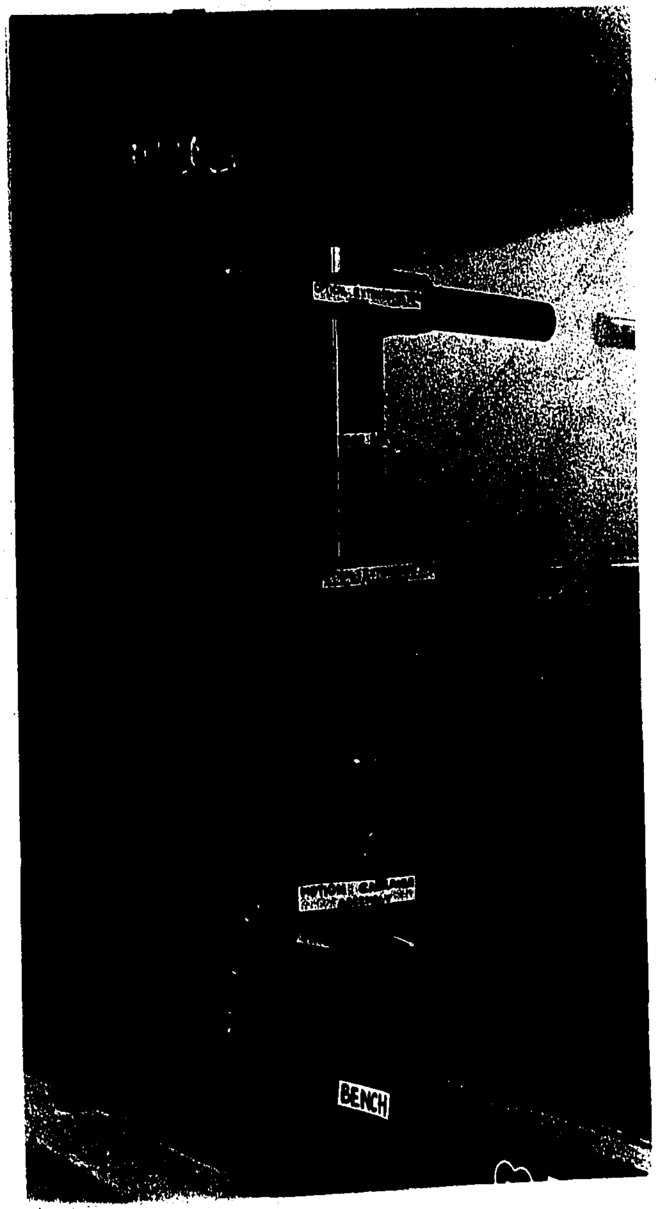

PLATE 3.10 - OPTICAL DEFORMATION MEASURING ASSEMBLY

The optical extensometers attached to the invar bar are mounted on the motion carriage assembly resting on the optical bench.

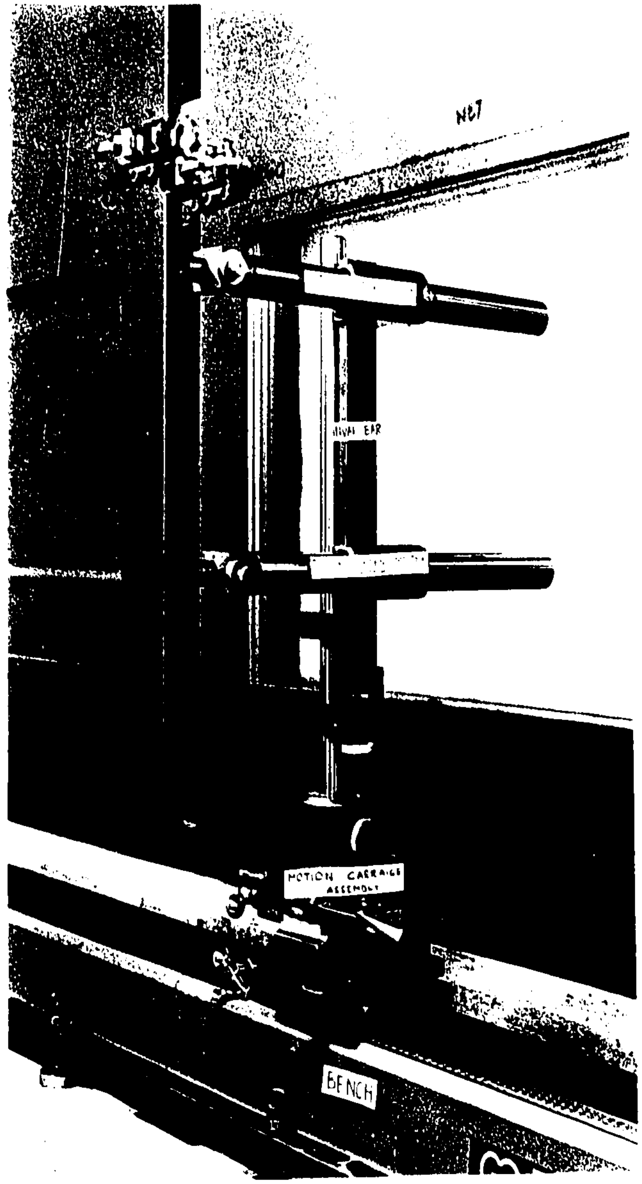

PLATE 3.10 - OPTICAL DEFORMATION [illegible]
ASSEMBLY

The optical extensometers attached to the [illegible] bar are mounted on the motion carriage [illegible] resting on the optical bench.

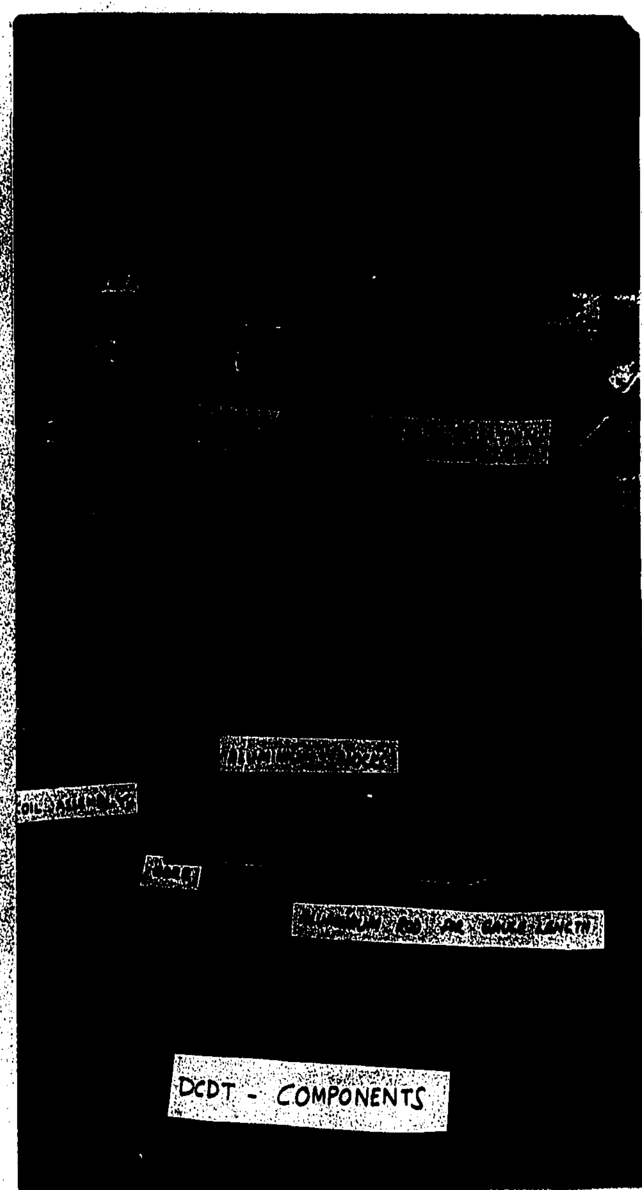

PLATE 3.11 - HEWLETT-PACKARD TRANSDUCERS
MODEL 7CDT - 100

DCDT: components (foreground) and assembled in position for deformation measurement (rear).

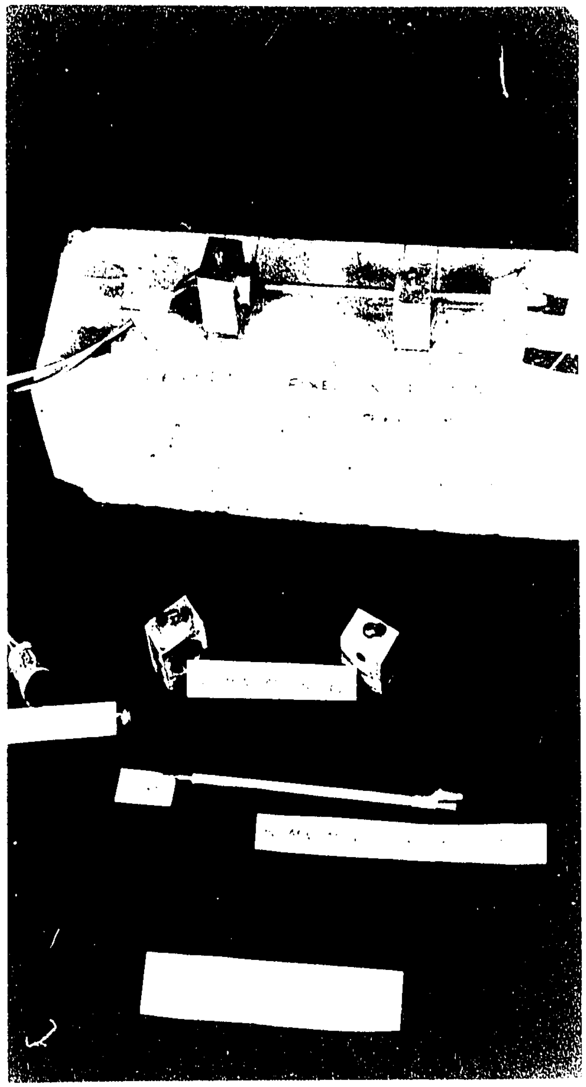

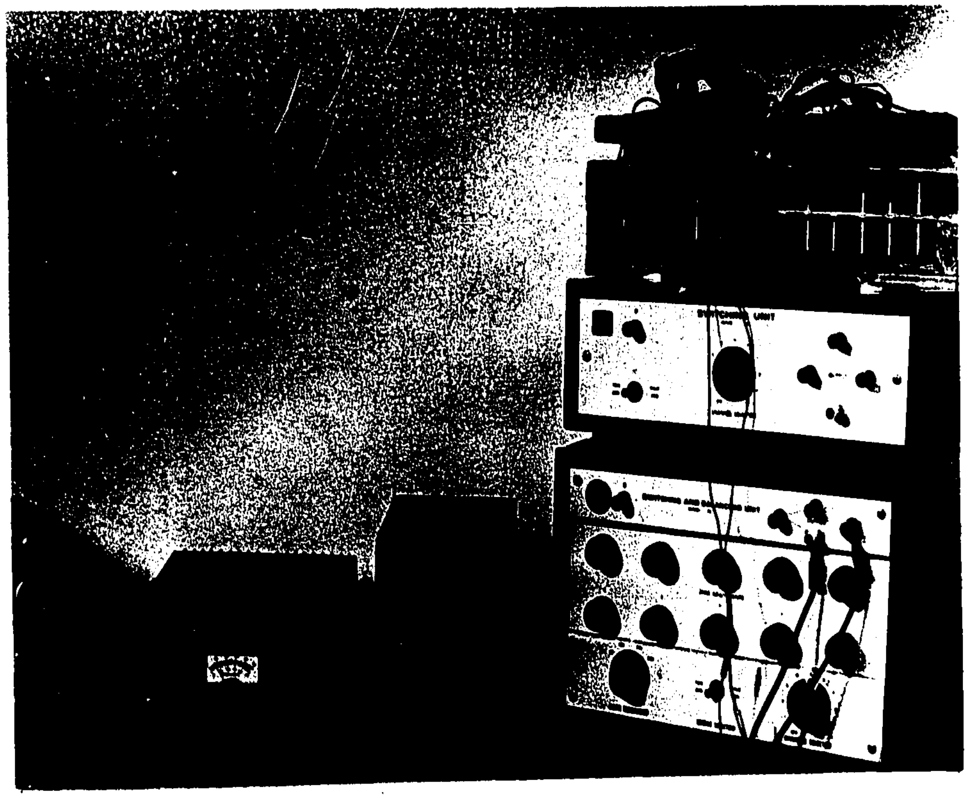

PLATE 3.12 - MEASURING DEVICES FOR DCDT

From left to right: voltage to frequency converter, DC power supply, frequency counter and mercuty pool switching panel on two switching units.

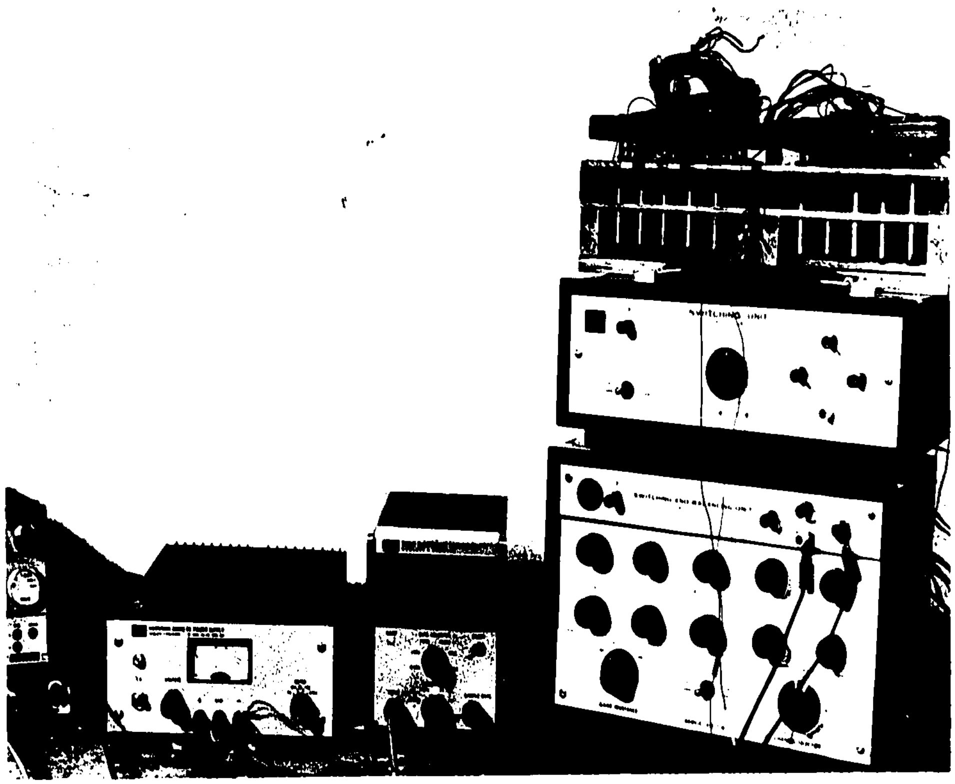

PLATE 3.12 - MEASURING DEVICES FOR DCDT

From left to right: voltage to frequency converter, DC power supply, frequency counter and mercuty pool switching panel on two switching units.

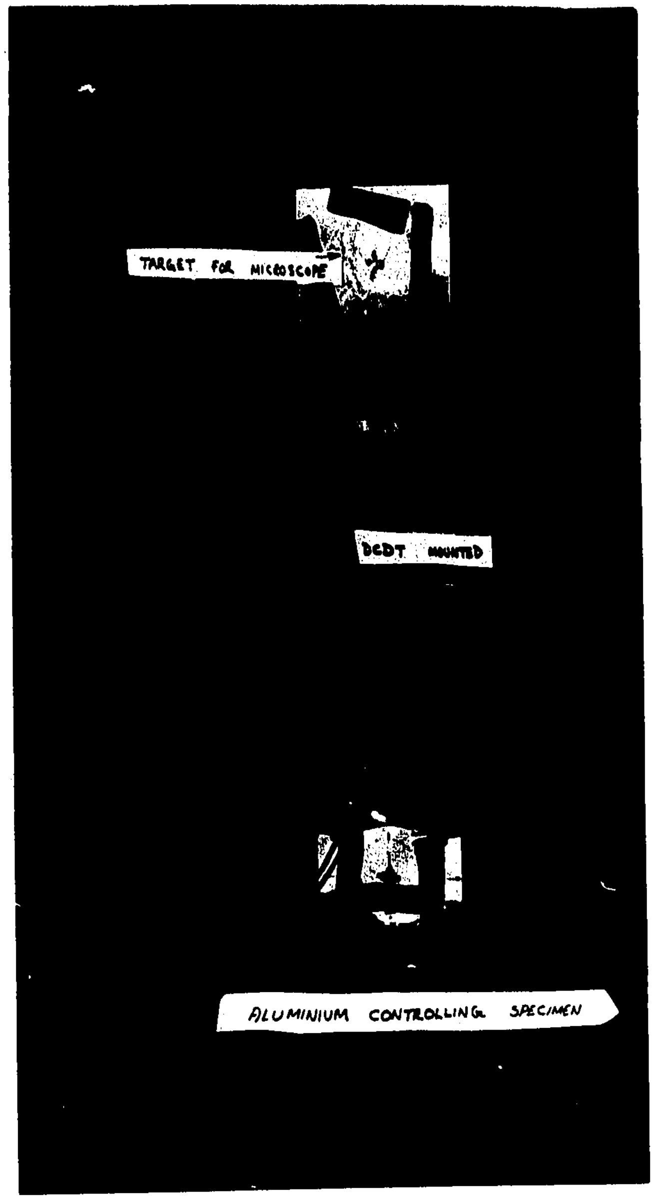

PLATE 3.13 - ALUMINIUM CONTROL PLATE

Targets for microscope (top and bottom) and DCDT (centre) are mounted for deformation measurement.

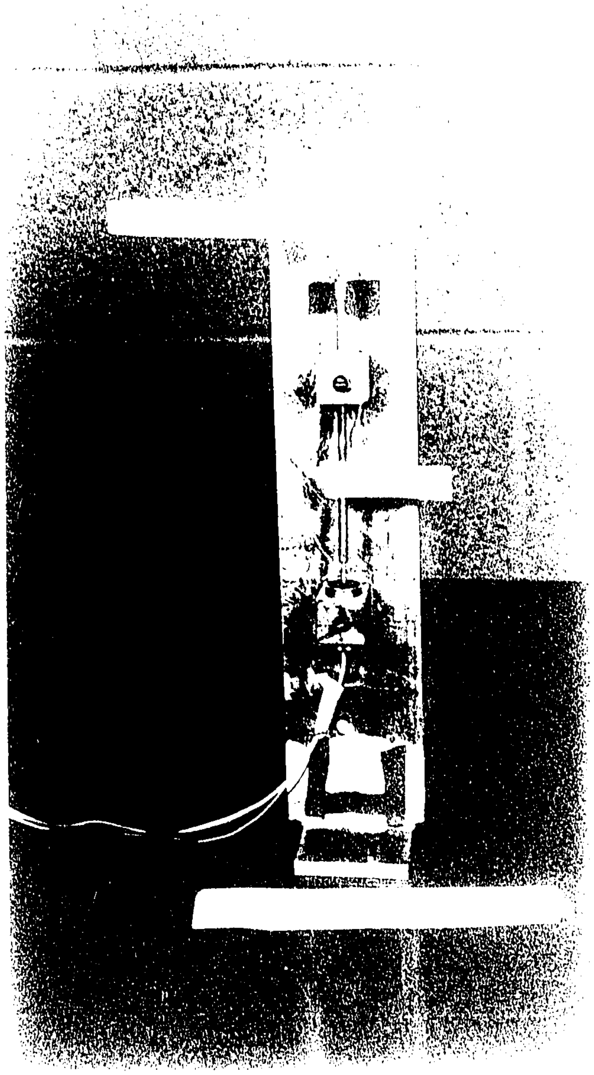

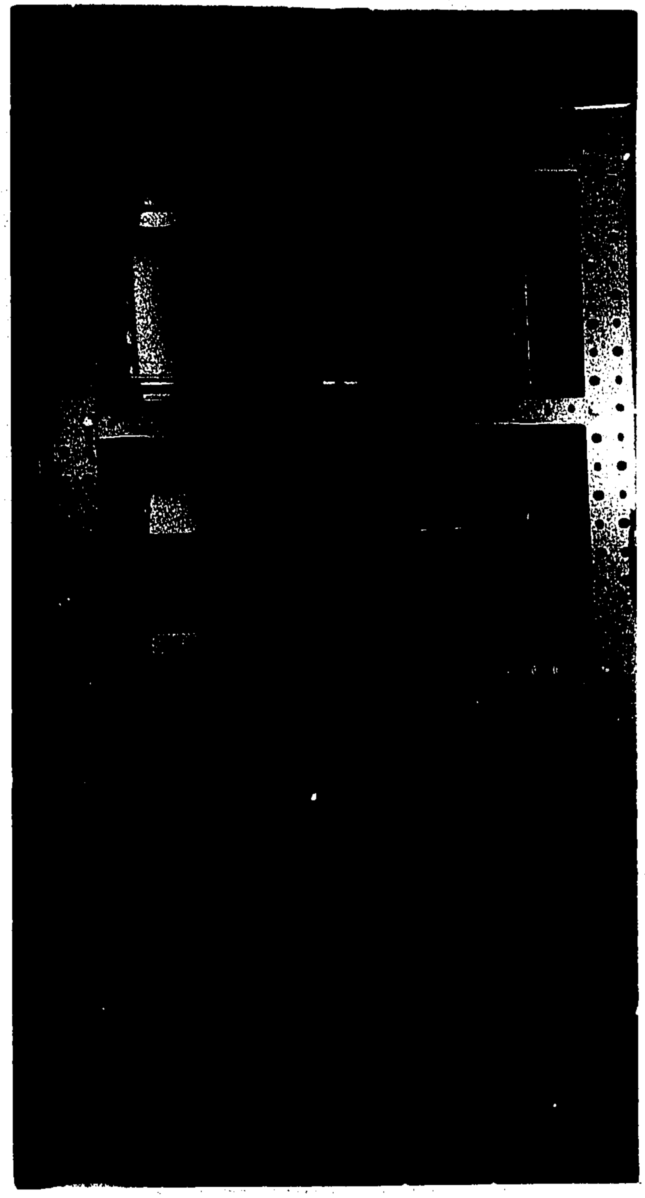

PLATE 3.14 - HALF INSIDE VIEW OF THE CHAMBER DURING TEST

Prism specimens mounted on sonic test benches are on the top two shelves. Slab specimens are on the third shelf.

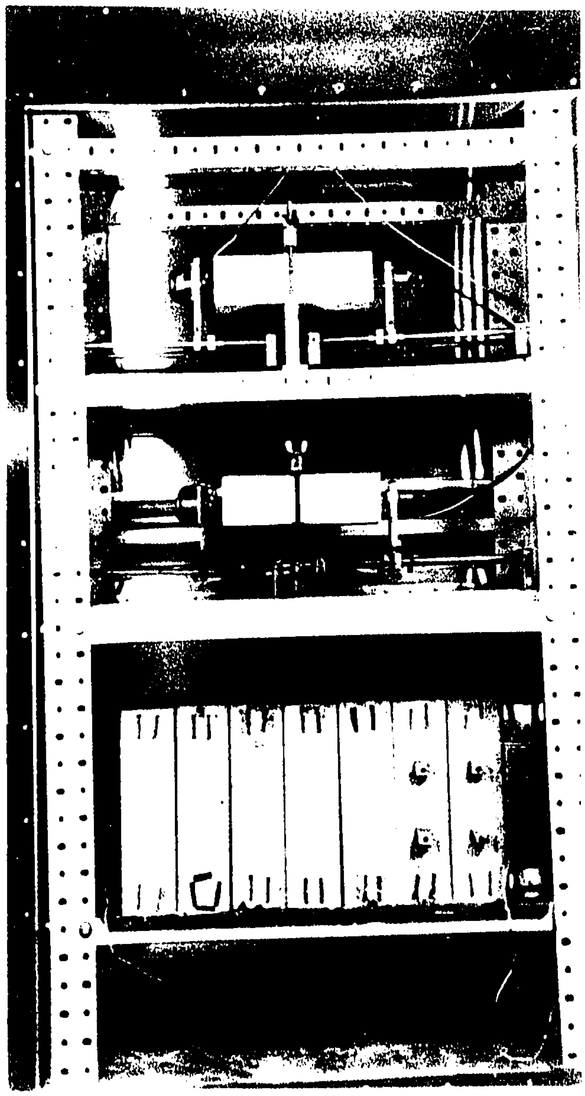

APPENDIX D: FLOW CHARTS AND SUBROUTINES

PROGRAMME C

DYNAMIC MODULUS ELASTICITY

(1) READ SERIES AND SPECIMEN IDENTIFICATION AND VARIABLES (AGE, WATER-CEMENT, WEIGHT OF SPECIMENS)

(2) READ TEMPERATURE AND SONIC RESONANCE FREQUENCY READINGS OF PRISM SPECIMENS

(3) CONVERT FREQUENCY READINGS INTO DYNAMIC MODULUS VALUES

(4) FIT SEPARATE CURVE TO DYNAMIC MODULUS VALUES FOR BOTH ABOVE AND BELOW THE FREEZING POINT

(5) FIND SLOPE OF FITTED CURVES AND THE INTERSECTING POINT (PROBABLE FREEZING POINT) OF THE FITTED CURVES OF ABOVE AND BELOW FREEZING TEMPERATURE

(6) REPEAT STEPS (3) TO (5) FOR ALL SPECIMENS

(7) PRINT OUT IN TABULAR FORM CALCULATED AND FITTED DYNAMIC-E VALUES, SLOPE OF FITTED CURVES AND INTERSECTING POINT OF THE FITTED CURVES

PROGRAMME D

ANALYSIS OF EXPERIMENTAL DEFORMATION DATA

(1) READ SERIES AND SPECIMEN IDENTIFICATION AND VARIABLES (AGE, WATER-CEMENT)

(2) READ TEMPERATURE AND DEFORMATION READINGS OF CONTROL SPECIMENS

(3) READ TEMPERATURE AND DEFORMATION READINGS OF SLAB SPECIMENS

(4) CORRECT DEFORMATION READINGS OF SLAB SPECIMENS FROM CONTROL SPECIMEN RESULTS

(5) FIT CURVE TO CORRECTED DEFORMATION DATA FOR ABOVE FREEZING TEMPERATURE. FIND COEFFICIENT OF EXPANSION FROM SLOPE OF FITTED LINE

(6) PRINT OUT FITTED VALUES OF DEFORMATION, COEFFICIENT OF EXPANSION AND INTERCEPT WITH Y-AXIS

(7) CALCULATE ESTIMATE OF ERROR, STANDARD DEVIATION, AND COEFFICIENT OF CORRELATION FOR THE FITTED CURVE AND PRINT OUT VALUES

(8) PLOT FITTED CURVE

(9) SUPERIMPOSE EXPERIMENTAL POINTS ON THE FITTED CURVE

X

PROGRAMME D

ANALYSIS OF EXPERIMENTAL DEFORMATION DATA

(1) READ SERIES AND SPECIMEN IDENTIFICATION AND VARIABLES (AGE, WATER-CEMENT)

(2) READ TEMPERATURE AND DEFORMATION READINGS OF CONTROL SPECIMENS

(3) READ TEMPERATURE AND DEFORMATION READINGS OF SLAB SPECIMENS

(4) CORRECT DEFORMATION READINGS OF SLAB SPECIMENS FROM CONTROL SPECIMEN RESULTS

(5) FIT CURVE TO CORRECTED DEFORMATION DATA FOR ABOVE FREEZING TEMPERATURE. FIND COEFFICIENT OF EXPANSION FROM SLOPE OF FITTED LINE

(6) PRINT OUT FITTED VALUES OF DEFORMATION, COEFFICIENT OF EXPANSION AND INTERCEPT WITH Y-AXIS

(7) CALCULATE ESTIMATE OF ERROR, STANDARD DEVIATION, AND COEFFICIENT OF CORRELATION FOR THE FITTED CURVE AND PRINT OUT VALUES

(8) PLOT FITTED CURVE

(9) SUPERIMPOSE EXPERIMENTAL POINTS ON THE FITTED CURVE

X

PROGRAMME D (CONT'D)

X

(10) REPEAT STEPS (5) THROUGH (9) FOR BELOW FREEZING POINT CORRECTED DEFORMATION DATA

(11) PRINT OUT IN TABULAR FORM COEFFICIENT OF EXPANSION OF CONCRETE SLABS (AT BOTH FACES) FOR ABOVE AND BELOW FREEZING POINT

PROGRAMME E

THEORETICAL ANALYSIS

(1) READ SERIES AND SPECIMEN IDENTIFICATION, DIFFERENT STEEL PERCENTAGES, REINFORCEMENT TYPE

(2) READ TEMPERATURE AND MODULII OF ELASTICITY AND COEFFICIENT OF EXPANSION OF PLAIN CONCRETE AND STEEL AT DIFFERENT TEMPERATURES

SYMMETRICAL REINFORCEMENT

(3) CALCULATE INTERNAL FORCE DEVELOPED AT EACH TEMPERATURE INTERVAL

(4) FROM COMPATIBILITY OF DEFORMATION CALCULATE STRAIN AND COEFFICIENT OF EXPANSION OF SLAB AT EACH TEMPERATURE INTERVAL

(5) CALCULATE AVERAGE VALUE OF COEFFICIENT BOTH ABOVE AND BELOW THE FREEZING POINT

(6) REPEAT STEPS (3) TO (5) FOR DIFFERENT PERCENTAGES OF STEEL

(7) PRINT OUT IN TABULAR FORM COEFFICIENT OF EXPANSION OF CONCRETE SLABS WITH DIFFERENT PERCENTAGES OF STEEL FOR BOTH BELOW AND ABOVE FREEZING POINT

UNSYMMETRICAL REINFORCEMENT

(8) FROM THE GEOMETRY OF THE SECTION CALCULATE LOCATION OF NEUTRAL AXIS AND MOMENT OF INERTIA OF THE CONCRETE SECTION

(9) REPEAT STEPS (3) THROUGH (7) FOR BOTH FACES OF SLAB

SUBROUTINE FIT 1


```
      SUBROUTINE FIT1(X,M,L)
C     PURPOSE: TO FIT BY THE LEAST SQUARE METHOD FIRST DEGREE POLYNOMIAL
C     CURVE TO THE EXPERIMENTALLY OBTAINED POINTS. THE PROGRAMME GIVES
C     THE FITTED VALUES, SLOPE OF FITTED CURVE AND THE INTERCEPT OF THE
C     FITTED CURVE ON THE Y-AXIS.
      DIMENSION Y(20),X(20),YFT(20)
      DIMENSION BY(20),PTY(20)
      DIMENSION SP(7)
      DIMENSION CK(2,2,7)
      COMMON SP,NG,J,K,SERIES,WCEM,AGE,YFT,BY,PTY,NTT,NTU,NTV,NTW,CK
      SUMX=0.0
      SUMY=0.0
      SUMXY=0.0
      SUMXSQ=0.0
      SUMXQB=0.0
      N=L-M+1
      DO 1 I=M,L
      Y(I)=BY(I)
      SUMX=SUMX+X(I)
      SUMY=SUMY+Y(I)
      SUMXY=SUMXY+X(I)*Y(I)
      SUMXSQ=SUMXSQ+X(I)*X(I)
      SUMXQB=SUMXQB+X(I)*X(I)*X(I)
    1 CONTINUE
      R1=N
      R2=SUMX
      R3=SUMXSQ
      R4=SUMY
      R5=SUMXQB
      R6=SUMXY
      AFT1=(R3*R4-R2*R6)/(R1*R3-R2*R2)
      BFT1=(R1*R6-R2*R4)/(R1*R3-R2*R2)
      DO 2 I=M,L
    2 YFT(I)=AFT1+BFT1*X(I)
      WRITE (3,307)
  307 FORMAT (1H1)
      WRITE (3,437)SERIES,WCEM,AGE
  437 FORMAT (/,5X,A4,2X,F5.3,5X,F8.2,2X,'DAYS')
      WRITE (3,439) SP(J),K
  439 FORMAT (/,5X,'SPECIMEN NO.',2X,A4,5X,'FACE',2X,I2)
      WRITE (3,340)
  340 FORMAT (///,10X,'TEMPERATURE',08X,'SPECIMEN LENGTH',/,26X,'CORRECT
     %ED',5X,'FITTED',//)
```

SUBROUTINE FIT 1 (CONT'D)


```
             DO 415 I=M,L                                                         00002980
       415   WRITE (3,345)X(I),Y(I),YFT(I)                                        00002990
       345   FORMAT (/,11X,F7.2,5X,F10.4,4X,F10.4)
             WRITE (3,1001) AFT1,BFT1                                             00003010
      1001   FORMAT (//,10X,'AFT1 =',F13.8,'   BFT1 =',F12.8,/)
             BFT1=BFT1*(10.0**5)
             IF(M.GT.3)GO TO 3001
             CK(1,K,J)=BFT1
             GO TO 3005
      3001   CK(2,K,J)=BFT1
      3005   CONTINUE                                                             00003030
             RETURN                                                               00003040
             END
```

SUBROUTINE COREL

```
FORTRAN IV G LEVEL  19              COREL              DATE = 72078          01/27/59              PAGE

 0001            SUBROUTINE COREL(X,M,L)                                                     00003050
           C     PURPOSE: TO CORELATE THE FITTED CURVE TO THE EXPERIMENTALLY
           C     OBTAINED POINTS. THE PROGRAMME FINDS OUT STANDARD DEVIATION,
           C     COEFFICIENT OF CORELATION AND ESTIMATE OF ERROR IN Y-DIRECTION.
           C     CORRECTION DUE TO SMALL SAMPLE SIZE IS TAKEN INTO CONSIDERATION.
           C        SDY=STANDARD DEVIATION OF Y                                             00003080
           C        R=CO-EFF. OF CORELATION                                                 00003090
           C        RR='R' CORRECTED FOR SMALL SAMPLE EFFECT                                00003100
           C        SYX=ERROR ESTIMATE OF Y ON X                                            00003110
           C        SMYDSQ=SUMMATION OF YDF(I) SQUARE                                       00003120
           C        SMYSQ=SUMMATION OF Y(I) SQUARE                                          00003130
           C        CSY=CORRECTED 'SYX' FOR SMALL SAMPLE EFFECT                             00003140
 0002            DIMENSION BY(20),PTY(20)                                                    00003150
 0003            DIMENSION YFT(20),X(20),Y(20),YDF(20)                                       00003160
 0004            DIMENSION DEVY(20)                                                          00003170
 0005            DIMENSION SP(7)                                                             00003180
 0006            DIMENSION CK(2,2,7)
 0007            COMMON SP,NG,J,K,SERIES,WCEM,AGE,YFT,BY,PTY,NTT,NTU,NTV,NTW,CK              00003200
 0008            N=L-M+1                                                                     00003210
 0009            SUMY=0.0                                                                    00003220
 0010            SMYSQ=0.0                                                                   00003230
 0011            SMYDSQ=0.0                                                                  00003240
 0012            SDVYSQ=0.0                                                                  00003250
 0013            DO 9 I1=M,L                                                                 00003260
 0014            YDF(I1)=0.0                                                                 00003270
 0015      9     DEVY(I1)=0.0                                                                00003280
 0016            DO 10 I1=M,L                                                                00003290
 0017            Y(I1)=BY(I1)                                                                00003300
 0018            SUMY=SUMY+Y(I1)                                                             00003310
 0019     10     SMYSQ=SMYSQ+Y(I1)*Y(I1)                                                     00003320
 0020            RN=N                                                                        00003330
 0021            YBAR=SUMY/RN                                                                00003340
 0022            DO 11 I1=M,L                                                                00003350
 0023            DEVY(I1)=Y(I1)-YBAR                                                         00003360
 0024     11     SDVYSQ=SDVYSQ+DEVY(I1)*DEVY(I1)                                             00003370
 0025            SDY=SQRT(SDVYSQ/RN)                                                         00003380
 0026            DO 15 I1=M,L                                                                00003390
 0027            YDF(I1)=YFT(I1)-Y(I1)                                                       00003400
 0028     15     SMYDSQ=SMYDSQ+YDF(I1)*YDF(I1)                                               00003410
 0029            SYX=SQRT(SMYDSQ/RN)
 0030            RSQ=1.-((SYX*SYX)/(SDY*SDY))
 0031            R=SQRT(RSQ)
 0032            RRSQ=1.-((1.-R*R)*((RN-1.)/(RN-2.)))
```

SUBROUTINE COREL (CONT'D)

```
FORTRAN IV G LEVEL  19                    COREL              DATE = 72078          01/27/59            PAG
 0033                  WRITE (3,16)RSQ,RRSQ
 0034          16      FORMAT (/,5X,'CHECK -VE VALUES   RSQ=',F15.8,5X,'RRSO=',F15.8,/)
 0035                  CSYXSQ=(SYX*SYX)*((RN-1.)/(RN-2.))                                          00003450
 0036                  RR=SQRT(RRSQ)                                                               00003460
 0037                  CSYX=SQRT(CSYXSQ)                                                           00003470
 0038                  WRITE (3,65)SYX,CSYX                                                        00003480
 0039          65      FORMAT (//,10X,'ESTIMATE OF ERR IN Y-DIRECTION',/,10X,'UNCORRECTED00003490
                      @ =',F10.4,'CORRECTED =',F10.4,/)                                            00003500
 0040                  WRITE (3,66)SDY                                                             00003510
 0041          66      FORMAT (10X,'STANDARD DEVIATION =',F10.4,/)                                 00003520
 0042                  WRITE (3,67)R,RR                                                            00003530
 0043          67      FORMAT (/,10X,'COEFF. OF CORRELATIONS*',/,10X,'CALCULATED =',F10.400003540
                      @,'CORRECTED =',F10.4,/)                                                     00003550
 0044                  RETURN                                                                      00003560
 0045                  END
```